INVESTIGATION OF EPHRIN REGULATION DURING HINDBRAIN SEGMENTATION

James Cameron Brodie

Division of Developmental Neurobiology
National Institute for Medical Research,
The Ridgeway, Mill Hill,
London, NW7 1AA

University College London
Gower Street,
London WC1E 6BT

Submitted for the degree of Doctor of Philosophy

September 2000

ProQuest Number: U643138

All rights reserved

INFORMATION TO ALL USERS
The quality of this reproduction is dependent upon the quality of the copy submitted.

In the unlikely event that the author did not send a complete manuscript
and there are missing pages, these will be noted. Also, if material had to be removed,
a note will indicate the deletion.

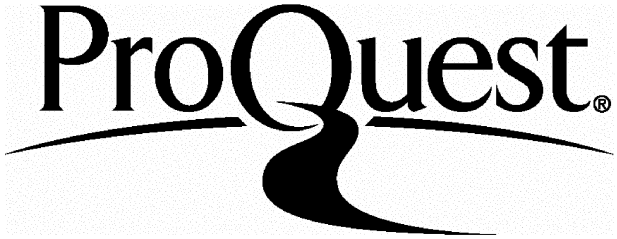

ProQuest U643138

Published by ProQuest LLC(2016). Copyright of the Dissertation is held by the Author.

All rights reserved.
This work is protected against unauthorized copying under Title 17, United States Code.
Microform Edition © ProQuest LLC.

ProQuest LLC
789 East Eisenhower Parkway
P.O. Box 1346
Ann Arbor, MI 48106-1346

Abstract

Early in the development of the vertebrate central nervous system, the hindbrain is transiently segmented into morphological units termed rhombomeres (r). Eph-family receptor tyrosine kinases such as EphA4 and EphB2 are expressed in rhombomeres 3 and 5, while their ligands – the ephrins – such as ephrin-B2, are expressed in r2, r4 and r6. The interaction between receptor and ligand in these complementary domains is important in the restriction of cell-mixing between rhombomeres. *Hox* genes are important in the parallel process of assigning axial identity to the resulting segments. These pathways are interconnected both by upstream factors such as Krox-20 and kreisler that regulate *Hox* genes as well as an Eph receptor, and by regulatory links between *Hox* genes and *Eph*s.

In order to discover more about the regulation of *ephrin*s during hindbrain development, two main approaches were selected. Preparatory work has been carried out for the analysis of the *ephrin-B2* regulatory region and a number of candidate regulatory factors have been investigated. Analysis of *kreisler* mutant embryos and transgenic embryos expressing *kreisler* in r3 has shown that this transcription factor does not regulate *ephrin-B2* or *-B3* in r5/6. These data also provide new insights into the nature of the disruption to segmentation in the *kreisler* mutant. Analysis of *Krox-20* mutant embryos indicates a role in the repression of *ephrin-B2* expression in r3/5. Analysis of *Hoxa1* and *Hoxb1* mutant embryos has shown that the loss of either of these factors individually does not affect *ephrin* expression in the caudal hindbrain. Regulation of *ephrin-B2* by retinoids was investigated by exposing zebrafish embryos to all-*trans*-retinoic acid or the retinoic acid-antagonist – BMS 493. These analyses have demonstrated a role for retinoids in *ephrin* regulation and have also provided further insights about the mechanisms underlying hindbrain development.

Contents

Figures

Tables

Abbreviations

A-P	antero-posterior
BAC	bacterial artificial chromosome
CNS	central nervous system
DN	dominant-negative
DNA	deoxyribonucleic acid
dpc	days postcoitum
D-V	dorso-ventral
GPI	glycosylphosphatidylinositol
IRES	internal ribosome entry site
kr	*kreisler*
ORF	open reading frame
PAC	P1 artificial chromosome
PCR	polymerase chain reaction
pGKPA	phosphoglycerate kinase polyadenylation sequence
r	rhombomere
RA	retinoic acid
RALDH	retinal dehydrogenase
RAR	retinoic acid receptor
RARE	retinoic acid response element
RNA	ribonucleic acid
ROLDH	retinol dehydrogenase
RTK	receptor tyrosine kinase
RXR	retinoid X receptor
val	*valentino*

Acknowledgements

First thanks to my supervisor, Dave Wilkinson, for coming up with the goods when it counted. Thanks too to lab-mates past and present for being there with a ready word of advice, a helping hand and those kindnesses which alleviate the daily grind. Special mention (in strict alphabetical order) to Jeff Christiansen, Andrea Pasini, Vicky Robinson, Dorothy Sobieszczuk and Thomas Theil. Neither will I forget the beneficial association with members of other labs in the Division and further afield. Special thanks here to my second supervisor – Robb Krumlauf – Miguel Manzanares, Stephan Nonchev, Nobue Itasaki, Maite Martinez, Linda Ariza-McNaughton, Heather Marshall, Christiana Ruhrberg, Steve Sedgewick, Baljinder Mankoo, Dipa Natarajan and the Director of Studies at the Institute – Rod King. Sincere thanks to Pierre Chambon for the gift of the BMS 493. Let's hear it for the people who look after the mice in Laidlaw Green – especially Amanda Hewett! Thank you to my parents and wider family for all their support and encouragement through the years, it's meant more to me than you may realise. Thanks to my dear friends, Antony Black, Ken Macrae and Martin Moneke, for keeping me insane in the midst of this madness. Finally, to the one who's borne the brunt of it all and still kept on loving me – Sonja Theuerkauf – thank you.

The work described in this thesis was carried out at the National Institute for Medical Research and was supported by the Medical Research Council.

Chapter 1 – Introduction

1.1 General Background

1.1.1 The Central Nervous System

The vertebrate central nervous system (CNS) is a study in complexity. From an initially homogeneous embryonic tissue, many hundreds and perhaps even thousands (Stevens, 1998) of specific neuronal subtypes are generated and patterned into a finely-tuned functional unit. Raw numbers, however, belie the elegance of co-ordination of the developmental processes involved and the genetic interactions which regulate them. The same principle of regionalisation employed by the developing embryo to such great effect in generating complex structures brings the process within reach of study and understanding.

During gastrulation, the three germ layers of the embryo – endoderm, mesoderm and ectoderm – are generated and become established in their relative positions. Also during this time, the primary antero-posterior (A-P) body axis is laid down and the process of organogenesis begins. Cross-talk between the mesoderm and overlying ectoderm is critical for many aspects of organogenesis, including the development of the nervous system. What follows is a brief description of the morphological progress of neurulation before looking at the underlying mechanisms which drive these events.

1.1.2 Neurulation

During neurulation the ectodermal layer of the gastrula is partitioned into the neural tube, the epidermis and the neural crest. The first visible event in neural tube formation is the delineation of the neural plate by elongation of the ectodermal cells along the midline as they develop into the columnar neural plate cells. The more laterally located cells in the ectodermal sheet represent the presumptive epidermis and these take on a flatter shape. These cell-shape changes produce a ridge along the boundary of the presumptive neural plate as the neural ectoderm thickens, marking the region that will later fuse along the dorsal midline and give rise to the neural crest.

The conversion of the flat neural plate into a neural tube is accomplished by a series of tightly controlled cell movements and shape changes involving the cells of the neural plate, the notochord and the presumptive epithelium. The result is that the plate bends and loops up until the edges of the neural plate meet and fuse, with the neural crest cells delaminating and migrating away from the dorsal lip either just before or just after closure, depending on the species and the position along the A-P axis.

1.1.3 Regionalisation of the neural tube

The first broad division of the neural tube is between the cephalic (head-forming) region and the trunk region, which will give rise to the spinal cord. While the trunk region persists as a simple tube, parts of the cephalic region become further subdivided into a series of bulges, known as neuromeres, which will give rise to the various regions of the brain.

The first bulges to form are the three primary vesicles: the prosencephalon, mesencephalon and rhombencephalon (from anterior to posterior), giving rise to the forebrain, midbrain and hindbrain respectively. The prosencephalon is then divided into telencephalon and diencephalon and later into smaller prosomeres. The rhombencephalon subsequently becomes further divided into the metencephalon and myelencephalon, with the myelencephalon being transiently divided into smaller rhombomeres.

1.1.4 The organiser

The bulk of historical work on neural induction and regionalisation has been carried out on the amphibian embryo, due to its availability, accessibility and amenability to surgical manipulation. The onset of gastrulation in this system is marked by the appearance of the blastopore, through which the superficial marginal zone cells of the blastula invaginate to create the archenteron. These cells are fated to form the endodermal lining of the archenteron, while cells of deeper involuting layers will give rise to the mesoderm. The outer cells, which cover the entire surface of the embryo, form the ectoderm. Thus, the three embryonic tissue layers are established. Classical experiments determined the dorsal lip of the blastopore to be a source of patterning information which, when transplanted to a host embryo, is capable of

inducing an ectopic dorsal axis in the host tissue leading to the formation of a complete nervous system (Spemann and Mangold, 1924). This entity is known as the organiser and its two main functions are the induction of neural tissue in competent ectoderm and dorsalisation of mesoderm, which would otherwise be ventral (blood, mesenchyme), to form trunk mesoderm (muscle). The equivalent structures in other vertebrate models are the embryonic shield in fish (Shih and Fraser, 1996) and the node in chick (Storey *et al.*, 1992) and mouse (Beddington, 1994). In the mouse, there is a growing body of evidence which indicates the presence of another organising activity within an extra-embryonic tissue – the anterior visceral endoderm – which initiates extreme anterior patterning (see Beddington and Robertson, 1998 for review). In zebrafish too, transforming signals have been located which originate outside the organiser in the germring (non-axial mesoderm) (Woo and Fraser, 1997). However, the similarities between systems are broad enough to warrant including a summary of events in the amphibian model, where the bulk of work in this area has been carried out.

Prior to the onset of gastrulation, during the blastula stage, distinct regions of the embryo are fated to give rise to ectoderm, endoderm and ventral and dorsal mesoderm. The organising activity resides within the dorsal mesoderm, located at the dorsal marginal zone (see Slack and Tannahill, 1992 for review). Gastrulation is initiated here and, during the movements which follow, this tissue comes to reside along the midline, subjacent to the dorsal ectoderm, giving rise to pre-chordal plate, notochord and axial mesoderm. Extensive signalling takes place throughout the process as successive inductive events occur. In the course of gastrulation, signals from the organiser both induce neural tissue to form from the overlying ectoderm and regionalise it along the A-P axis (reviewed in Slack and Tannahill, 1992; Sasai and De Robertis, 1997; Wilson and Hemmati-Brivanlou, 1997; Niehrs, 1999). Signals from the organiser are propagated both vertically, from the chordamesoderm to the neural ectoderm opposed to it and horizontally, within the plane of the ectoderm from the dorsal lip of the blastopore.

Evidence for the transmission of antero-posterior regional identity from the mesoderm to overlying neural tissue comes from the disruption of such genes as *Lim1* (Shawlot and Behringer, 1995). *Lim1* is expressed early in a restricted region of the epiblast, where the primitive streak will form, and later in the prechordal mesoderm. In null mutant embryos, the most rostral domain of the neural tube is represented by a reduced r3 *Krox-20* stripe and all neural structures anterior to this are absent, though the posterior neuraxis is unaffected (Shawlot and Behringer, 1995). In the chick, prechordal tissue has variously been reported as being competent to induce anterior neural structures from undifferentiated ectoderm (Pera and Kessel, 1997) or to anteriorise more posterior neural tissue towards forebrain identity (Foley *et al.*, 1997).

1.1.5 Neural induction

The most widely accepted model explaining how the neural tube is induced and regionalised is the activation-transformation model (Nieuwkoop *et al.*, 1952). Several variants of the basic model exist, but in essence, it proposes that neuralisation is a two-step process. In the first step, neural tissue is induced to form from the ectoderm by one set of signals and in the second, it is regionalised by a separate set of signals. Several factors, present in the organiser, are known to induce the formation of anterior neural structures in naïve ectoderm, while others then modify its antero-posterior character (see reviews cited above). This then leads to the organised layout of the neural tube from forebrain to spinal cord by the end of gastrulation. Signals from the organiser set in train a cascade of inductive events which ultimately give rise to a complete nervous system.

1.1.6 The hindbrain

Cells in the neural tube become committed to a hindbrain fate during mid-gastrulation (Woo and Fraser, 1998; Muhr *et al.*, 1999), as part of the broad regionalisation occurring at this time. Finer patterning subsequently occurs within smaller regional units. The hindbrain represents an attractive and accessible system for the study of local CNS patterning due to the relatively low number of cell types generated within it and the segmental nature of its

development. In segmented development, a tissue is partitioned into a series of lineage-restricted blocks, which then differentiate according to their position along the body axis. Segmentation is often used in animal development to generate homologous, yet distinct structures from reiterated blocks of tissue along the body axis and, as mentioned above, the hindbrain is transiently segmented into morphological units termed rhombomeres (r). Although hindbrain segmentation bears a superficial resemblance to that seen in diverse members of the animal kingdom such as *Drosophila melanogaster* (Lumsden, 1990), the strategy is thought to have evolved independently many times (Newman, 1993). Nevertheless, the systems share a number of conceptual features. The segment as a developmental compartment is one example.

A developmental compartment may be defined as a block of cells which does not intermingle with adjacent populations and which corresponds with domains of gene expression and action (Garcia-Bellido *et al.*, 1973; Lewis, 1978; Lawrence and Struhl, 1996). This grouping and partial isolation of cells allows them to assume a collective identity and follow a co-ordinated programme of differentiation. Compartments are also seen to have a role in limiting cell proliferation, providing a check on growth. Although compartments are often separated by a morphological boundary, this is not prerequisite as there are a number of different mechanisms for preventing intermingling between adjacent cell populations.

Visible segmentation of the hindbrain occurs in the chick (the process is similar for other vertebrate models) between stages 9 and 12 (for HH stages see Hamburger and Hamilton, 1951). Boundaries appear as bulges of the neuroepithelial sheet into the neurocoel, partitioning the neural tube at this axial level into a series of 8 rhombomeres (7 in the mouse). Each rhombomere is a polyclonal block of neuroepithelial cells with limited intermingling between adjacent segments (Fraser *et al.*, 1990; Birgbauer and Fraser, 1994).

1.1.7 Hindbrain segmentation

Restriction of cell-mixing between segments is thought to be a key precondition for the establishment and maintenance of rhombomere-specific

domains of gene expression and by extension, rhombomeric identity. This may be achieved by erecting a mechanical barrier which prevents cells crossing or by rendering the two cell populations immiscible with each other by means of cell adhesion or repulsion properties (or both). As the onset of segmentally-restricted gene expression, the appearance of morphological boundaries and lineage restriction between rhombomeres all occur within a narrow time window, it was for some time unclear which of these mechanisms has the primary role.

Rhombomere boundary regions have a number of features which make them distinct from the rest of the rhombomere, such as altered shape and increased extracellular spaces (Heyman *et al.*, 1993), changes in the extracellular matrix (Heyman *et al.*, 1995) and reduced rates of cell division (Guthrie, 1991). These properties on their own would certainly inhibit the passage of cells between rhombomeres, but two key pieces of evidence suggest that boundaries form as a result of inherent differences between the cells of adjacent rhombomeres. Firstly, rhombomere-specific patterns of gene expression are observed before the appearance of morphological boundaries (e.g. Wilkinson *et al.*, 1989a) and secondly, boundaries regenerate following their surgical removal (Guthrie and Lumsden, 1991). Grafting and cell-transplantation experiments have confirmed that cells from neighbouring rhombomeres (e.g. r4 and r5) have a limited capacity for intermingling and will sort out if artificially mixed (Guthrie *et al.*, 1993; Wizenmann and Lumsden, 1997). By contrast, cells of alternate rhombomeres (e.g. r2 and r4) are capable of mixing, though to a lesser degree than those from the same rhombomere (Guthrie and Lumsden, 1991; Wizenmann and Lumsden, 1997). Small groups of cells grafted into neighbouring rhombomeres are capable of autonomously maintaining their molecular identity as long as they remain in contact with each other and switching identity when dispersed (Trainor and Krumlauf, 2000). Thus the fundamental factor in preventing cells straying between rhombomeres is repulsive interactions or differences in adhesivity, alternate rhombomeres sharing similar properties.

1.2 Hindbrain patterning

In addition and parallel to the mechanical aspects of segmentation, the axial identity of the rhombomeres must also be correctly specified, as their metameric organisation forms the basis of patterned differentiation. Reticular neurons are repeated through the rhombomeres with little axial variation (Clarke and Lumsden, 1989), but the organisation of the branchiomotor neurons displays a two-segment periodicity. Groups of branchiomotor neurons occupy a pair of segments, while their axons innervate a single branchial arch (segmented structures located ventrolaterally to the hindbrain) (Lumsden and Keynes, 1989). The trigeminal (V^{th}) ganglion arises in rhombomeres 2 and 3, exiting from r2, while the facial (VII^{th}) and glossopharyngeal (IX^{th}) arise in r4/5 and r6/7 and exit from r4 and r6 respectively. Neural crest cells originating from the hindbrain also largely conform to this two-segment rule, streaming out from rhombomeres 2, 4 and 6 into the first, second and third branchial arches respectively. Here, they contribute to the formation of muscular, skeletal, neurogenic and vascular structures (Le Lievre and Le Douarin, 1975; Noden, 1983; Bockman and Kirby, 1984; Couly *et al.*, 1993; Könteges and Lumsden, 1996) and they carry at least some of the positional information derived from their hindbrain origins with them (Kuratani and Eichele, 1993; Prince and Lumsden, 1994; Saldivar *et al.*, 1996) but see (Mallo and Brändlin, 1997; Trainor and Krumlauf, 2000).

1.2.1 *Hox* genes

This positional information is conveyed by members of the *Hox* gene family (reviewed in McGinnis and Krumlauf, 1992). The vertebrate *Hox* genes are arranged in 4 separate clusters which have arisen through duplication of the ancestral complex and are homologous to the *HOM-C* genes of *Drosophila*. The *Drosophila* homeotic genes were found to be organised in a complex which reflects their action along the body axis (Lewis, 1978). These genes play a central role in specifying axial tissue identity along the anterior-posterior axis of multicellular animals from *C. elegans*, to vertebrates (see Krumlauf, 1994 for review).

Mutations in fly *HOM-C* genes lead to homeotic transformations of segment identity, i.e. the transformation of identity of one body segment to another. For example, when the *Ubx* gene is mutated, the third thoracic segment, normally endowed with halteres (small organs aiding balance in flight), assumes the character of the second thoracic segment and produces a second pair of wings (Lewis, 1978). Other extraordinary features of the *Hox* genes include their genomic organisation within the cluster which coincides with the order in which they are expressed along the anterior-posterior axis (termed colinearity) and the fact that this arrangement is evolutionarily conserved throughout the animal kingdom (Lewis, 1978; Duboule and Dollé, 1989; Graham *et al.*, 1991). Genes at the 5'-end of the complex are the most posteriorally restricted, with further 3' genes having more anterior limits of expression.

A key observation which helped confirm the importance of rhombomeres in hindbrain patterning was the coincidence of 3'-*Hox* gene expression with rhombomere boundaries (Wilkinson *et al.*, 1989a; Hunt *et al.*, 1991). A two-segment periodicity is evident here too as successive members of the *Hoxb* complex have anterior limits of expression differing by two rhombomeres (Wilkinson *et al.*, 1989a). *Hoxb4* has an anterior expression limit at the r5/6 boundary, while *Hoxb3* and *Hoxb2* reach the r4/5 and r2/3 boundaries respectively. Superimposed on this pattern are rhombomere-specific variations in expression levels. *Hoxb3* expression, for example, is elevated in r5 and *Hoxb2* is expressed at higher levels in rhombomeres 3–5 (Wilkinson *et al.*, 1989a). In vertebrates, as in *Drosophila*, disruption of *Hox* gene expression leads to disruption of axial patterning and homeotic transformations of tissues in their anterior expression domain (reviewed in Krumlauf, 1994). Thus we see rhombomeres acting as domains of *Hox* gene expression and action as well as lineage restriction, analogous to the developmental compartments of *Drosophila*.

A number of other genes with rhombomere-specific expression patterns are believed to be important in the segmental development of the hindbrain. *Krox-20, kreisler* and members of the Eph family of receptor tyrosine kinases and their ligands the ephrins all play pivotal roles. I will

briefly introduce each of them here to set the context for a thorough discussion of their roles in subsequent sections.

1.2.2 *Krox-20*

Krox-20 was originally identified as a serum-responsive gene in mouse NIH 3T3 fibroblasts and encodes a transcription factor with three zinc-finger domains (Chavrier *et al.*, 1988). Soon after it was cloned, it was found to be segmentally expressed in the developing hindbrain (Wilkinson *et al.*, 1989b), in rhombomeres 3 and 5, leading to speculation that it may be involved in segmentation. Indeed, a loss of functional Krox-20 results in the complete loss of r3 and r5, although they are initially formed correctly (Schneider-Maunoury *et al.*, 1993; Swiatek and Gridley, 1993), indicating an important role in the maintenance of these rhombomeres.

1.2.3 *kreisler*

kreisler has been known since the early 1940s, arising as an allele in X-ray mutagenesis studies on mice (Hertwig, 1942; Hertwig, 1944). Mutants attracted attention because of the distinctive circling behaviour and deafness observed in adult animals. These aspects of the mutant phenotype are due to defective inner ear development which is secondary to defects in hindbrain segmentation (Deol, 1964). The *kreisler* (*kr*) gene encodes a basic domain-leucine zipper transcription factor of the Maf subfamily and is expressed in rhombomeres 5 and 6 (Cordes and Barsh, 1994). In homozygous *kr* mutants, there is a complete breakdown in overt segmentation posterior to rhombomere 3. Rhombomeres 1-3 appear outwardly normal, but at the level of r4-r7, the neural tube is smooth and morphologically unsegmented. It was for this smooth appearance of the hindbrain that the zebrafish homologue of *kreisler* – *valentino* – was named (Moens *et al.*, 1996).

1.2.4 *Ephs/ephrins*

In recent years, a considerable body of evidence has accrued regarding the involvement of the Eph-family of receptor tyrosine kinases (RTKs) and their ligands, the ephrins, in setting up regions of differential adhesion/repulsion. Indeed, it was the Eph-receptors' rhombomere-specific expression patterns in

the hindbrain which first attracted the attention of developmental biologists (Nieto *et al.*, 1992). The Eph-family has since been found to comprise the largest known family of RTKs, consisting of at least 14 members in vertebrates, and fewer genes in invertebrates such as *Drosophila* and *C. elegans*. Amino acid sequence comparisons reveal that all family members have several conserved characteristics. The cytoplasmic kinase domain is highly conserved and has strong similarity to that of other families of RTKs. The distinctive feature of Eph receptors is the primary structure of the extracellular region, which includes 2 fibronectin type III motifs (Pasquale, 1991), 20 conserved cysteines, many of which are clustered in a cysteine-rich region, and an N-terminal ligand binding domain (Labrador *et al.*, 1997; Lackmann *et al.*, 1998). The N-terminal domain was initially proposed to have an immunoglobulin-like structure, but X-ray crystallographic determination of the structure has now shown that it is comprised of 11 antiparallel β-sheets with a loop that is predicted to interact with the ligand (Himanen *et al.*, 1998). Many Eph receptors display complementary expression patterns with their ligands in the hindbrain (as well as in other tissues) (Becker *et al.*, 1994; Flenniken *et al.*, 1996; Gale *et al.*, 1996). *EphA4*, *EphB2* and *EphB3*, for example, are expressed in rhombomeres 3 and 5, while their interacting ligands – *ephrin-B1*, *-B2* and *-B3* – are expressed in rhombomeres 1, 2, 4 and 6. The ligands are all membrane bound; either via a GPI-linkage (ephrin-A-class) or by a transmembrane domain (ephrin-B-class) and receptors are classified based on which group of ligands they bind to: EphA receptors bind GPI-linked ligands, EphB receptors bind transmembrane ligands (the only exception being EphA4 which binds to members of both) (Gale *et al.*, 1996). Proteins of the ephrin-B class have a short cytoplasmic region with, at the C-terminal end, 33 highly conserved amino acids including 5 tyrosines. The sequence identity of the extracellular region of different ephrin family members is relatively low (18–55%), but there are a number of strictly conserved residues, including 4 cysteine residues. Unless artificially clustered, the ligands are only active when membrane-bound (Davis *et al.*, 1994) and there is ample evidence that ephrin-B proteins are capable of transducing signals on receptor binding, such that bi-directional signalling

occurs at the interface of complementary ligand/receptor expression domains (Henkemeyer *et al.*, 1996; Holland *et al.*, 1996; Bruckner *et al.*, 1997; Xu *et al.*, 1999; Mellitzer *et al.*, 1999).

Ephs and ephrins are involved in developmental processes such as axonal pathfinding, retino-tectal mapping, neural crest migration and hindbrain segmentation (see Wilkinson, 2000; Frisén *et al.*, 1999 for recent reviews). The common theme to their involvement is the mediation of cell-contact dependent signals that regulate repulsion or differential adhesion and so restrict the movement of axons or cells.

Overexpression (in *Xenopus* and zebrafish) of a dominant negative (truncated - lacking the cytoplasmic tyrosine kinase domain, but still anchored to the membrane) version of the EphA4 receptor, normally expressed in r3 and r5, leads to abnormal cell mixing and disruption of hindbrain patterning (Xu *et al.*, 1995). Ectopic r3 and r5 cells are now observed in rhombomeres 2, 4 and 6. Neural crest migration is also disrupted; cells which would normally only migrate into the third branchial arch now enter second and fourth arch territories as well (Smith *et al.*, 1997). Overexpression of a full length transmembrane ligand, *ephrin-B2*, likewise leads to abnormal rostral and caudal straying of third arch neural crest cells with an even more pronounced effect than the dominant negative receptor (Smith *et al.*, 1997). Mosaic analysis and *in vitro* assays have now provided direct evidence that Eph receptors and ephrins mediate cell sorting responses that restrict the intermingling of odd and even numbered rhombomeres (Xu *et al.*, 1999; Mellitzer *et al.*, 1999).

An outstanding and important question is how the mediators of positional identity are coupled with the process of segmentation such that orderly segments, each with a distinct and homogeneous identity correctly positioned along the A-P axis, are produced. Global patterning events which occur during gastrulation initiate a cascade of regulatory interactions, leading to refinement of pattern on an increasingly localised scale. I will attempt to follow some threads of this process which lead to the establishment of A-P pattern in the hindbrain.

The stage has been set by the end of gastrulation with the induction of neural tissue and relatively broad-brush regionalisation in response to signals from the organiser and its derivatives. One of the molecules thought to be involved in the refinement of pattern at this stage with particular relevance to the hindbrain is retinoic acid (RA).

1.3 Retinoids in hindbrain development

Many aspects of vertebrate development are affected by retinoids (see e.g. Morriss-Kay and Sokolova, 1996 for review) and the hindbrain is among the most sensitive systems to this perturbation. The retinoids are derivatives of vitamin A (retinol), an essential dietary component, and exist in two main physiologically active forms: all-*trans*-retinoic acid and 9-*cis*-retinoic acid. The developing mammalian embryo is ensured an adequate supply of retinol from the maternal blood supply through a supply system considerably buffered against variation in maternal stores. Active retinoids are then synthesised within the embryo.

The retinoid receptors are ligand-activated transcription factors which reside within the nucleus and are divided into two families: retinoic acid receptors (RARs) and retinoid X receptors (RXRs) (see Chambon, 1996 for review). Both groups are further classed into three subtypes: α, β and γ, each of which exists in several different isoforms. Upon ligand (all-*trans*- or 9-*cis*-RA) binding, heterodimeric (RAR/RXR) receptor pairs become transcriptionally active, binding to *cis*-acting retinoic acid response elements (RAREs – themselves polymorphic) within the regulatory elements of target genes. RXR/RXR homodimers are activated by 9-*cis*-RA only and bind to RXREs. These, however, do not appear to be involved in hindbrain development (van der Wees *et al.*, 1998) and so will not be considered here.

1.3.1 Retinoic Acid Response Elements (RAREs)

The final link in the chain is the RARE to which ligand-activated RARs bind and mediate their effects on transcription. Functional RAREs have been found within the regulatory region of several *Hox* genes and show extensive conservation between species (Pöpperl and Featherstone, 1993; Langston *et*

al., 1997) and they have been demonstrated to be directly involved in the regulation of their respective genes. For example, two DR2 RAREs are known to be vital for the correct regulation of *Hoxb1* expression (Marshall *et al.*, 1994; Studer *et al.*, 1994; Studer *et al.*, 1998). An 800 bp fragment lying 3′ to the *Hoxb1* gene, capable of driving expression in a subset of the normal domains and ectopic expression in response to retinoic acid, was found to contain a motif related to a consensus RARE sequence (Marshall *et al.*, 1994). *In vitro*, this was shown to bind RAR/RXR heterodimers and point mutations within the RARE abolish this binding. Likewise, disruption of the RARE, by deletion or point mutation, abrogated the activity of this enhancer *in vivo*, highlighting its importance in the establishment of early neural expression. This RARE has also been mutated in the context of the endogenous gene, confirming its role in the early induction of *Hoxb1* (Studer *et al.*, 1998). Another RARE, this time a component of an enhancer lying 5′ to the *Hoxb1* gene, has been shown to negatively regulate expression in rhombomeres 3 and 5 (Studer *et al.*, 1994). This element co-operates with an enhancer capable of driving expression in rhombomeres 3, 4 and 5 to give a domain sharply restricted to r4.

The early neural enhancer of the *Hoxb4* gene has also been shown to contain a DR5 RARE which is absolutely required for all phases of its activity (Gould *et al.*, 1998). Replacing only the DR5 RARE component of this enhancer with the *Hoxb1* DR2 (the 3′ RARE mentioned above) results in an alteration of its expression domain such that it approximates that of *Hoxb1*. This result provides very strong evidence for the presence of information important for A-P positioning of *Hox* gene expression in the hindbrain encoded in RARE composition.

1.3.2 Retinoic acid metabolism

Several studies using high pressure liquid chromatography, reporter cell lines (with reporter expression driven by a RARE) and transgenic constructs (again with a RARE-driven reporter) have demonstrated the presence of endogenous retinoids in the embryo (Rossant *et al.*, 1991; Chen *et al.*, 1993; Maden *et al.*, 1998). They have shown that, around the onset of somitogenesis, retinoids are present in posterior regions of the embryo up to the level of the hindbrain.

The embryo must convert retinol obtained from maternal blood by dehydrogenation into retinoic acid in the tissues where it is required. This is achieved in two steps: first the conversion of retinol to retinal by a retinol dehydrogenase (ROLDH), followed by conversion to RA by a retinal dehydrogenase (RALDH). Other enzymes then further metabolise RA into inactive by-products. Regulating the availability of transcriptionally active retinoids is an important means by which the embryo may control this signalling system. *RALDH-2* (an RA synthesis enzyme) and *CYP26* (which breaks it down) have been found to be expressed in mutually exclusive regions of the chicken embryo which border the hindbrain (Berggren *et al.*, 1999; Swindell *et al.*, 1999). Mouse *Raldh-2* is similarly expressed (Niederreither *et al.*, 1997) and another enzyme which degrades RA – $P450_{RA}$ – is expressed in the anterior region of the embryo between 7.5 and 8.0 dpc (Fujii *et al.*, 1997).

Work in the chick has shown that expression of these enzymes correlates with retinoic acid synthesis and degradation respectively (Swindell *et al.*, 1999). *RALDH-2* is expressed in posterior mesodermal tissues from early in development (HH stage 4) (Swindell *et al.*, 1999; Berggren *et al.*, 1999). It is particularly strongly expressed in the nonaxial mesoderm surrounding Hensen's node, though not in the node itself. The node had been proposed as a site of RA-synthesis (Hogan *et al.*, 1992), but the source appears rather to be the surrounding mesoderm (Ang and Duester, 1997; Berggren *et al.*, 1999; Niederreither *et al.*, 1997). At stage 7, *RALDH-2* expression extends to a sharp anterior boundary at the level of the first somite. *CYP26* expression begins slightly earlier than *RALDH-2* in the ectoderm anterior and lateral to the node, corresponding to the presumptive fore- and midbrain regions. The gap between expression domains of these two genes corresponds to the presumptive hindbrain – strongly reminiscent of the classic source-sink model for establishing a morphogen gradient (Wolpert, 1969). RA production in the somites, diffusion into the hindbrain and degradation in the midbrain could give rise to an RA gradient across the hindbrain.

The presence of retinoic acid in somites is consistent with their ability to induce *Hox* gene expression in co-culture with hindbrain tissue. *Hoxb4*

expression is induced in explanted hindbrain tissue in response either to co-culture with somitic tissue or addition of RA to the culture medium (Gould *et al.*, 1998). This induction is more pronounced when somites from more posterior regions are used than when occipital somites are used. *Hoxb4* may be induced rostrally to its endogenous domain by increasing RA dosage, culturing with more posterior somites or increasing the proximity of more rostral hindbrain tissue to the somitic explants, though this ectopic induction occurs only after a delay relative to endogenous expression. Although capable of replicating the effect of somites, it is clear that RA is not the only factor involved *in vivo*, as the insertion of filters with molecular weight cut-offs between 10 and 200 kDa between somite and hindbrain tissue prevents induction of *Hoxb4*. This points to the involvement of other diffusable factor(s) which may act in concert with the retinoid signal, perhaps potentiating the RARE (see section 1.3.1) to respond to lower, physiological, concentrations of retinoic acid. Indeed, it has been shown that retinoic acid treatment causes the appearance of a DNAse I hypersensitive site 3′ of *Hoxa1*, indicative of a change in chromatin structure (Langston and Gudas, 1992). This site contains not only a RARE, but also another site which binds a novel RA-inducible factor of approximately 170 kDa that appears to have a negative regulatory effect on gene expression (Langston *et al.*, 1997).

1.3.3 Disruption of retinoid levels

Retinoid levels in the embryo may be altered by various means, from dietary supplement to disruption of endogenous enzymes required for their synthesis, and effective signalling levels may be altered by several other means. Experiments of this type began several decades ago with dietary studies demonstrating that either excess or deficiency of vitamin A led to embryological defects (Kalter and Warkany, 1959). More recent studies focusing on effects on the CNS have found the hindbrain to be particularly sensitive.

1.3.3.1 Increased retinoid signalling

The effects of altering embryonic retinoid levels show considerable dose and stage dependency. Application of exogenous retinoic acid to

gastrula/neurula stage embryos results in increasingly severe anterior truncations and/or antero-posterior transformations with increased dosage in *Xenopus* (Durston *et al.*, 1989), zebrafish (Holder and Hill, 1991) and mouse (Morriss-Kay *et al.*, 1991). Likewise, deprivation of retinoids as seen in vitamin A-deficient quail embryos (Maden *et al.*, 1996) leads to anteriorisation/truncation of the caudal hindbrain. Effects on A-P identity suggest a role for endogenous retinoids in its initial specification.

1.3.3.1i *Xenopus*

The CNS of *Xenopus* embryos is sensitive to retinoic acid treatment perhaps to uniquely high degree. While initial reports of RA effects suggested the deletion of much of the anterior CNS and its replacement with caudal hindbrain (Durston *et al.*, 1989; Sive *et al.*, 1990), subsequent studies using reduced concentrations produced less severe results. Even very low concentrations of RA cause the loss of rhombomeres 1-3 and the expansion of r4 and r5 (Papalopulu *et al.*, 1991; Kolm and Sive, 1997). The overexpression of constitutively active retinoic acid receptors reproduces many of these effects (Blumberg *et al.*, 1997). Anterior gene expression is affected by successive RA thresholds (Godsave *et al.*, 1998). Increasing RA concentration leads to activation of further posterior hindbrain markers with concomitant inactivation of anterior ones, until caudal hindbrain markers such as *Hoxb3* and *Hoxb4* reach the front end of the embryo (Godsave *et al.*, 1998).

Hox genes with normal expression boundaries in the hindbrain show a colinear, anterior-to-posterior sequence of concentration dependencies for induction in anteriorised neural explants (Godsave *et al.*, 1998). This is consistent with earlier results observed in embryonic carcinoma cell lines (Simeone *et al.*, 1991). It is noteworthy that RA alone is not capable of inducing *Krox-20* expression in this type of assay, whereas posterior dorsal mesoderm is (Kolm *et al.*, 1997). This highlights the presence *in vivo* of additional factor(s) required to achieve full posterior respecification of anterior neural tissue.

1.3.3.1ii Zebrafish

RA treatment of zebrafish embryos produces a series of morphological and neuroanatomical changes, correlated with alterations in underlying gene expression, which are mainly confined to the caudal-midbrain/rostral-hindbrain region (Holder and Hill, 1991; Hill *et al.*, 1995). High doses of retinoic acid at mid-gastrulation stage give rise to severe disruptions in the anterior CNS. There is a failure of clear differentiation of neurons in the forebrain, midbrain and hindbrain and neither eyes nor otocysts are formed. The trunk, although not entirely normal, remains recognisable.

Lower doses result in disruptions of the area between the otocyst and the eye, the distance between these structures being dramatically reduced. The rostral hindbrain of these embryos is most seriously affected: rhombomeres 1, 2 and 3 fail to form recognisable separate units and show some disruptions in A-P identity, while those adjacent and caudal to the otocyst (4,5, and 6) are clearly formed. *Krox-20* expression is often abnormal, the r3 stripe being reduced to two lateral spots, and occasionally absent altogether. The midbrain-hindbrain border, as assessed by the presence of engrailed protein (Holder and Hill, 1991) and the band of *Pax2* expression, which normally lies just rostral to that of *engrailed* (Hill *et al.*, 1995), appears to be deleted.

The neuranatomy of the rostral hindbrain (anterior to the otocyst) is severely affected, suggesting disruptions of neural crest patterning (Holder and Hill, 1991). Effects on the reticulospinal neurons are particularly informative in terms of A-P patterning (Hill *et al.*, 1995). The Mauthner neuron, normally specific to r4, is duplicated in r2, while other rhombomere-specific neurons such as the vestibulospinal nucleus of r4 and the RoL2 neuron of r2 remain unchanged. This suggests a novel hybrid identity for r2. More severely affected embryos show progressive deletion of rhombomeres 1, 2 and 3 bringing, in extreme cases, the anterior midbrain into juxtaposition with r4 (Hill *et al.*, 1995).

1.3.3.1iii Mouse

Many analogous effects to those observed in zebrafish are also seen in mouse embryos treated with RA. Gastrulation in the mouse begins at around 6.5 dpc, neurulation at approximately 7.5 dpc and somitogenesis around 8.0 dpc. The critical window for retinoid involvement in hindbrain patterning appears to lie between 7.5 and 8.5 dpc. Treatment with exogenous RA during this time results in ectopic anterior induction of 3′ members of the *Hox-B* complex in a stage-specific manner (Conlon and Rossant, 1992; Marshall *et al.*, 1992; Morriss-Kay *et al.*, 1991; Wood *et al.*, 1994). Two main phenotypes have been reported in animals treated around this time. In the more severe phenotype, the hindbrain fails to undergo correct morphological segmentation. Examined on day 9, the pre-otic hindbrain appears to consist of a single large rhombomere, which expresses *Hoxb1* and *Hoxb2* throughout its length and does not express *Krox-20*, suggesting an r4-like identity (Morriss-Kay *et al.*, 1991; Wood *et al.*, 1994). In the less severe phenotype, the hindbrain is properly segmented, but with apparent homeotic transformations of rhombomeres 2/3 into partial 4/5 identity (Wood *et al.*, 1994; Marshall *et al.*, 1992). *Hoxb1* expression resolves into two stripes – in r2 and r4 – and *Hoxb2* is also ectopically expressed in r2. r3 appears to recapitulate the normal r5 *Krox-20* expression dynamics, but does not express other posterior markers such as *Hoxb3*. The underlying neural anatomy is consistent with this. The trigeminal (V^{th}) ganglion which arises in r2 and r3 and exits from r2 appears from its morphology and gene expression profile to assume characteristics of the facial (VII^{th}) ganglion of r4/5 (Marshall *et al.*, 1992).

In animals treated later on embryonic day 8, more posteriorally expressed genes are affected (Conlon and Rossant, 1992). The hindbrain expression domains of *Hoxb1* and *Hoxb2* become refractive to RA-treatment and *Krox-20* expression in r5 is reduced. A more 5′ member of the *Hox* complex, *Hoxb4*, now becomes sensitive, its anterior boundary of expression shifting by one rhombomere from r7 into r6.

1.3.3.2 Decreasing retinoid signalling

The retinoid-deficient quail embryo, in addition to numerous neural crest defects (trunk and cranial) and a dramatic reduction in somite size, shows evidence of a respecification of hindbrain tissue such that rhombomeres 4–7 are lost while rhombomeres 1–3 expand to take their place (Maden *et al.*, 1996; Gale *et al.*, 1999). There are only three rhombomere boundaries and two bulges visible rather than the usual six and five respectively. The r4 band of *Hoxb1* expression fails to appear, as do the r5 *Krox-20* stripe, expression of FGF-3 (normally present in r4-6), and *MafB* (the chick homologue of mouse *kreisler*, normally expressed in rhombomeres 5 and 6). The hindbrain expression of *Hoxb4*, which ordinarily reaches to the r6/7 border, is also absent. Evidence that what remains of the hindbrain are expanded versions of rhombomeres 1-3 comes from the expression of *Hoxa2* which retains its normal pattern relative to them (Maden *et al.*, 1996) and the r3 band of *Krox-20* expression which occupies the posterior third of the altered hindbrain (Gale *et al.*, 1999).

Expression of midbrain/hindbrain boundary markers, *Fgf8* and *Pax2*, are largely unaffected in the retinoid-deficient animals. Interestingly, the phenotype can be rescued by a single injection of all-*trans*-retinol into the albumin layer of the egg as late as the 5 somite stage (though more optimally at the 2-4 somite stage), pointing to this as the critical window for retinoid involvement in the regionalisation of the hindbrain. This indication of the importance of the 5 somite stage in hindbrain development is also supported by the discovery that rhombomeric fate is respecified in the avian embryo when rhombomeres are transplanted caudally at this time (Grapin-Botton *et al.*, 1995; Grapin-Botton *et al.*, 1997; Grapin-Botton *et al.*, 1998; Itasaki *et al.*, 1996).

The endogenous supply of retinoic acid has been disrupted in *Xenopus* by overexpression of XCYP26 (Hollemann *et al.*, 1998) and in the mouse by targeted disruption of *Raldh2* (Niederreither *et al.*, 1999). Both approaches mimic certain effects of RA-deprivation in anteriorising the developing hindbrain, but with some important differences. XCYP26 overexpression was found to rescue RA-induced developmental defects and to selectively

anteriorise aspects of the hindbrain (Hollemann *et al.*, 1998). Depending on the dose, both the r3 and r5 stripes of Krox-20 expression were shifted posteriorally by one or two rhombomeric units. Pax6, normally expressed in r3 and r5, also shifted posteriorally by one rhombomere at the lower dose, but at the higher dose only one stripe (presumed to be r3) remained – in the normal position of r5. Hoxb3, which also marks r5, was similarly affected but both the anterior and posterior boundaries of the hindbrain appeared normal. Intriguingly, the trigeminal (V^{th}) ganglion, rather than simply relocating posteriorally, is duplicated – indicating that not all aspects of A-P identity are affected in the same way as Krox-20 expression.

Raldh2 null mutants do not survive beyond 10.5 dpc and show multiple abnormalities consistent with RA deprivation (Niederreither *et al.*, 1999). The hindbrains of *Raldh2* mutant mice appear to be unsegmented caudally and poorly segmented rostrally (Niederreither *et al.*, 2000). *Krox-20* is expressed in a single broad domain throughout the caudal hindbrain, which lacks a sharp posterior boundary. There is a low level of *Fgf-3* expression throughout this domain and patchy expression of *Hoxb1* is also found, but *kreisler* expression is entirely absent. Similarly, *Hoxa3* and *Hoxb3* (normally expressed up to the r4/5 boundary) are dramatically downregulated while *Hoxa4, b4* and *d4* (normally expressed up to rhombomere 7) are no longer expressed in the hindbrain. Thus it appears that at least some portion of the caudal hindbrain is missing. Rhombomeres 2 and 3 appear to be enlarged, based on the expression of *Meis2, CRABPI* and *Hoxa2,* but the midbrain/hindbrain boundary is not affected. These defects are partially rescued by the addition of sub-teratogenic doses of RA. The effects of the *Raldh-2* mutation are largely analogous to those seen in the retinoid-deficient quail embryo, with the important exception of the persistence of post-r3 markers such as *Hoxb1*. This may indicate differences of regulation of this gene in the mouse or the continued synthesis of RA by an alternative enzyme in the *Raldh-2* mutant animal. Indeed, another enzyme with retinal dehydrogenase activity – class I aldehyde dehydrogenase (ALDH-I) – has been shown to be expressed in many of the same tissues as *Raldh-2* from 7.5 dpc onwards (Ang and Duester, 1997).

1.3.3.2i Retinoic acid receptors

RA acts as a ligand to the retinoic acid receptors (RAR/RXRs). Ligand binding makes them transcriptionally active – providing direct regulation of target genes. One experimental approach to this system has been the use of dominant-negative forms of these receptors in *Xenopus*, another method of reducing retinoid signalling levels. Several such studies have in common the fact that embryos overexpressing the dominant-negative (DN) constructs are protected from the teratogenic effects of exogenous RA (Blumberg *et al.*, 1997; van der Wees *et al.*, 1998; Kolm *et al.*, 1997). This demonstrates that these receptors really are the agents that mediate the effects of retinoic acid and that they efficiently block this signalling. Significant differences arise depending on which member of the receptor family is used – reflecting the complexity of their overlapping expression patterns and functions. Overexpression of a DN version of RARα2.2 completely eliminates expression of HoxD1, whose domain of expression it shares (Kolm *et al.*, 1997). It also leads to a downregulation of *Krox-20* expression in r5, while leaving more anterior markers such as *En-2* and *Otx2* unaffected. This contrasts slightly with another study using a DN version of another RARα isotype – RARα1 (Blumberg *et al.*, 1997). In this case, although *Krox-20* is similarly affected, there is an expansion of the *Otx2* and a posterior shift of the *En-2* expression domains. Electroporation of this construct into early chick embryos (7-10 somite stage) results in a failure to properly induce *Hoxb4* expression in the hindbrain and spinal cord (Gould *et al.*, 1998).

More severe effects on the hindbrain are produced by the use of a DN RARβ construct (van der Wees *et al.*, 1998). This leads to a reduction in hindbrain length and, in more extreme examples, the loss of visible rhombomere boundaries. Supernumerary Mauthner neurons are produced (see section 1.3.3.1ii), appearing in rhombomeres 4, 5 or 6, suggesting partial anteriorisation of these rhombomeres. *Krox-20* expression is considerably disrupted, appearing in an extremely patchy ectopic domain throughout rhombomeres 4, 6, 7, and even 8. Expression of *Hoxb1* in r4, by contrast, remains unaffected, even though it lies right in the middle of these perturbations.

It is clear that functional redundancy exists between the receptor classes. This is most evident in targeted inactivations of the RAR genes in the mouse, where various single null RAR mutants are largely normal but combination of multiple null mutants leads to serious effects which recapitulate aspects of vitamin A deficiency (Lohnes *et al.*, 1994). Disruptions in the post-otic hindbrain are observed in RARα/RARβ double-mutants (Dupé *et al.*, 1999). Double-mutant animals exhibit disorganisation of the post-otic cranial nerves and fusion of the 3rd and 4th branchial arches along with associated arteries and nerves. Rhombomere 5 is expanded, and the morphological boundary between r6 and r7 is absent. Correlated with this are the enlargement of the r5 *Krox-20* stripe and its expansion into r6 territory, as well as posterior expansion of *kreisler* expression and the induction of supernumerary otic vesicles. This suggests a normal role for retinoic acid in restricting the caudal expression limit of these genes. The expression of several *Hox* genes is also affected. *Hoxb1* gains an ectopic, posterior expression domain with an anterior limit at the prospective r6/7 boundary, suggesting that this is normally repressed by retinoic acid. *Hoxb3*, normally specifically upregulated in r5, now shows high expression throughout r5 and r6 and *Hoxd4* expression, normally extending to the r6/7 boundary, now recedes to the caudal-most region of the neural tube. These characteristics are strikingly similar to those of rat embryos carried by vitamin A deficient dams maintained on a minimal dose of all-*trans*-RA required to support pregnancy (White *et al.*, 1998). These animals also present with supernumerary otic vesicles, as well as loss of post-otic pharyngeal arches and cranial nerves IX – XII.

1.4 The rostral hindbrain

As we have seen, retinoids play a key role in the development of the caudal hindbrain, but are less vital to the rostral hindbrain. What is the source of the patterning information which leads to the development of rhombomeres 1–3, even in the absence of more posterior rhombomeres as seen in the retinoid-deficient quail (see above)? The apparent separability of the rostral and caudal portions of the hindbrain as patterning units is further supported by

perturbations which result in the loss of rhombomeres 1–3, but leave more caudal rhombomeres intact. Mutations in genes such as *Gbx2* and *Otx2* affect the rostral hindbrain in just this way (Wassarman *et al.*, 1997; Rhinn *et al.*, 1998; Matsuo *et al.*, 1995). The isthmus, at the junction between the midbrain and hindbrain, is a source of patterning signals which affect this region. Although it is chiefly important for the correct specification of the midbrain and cerebellum (derived from r1), signals from the isthmus may penetrate as far as rhombomere 3 (Wassef and Joyner, 1997; Wingate and Hatten, 1999). FGF8 signalling from the isthmus is thought to repress *Hox* gene expression in rhombomere 1 and may antagonise posteriorising influences such as retinoids (Irving and Mason, 2000). Interfering with genes involved in setting up or maintaining this signalling centre results in deletions of the anterior hindbrain (McMahon *et al.*, 1992; Matsuo *et al.*, 1995; Rhinn *et al.*, 1998; Irving and Mason, 2000). The isthmic organiser itself is thought to be set up in response to signals from mesendoderm and between nascent hindbrain and midbrain (Ang *et al.*, 1994; Wassarman *et al.*, 1997; Millet *et al.*, 1999; Grapin-Botton *et al.*, 1999; Irving and Mason, 2000).

Sources of patterning information such as RA which originate externally to the hindbrain set in motion a series of finer patterning events. *Hox* genes are known targets of retinoid regulation and, once established in the hindbrain, co-ordinate much of its patterning.

1.5 Regulatory relationships

1.5.1 *Hox* genes

Different phases of *Hox* gene regulation exist in which separate enhancers respond to different early and late signals (Gould *et al.*, 1998). The early signals set up more broadly defined initial domains of expression, which are then refined by later interactions. These subsequent interactions proceed in a complex cascade reinforced by overlap of functions and partial redundancy to give a robust patterning process. Auto-, cross- and para-regulatory interactions between members of the *Hox* family are involved in setting up and maintaining their expression domains (Pöpperl *et al.*, 1995; Gould *et al.*, 1997; Studer *et al.*, 1998). To take an example, the regulation of *Hoxb1*

expression in rhombomere 4 has been extensively studied. As discussed above, the involvement of retinoids is critical for its early activation, but there are additional factors involved in its establishment and maintenance. When the RARE involved in the early neurectodermal expression of *Hoxb1* is disrupted in the endogenous locus *in vivo*, early expression is reduced (though not eliminated) and later r4-specific expression is unchanged (Studer *et al.*, 1998). The other agent responsible for this residual induction was found to be the paralogous gene *Hoxa1* (itself upregulated in response to retinoic acid (Dupé *et al.*, 1997) – providing an example of para-regulation (Studer *et al.*, 1998). This overlap between retinoids and *Hoxa1* in the regulation of *Hoxb1* is only partial, as *Hoxa1* has been shown to be absolutely required to specify the correct rostral *Hoxb1* expression boundary (Barrow *et al.*, 2000). The Hoxb1 protein also positively regulates its own expression, binding to its promoter in conjunction with the co-factor pbx1 (a homologue of the *Drosophila* extradenticle protein) and giving rise to sustained high-level expression in r4 (Studer *et al.*, 1998; Pöpperl *et al.*, 1995). Thus, early transcription, induced both directly and indirectly by retinoids and other *Hox* genes, leads to activation of the autoregulatory loop to give strong, r4-specific expression. This is limited to r4 by means such as the availability of co-factors required by *Hoxb1* in its autoregulation (Pöpperl *et al.*, 1995) and through negative regulation by retinoids (Studer *et al.*, 1994).

Interfering with *Hox* gene expression *in vivo* affects segmental identity through multiple disruptions of the regulatory networks (reviewed in Krumlauf, 1994). The loss of *Hoxb1* leads to at least a partial transformation of r4 to an r2 identity (Studer *et al.*, 1996; Goddard, 1996). Conversely, *Hoxb1* misexpression leads to a transformation of r2 towards r4 identity (Bell *et al.*, 1999), analogous to that seen in animals treated with exogenous retinoic acid (see above) (Marshall *et al.*, 1992).

Similar experiments with *Hoxa1*, however, give a more complex set of results. Overexpression of *Hoxa1* (in the mouse) produces similar effects to those observed following *Hoxb1* misexpression (Zhang *et al.*, 1994). These results resemble those seen following treatment with retinoic acid (Marshall *et al.*, 1992), suggesting shared downstream pathways of these paralogues.

Similar studies in zebrafish have confirmed these results (Hill *et al.*, 1995; Alexandre *et al.*, 1996). In these animals, alterations in the pharyngeal skeleton and the duplication of the Mauthner cell, normally specific to r4, in r2 – suggest a posterior transformation of this rhombomere. Both RA treatment and *Hoxa1* overexpression lead to the ectopic accumulation of *Hoxa1* and *Hoxb1* transcripts in the rostral hindbrain (Alexandre *et al.*, 1996), which ectopically activate the *Hoxb1* autoregulatory loop in r2. Thus, ectopic activation of the *Hox1* paralogues leads to similar phenotypes, due to overlap in their abilities to activate downstream targets. The phenotype of the *Hoxa1* null mutant, however, is more severe. In this case, defects in segmentation are observed which interfere with the specification of r5 such that it is drastically reduced (Mark *et al.*, 1993; Dollé *et al.*, 1993) or deleted (Carpenter *et al.*, 1993) and r4 which is also reduced in size. The hindbrain of the null mutant is correspondingly shorter by approximately one rhombomere's length. Some of these effects are partially reproduced in animals where only the *Hoxa1* 3′ RARE has been inactivated (Dupé *et al.*, 1997). The main defects in these animals are a delay in the spreading of *Hoxa1* expression to its correct anterior limit and an overall reduction of its expression levels. That its expression ultimately reaches the correct A-P level points to regulatory compensation by other factors such as *Hoxb1*.

The existence of redundancy and synergistic interactions between the paralogues is revealed when both *Hoxa1* and *b1* are disrupted. *Hoxb1* is the only member expressed in the hindbrain by the stage when segmentation occurs. Earlier, however, both *Hoxa1* and *b1* share a rostral expression limit at the presumptive r3/4 boundary. In the *Hoxb1* single null mutant, r4 is thought to be specified correctly, but then fails to maintain all aspects of its identity, though it does continue to express r4-specific genes such as *EphA2* – its earliest known marker (Becker *et al.*, 1994; Studer *et al.*, 1996; Studer *et al.*, 1998). In the *Hoxa1* single null mutant the r4 territory, though reduced in size, expresses *Hoxb1* (upregulated by retinoic acid) and *EphA2* (Studer *et al.*, 1998). In both cases, one of the paralogues is still expressed in at least part of the r4 territory during part of its development – leading to partial specification. Combining an allele of *Hoxb1* which has its 3′ RARE disrupted with the *Hoxa1*

null mutant leads to a complete absence of both in r4, though other parts of the *Hoxb1* expression domain are unaffected (Studer *et al.*, 1998). There remains a reduced rhombomeric territory in the position of r4, but its identity is uncertain as it fails to express any of the known r4 markers which have been examined, including *EphA2*. *Hoxa1* and *Hoxb1* may therefore be seen to have overlapping functions in the specification of r4. The regulation of *EphA2* by *Hoxa1/b1* has been shown to be direct – through an enhancer element which contains multiple binding sites for these *Hox* genes and their co-factor Pbx1 (Chen, 1998) (also involved in *Hoxb1* auto-regulation Pöpperl *et al.*, 1995).

Cross-regulatory relationships exist between non-paralogous *Hox* genes and are thought to be generally important for the maintenance of overlapping expression patterns. *Hoxb2* expression, for example, is directly upregulated in r4 by *Hoxb1* (Machonochie *et al.*, 1997). *Hoxb3* and *Hoxb4* (neighbours in the complex) share a regulatory element which is activated by multiple group 4–6 *Hox* genes and maintains them up to the r6/7 boundary (Gould *et al.*, 1997). Again, this limit is only affected when both of the paralogues present at this level – *Hoxb4* and *d4* – are removed simultaneously, either one alone being sufficient to induce expression from this enhancer (Gould *et al.*, 1997).

In addition to regulating themselves and each other, *Hox* genes also regulate other genes involved in hindbrain segmentation. *Hoxa2*, for instance, has been shown to be genetically upstream of *EphA7* in rhombomeres 2–4 (Taneja *et al.*, 1996) and *EphA4* in r2 (Gavalas *et al.*, 1997). *Hoxa2* is the most rostrally expressed of the *Hox* genes, having an anterior limit at the r1/2 boundary. It is expressed throughout the remainder of the hindbrain caudally and at high levels in rhombomeres 3 and 5 (Krumlauf, 1993). FGF8 signalling from the isthmic organiser (see section 1.4) is thought to be involved in specifying the anterior expression boundary of this gene (Irving and Mason, 2000), which is the only member of the *Hox* family expressed in r2. In *Hoxa2* null mutant animals the r1/2 and r2/3 boundaries fail to form (Gavalas *et al.*, 1997; Barrow *et al.*, 2000). This presumably results in an abnormal caudal spreading of signals from the isthmus as evinced by an expansion of the *En-2*

domain and cerebellar r1 territory at the expense of r2 and r3 territory (Irving and Mason, 2000; Gavalas *et al.*, 1997). Neural differentiation is also altered in the r2–r3 region such that it resembles the normal r1 pattern (Davenne *et al.*, 1999) and duplications of first branchial arch structures are seen in the second arch (Rijli *et al.*, 1993). *EphA4* expression is eliminated in r2 (Gavalas *et al.*, 1997) and expression of *EphA7* is lost in r3 and altered in r2 and r4 (Taneja *et al.*, 1996). Other downstream effectors of *Hoxb1* in r4 include the transcription factors GATA2 and GATA3 (Pata *et al.*, 1999). The altered migratory behaviour of r4 motor neurons in GATA3 mutants is similar to that in *Hoxb1* mutants and both GATA2 and 3 are ectopically induced in response to *Hoxb1* misexpression and abolished in *Hoxb1* mutants (Pata *et al.*, 1999; Studer *et al.*, 1996).

When *Hoxa2* and *Hoxa1* null mutations are combined, the hindbrain segmentation defects are compounded. The hindbrains of double-null mutant animals are completely smooth – lacking any visible rhombomere boundaries (Barrow *et al.*, 2000). Some of the effects are additive – the failure of r5 differentiation in *Hoxa1* mutants means a corresponding failure of boundary formation between r4 and r6, now juxtaposed (Carpenter *et al.*, 1993), and in *Hoxa2* single null mutants there are problems with r1/2 and r2/3 boundary formation (Barrow *et al.*, 2000; Gavalas *et al.*, 1997). The additional loss of the r3/4 boundary in double mutants indicates synergistic effects between these genes in boundary formation.

Disruption of the *Hoxa2* paralogue, *Hoxb2*, on its own does not appear to affect boundary formation, but when combined with the *Hoxa2* null mutant, it exacerbates the effects seen therein (Davenne *et al.*, 1999). In this case, no boundaries are visible between rhombomeres 1–4, though the sharp segmentally-restricted domain of *Krox-20* and *EphA4* in r3 is still evident (Davenne *et al.*, 1999). This highlights a disparity between these paralogues in their ability to functionally compensate for one another. It also suggests that possible misregulation of *Hoxb2* in the *Hoxa1/a2* mutant could be involved in the failure of r3/4 boundary formation. *Hoxa2* and *Hoxb2* also have distinct non-overlapping roles in the differentiation of neurons along both the A-P and D-V axes which reflect their expression patterns (Davenne *et al.*, 1999).

Hoxb2 is known to be downstream of *Hoxb1* in r4 (Machonochie *et al.*, 1997) and mutants of both genes are similarly affected (Barrow and Capecchi, 1996), identifying *Hoxb2* along with GATA2/3 (see above) as important members of the *Hoxb1* signalling pathway. Whether they are members of the same or parallel pathways has not been determined – it would be interesting to know how GATA2/3 expression is affected in the *Hoxb2* mutant.

One method of studying global regulation of *Hox* genes in a given segment is to alter its environment by surgical transposition to another axial level – a manipulation particularly suited to the avian embryo. This type of experiment has further highlighted the role of signals from the paraxial mesoderm and within the plane of the neural epithelium in regulating *Hox* gene expression (Grapin-Botton *et al.*, 1995; Itasaki *et al.*, 1996; Grapin-Botton *et al.*, 1997). They have also shown that the fate of particular rhombomeres can retain plasticity in response to these signals even after the appearance of rhombomere boundaries (Grapin-Botton *et al.*, 1995). This is, however, conditional on factors such as the axial level and size of the transplant and its direction along the A-P axis as segments transposed rostrally retain their *Hox* gene expression profiles and *vice versa* (Guthrie *et al.*, 1992; Grapin-Botton *et al.*, 1995; Itasaki *et al.*, 1996; Grapin-Botton *et al.*, 1997). This effect has been interpreted as demonstrating an increasing gradient of signal from anterior to posterior to which the segments are responding.

1.5.2 *Krox-20*

Krox-20 is an early marker of r3/5 identity, its onset of expression occurring on day 8, prior to the appearance of morphological boundaries (Wilkinson *et al.*, 1989b; Schneider-Maunoury *et al.*, 1993). As previously indicated, rhombomeres 3 and 5 initially form correctly in *Krox-20* mutants, but subsequently disappear (Schneider-Maunoury *et al.*, 1993; Swiatek and Gridley, 1993). The hindbrain of these mutants is smooth in morphology and was initially thought to be unsegmented from r2-r6 (Schneider-Maunoury *et al.*, 1993). More careful analysis has revealed the presence of boundaries between r2/4 and r4/6, following the loss of r3/5 (Schneider-Maunoury *et al.*, 1997).

In addition to its role in directly activating *Hoxb2* in r3/5 (Sham *et al.*, 1993) (see above), *Krox-20* also regulates its paralogue, *Hoxa2*, in these rhombomeres (Nonchev *et al.*, 1996), though the r5 domain is also lost in the *Hoxa1* 3′ RARE mutant (Dupé *et al.*, 1997). It is also important to point out that, although *Krox-20* specifically upregulates these genes in r5, low-level expression persists in r5 (prior to the loss of the rhombomere) even in *Krox-20* mutants (Schneider-Maunoury *et al.*, 1993; Nonchev *et al.*, 1996). This expression demonstrates activation independent of *Krox-20*, as in more posterior regions. Similar effects have been noted on *Hoxb3* expression in r5 (Seitanidou *et al.*, 1997), though it is not yet known whether this relationship is direct. *CRABPI* expression is also maintained in r5 of *Krox-20* mutants, indicating that some aspects of r5 identity are retained (Seitanidou *et al.*, 1997).

The specific upregulation of *EphA4* in rhombomeres 3 and 5 is dependent on *Krox-20* and this activation has been shown to be direct (Seitanidou *et al.*, 1997; Theil *et al.*, 1998). Again, the early broad expression domain of this gene, which includes presumptive r3 and precedes *Krox-20* expression, is unaffected in the *Krox-20* mutant, demonstrating early involvement of other regulatory factors (Seitanidou *et al.*, 1997). *Krox-20* is also required for the specific downregulation of *follistatin* in r3 (Seitanidou *et al.*, 1997). Thus, its role extends well beyond the regulation of *Hox* genes to members of multiple gene families, highlighting the importance of *Krox-20* in patterning this region.

How is *Krox-20* itself regulated? Signals downstream of *Hoxa1* and *b1* in r4 have been proposed to have a role *Krox-20* induction in r3 (Barrow *et al.*, 2000). Capecchi and colleagues suggest, based on their observations of expression domains related to morphological markers, that in the double mutant *Krox-20* is not expressed at the normal A-P level of r3, but rather in r4, where it would normally be repressed by the *Hox1* paralogues (Rossel and Capecchi, 1999; Barrow *et al.*, 2000). The findings that, in *Hoxa1* null mutants, r3 *Krox-20* expression is patchy, that the non-expressing patches present an r2-like molecular identity and the area of these patches increases when only one functional copy of *Krox-20* is present (Helmbacher *et al.*, 1998) are not

inconsistent with this interpretation and support a role for *Hoxa1* in *Krox-20* induction. Rhombomere grafting experiments have shown that r3 *Krox-20* expression is not maintained in the absence of r4 (Graham and Lumsden, 1996). *Krox-20* expression was rapidly downregulated either when r3 was grafted into the normal position of r4 or when isolated in explant culture (Graham and Lumsden, 1996). When contact between rhombomeres 3 and 4 was preserved in explant culture, however, *Krox-20* expression was maintained in r3. This study also revealed an important difference between *Krox-20* regulation in rhombomeres 3 and 5. Whether grafted into the position of r4 or cultured in isolation, *Krox-20* expression was maintained in r5. Thus r5 does not require signals from its neighbours to maintain *Krox-20* expression (Graham and Lumsden, 1996).

Further clues have come from single-rhombomere transplantations in which it was shown that r6 is also capable of upregulating *Krox-20* when it is grafted either into the position of r5 or more caudally (Marín and Charnay, 2000). This upregulation occurred whether the graft was in contact with the neural plate or when it was placed more laterally in the adjacent mesoderm. Rhombomere 7, grafted into the same positions, did not express *Krox-20*. *Krox-20* was also induced in r6 when the embryo was severed at the r6/7 boundary but only providing the first pair of somites were also removed, as either their retention or the retention of neural tube to the r7/8 boundary abrogated this effect (Marín and Charnay, 2000). r5 *Krox-20* expression was downregulated following grafting to the position of r6 or r7. Together, these results suggest that signals from more caudal regions are important for repressing *Krox-20* expression in r6 and that, similar to r5 in the experiments of Graham *et al.*, this rhombomere may have an intrinsic ability to express *Krox-20*.

Interestingly, overexpression of *Hoxb2* in the zebrafish embryo leads to ectopic expression of *Krox-20* in the rostral hindbrain, whereas overexpression of *Krox-20* does not induce ectopic *Hoxb2* (Yan *et al.*, 1998). In the mouse, *Hoxb2* is known to be downstream of *Hoxb1* in r4 (Machonochie *et al.*, 1997) and directly activated by *Krox20* in r3 and r5 (Sham *et al.*, 1993; Vesque *et al.*, 1996). It is possible that *Hoxb2* is part of the *Hoxb1* signalling

pathway that leads to the induction of *Krox-20* in r3. The failure of *Krox-20* to induce ectopic *Hoxb2* expression in the zebrafish experiment may reflect the requirement for a co-factor acting in concert with *Krox-20*, which is not present outside of its usual domain (Vesque *et al.*, 1996).

Recent work on Nab protein inhibitors of *Krox-20* has shown that they are involved in a negative-feedback loop with *Krox-20* in the hindbrain (Mechta-Grigoriou *et al.*, 2000). Misexpression of these proteins not only affects known targets of *Krox-20* regulation such as *EphA4*, but also the expression of *Krox-20* itself, supporting the hypothesis that it is required for its own maintenance (Mechta-Grigoriou *et al.*, 2000; Schneider-Maunoury *et al.*, 1993).

1.5.3 *kreisler*

Like *Krox-20*, *kreisler* has been shown to be a regulator of *Hox* genes. Both *Hoxb3* in r5 and its paralogue, *Hoxa3* in r5 and r6, are directly upregulated by *kreisler* (Manzanares *et al.*, 1997; Manzanares *et al.*, 1999a). Also like *Krox-20*, hindbrain segmentation is disrupted in *kreisler* mutants with the loss of at least r5 (there are conflicting interpretations regarding the fate of r6) (Frohman *et al.*, 1993; McKay *et al.*, 1994; Cordes and Barsh, 1994; Manzanares *et al.*, 1999b). *kreisler* appears to act before *Krox-20* in the specification of r5 as no trace of the r5 domain of *Krox-20* expression is ever observed in mutant animals (McKay *et al.*, 1994; Frohman *et al.*, 1993). Thus, *kreisler* is genetically upstream of *Krox-20* in r5 and the expression of other genes downstream of *Krox-20* such as *Hoxa2* and *Hoxb2* (see above) is also lost. Surprisingly, several molecular changes in rhombomere 3 are also noted in *kr* mutants. The longer perdurance of *Krox-20* expression and weak ectopic activation of *Fgf-3* and *Hoxb-3* (Frohman *et al.*, 1993) are all suggestive of a partial transformation of r3 towards r5 identity, though no mechanism has been proposed to account for this. This effect is also observed with reporter gene expression driven by the r5/6 enhancer of *Hoxa3*, both in *kr* heterozygous and homozygous mutants (Manzanares *et al.*, 1999b). This is particularly intriguing as heterozygotes had previously been thought of as effectively wild-type and reveals a dose-dependency of r3 on *kreisler*. The effects on *Hox* gene expression naturally lead to corresponding defects in neural crest-derived

structures and neural architecture (Frohman *et al.*, 1993; McKay *et al.*, 1994). Interpretation of the phenotype is, however, complicated by the retention of certain aspects of r5 neural architecture (though these may be specified prior to the requirement for *kr* input) (McKay *et al.*, 1997) and the loss of certain genes normally expressed in r6 such as *Fgf-3*, *Hoxa3* and *CRABPI* (Frohman *et al.*, 1993; McKay *et al.*, 1994). These results have led some to argue that r6 is also lost in the *kreisler* mutant.

Analysis of the zebrafish homologue of *kreisler*, *valentino* (*val*) (Moens *et al.*, 1998), has revealed many similarities, but also some important differences between the two systems (Moens *et al.*, 1996; Prince *et al.*, 1998). As in *kreisler* mutants, the hindbrains of *val* mutant embryos are reduced by the length of one rhombomere and appear unsegmented posterior to rhombomere 3 (Moens *et al.*, 1996). Some aspects of neural architecture specific to r5 and r6 are retained, while others are lost and some neural crest-derivatives and *Hox* gene expression patterns are altered in a manner analogous to that seen in the mouse system (Moens *et al.*, 1996; Moens *et al.*, 1998; Prince *et al.*, 1998). In mosaic analyses which test the ability of *val* mutant cells to contribute to wild-type embryos, however, it was shown that they are specifically excluded from both r5 and r6, suggesting that *val*$^-$ cells are unable to assume the mature characteristics of either rhombomere (Moens *et al.*, 1996). In the converse experiment, wild-type cells which come to lie in the r5/6 region of *val* mutant embryos do not mix freely with the surrounding *val*$^-$ cells, although those in the rostral half express *Krox-20* in response to upstream signals (Moens *et al.*, 1996). These results led to the suggestion that *valentino* is autonomously required for the sub-division of a 'proto-rhombomere' which normally gives rise to rhombomeres 5 and 6 (Moens *et al.*, 1996). In *val* mutants this proto-rhombomere is proposed to continue an anachronistic existence as the immature precursor of r5/6, displaying some characteristics of both while being unable to assume the mature character of either (Moens *et al.*, 1996; Moens *et al.*, 1998; Prince *et al.*, 1998). Another important difference between *kreisler* and *valentino* is that *val* is not required for the initial upregulation of *Krox-20* in r5 (Moens *et al.*, 1996). Although *Krox-20* expression is first seen at the 1-somite stage, mutant

embryos are indistinguishable (based on *Krox-20* expression) from wild-type until after the 2–3 somite stage (Moens *et al.*, 1996). This suggests a difference in the regulatory relationship of these genes between the mouse and fish systems.

Relatively little is known about how *kreisler* itself is regulated. In zebrafish with a point mutation in *valentino* which inactivates the protein without affecting its regulation, transcripts are initially detected in the r5/6 region, but subsequently lost – demonstrating a requirement for *val* in the maintenance of its own expression (Moens *et al.*, 1998). Some clues have come from rhombomere transplantation experiments. In the same series of experiments in which they examined *Krox-20* regulation in rhombomeres 5 and 6, Marín and Charnay also looked at *kreisler* regulation (see above) (Marín and Charnay, 2000). They found that, similar to *Krox-20* in r6, *kreisler* could be upregulated in r7 in response to grafting to more anterior regions, while r8 was refractory to this transformation. Some important differences were also uncovered. Severing the embryo at the r7/8 boundary did not lead to upregulation of *kr* in r7 although severing at the r5/6 boundary led to its downregulation in r6. When the embryo posterior to r7 was replaced by an inverted r3–r5 region, however, *kreisler* was upregulated in r7. These results suggest that influences from the rostral hindbrain may be important for the normal activation of *kreisler* in r5/6. The finding that *kreisler* is down-regulated in r5/6 in response to grafting into the region of r7/8 is consistent with this interpretation (Grapin-Botton *et al.*, 1998), although this also entails an increase in the strength of posteriorising signals. In agreement with this is the finding that this effect can be reproduced by grafting posterior somites laterally to r5/6 (Grapin-Botton *et al.*, 1998). It was also demonstrated that *kr* can be activated in r4 when confronted with posterior somites and that this is reproduced when retinoic acid-soaked beads are placed laterally to r4. Furthermore, increasing the RA concentration leads to more anterior induction of *kr*, ultimately reaching r1 (Grapin-Botton *et al.*, 1998). These results indicate that a posteriorising influence from caudal tissues has a critical role in normal *kreisler* induction.

1.5.4 Eph/ephrins

Known regulatory relationships involving the *Eph*s have been mentioned in the context of the regulatory agents and are summarised here. *EphA2* is directly regulated by *Hoxa1/b1* in r4 (Chen, 1998; Studer *et al.*, 1998). *Hoxa2* is upstream of *EphA7* in rhombomeres 2, 3 and 4 (Taneja *et al.*, 1996) and *EphA4* in r2 (Gavalas *et al.*, 1997). *EphA4* is also known to be regulated directly by *Krox-20* in rhombomeres 3 and 5 (Seitanidou *et al.*, 1997; Theil *et al.*, 1998). The joint regulation of both a member of the Eph family and *Hox* genes (see section 1.2.4) is particularly interesting as it represents a coupling of the mechanical segmentation process with A-P identity. Overall, very little is known about the regulation of the *Eph*s and even less about *ephrin*s. The importance of the role of Eph/ephrins in hindbrain segmentation makes their position within the regulatory networks outlined in this Introduction of considerable interest.

Chapter 2 – Materials and methods

2.1 Bacterial media and strains and bacteriophage types

Luria-Bertani (LB) broth (1% bacto-tryptone, 0.5% yeast extract, 1% NaCl) and LB agar (1.5% supplemented with 50μg/ml ampicillin) were used routinely in the propagation of DH5α*E. coli* carrying plasmid vectors. NZCYM broth, 1.5% agar and top-agarose (0.8%) were used to maintain *E. coli* strains containing bacteriophage vectors. Long-term storage of bacterial strains was at -70°C in LB broth with 15% glycerol.

E. coli genotypes:

DH5α *supE44* Δ*lac* U169(ϕ80 *lacZ*ΔM15) *hsdR*17 *recA*1 *endA*1 *gyrA*96 *thi*-1 *relA*1 (Hanahan, 1983)

DH10B F′-*mcr*A Δ(*mrr-hsd*RMS-*mcr*BC) ϕ80d*lacZ*ΔM15 Δ*lac*X74 *deo*R *rec*A1 *end*A1 *ara*D139 Δ(*ara, leu*)7697 *gal*U *gal*K λ^- *rps*L *nup*G

LE392 F^- $e14^-$ ($mcrA^-$) *hsdR514* (r_K- m_K+) *supE44 supF58 lacY1 or Δ(lacIZY)6 galK2 galT22 metB1 trpR55* (Sambrook *et al.*, 1989)

Bacteriophage types:

λFIXII λ*sbh*Iλ1° *b*189 {T7 promoter – polycloning site *sr*Iλ3° *nin*L44*bio* polycloning site - T3 promoter} KH54 *chi*C *sr*Iλ4° *nin*5 *shn*dIIIλ6° *sr*Iλ5° (Stratagene Cloning Systems)

Bacteriophage stocks were diluted in SM buffer (50mM Tris.Cl (pH 7.5), 100mM $MgSO_4.7H_2O$) and stored in the same solution at 4°C following the addition of one drop of chloroform.

2.2 Production and transformation of competent cells

2.2.1 Tfb protocol

A single colony of DH5α cells was used to inoculate 10ml L. broth and cultured overnight on a gyratory shaker (set to 250rpm) at 37°C. The 10ml culture was then sub-cultured into 200ml of fresh medium, prewarmed to 37°C and grown until the OD_{550} was between 0.45 and 0.5. The culture was chilled on ice for 5 min. and the cells were pelleted by centrifugation at 2500rpm for 10 min. at 4°C in a Sorvall GS-3 rotor. The supernatant was discarded and the pellet was resuspended in 40ml of TfbI (30mM KOAc, 100mM RbCl, 10mM $CaCl_2.2H_2O$, 50mM $MnCl_2.4H_2O$, 15% glycerol, pH adjusted to 5.8 with 0.2M acetic acid, filter sterilised and stored at 4°C). The cells were placed on ice for 5 min. before further centrifugation at 2000rpm for 10 min. at 4°C in a Sorvall HS4 rotor. The cells were resuspended in 8ml of TfbII (10mMOPS, 75mM $CaCl_2.2H_2O$, 10mM RbCl, 15% glycerol, pH adjusted to 6.5 with KOH, filter sterilised and stored at 4°C) and stored on ice for 15 min. before separating into 200μl aliquots in 1.5ml microfuge tubes and snap-freezing on dry ice. The tubes were stored at -70°C.

2.2.2 Heat-shock transformation of competent cells

The cells were thawed on ice and 50μl dispensed into a prechilled 1.5ml microfuge tube. 1-5μl of DNA solution was added and mixed gently with the pipette tip. The mixture was incubated on ice for 20 min. before a 5 min. heat shock at 37°C. 200ml of L. broth was added and the cells were incubated for a further 20 min. at 37°C before being plated out onto selective agar. The plates of bacteria were incubated at 37°C for 12-16 hours. If required, "blue/white" selection (testing for α-complementation) was performed according to Sambrook *et al.* (1989).

2.3 Nucleic acid handling

2.3.1 Small scale isolation of plasmid DNA

Small scale preparation of plasmid DNA was performed according to the alkaline lysis 'mini-prep' method (Sambrook *et al.*, 1989).

2.3.2 Large scale isolation of plasmid DNA

Large scale isolation of plasmid DNA was performed using either the Wizard™ *Plus* Maxipreps DNA Purification System from Promega or the alkaline lysis method (Sambrook *et al.*, 1989).

2.3.3 Preparation of phage DNA

2.3.3.1 Preparation of LE392 cells

A single colony of LE392 cells was cultured overnight on a gyratory shaker (set to 250rpm) in 50ml LB, supplemented with 0.2% maltose and 10mM $MgSO_4$. The cells were pelleted by centrifugation at 3000rpm for 10 min. at 4°C in a Sorvall GS-3 rotor. The supernatant was discarded and the cells resuspended in 15ml of ice-cold 10mM $MgSO_4$.

2.3.3.2 Liquid culture of bacteriophage

For liquid culture, a bacteria to phage ration of 1000:1 is required. The bacterial OD_{600}=1 for approximately 8 x 10^8 cells/ml. A rough estimate is that a phage plaque contains 10^6 plaque forming units (pfu).

Approximately 2 x 10^5 pfu were added to 200µl 10mM $MgSO_4$ containing approximately 2 x 10^8 bacteria, mixing gently with the pipette tip. The mixture was incubated at 37°C with gentle shaking for 20 min. This was then added to 500ml of LB (0.2% maltose, 10mM $MgSO_4$) and cultured overnight at 37°C with shaking (250rpm).

2.3.3.3 Isolation of phage DNA

After checking for lysis, 10ml of chloroform was added to the liquid culture. 50µl each of DNAseI and RNAseA (10mg/ml) and 29g of NaCl were added and the mixture incubated with vigorous shaking (>300rpm) at 37°C for 30 min. The contents were allowed to settle before pouring into two 500ml Nalgene centrifuge bottles leaving the chloroform behind. The bottles were centrifuged at 8000rpm in a Sorvall GS-3 rotor for 10 min. at 4°C. The supernatant was transferred into fresh bottles and 25g of solid PEG8000 was dissolved into each. The mixture was then chilled to 4°C for at least one hour. This was centrifuged at 8000rpm for 20 min. to recover the phage. The supernatant was discarded, the pellet resuspended in 3ml of SM buffer and

transferred to a 30ml Corex tube. 1.5μl of DNAse and 30μl of RNAse were added and the mixture incubated at 37°C for 30 min. 150μl of 10% SDS, 120μl of 0.5M EDTA (pH 8.0) and 30μl of 10mg/ml proteinase K were added and incubated at 68°C for 30 min. This was extracted, with equal volumes, first of phenol, then 1:1 phenol/chloroform, and finally chloroform, before adding 1.5ml of 5M NH_4OAc, 6ml ethanol and chilling on ice for 15 min. The tube was centrifuged at 9250rpm in a Sorvall SS34 rotor at 4°C for 20 min., the supernatant discarded, the pellet air-dried and redissolved in 1.6ml H_2O. 400μl of 4M NaCl and 2ml of 13% PEG8000 were added and the mixture chilled on ice for 1 hour to overnight. Following centrifugation at 9250rpm for 20 min. at 4°C, the supernatant was discarded, the pellet rinsed with 70% ethanol, air-dried and resuspended in 200-500μl dH_2O.

2.3.4 Extraction and precipitation of DNA and RNA

Extraction of DNA or RNA with phenol/chloroform was routinely used to remove contaminating proteins. An equal volume of either Tris.Cl (pH7.5) equilibrated (for DNA) or DEPC H_2O saturated (for RNA) phenol and chloroform (1:1) was added, mixed vigorously and then the phases separated by centrifugation at 12000g for 2 min. The upper (aqueous) phase was then removed and the DNA or RNA recovered by precipitation with ethanol. To one volume of DNA, $^1/_{10}$ volume of 3M NaOAc (pH 4.9) and 2.5 volumes of ethanol were added. Following incubation either on dry ice for 15 min. or at -20°C from $^1/_2$ hour to overnight, the sample was centrifuged at 12000g for 20 min. at 4°C. The nucleic acid pellet was then washed with 70% ethanol and air-dried prior to resuspension.

2.3.5 Quantitation of nucleic acid concentrations

Rough estimates of nucleic acid concentration were made by comparison of sample material with a standard on an agarose gel. More accurate determinations were made by spectrophotometric scanning at the wavelength of 260nm. An A_{260} value of 1 represents an approximate concentration of 50μg/ml for double-stranded DNA, 40μg/ml for single-stranded RNA and 33μg/ml for oligonucleotides.

2.3.6 Restriction enzyme digestion of DNA

Restriction digests were carried out according to the specifications of the manufacturer of the particular restriction endonuclease (Boehringer Mannheim or New England Biolabs). Sample DNA was diluted in sterile distilled water (SDW) and restriction endonuclease was always added in at least a two-fold excess of the 1U/μg recommended by Sambrook *et al.* (1989).

2.3.7 Electrophoretic separation of DNA

Following restriction endonuclease digestion, DNA samples were separated using agarose gel electrophoresis and TAE buffer (40mM Tris.acetate (pH 7.0), 1mM EDTA). The concentration of agarose used depended on the size of the fragments that were to be separated, but generally 1% gels were used unless indicated otherwise. DNA samples were loaded with one tenth volume of 0.1% Orange G and 50% glycerol into the wells. Ethidium bromide-stained DNA bands were visually detected with ultraviolet light and subsequently photographed. In order to purify DNA fragments from agarose gels, the QIAEX II Gel Extraction Kit (500) from QIAGEN was used according to the manufacturer's instructions. An alternative method employed was to pierce a small hole in the bottom of a 0.5ml eppendorf tube, place first a small quantity of glass wool and then the excised gel fragment inside and to place the entire construct in a 1.5ml eppendorf tube. This was then spun at 6000rpm for 10 min. to elute the buffer containing the DNA from the gel fragment. The DNA was precipitated and resuspended in an appropriate volume of sterile distilled water.

2.3.8 Blunt-ending, phosphatasing and ligation of DNA fragments

If fragments were to be ligated which had been digested with different restriction enzymes, the single-stranded overhangs were eliminated using one of two methods. To end-fill the overhang, the Klenow fragment of DNA polymerase was used as follows: 0.1U of Klenow per μl in a solution of 10mM Tris (pH 7.4), 5mM $MgCl_2$ and 1mM of each of the four dNTPs, which was incubated at 37°C for 15 min. The DNA was then extracted and precipitated.

To remove the overhang, mung bean nuclease was used to digest the single-stranded DNA. 10mM $ZnCl_2$ was added to the restriction digest to a final concentration of 1.5mM and mung bean nuclease to a final concentration of $0.1U\mu l^{-1}$. Sufficient sterile distilled water was added to keep the concentration of glycerol in the reaction to 10% or less. The reaction was incubated at 30°C for 30 minutes, and then gel-purified. Blunt-ended vector molecules (or those which had only been cut with a single restriction endonuclease) were treated with calf intestinal alkaline phosphatase from Boehringer Mannheim according to the manufacturer's instructions to inhibit intramolecular ligation of vector without insert. Vector and insert fragments were mixed in a molar ratio of 1:3 and ligations were either carried out at 16°C overnight in 10μl reactions using T4 DNA ligase (100 ligation units for cohesive reactions) containing one tenth volume of 10x ligase buffer (200mM Tris.Cl (pH7.6), 100mM $MgCl_2$, 100mM dithiothreitol, 1mM ATP) or using Ready-To-Go™ T4 DNA Ligase from Pharmacia according to the manufacturer's instructions.

2.3.9 Double stranded DNA sequencing

Double stranded plasmid DNA was sequenced (Sanger dideoxy chain termination method) using a Pharmacia ^{T7}Sequencing kit according to the manufacturer's instructions. Glass sequencing plates were washed with detergent, rinsed well with tap water and finally with dH_2O. They were then rinsed with 70% ethanol and left to air-dry before a final rub with chloroform. The surface of one plate was treated with dimethyldichlorosilane solution (BDH #33164) to prevent the gel sticking tightly to both plates. Plastic spacers (0.4mm) positioned along the sides separated the two plates which were clamped together using bulldog clips and the plates were placed horizontally over a suitable object. The polyacrylamide gel was prepared by mixing 100ml of 5% acrylamide/urea solution (SEQUAGEL™ Sequencing System from National Diagnostics) with 800μl of 10% ammonium persulphate solution and 40μl of TEMED. The mixture was immediately drawn into a 50ml syringe and slowly injected between the horizontal glass plates, allowing capillary action two draw the solution through, assisted by tilting the plates as necessary. The flat side of a shark's tooth comb was then inserted

approximately 0.5cm into the solution and the gel allowed to polymerise overnight. Electrophoresis was carried out at a constant voltage of 25kV. The gel was then fixed with 10% methanol/10% acetic acid for 30 min. before transferring onto a sheet of Whatman 3MM paper and drying under a vacuum, using a Bio-Rad slab gel drier, for 1-2 hours. The labelled DNA fragments were visualised by autoradiography using Kodak X-OMAT AR film.

2.3.10 Southern blotting

DNA to be blotted was separated by agarose gel electrophoresis. The gel was photographed alongside a ruler to allow the calculation of fragment sizes from the autoradiograph. The gel was soaked twice for 30 min. in denaturing solution (0.5M NaOH, 1.5M NaCl) and once, for at least 10 min. in neutralising solution (0.5M Trizma base, 1.5M NaCl, pH 7.5). Blotting onto Hybond-N nylon membranes (Amersham) was performed by capillary transfer. A pre-wet wick of Whatman 3MM paper (three layers) was laid on a raised platform over a reservoir of 20xSSC (3M NaCl, 0.3M Tri-sodium citrate pH 7.0). The membrane, soaked with 20xSSC, was laid on top of this, followed by three sheets of 3MM paper (also saturated with 20xSSC) and then a stack of paper towel. This was then weighted down to aid the transfer. Following overnight transfer of DNA onto the filter, DNA was crosslinked to the filter using a UV Stratalinker™ 1800 (Stratagene) ultraviolet crosslinker (energy setting of 1200).

2.4 Lambda bacteriophage library plating and lifts

Prior to plating the Mouse 129SV Genomic Library (Stratagene) in the Lambda FIX™ II vector, the titre was calculated. Plating cells were prepared by seeding 50ml NZCYM, 0.2% maltose broth with 100μl of an appropriate starter culture. Following overnight incubation at 37°C, the cells were ready for use. 650μl of plating cells were mixed with an appropriate amount of λ stock in a 10ml tube. The cells were left at 37°C for 15 min. to allow preadsorption of λ particles and then 8ml NZCYM top agarose at 42°C was added to each tube, quickly mixed by inversion of the tube and poured onto

the surface of a prewarmed NZCYM plate (55°C) with swirling of the plate to ensure even coverage. The top agarose was allowed to set, and then the plates inverted and incubated at 37°C overnight. The following morning plaques of dead cells caused by λ infection were seen in a bacterial lawn. The titre of the library was calculated as plaque forming units (pfu) per unit of volume and then the library was plated at 1 x 10^5 pfu per 137mm plate. To ensure complete representation of the library, 1 x 10^6 pfu in total were plated. Two replicas of each plate to be screened by hybridisation were taken by overlaying Colony/Plaque Screen™ hybridisation transfer membranes (DuPont NEN® Research Products) onto the plate and punching orientation marks through the filters and into the agar (the first filter was laid on the plate for 30 seconds, the second for 60 seconds). Filters were removed from the plate and then laid in a 2ml pool of denaturing solution (see Southern blotting) on a sheet of Saran wrap for 5 min., dried briefly on 3MM paper, and then in a similar pool of neutralising solution for 5 min. Following a further 5 min. rinse in neutralising solution, the filters were washed with 5xSSC for 5 min. and then dried between two sheets of 3MM paper. DNA was crosslinked to the filters using a UV cross-linker followed by baking at 80°C for two hours as previously described (see Southern blotting – section 2.3.10).

2.5 Radioactive labelling of DNA

2.5.1 Double-stranded probes

Fragments to be used as templates were excised from 1% agarose gels as previously described (see Electrophoretic separation of DNA). This was then labelled using the Megaprime DNA Labelling System (Amersham) according to the manufacturer's instructions. The labelling reaction was purified by gel exclusion chromatography through Sephadex G-50 (Pharmacia) equilibrated with TE (10mM Tris.Cl (pH 8.0), 1mM EDTA (pH 8.0), autoclaved). The specific activity of the probes was determined by scintillation counting (Beckman LS600IC).

2.5.2 End-labelling of oligonucleotide primers

Single-stranded oligonucleotides were labelled by the addition of ^{32}P to the 5′ end by T4 DNA polynucleotide kinase. 150ng of the oligonucleotide primer was mixed with 2μl of kinase buffer (100mM Tris.Cl pH 7.6, 100mM $MgCl_2$, 50mM DTT, 1mM spermidine HCl), 50μCi [γ-^{32}P] ATP and 10U of T4 polynucleotide kinase. Following incubation at 37°C for 1 hour, the probe was purified by gel exclusion chromatography through Sephadex G-25 (Pharmacia) equilibrated with TE. Specific activity of the probe was determined by scintillation counting (Beckman LS600IC).

2.6 Hybridisation of filters

2.6.1 Southerns and library screens

Filters were hybridised according to the manufacturers' instructions (Colony/Plaque Screen™ from DuPont for library, Hybond-N from Amersham for Southerns). Aqueous hybridisation buffer (10% Dextran Sulphate, Na salt (MW ~ 500 000), 1% SDS, 1M NaCl) was used in both cases. Filters were incubated in Techne hybridisation bottles or plastic petri dishes at either 42°C (when labelled oligonucleotide primers were used) or 65°C (when double-stranded oligonucleotide primed probes were used). Following hybridisation and washing, the filters were wrapped in clingfilm and exposed to X-ray film (Kodak). Intensifying screens were used at -70°C when required. Exposed film was developed in an automatic developing machine (Kodak).

2.7 Production of transgenic mice

Fragments to be tested for enhancer activity were subcloned into the lacZ expression vector pGZ40, which contains the lacZ ORF flanked by a β-globin minimal promoter. Fragments were inserted 5′ to this minimal promoter which would then be driven by any tissue-specific enhancer elements therein. Throughout these experiments, (CBA x C57Bl10)F_1 mice were used as embryo donors and pseudopregnant females. All techniques performed on animals

were licensed under the Animals (Scientific Procedures) Act 1986, license no. PPL 70/4124.

2.7.1 Transgenic media

The most commonly used embryo culture media is M16, which is very similar to Whitten's medium and is bicarbonate-buffered. This medium was incubated at 37°C in 5% CO_2, 95% air during use. Embryos were collected and stored in the incubator in this solution. For microinjection, when the embryos were handled for prolonged periods outside the incubator, HEPES buffer was added in place of the bicarbonate to maintain the correct pH. This medium with HEPES supplement is named M2 and the components are shown in Table 2.1. Stock E was adjusted to pH 7.4 with NaOH. The stock solutions for M2 could be stored for 3 months at -20°C. To make up 50ml of M2 the following were mixed: 5ml stock A, 0.8ml stock B, 0.5 ml stock C, 0.5ml stock D, 4.2ml stock E, 39ml SDW and 200mg BSA.

2.7.2 Preparation of DNA for microinjection

Linear DNA fragments were prepared using GELase™ Agarose Gel-Digesting Preparation (Epicentre Technologies), redissolving the DNA in injection buffer (10mM Tris.Cl (pH 7.6), 0.1mM EDTA) instead of dH_2O. The concentration was determined by running an aliquot of the solution through an agarose gel next to the *HindIII* DNA marker. The concentration was then adjusted to 1-3ngμl^{-1} (final adjustments of concentration had to be made after testing a given construct empirically), and the final solution was cleaned by centrifugation through a Spin-X column (Costar #8162).

2.7.3 Preparation of egg donors by superovulation

Naturally ovulating females will typically produce 6-10 eggs, so to reduce the number of females needed for each experiment the females used for this purpose were superovulated. This results in 20-30 eggs being produced from each 3-4 week old animal. The females, which are adjusted to a light period of 5am-7pm, were given an intraperitoneal injection with 5IU of pregnant mare's serum (PMS) at about 3pm, 3 days before the eggs were to be recovered. A second injection of 5IU human chorionic gonadotrophin (hGC)

was given at about 1pm, the day before the experiment. Both hormones were obtained from Intervet Laboratories, as Folligon and Chorulon respectively. Following hGC injection, each female was placed in a cage with a stud F_1 male. The males used were between 2 and 5 months old. The number of viable, fertilised eggs obtained from a mating with a male older than 5 months was significantly reduced, so the stud males were replaced every 3 months. Copulation plugs were checked the following morning and these females removed for oviduct dissection. The oviducts were dissected into M2 medium and the eggs released by opening them with forceps. Cumulus cells were removed from the zygotes by adding hyaluronidase to the M2 to a final concentration of 300μg/ml and the eggs removed to fresh M2 as they were freed from cumulus cells. The eggs were then rinsed three times in M2 and three times in M16 before being stored in the 37°C incubator (in M16, with 5% CO_2). The drop of M16 was prevented from evaporating by a covering of mineral oil.

TABLE 2.1: Preparation of M2 media.

STOCK A (10 x conc.)	**COMPONENT**	**g/100ml**
	NaCl	5.534
	KCl	0.235
	KH_2PO_4	0.162
	$MgSO_4.7H_2O$	0.293
	Sodium lactate (60% syrup)	3.4ml
	Glucose	1.000
	Penicillin G	0.060
	Streptomycin sulphate	0.050
STOCK B (10 x conc.)	**COMPONENT**	**g/100ml**
	$Na\ HCO_3$	2.101
	Phenol Red	0.010
STOCK C (100 x conc.)	**COMPONENT**	**g/10ml**
	Sodium pyruvate	0.036
STOCK D (100 x conc.)	**COMPONENT**	**g/10ml**
	$CaCl_2.2H_2O$	0.252
STOCK E (10 x conc.)	**COMPONENT**	**g/100ml**
	HEPES	5.958
	Phenol Red	0.010

2.7.4 Pseudopregnant recipients

Pseudopregnant female mice, between 6 and 8 weeks of age, were prepared by mating females in natural oestrus with vasectomised males. Vasectomised males were prepared in the SPF facility of the NIMR, and pseudopregnant females were ordered from the unit as required. The females were anaesthetised at 0.5dpc by and intraperitoneal injection of 200μl of Hypnovel/Hypnorm. Microinjected embryos, at the one- or two-cell stage were then transferred through the infundibulum into the oviducts, using a heat-polished pulled-capillary needle. 15 embryos were transferred into each oviduct.

2.8 Analysis of transgenic mice

2.8.1 Transgenic detection by PCR

Yolk sac tissue was retained following dissection of embryos for PCR analysis. The tissue was placed in 100μl of tail lysis buffer (100mM NaCl, 10mM Tris pH 7.5, 1mM EDTA, 1% SDS, 100ng/ml proteinase K) and incubated overnight at 55°C. Following phenol/chloroform extraction (to remove protein), 1μl of the DNA solution was added to: 2μl 10x PCR salt solution, 2μl 10x dNTP solution, 0.5μl (50ng) each of the relevant primers (the primers used are listed at the end of this section), 0.1μl *Taq* polymerase and 13μl dH_2O. The samples were denatured for 3min. at 94°C, followed by 30 cycles of denaturation at 94°C (20 sec.), annealing at 57°C (1 min.), and primer extension at 72°C (2 min.). A final extension cycle was performed at 72°C for 3 min. The resulting PCR products were loaded onto a TAE-buffered 2% agarose gel for electrophoresis (30 min. at 120 volts). Two control primers from the myogenin gene were used as a positive control for the PCR reaction in each case (MGP1 and MGP2). Primers LZ3 and ZT4 were used to assay the presence of the lacZ transgene. The MGP primers give a band of around 200bp, while the lacZ primers give a PCR product of around 500bp.

MGP1 - CCAAGTTGGTGTCAAAAGCC

MGP2 - CTCTCTGCTTTAAGGAGTCAG

LZ3 - GCGACTTCCAGTTCAACATC

ZT4 - GATGAGTTTGGACAAACCAC

2.8.2 Assay for β-Galactosidase

Embryos were dissected from pregnant females, washed in PBS and stained for β-galactosidase activity as follows: 30-90 min. in fix (1% formaldehyde, 0.2% gluteraldehyde, 2mM $MgCl_2$, 5mM EGTA, 0.02% NP-40 in PBS), followed by three 30 min. washes (0.02% NP-40 in PBS). The embryos were then incubated in staining solution (5mM $K_3Fe(CN)_6$, 5mM $K_4Fe(CN)_6$, 2mM $MgCl_2$, 0.02% NP-40, 1mg/ml X-Gal in PBS) in the dark at 37°C. The strength of expression varies greatly between constructs and the length of incubation time therefore ranged from a few hours to a couple of days.

2.9 Wholemount *in situ* hybridisation

2.9.1 Synthesis of probe

The following synthesis reaction was incubated from 2 hours to overnight at 37°C: 10μl of dH_2O, 4μl of 5x transcription buffer (Promega), 2μl of 0.1M DTT, 2μl of 10x DIG-labelled nucleotide mix, 1.5μl of linearised DNA template (at 1μg/μl), 0.5μl of Rnasin ribonuclease inhibitor and 1.5μl of SP6, T7 or T3 RNA polymerase (depending on the promoter used). After synthesis, 1μl was removed and run on an agarose gel to estimate the amount of RNA present. 2μl of DNAse was added and the reaction incubated at 37°C for 15-25 min. The RNA was precipitated by adding 50μl of dH_2O, 1μl of glycogen, 25μl of 10M ammonium acetate and 200μl of ethanol, mixing well, incubating on dry ice for 30 min. and then centrifuging at 13000rpm for 20 min. at 4°C. The pellet was washed in 70% ethanol and air-dried briefly before re-dissolving in 20μl of DEPC-treated water and storage at -80°C.

2.9.2 Pretreatment of embryos: mice and fish

Embryos were dissected in PBS, fixed overnight at 4°C in 4% paraformaldehyde and rinsed twice in PBT (0.1% Triton X-100 in PBS) at 4°C for 5 min. They were then taken through a graded methanol series: 10 min. in each of 25%, 50%, 75% (in PBT) and 100% and could be stored for weeks at -20°C in 100% methanol. To rehydrate the embryos ready for use, they were taken back down through the same graded methanol series. The embryos

were rendered more permeable to the probe by treatment with 10μg/ml of proteinase K in PBT for 5-10 min. (max. 5 min. for fish) at room temperature. They were then rinsed twice in PBT for 5 min. before refixing for 30 min. (20 min. for fish) in 4% paraformaldehyde at 4°C, a further 2 rinses in PBT and then placed in the prehybridisation mix (50% deionised formamide, 5xSSC, 2% Boehringer Blocking Powder, 0.1% Triton X-100, 0.1% Chaps, 50μg/ml Heparin, 1mg/ml t-RNA, 5mM EDTA in DEPC-treated water) overnight with gentle rocking at 62-65°C (fish were only pre-hybridised for 2 hours).

2.9.3 Hybridisation: mice and fish

The hybridisation process was carried out under the same conditions as prehybridisation, with the addition of fresh, pre-warmed hybridisation buffer containing 500–1000ng of probe. Hybridisation was allowed to proceed overnight or over the weekend.

2.9.4 Post-hybridisation washes: mice

The embryos were washed with gentle rocking in solutions prewarmed to 65°C as follows: prehyb. mix, twice for 30 min.; solution 1 (50% formamide, 1 x SSC, 0.1% Triton X-100) twice for 30 min.; 1:1 solution 1: MABT (100mM maleic acid pH 7.5, 150mM NaCl, 0.1% Triton X-100) for 20 min. The embryos were then washed a further two times for 10 min. at room temperature in MABT before preblocking in Blocking Solution (2% Boehringer blocking reagent in MABT) for 2-4 hours at room temperature. The blocking solution was removed and replaced with anti-digoxygenin FAB fragments (Boehringer) diluted 1:1000 in blocking solution and left rocking gently at 4°C overnight.

2.9.5 Post-hybridisation washes: fish

The following washes were performed at 65°C. The embryos were first washed three times for 10 min in 25% hyb. mix/2 x SSC, diluted in DEPC-treated sterile-distilled water (20 x SSC: 3M NaCl, 0.3M Tri-sodium citrate pH 7.0). They were then washed a further two times in 2 x SSC and three times in 0.2 x SSC, all for 10 min. Following a rinse in PBT at room temperature, they were incubated in PBT containng 2% sheep serum with gentle agitation for

two hours at room temperature. This solution was then replaced with anti-DIG-AP antibody diluted 1:1000 in PBT containing 2% sheep serum and the embryos incubated at 4°C over night with gentle agitation.

2.9.6 Post-antibody washes and histochemistry: mice

The embryos were washed 5-6 times for one hour – each wash at room temperature and then overnight at 4°C in MABT. They were then washed twice at room temperature for 10 min. in NTMT (100mM NaCl, 100mM Tris.HCl pH 9.5), 50mM $MgCl_2$, 0.1% Tween, made from concentrated stocks on the day of use). The embryos were transferred to a glass embryo dish containing 2ml NTMT including 4.5μl/ml NBT (75mg/ml in 70% dimethylformamide, store at -20°C) and 3.5μl/ml BCIP (50mg/ml in dimethylformamide, store at -20°C) and left in the dark at room temperature with gentle shaking. The colour reaction was monitored periodically under a dissecting microscope. When colour had developed to the desired extent, the embryos were washed with NTMT and stored in PBT. The stain was fixed before photography overnight in 4% PFA at 4°C. Embryos (or portions thereof) that were to be flat-mounted were usually equilibrated in 70% glycerol at least over night.

2.9.7 Post-antibody washes and histochemistry: fish

The embryos were washed 8 times for 15 min. each wash in PBT at room temperature. They were then washed twice for 5 min. in NTMT at room temperature and stained as for mice embryos (see previous section). When the colour had developed to the desired extent, the embryos were washed 3 times for 5 minutes in PBT and they were refixed in 4% PFA for 2 hours. Following refixing, they were washed twice for 5 minutes in PBT and equilibrated at least overnight in 70% glycerol for flat-mounting.

2.9.8 Double *in situs*: fish

For double *in situs*, both probes were added at once (e.g. one labelled with digoxygenin, one with fluorescein). The first colour reaction was then developed as normal and washed three times 5 min. with PBT. The embryos were incubated twice for 20 min. in 0.1M glycine-HCL pH 2.2, 0.1% Tween at

RT to inactivate the first antibody. Following this, they were washed twice for 5 min. in PBT and incubated in PBT for one hour at 65°C. The embryos were then refixed in 4% PFA for 20 min. at 4°C before washing a further two times 5 min. in PBT. They were then incubated at RT for 30 min. in PBT containing 2% sheep serum and overnight at 4°C in PBT 2% sheep serum containing the second antibody.

2.9.9 Fast Red staining

Owing to the light-sensitive nature of fluorescein, *in situs* were kept in the dark as much as possible following the addition of a fluorescein-labelled probe. Following the post-antibody washes, the embryos were equilibrated for 2 x 5 min. in FR buffer (0.1M Tris-HCl pH 8.2, 0.1% Tween). To prepare the staining solution, one Fast Red tablet (Boehringer Mannheim) was dissolved in 2ml of FR buffer and the solution passed through a 0.45μm filter. The equilibrated embryos were transferred to the staining solution and incubated for up to 24 hours at room temperature in the dark. When the colour had developed to the desired extent, the embryos were rinsed twice in PBT and refixed in 4% PFA for 30 min. at 4°C. They were then washed twice for 5 min. in PBT and equilibrated in 70% glycerol for flat-mounting.

2.9.10 Flat-mounting: fish

Using a pair of fine tungsten needles, all of the yolk cells were carefully removed from the embryo before laying it flat on a microscope slide, covering with a glass cover-slip, filling the space with 70% glycerol and sealing the slide with nail varnish. This facilitated clear and detailed photography of *in situ* patterns without the impediment of opaque yolk cells.

2.10 Photography

Bright field low power pictures of whole embryos were taken on a Leica Wild M10 stereo-microscope with a photographic attachment, using an agarose bed flooded with PBT to position the embryos. Flat-mounts were photographed on a Zeiss Axoiphot microscope using Nomarski optics. Photographs were taken using Kodak Ectachrome 64T film and processed by the NIMR photographics division.

2.11 Wholemount immunohistochemistry

Embryos were dissected in ice-cold PBS and fixed for 1 hour at 4°C in 2% TCA. After fixation, embryos were washed 3 times in PBT for 10 min. at RT and then incubated in 0.05% hydrogen peroxide for several hours at 4°C. The embryos were washed in PBT 3 times for 10 min., followed by blocking in 5% sheep serum in PBT for 1-2 hours at room temperature (RT) with gentle agitation. The embryos were incubated in the appropriate dilution of primary antibody in 5% sheep serum PBT overnight or over the weekend at 4°C with gentle agitation. They were then rinsed once in PBT and washed 8 times 15-30 min. in PBT at RT with gentle agitation. The embryos were then incubated in the appropriate dilution of secondary antibody in 5% sheep serum PBT overnight at 4°C, followed by the same series of post-antibody washes. An optional final wash for lower backgrounds was a final overnight incubation at 4°C in PBT with gentle agitation. For alkaline phosphatase coupled secondary antibodies, the detection was carried out as for *in situ* colour reactions.

2.12 Maintenance of fish and treatment with chemical agents

Breeding fish were maintained at 28.5°C on a 14-hour light/10-hour dark cycle. Embryos were collected by natural spawning, raised in aquarium water at 28.5°C and staged according to (Kimmel *et al.*, 1995).

2.12.1 Retinoic acid treatment

Embryos were treated in the dark with all-*trans*-retinoic acid at 10^{-7} M (final concentration) in aquarium water containing 10% Hank's balanced salt solution (Sigma) for one hour at 50% epiboly (Holder and Hill, 1991). Retinoic acid was prepared as a stock solution of 10^{-4}M in DMSO in a darkroom under photographic safety light and the stock was shielded from exposure to light as much as possible. Following treatment, the embryos were washed several times in aquarium water. When embryos had reached at least 80% epiboly, they were transferred to a 16°C incubator overnight and back to 28.5°C the

following morning until the desired somite-stage was reached in the early afternoon.

2.12.2 Retinoic acid antagonist (BMS 493) treatment

The retinoic acid antagonist BMS 493 was used as it is reported to block all RAR receptor isotypes (P. Chambon, pers. comm.) Embryos were treated under identical conditions to those used for retinoic acid treatment, with the substitution of 10^{-6}M BMS 493 for all-*trans*-RA, either from pre-1000 cell stage or from 50% epiboly overnight. The optimal antagonist concentration was determined by the treatment of chick embryos with various concentrations and analysing them for *Hoxb4* expression (N. Itasaki, pers. comm.). Effects were noted with concentrations as low as 0.25μM. 1μM concentration phenocopied the effect of the *Raldh2* mutation in the mouse (loss of *Hoxb4* expression in the hindbrain Niederreither *et al.*, 2000). Increases beyond 1μM did not enhance the effect any further. As with retinoic acid treatment, embryos under exposure to BMS 493 were kept in the dark. When treating from pre-1000 cell stage, embryos were transferred to fresh media and antagonist 6–7 hours into the treatment followed by incubation overnight.

2.13 P1 Artificial Chromosome (PAC) manipulations

Gridded filters and subsequently clones from the mouse PAC library RPCI-21 (created by K. Osoegawa and P. de Jong – http://www.chori.org/bacpac/) were supplied by the UK HGMP Resource Centre, Cambridge. PAC clones carried by DH10B bacterial cells were modified by ET-recombination (Zhang *et al.*, 1998; Muyrers *et al.*, 1999). The plasmid pBAD-ETγ (see Appendix 3) was introduced into PAC-containing cells by heat-shock to prepare them for the following procedure.

2.13.1 Preparation of electrocompetent cells

A single isolated colony of cells containing the PAC clone and pBAD-ETγ was picked and grown over night on a rotary shaker set to 250rpm at 37°C in 5 ml of LB containing ampicillin (100μg ml^{-1}) and kanamycin (60μg ml^{-1}). Sufficient 10% glycerol in sterile distilled water was prepared and chilled on ice for at least three hours before use. The 5ml overnight culture was then transferred

into 250 ml of prewarmed LB (plus antibiotics) and this larger culture was incubated at 37°C on a rotary shaker set to 250rpm for 1.5-2 hours until the OD600 was 0.2. Arabinose was then added to a final concentration of 0.1% to induce *recE* and *recT* as well as *gam* expression. The bacterial cells were then harvested after 1.5 hours (final OD600 = 0.35-0.4). They were transferred into 500ml centrifuge tubes and chilled on ice-water for 15 min. During this period, the centrifuge rotor (Beckmann JLA-10500) was cooled down to -7°C by spinning at 4000rpm for 10 min. The cells were then pelleted by centrifuging for 10 min. at 7000rpm at -7°C. The supernatant was then discarded and the cells placed immediately on ice before resuspending them in 250ml of ice-cold 10% glycerol. The cells were pelleted as before, followed by a repetition of the glycerol wash. After this final wash, the supernatant was discarded, retaining a small volume (several hundred μl) in which to resuspend the cells for snap-freezing in pre-cooled eppendorf tubes on dry ice in 50μl aliquots. Competent cells were stored at -80°C for subsequent use.

2.13.2 Transformation

The DNA fragment designed for PAC modification by homologous recombination was introduced into competent cells prepared as described above by electroporation. Cuvettes were pre-cooled on iced for at least 5 min. Competent cells were thawed on ice before adding 1μl of DNA and gently mixing. They were then introduced into the cuvette. Cells were electroporated at 2.5kV (Bio-Rad Gene Pulser, 25μF with pulse controller set to 200 ohms). 1ml of chilled LB was immediately added before transferring the cuvette to ice for several minutes. The cells were then removed to an eppendorf tube for incubation at 37°C with shaking for 15-30 min. before plating on suitable antibiotic plates.

2.13.3 PAC DNA preparation

PAC-containing cells were seeded into 30ml of LB, supplemented with the appropriate antibiotic(s), and grown overnight at 37°C with shaking. Cells were pelleted the following morning by spinning for 15 min. at 2000rpm in a bench-top centrifuge. They were then gently resuspended in 1ml of GET (50mM glucose, 10mM EDTA pH 8.0, 25mM Tris-HCl pH 8.0) and 30μl of

50mgml^{-1} lysozyme in TE was added, mixing gently. The suspension was incubated at room temperature for 5 min. 2ml of 0.2M NaOH/1% SDS was then added, the solution mixed gently and placed on ice for 5 min. Following this, 1.5 ml of 3M potassium acetate was added and mixed gently by inversion before placing on ice for 5 min. The precipitate was then pelleted by centrifugation at 10000g for 10 min. The supernatant was carefully transferred into a 15ml conical polypropylene centrifuge tube and DNase free RNase A added to a final concentration of 50 mgml^{-1} before incubating at 37°C for 1 hour. The mixture was then phenol/chloroform extracted (mixing very gently) and the DNA precipitated by addition of an equal volume of isopropanol. The DNA was pelleted by centrifugation at 10000g for 20 minutes, washed with 70% ethanol and resuspended in a suitable volume of sterile distilled water.

2.13.4 Pulsed-field gel electrophoresis

Pulsed-field gel electrophoresis was carried out on a Bio-Rad CHEF-DR® II unit according to the manufacturer's instructions.

2.13.5 Fusaric acid selection

In order to select against tetracycline-resistant bacteria, cells were grown on fusaric acid plates. These were prepared according to Maloy and Nunn (Maloy and Nunn, 1981) or Yang *et al.* (Yang *et al.*, 1997) (the methods are nearly identical), with the single modification of doubling the fusaric acid concentration.

Chapter 3 – The search for *ephrin-B2* regulatory elements

3.1 Introduction

The aim of this project has been to discover more about the regulation of *ephrin*s during hindbrain segmentation. As they play an important role in restricting the movement of cells between rhombomeres, the position of *Eph*s and *ephrin*s within the regulatory hierarchy is of interest. Some information has been forthcoming regarding the regulation of a few *Eph* receptors (see section 1.5.4), but less is known about the regulation of *ephrin*s. As has been demonstrated with members of the *Hox* complex, transgenic analysis of a gene's regulatory region is one useful method of identifying upstream factors. This approach has also been successful with *EphA4* (Theil *et al.*, 1998). Previous work indicated that *ephrin-B2* is expressed in rhombomeres 2, 4 and 6 (Bergemann *et al.*, 1995), making this a suitable subject for enhancer analysis. A thorough analysis of *ephrin-B2* expression in the hindbrain including a detailed time-course had, however, not previously been carried out. As detailed knowlege of its expression is important when studying the regulation of a gene, I carried out such an analysis of *ephrin-B2* expression. This is followed here by the approaches used in generating constructs for transgenic analysis in the search for regulatory elements controlling *ephrin-B2* expression.

3.2 Time-course of *ephrin-B2* expression

A detailed time-course analysis of *ephrin-B2* expression by *in situ* hybridisation was carried out (fig. III.1). At the earliest stage examined, the egg cylinder stage (fig. III.1A), expression is seen in a broad, posterior domain. There is also a ring of expression around the egg cylinder, possibly at the junction between embryonic and extra-embryonic tissue. As the first somite is forming (fig. III.1B, C), a strong domain of expression is seen in the forming somite, as well as a double ring of expression, which seems to

delineate the neural plate. Expression in the hindbrain region is broad and uniform. At the 4 somite stage (fig. III.1D), expression occurs in the posterior half of somites and throughout the forming somite (this is a consistent feature of the expression pattern for the duration of somitogenesis) and in a strong, uniform manner in the hindbrain. At the 7 somite stage (fig. III.1E, F), expression is additionally seen in the forebrain and the onset of segmentally restricted expression is seen in the hindbrain. Expression is becoming upregulated in r2 and downregulated in r3. The rest of the hindbrain continues to express at a moderate and uniform level. At the 9 somite stage (fig. III.1G, H), further downregulation has occurred in r3, and r5 expression is beginning to diminish. By the 12 somite stage (fig. III.1I), expression is seen at high levels in r1, r2, r4 and r6 and at low levels in r3 and r7 and is absent from r5. Expression is also seen in the eye and in the branchial arches. This pattern persists through to the latest stages examined (22-23 somites).

3.3 Transgenic analysis of the genomic region of *ephrin-B2*

Two separate approaches were used to generate constructs for transgenic analysis. In the first, a mouse genomic library in the bacteriophage vector λFIXII was screened for clones spanning the genomic region of *ephrin-B2*. The clones identified were mapped relative to each other and fragments were tested for enhancer activity by subcloning them into a vector with a minimal promoter driving lacZ and producing transient transgenic mice with the resulting constructs. In the second approach, a mouse genomic PAC library was used in order to obtain clones spanning a larger area surrounding the *ephrin-B2* coding region which could be modified by homologous recombination in bacteria, inserting the reporter gene near the start codon.

3.3.1 Screening of the phage library

A mouse genomic library (see Materials and Methods section 2.1) was screened using the entire 1kb open reading frame (ORF) of the *ephrin-B2* cDNA as a probe to obtain genomic DNA of the *ephrin-B2* region. 10 separate phage clones were purified to the single-plaque stage. Preliminary mapping

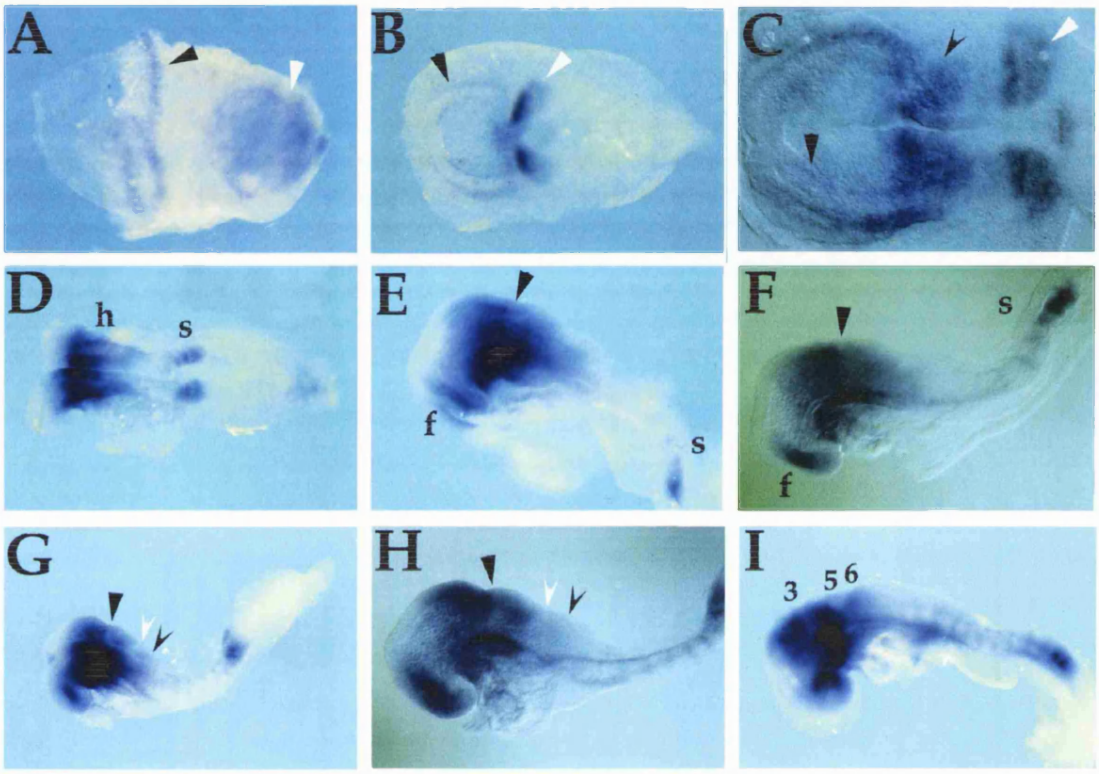

Figure III.1 *In situ* hybridisation time-course of *ephrin-B2* expression in wildtype embryos. **A.** Egg cylinder stage. Expression in a ring around the cylinder (black arrow), possibly at the junction between embryonic and extra-embryonic tissue and a broad domain in the embryonic tissue (white arrow). **B,C.** 0-1 somite stage. Double ring of expression which appears to delineate the neural plate (black arrow) plus strong expression in forming somite (white arrow) and in the hindbrain region. C is a flatmount of the embryo in B. The region encompassing the hindbrain is indicated by the indented black arrow. **D.** 4 somites. Expression in the posterior half of somites (s) and strong throughout the hindbrain (h). **E,F.** 7 somites. Expression coming up in the forebrain (f) and first hint of segmental restriction in the hindbrain (black arrow), most clearly seen in the flatmount (F). Slight reduction of intensity in r3 as gauged by the position of the pre-otic sulcus. **G,H.** 9 somites. From the initial uniform domain in the r5/6 region, r6 expression has become elevated (indented black arrow), while being reduced in r5 (white arrow). The low-level r3 domain is indicated by the black arrow. H is the flatmount of the embryo in **G. I.** 12 somites. Expression in the eye and branchial arches. Expression has cleared from r5 and is strong in r6. This general pattern persists through to the latest stages examined (22-23 som.).

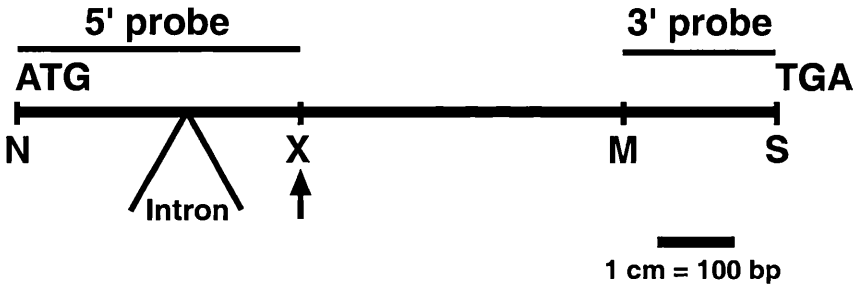

Figure III.2. The position of the 5′ and 3′ probes within the *ephrin-B2* ORF. The point of insertion of the first intron is also indicated as is the 3′ end of the B25′X2 fragment (black arrow). N – *Nco*I; X – *Xba*I; M – *Msc*I; S – *Stu*I

experiments were carried out on these by Southern hybridisation using a 5′ and a 3′ probe created from sections of the cDNA (fig. III.2): bases 168-538 (*Nco*I-*Xba*I) and 987-1174 (*Msc*I-*Stu*I) respectively. (The *ephrin-B2* cDNA sequence can be found in Appendix 1.) The most 5′ clone, c8, was selected for further analysis.

3.3.1.1 Subcloning fragments and transgenic analysis

I first subcloned a 2kb *Xba*I fragment (B25′X2) identified by the 5′ cDNA probe which, by reference to the cDNA sequence, should extend approximately 1.5kb 5′ to the ATG (fig. III.2). This could then used as a probe to identify 5′ fragments. Restriction analysis, however, showed that the expected *Nco*I site was not present in this fragment, suggesting that the cDNA sequence at this point is interrupted by an intron. This hypothesis was confirmed by sequence analysis, placing the intronic interruption at base 292 of the cDNA sequence. In an effort to identify fragments 5′ of the ORF, a 40 bp oligo designed against the 5′ most extent of the published cDNA sequence was used as a probe in Southern hybridisation. Two fragments identified by this method were cloned following prolonged and strenuous efforts and subsequently found to have a probable origin elsewhere in the genome. I next subcloned and tested for enhancer activity in transgenic mice two fragments which hybridised weakly with the 5′ cDNA probe, neither of which had any enhancer activity at the stages examined (40 transgenics out of 71 embryos, harvested at 9.5dpc).

3.3.2 Approaches for targeted modification in bacteria

In order to secure a larger genomic fragment with maximum probability of containing the *ephrin-B2* regulatory elements, it was decided to screen and obtain clones from a PAC library, with an average insert size of 147kb. The method initially selected for the introduction of the *LacZ* reporter gene into the PAC clones by homologous recombination in bacterial cells was that of Yang and colleagues (Yang *et al.*, 1997). In this method, a recombination cassette is constructed by cloning two genomic fragments of at least 500 bp each on either side of a cassette containing the *lacZ* reporter gene flanked by an internal ribosome entry site (IRES) (5′) and a pGKPA sequence (3′). This is

carried out in the building vector (see Appendix 2) and the assembled recombination cassette is then subcloned into the shuttle vector, which also carries a bacterial *recA* gene, tetracycline resistance and a temperature-sensitive origin of replication. This construct is then transformed into chemically competent PAC-carrying bacteria and co-integrates selected for by tetracycline and kanamycin resistance at 43°C (which prevents replication from the temperature-sensitive origin of the shuttle vector). The co-integrate must then be resolved through a further internal recombination event to leave the LacZ cassette inserted between the two homology arms in the PAC. Unresolved co-integrates are selected against by sensitivity to fusaric acid which is a consequence of tetracycline resistance.

While this work was in progress, I enjoyed the benefit of regular discussions with a colleague in the laboratory of Robb Krumlauf who was also using this system for targeted homologous recombination in bacteria. In this way, I learned of several difficulties encountered in the execution of the method outlined above, namely the sub-cloning of the recombination cassette into the shuttle vector and the correct resolution of co-integrates (M. Martinez, pers. comm.), and also of a newer method (ET-cloning – see below) which promised to be more straightforward. Having completed the construction of the recombination cassette (see section 3.3.2.2) and realising that this could equally well be used with the ET-cloning method, I decided to switch to this approach.

ET-cloning was devised in the laboratory of Francis Stewart (Zhang *et al.*, 1998; Muyrers *et al.*, 1999). As in the method of Yang and colleagues (Yang *et al.*, 1997), this approach is based on homologous recombination in *E. coli*. The key differences between the two methods are as follows. Whereas the method of Yang *et al.* involves the co-integration of two circular molecules mediated by the product of the *recA* gene and necessitates the subsequent resolution of this product by internal recombination (see above), ET-cloning relies on the products of the *recE* and *recT* genes to recombine a linear molecule with a circular one. This results in the insertion of a fragment

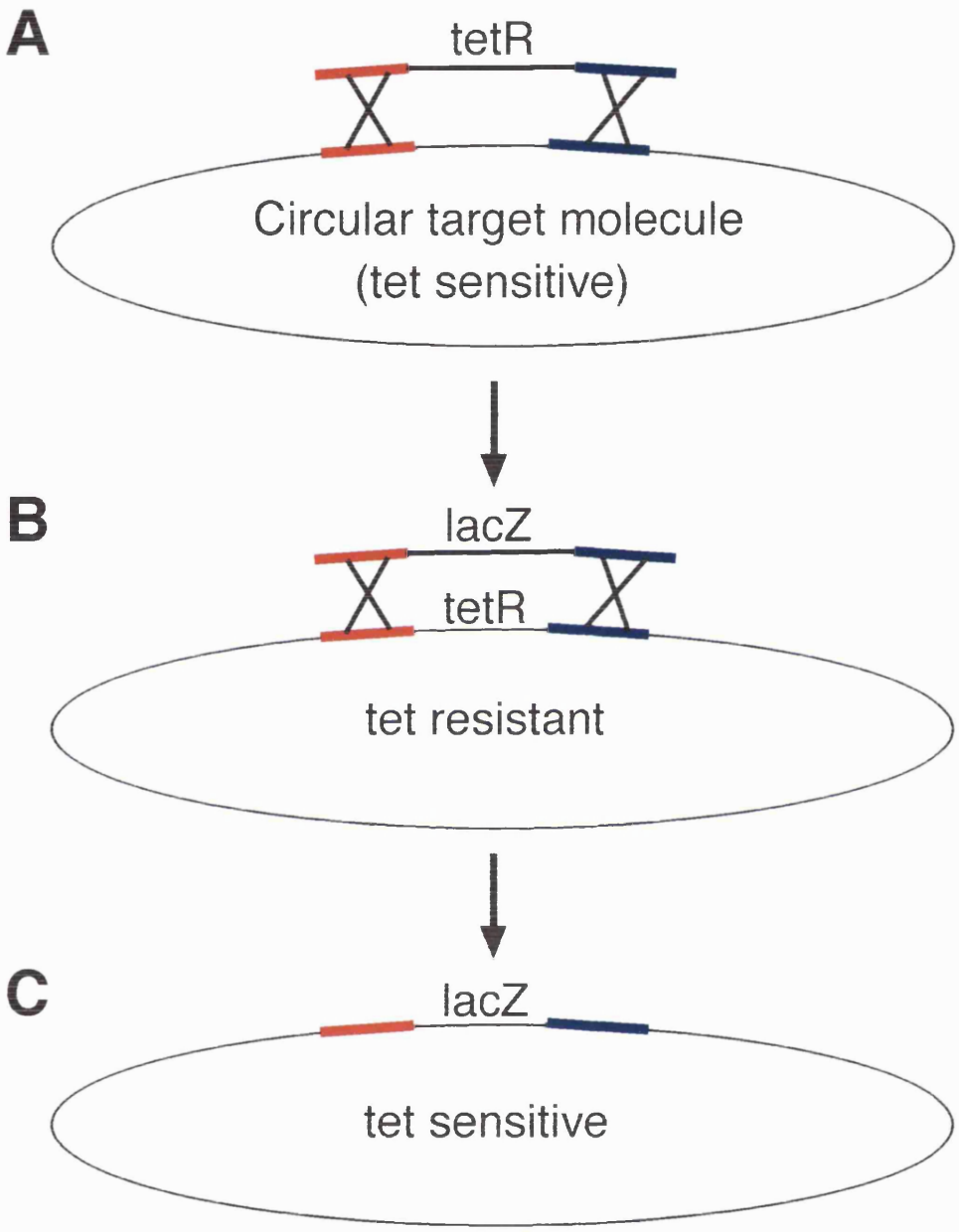

Figure III.3. ET cloning strategy for introducing lacZ into PAC clones.
A. In the first round of homologous recombination, tetracycline resistance (tetR) is introduced into the target PAC, replacing the sequence between the 5′ and 3′ homology arms (represented by the red and blue bars respectively). This event is selectable by exposure to tetracycline. **B.** In the second round, tetR is replaced by the lacZ reporter through the use of the same homology arms. This event is selectable by exposure to fusaric acid, which selects against tetracycline resistance. **C.** The final construct has the lacZ reporter inserted in the target PAC between the homology arms.

between the homology arms without the requirement for further resolution. I therefore devised a strategy for introducing the *lacZ* reporter gene into the coding region of *ephrin-B2*, near the start codon, which takes advantage of the ability to apply both positive and negative selection against tetracycline resistance and which requires two rounds of ET-cloning (fig. III.3). In the first round, a tetracycline resistance (*tetR*) gene, flanked by homology arms either cloned from the desired site of introduction or introduced by PCR (the arms may be as short as 50 nt (Zhang *et al.*, 1998) is introduced and selected for by exposure to tetracycline. In the second round, the same homology arms are used flanking the *lacZ* reporter to replace *tetR* with this cassette, the event being selectable by resistance to fusaric acid (Maloy and Nunn, 1981).

3.3.2.1 Screening of the PAC library and preliminary analysis of positive clones

Gridded filters of the mouse PAC library RPCI-21 (see section 2.13) were screened using the *ephrin-B2* ORF and 16 positive clones were obtained. Subsequent analysis of these clones by *Eco*RI restriction digest and Southern hybridisation with the *ephrin-B2* ORF revealed that 4 of the 16 original positives produced strong signals (see fig. III.4). Clones 383-I11, 491-E10, N22-548 and J19-385 were selected for further analysis. Using the B25'X2 fragment (see section 3.3.1.1) as a probe, each of these clones was analysed by restriction with *Eag*I and *Not*I (singly and in combination) and Southern hybridisation (see fig. III.5). *Not*I sites flank the insert in the pPAC4 vector (the insert is located between the *Bam*HI sites – see Appendix 3), so this digest was included to determine the insert size. *Eag*I is another rare cutter which also cuts at the *Not*I recognition site. As there is an *Eag*I site at base 111 of the *ephrin-B2* cDNA sequence (see Appendix 1) which lies 5′ of the B25'X2 fragment (see fig. III.2), this enzyme was considered suitable for basic mapping of the clones. This analysis revealed that clone 383-I11 contains approximately 70kb of sequence 5′ to the *ephrin-B2* start codon and clone 548-N22 contains approximately double this, while clones 385-J19 and 491-E10 contain little or no 5′ sequence (fig. III.5). To test this interpretation, PCR primers (008 and 009 – see Appendix 4) were designed based on the *ephrin-B2* cDNA sequence to amplify a fragment extending from base 17 to base 129.

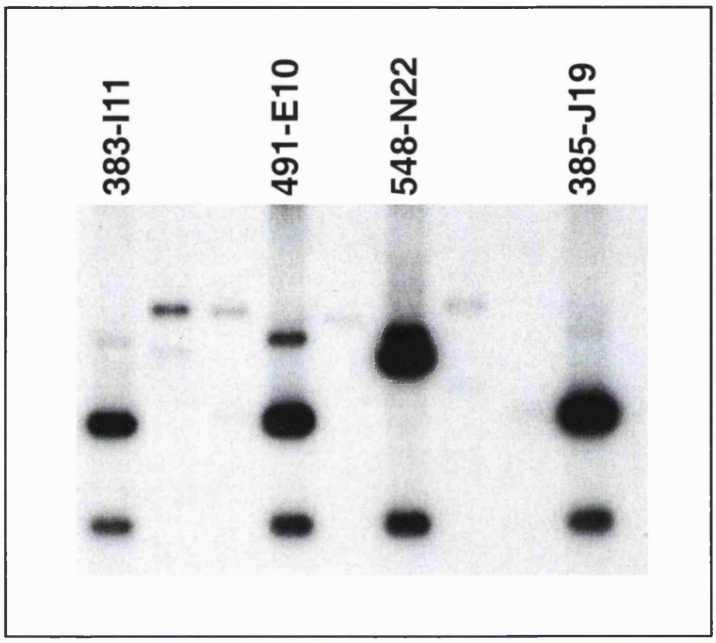

Figure III.4. PAC clones digested with *Eco*RI and and hybridised with the *ephrin-B2* ORF. The four clones indicated were the ones which gave the strongest signal.

Figure III.5. A–C. Autoradiographs of PAC clones probed with B25'X2 (see fig. III.2). Both the *Not*I and *Eag*I digests release the insert and the *Eag*I digest additionally cuts at base 111 of the *ephrin-B2* cDNA sequence (see Appendix 1), 5' to the site recognised by the B25'X2 probe. **A.** Clone 383-I11. The labelled fragment of approximately 180 kb in the *Not*I digest is reduced to approximately 110 kb in the *Eag*I digest , indicating the presence of approx. 70 kb of sequence 5' to the *Eag*I site in the cDNA sequence (c111). **B.** Clone 548-N22. In this case, the *Not*I fragment of approx. 190 kb and *Eag*I fragment of approx. 40 kb suggest approx. 150 kb of sequence 5' to c111. **C.** Clone 385-J19. The indistinguishable size of the *Not*I and *Eag*I fragments in this experiment suggests that the c111 *Eag*I site is near the 5' end of the clone and that there is relatively little sequence 5' to it. **D.** Maps of clones 383-I11 and 548-N22 based on the above results.

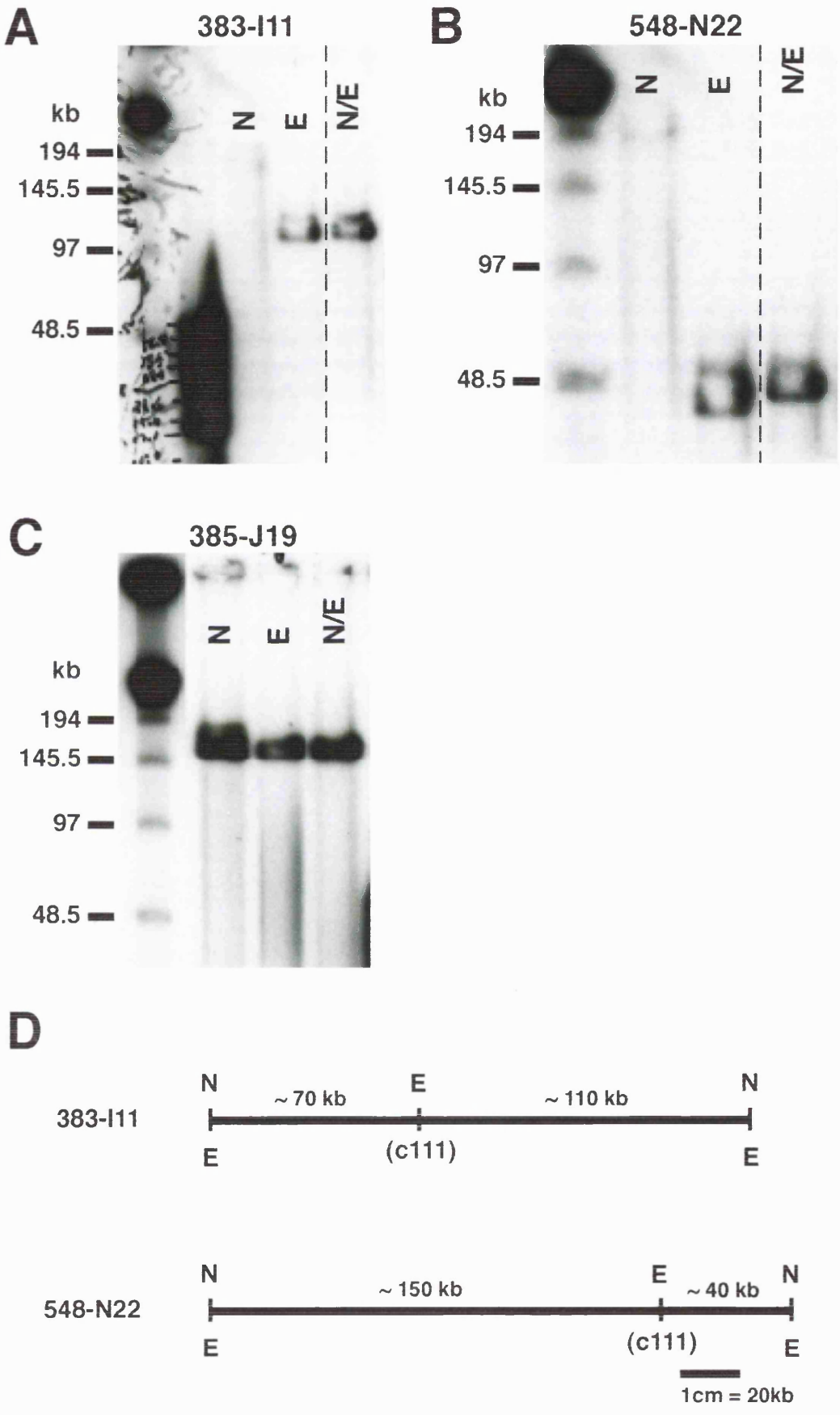
A
383-I11
kb
194
145.5
97
48.5
N
E
N/E
B
548-N22
kb
194
145.5
97
48.5
N
E
N/E
C
385-J19
kb
194
145.5
97
48.5
N
E
N/E
D
383-I11
N
~ 70 kb
E
~ 110 kb
N
E
(c111)
E
548-N22
N
~ 150 kb
E
~ 40 kb
N
E
(c111)
E
1cm = 20kb

The predicted product was generated from clones 383-I11 and 548-N22, but not from clones 491-E10 or 385-J19 (not shown), suggesting that the positioning of the latter excluded one or both of the oligonucleotide primers. Clones 383-I11 and 548-N22 were therefore selected for further work.

3.3.2.2 Subcloning of fragments and construct building

The PCR product referred to in the previous section was purified for use as a probe to identify fragments extending 5′ to the start codon from clone 383-I11. In this manner, a 3kb *Xba*I fragment (IX3) was identified and cloned. Mapping digests revealed that the start codon was quite close to the 3′ end of this fragment (fig. III.6). The 3′-most end of this fragment, approximately 200 bases from the *Nco*I site at the start codon to the *Xba*I site, was therefore used as a probe to identify a suitably sized fragment by Southern hybridisation for subcloning and use as the 3′ homology arm. This led to the identification and subcloning (into pBSKS) of an approximately 1kb *Eco*RI fragment (fig. III.7) selected for use as the 3′ homology arm. The approximately 1.6kb *Nco*I fragment of IX3 (see fig. III.6), extending 5′ from the *Nco*I site at the start codon, was selected for the 5′ homology arm. This fragment was cloned by blunt-end ligation into the *Eco*RI site of the polylinker at the 5′ end of the IRES sequence in the building vector pBV.IRES.LacZ.PA (see Appendix 2 and fig. III.8). The orientation of the inserted fragment was determined by double restriction digestion with *Eag*I and *Xho*I. Constructs with the correctly oriented insert release a fragment of slightly less than 1.6kb. The *Eco*RI fragment chosen for the 3′ homology arm was then blunt-end ligated into the *Xba*I site of the polylinker at the 3′ end of the polyadenylation sequence of the building vector. In order to identify constructs with the correct insert orientation, double restriction digests with *Xba*I and *Not*I were carried out. Those with a correctly oriented insert released a fragment of slightly less than 1kb. One of these was selected for further work and the completed construct with both homology arms inserted in the correct orientation was designated pBVHA12 (fig. III.8). The full LacZ cassette, flanked by the 5′ and 3′ homology arms was released by double digestion with *Not*I and *Xho*I.

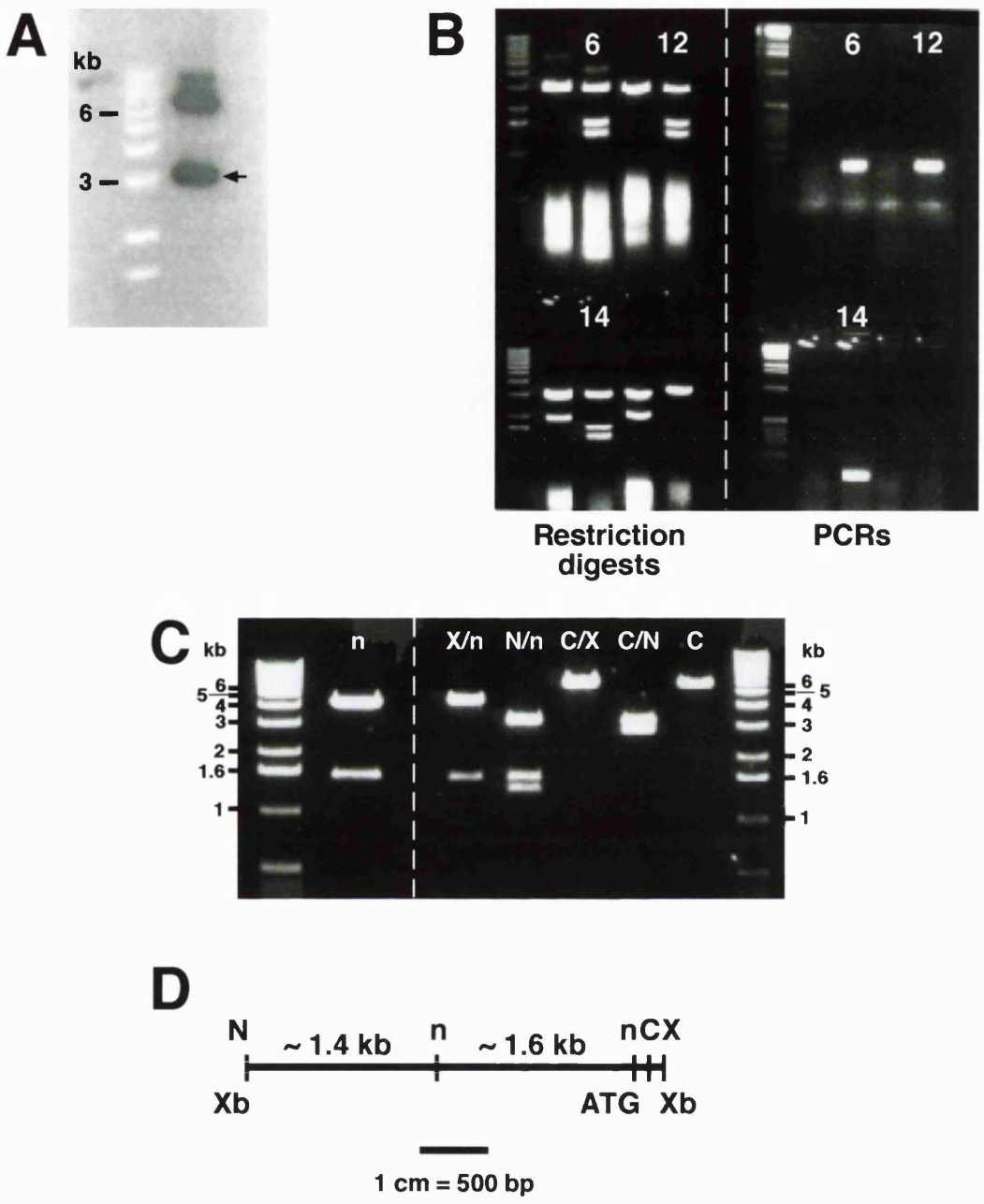

Figure III.6. The cloning and restriction mapping of fragment IX3. **A.** A fragment extending from base 17 to 129 of the *ephrin-B2* cDNA sequence was amplified by PCR (see Appendix 4), radio-labelled and used to probe *Xba*I-digested 383-I11 DNA. The approx. 3 kb labelled fragment (indicated by a black arrow) was selected for subcloning into pBSKS. The higher molecular weight labelling is the product of partial digestion of the PAC DNA. **B.** Clones containing the correct insert were identified in parallel by double restriction digest with *Xba*I and *Nco*I and by PCR, using the same oligonucleotide primers as used to amplify the probe fragment. Clone 14 was selected for further work. **C.** Mapping digests were carried out using enzymes with sites in the vector (*Not*I and *Xho*I) and in the *ephrin-B2* cDNA sequence (*Nco*I and *Cla*I). The results from these digests were used to generate the map shown in **D.**

C – *Cla*I; n – *Nco*I; N – *Not*I; Xb – *Xba*I; X – *Xho*I

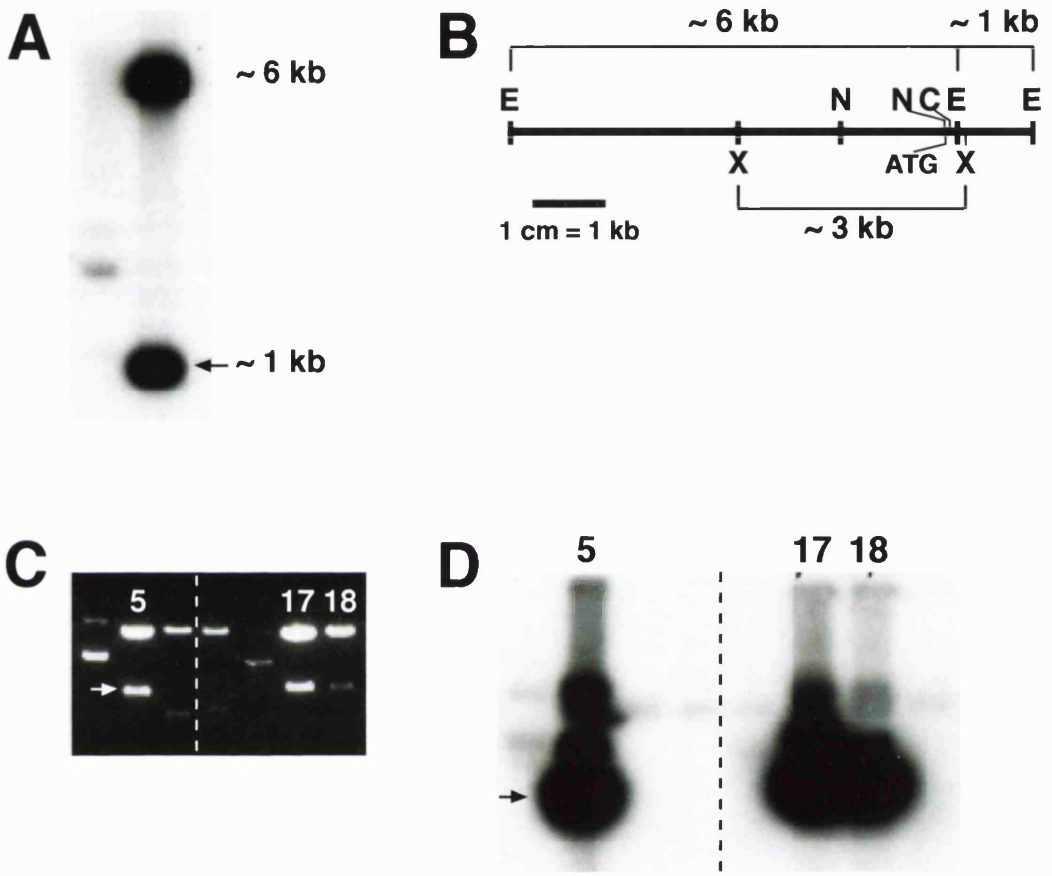

Figure III.7. The cloning of fragment IE1. **A.** The extreme 3' *Nco*I-*Xba*I fragment from IX3 (see fig. III.6) was used as a probe to identify fragments from *Eco*RI-digested 383-I11 DNA by Southern hybridisation (there is an *Eco*RI site at base 274 of the cDNA sequence). Fragments of approximately 1 and 6 kb were identified. In order to determine whether the 1 kb fragment was contained within IX3, this was digested with *Eco*RI (not shown). As no 1 kb fragment was released (the construct was linearised), the map was drawn as shown in **B. C.** The 1 kb fragment indicated by a black arrow in A. was subcloned into pBSKS. Clones with inserts of the expected size were identified by restriction digestion with *Eco*RI and their identity was further confirmed (**D**) by Southern hybridisation with the *Nco*I-*Xba*I fragment as in A.

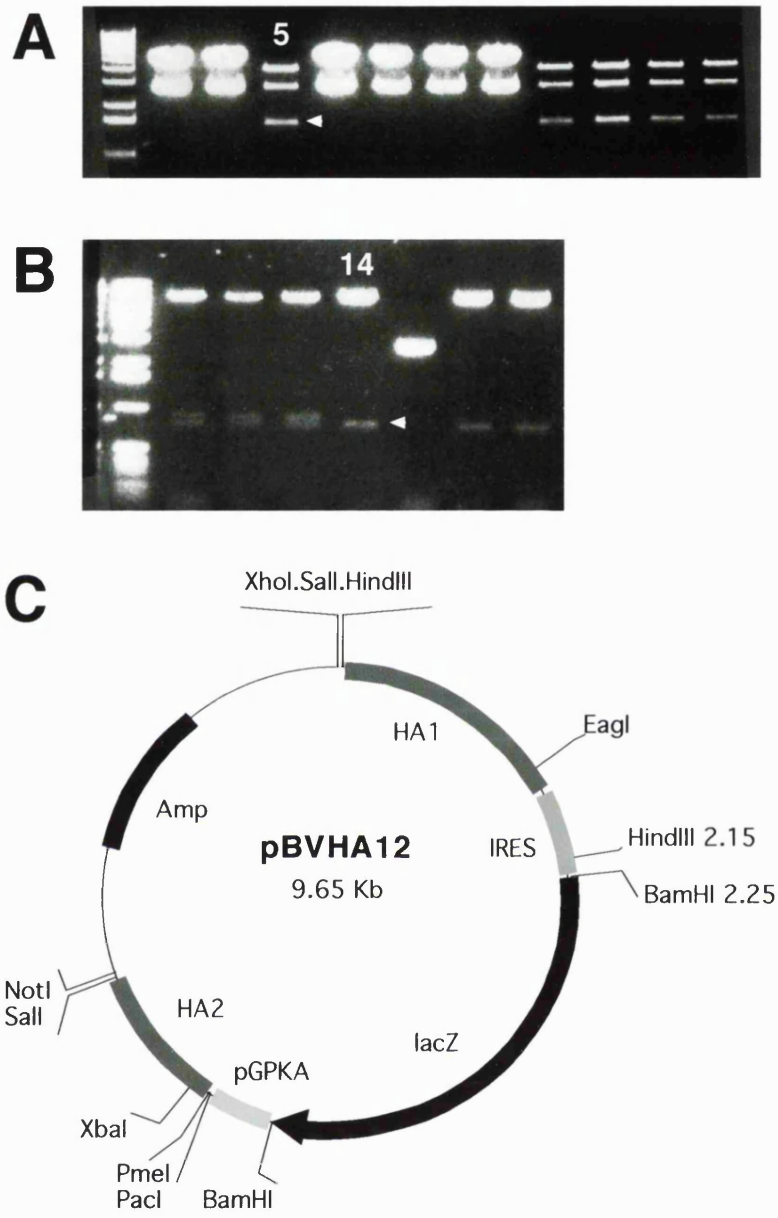

Figure III.8. The construction of pBVHA12. **A.** The 1.6 kb *Nco*I fragment extending 5′ from the *ephrin-B2* start codon was blunt-end ligated into the *Eco*RI site 5′ of the IRES in the building vector of Yang *et al.* (see Appendix 2). The orientation of the inserted fragment was determined by double restriction digestion with *Eag*I and *Xho*I, constructs with the correctly oriented insert release a fragment of slightly less than 1.6 kb (white arrow). Clone number 5 was selected for further work. **B.** The 1kb *Eco*RI fragment extending 3′ from the site at base 274 of the cDNA sequence was blunt-end ligated into the *Xba*I site 3′ of the polyadenylation sequence in the building vector. Double restriction digests with *Xba*I and *Not*I were carried out. Those with a correctly oriented insert released a fragment of slightly less than 1 kb (white arrow). Clone number 14, with both homology arms inserted in the correct orientation, was selected for further work and is designated pBVHA12. **C.** Map of pBVHA12.

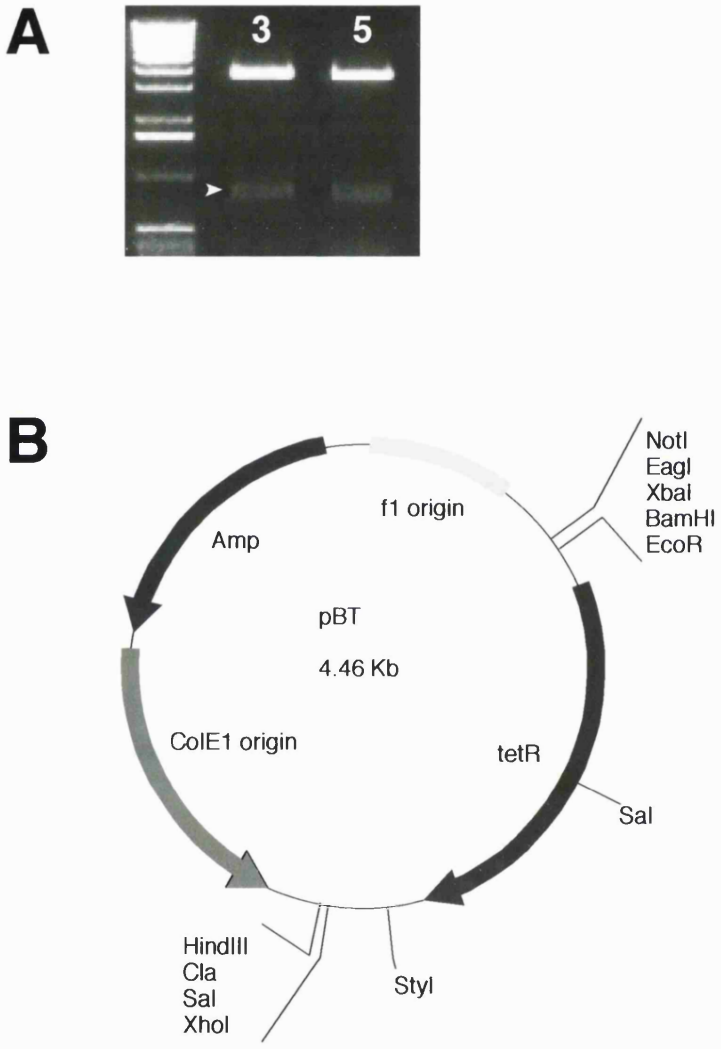

Figure III.9. The subcloning of tetracycline resistance (tetR) into pBSKS to create pBT. **A.** Positive clone numbers 3 and 5 following diagnostic digest with *Sal*I, releasing a fragment of slightly less than 1 kb (white arrowhead). Clone 3 was selected for further work. **B.** Map of pBT showing key polylinker sites either side of the insert and also the *Sty*I and *Sal*I sites within the insert.

For the ET-cloning strategy outlined in section 3.3.2, a construct containing tetracycline resistance flanked by the same homology arms was required for the first step. The tetracycline resistance gene was released from the plasmid pACYC184 by digestion with *Xba*I and *Ava*I and blunt-end ligated into the *Eco*RV site of pBSKS to create the plasmid pBT (see Appendix 3 and fig. III.9). The 5′ homology arm was released from pBVHA12 by double restriction digestion with *Eco*RI (from the polylinker) and *Eag*I (from the cDNA sequence, base 111). The overhangs were then removed by end-filling with Klenow fragment. This was then blunt-end ligated into the *Eco*RI site of pBT where the overhang had been removed by digestion with mung bean nuclease. This resulted in the recreation of the *Eco*RI site at the 5′ end of the insert and the fragment orientation was determined by double digestion with *Sal*I (present in the TetR sequence) and *Eco*RI. Constructs with correctly oriented insert released a fragment of approximately 2.3kb. The 3′ homology arm was released from pBlueScript by digestion with *Xba*I and *Eco*RI, thus removing a small piece (<100 bp) from its 5′ end, and blunt-end ligated into the *Sty*I site present at the 3′ end of the TetR cassette. Both sets of ends were filled using Klenow, resulting in the recreation of the *Eco*RI site at the 3′ end. Insert orientation was determined by double digestion with *Eag*I (present in TetR) and *Eco*RI (correct orientation gave an approximately 1.3 kb band) and confirmed with *Xho*I (from the BSKS polylinker) and *Eco*RI (incorrect orientation gave an approximately 1.1kb band). The completed construct was called pBTHA12 and the linear cassette with TetR flanked by the 5′ and 3′ homology arms is released by digestion with *Eco*RI (see fig. III.10).

3.3.2.3 PAC modification by ET-cloning

The recE and recT required for ET-cloning are supplied on another plasmid (pBAD-ETγ – see Appendix 3) under the control of an arabinose-inducible promoter. This plasmid was transformed into the DH10B cells carrying PAC clones 383-I11 and 548-N22. The resulting bacteria were designated IB and NB respectively. Electrocompetent IB and NB cells were prepared and approximately 100ng of tetracycline resistance cassette from construct pBTHA12 (previous section) was transformed in by electroporation (see

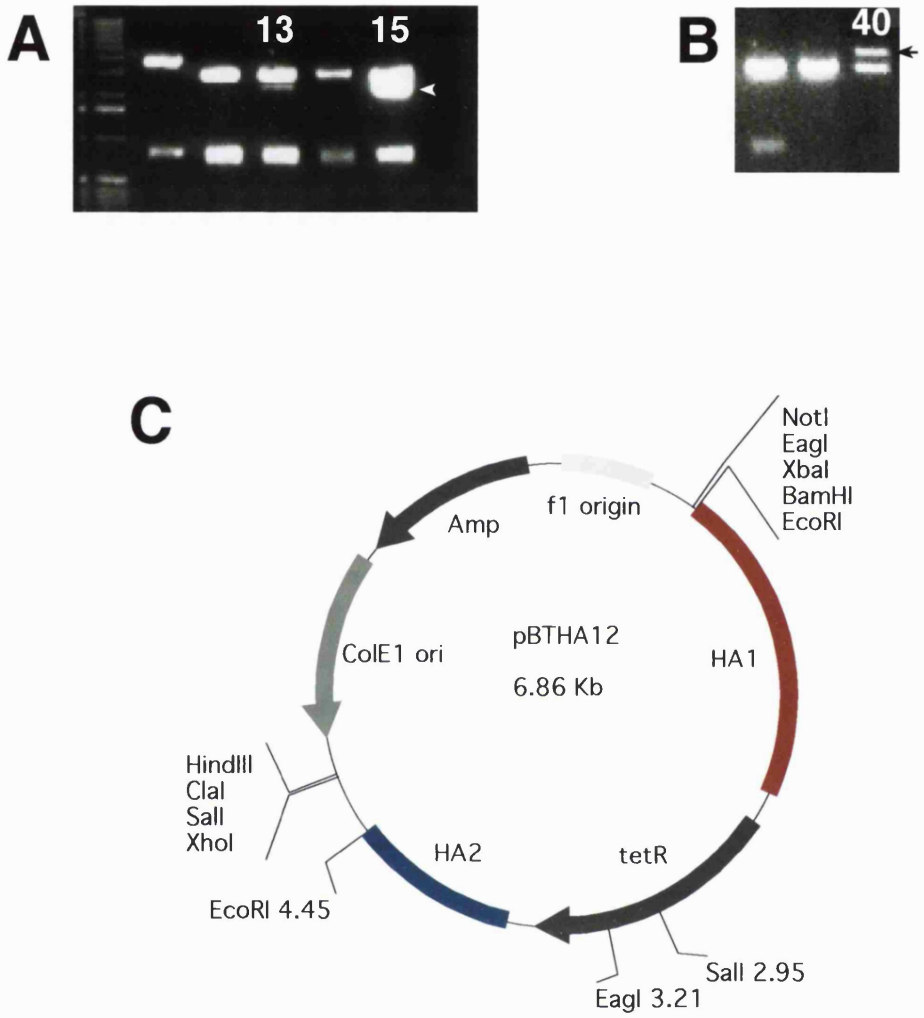

Figure III.10. The subcloning of homology arms HA1 and HA2 into pBT to create pBTHA12. **A.** Cloning of HA1. Positive clone numbers 13 and 15 release a fragment of approx. 1.3 kb (white arrow) on double digestion with *Eco*RI and *Sal*I. Clone number 15 was selected for further work. **B.** Cloning of HA2. Positive clone number 40 releases an approx. 4 kb (black arrow) fragment on double digestion with *Xho*I and *Eco*RI. Incorrectly oriented inserts result in the release of a fragment slightly less than 1 kb in size. Clone number 40 was selected for further work and named pBTHA12. **C.** Map of pBTHA12. HA1 and HA2 are labelled in red and blue for easy comparison with fig. III.3.

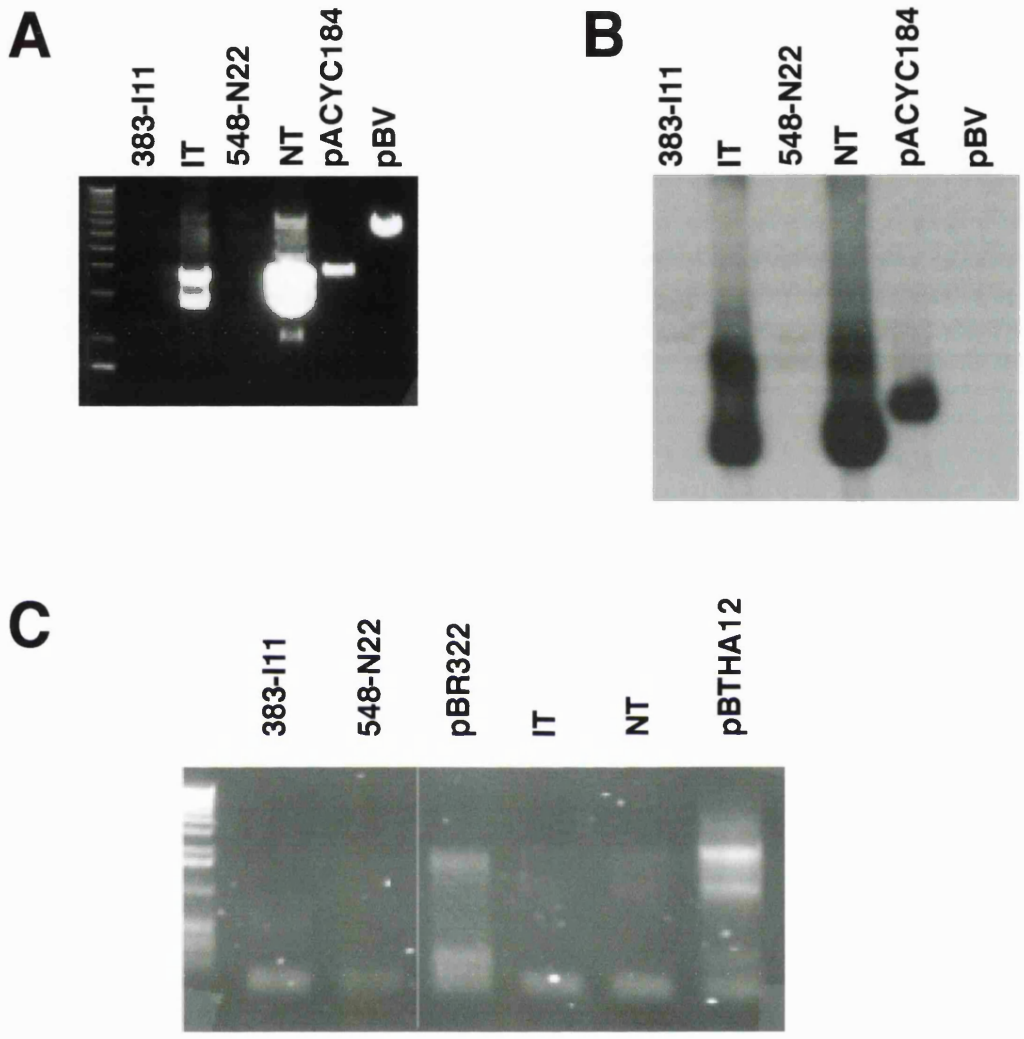

Figure III.11. Confirmation of the introduction of tetracycline resistance into IT and NT. **A.** Agarose gel with products of restriction digests by *Eco*RI. 383-I11, 548-N22 and pBV (see Appendix 2) were included as negative controls as they do not carry tetR. pACYC184 was included as a positive control. **B.** Autoradiograph of Southern hybridisation of the gel shown in A. The radio-labelled probe was an approximately 600 bp *Sal*I-*Cla*I fragment from the tetR region of pBT (see fig. III.9). **C.** PCR amplification using the primers B2P and TetF (see Appendix 4). Again, DNA from clones 383-I11 and 548-N22 was included as a negative control. pBR322 and pBTHA12 were included as positive controls. Only those constructs carrying tetR give a product.

section 2.13.2). A few tetracycline-resistant colonies were obtained in each case and the presence of the TetR cassette in the PACs was confirmed by Southern hybridisaiton and PCR (fig. III.11). The cells carrying the modified PACs were designated IT and NT.

Electrocompetent IT and NT cells were prepared and varying amounts (from 100–500 ng) of LacZ cassette (previous section) were introduced into the cells by electroporation. Some problems, however, were encountered with this second step. Although several hundred apparently tetracycline sensitive colonies were screened by PCR, none were found to contain the LacZ cassette. Replica plating of these colonies onto plates containing either kanamycin alone or kanamycin plus tetracycline revealed that they were in fact still tetracycline-resistant. Unfortunately I did not have sufficient time to pursue this matter to its conclusion. Possible reasons for the difficulties experienced at this stage are considered below (section 3.4).

3.3.2.4 Improved fusaric acid selection

The first difficulty encountered in my attempts to replace the TetR cassette in IT and NT cells with the LacZ cassette was the growth of tetracycline-resistant colonies on fusaric acid plates prepared according to the protocol of Maloy and Nunn (Maloy and Nunn, 1981). The possible explanations considered and tested for this were incompatablility between kanamycin (the resistance carried by PACs) and fusaric acid selection systems and a requirement for higher fusaric acid concentration. The results listed in Table 3.1 demonstrate that a two-fold increase in fusaric acid concentration was sufficient to prevent growth of tetracyline-resistant cells, while permitting growth of tetracycline-sensitive cells following overnight culture at 37°C. Some growth of tetR colonies did occur even on plates with increased fusaric acid concentration following two or three days at 37°C.

Cells	DH5α			IT
Resistance	none	Amp	Amp.Tet	Amp.Tet.Kan
Selection				
none	++++	++++	++++	++++
Tet	-	-	++ ++	++++
Fusaric acid	nd	nd	nd	++
Fus + Kan	nd	nd	nd	++
Amp + Fus	-	++	+	+
Amp + 2Fus	-	+	-	-

Table III.1. Growth of bacterial cells with different antibiotic resistances on selective media. Cells were cultured approximately 18 hours at 37°C. Doubling the suggested fusaric acid concentration (Maloy and Nunn, 1981) effectively prevented the growth overnight of tetracycline resistant cells while permitting that of ampicillin resistant, tetracycline sensitive cells. Amp – ampicillin; Tet – tetracycline; Fus – fusaric acid; 2Fus – doubled fusaric acid concentration; nd – no data.

3.4 Discussion

The time-course analysis of *ephrin-B2* expression has revealed that its regulation is more complex than suggested by published studies (Bergemann *et al.*, 1995) which described expression in rhombomeres 2, 4 and 6 at 9.5dpc. Hindbrain expression (fig. III.12) begins in an early broad domain, which later becomes restricted in specific segments, with a low level domain in r3 that overlaps with interacting Eph receptors. This is reminiscent of the dynamic regulation of *Hox* genes and *EphA4*. In these genes, distinct enhancers control early and late expression as well as expression in specific segments. It will be interesting to learn whether a similar situation exists for *ephrin-B2*.

Regulatory elements which control the expression of a given gene can often be located tens of kilobases distant from its coding region. Homologous recombination overcomes the limitations imposed by restriction sites and difficulty in handling large fragments of DNA. It thus offers a means of circumventing the lengthy and laborious process of 'walking' to distant elements by conventional techniques. The work detailed in this chapter demonstrates in principle that the new methods being developed using homologous recombination in bacterial systems can be adapted for use in enhancer-mapping experiments. The successful insertion of tetracycline resistance into the *ephrin-B2* coding region in two independent clones shows that the foundation of the method is sound. Technical difficulties are often encountered when first employing new methods and I feel that those experienced here can be overcome. Problems with the poor stringency of fusaric acid selection remain to be resolved. Although this was improved by increasing the fusaric acid concentration, tetracycline-resistant colonies still retained some ability to grow in spite of this selection. Further optimisation of this step is clearly required. One possiblility to be considered is that there may be a fault with the chlorotetracycline-induction system of the Tet operon which is required to keep the cells expressing Tet resistance in the presence of fusaric acid. Further control experiments are required to test this. Some problems were also experienced with the reliability of the PCR reaction used

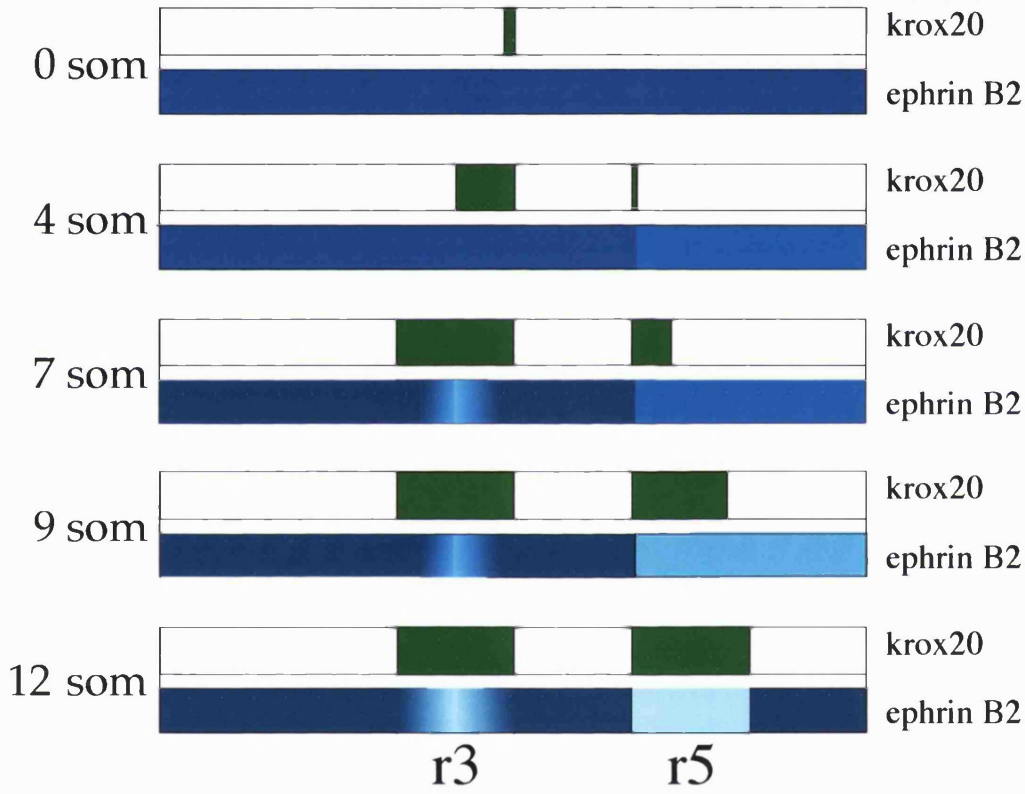

Figure III.12. Diagrammatic summary of the *ephrin-B2* time-course. *Krox-20* is included as a guide to the stage of development of r3 and r5 (data from Irving *et al.*, 1996) and because of its potential role as a suppressor of *ephrin-B2* in these rhombomeres (see Chapter 4).

for mass-screening of tetracycline-sensitive colonies. It is essential to the success of this method that the screening at this stage should be absolutely efficient and optimisation of the PCR parameters is probably all that is required. Colony hybridisation screening was also considered as a potential method for mass-screening of potential recombinants, but was judged to be impracticable owing to the presence of LacZ sequence within the bacterial genome.

Continuation of this work should address the points detailed above. Optimisation of parameters both in the recombination step and the subsequent screening proceedure are the primary objectives for the successful conclusion of this method. Once the LacZ cassette has been correctly inserted into the *ephrin-B2* coding region, the next step is to make transient transgenics using the modified PAC constructs. This is reported to be an efficient procedure (M. Martinez, pers. com.) and may even be carried out by pronuclear injection of whole circular BAC molecules (bacterial artificial chromosome – BAC – inserts are generally larger than those of PACs). Regulatory elements identified in this way may then be further localised by injection of sub-sections of the modified PACs until regions are left small enough to be dealt with by the conventional methods outlined in section 3.3.1.1.

Chapter 4 – The analysis of candidate upstream genes

4.1 Introduction

As discussed in section 1.5.4, several transcription factors with known roles in hindbrain development have been linked, directly or indirectly, to the regulation of a few Eph receptors. *EphA2* is directly regulated by *Hoxa1/b1* in r4 (Chen, 1998; Studer *et al.*, 1998). *Hoxa2* is upstream of *EphA7* in rhombomeres 2, 3 and 4 (Taneja *et al.*, 1996) and *EphA4* in r2 (Gavalas *et al.*, 1997). *EphA4* is also known to be regulated directly by *Krox-20* in rhombomeres 3 and 5 (Seitanidou *et al.*, 1997; Theil *et al.*, 1998). Each of these factors has been considered at some length in Chapter 1. These known relationships immediately suggest the same factors as possible regulators of the *ephrins*. *kreisler* too, with its known roles in the development of rhombomeres 5 and 6, particularly through regulation of genes such as *Hoxa3*, *Hoxb3* and *Krox-20*, is clearly a candidate regulator of the *ephrins* within its expression domain. Embryos mutant for several of these transcription factors individually were therefore analysed by *in situ* hybridisation for effects on *ephrin* expression.

4.2 Analysis of *kreisler* mutant embryos

As indicated above, there were several reasons for selecting *kreisler* as a candidate regulator of *ephrin* expression in r6. Firstly, it is a known regulator of *Krox-20* (Frohman *et al.*, 1993) and *Hoxb3* in r5 (Manzanares *et al.*, 1997) and *Hoxa3* in r5 and r6 (Manzanares *et al.*, 1999a). Secondly, it has been proposed that the zebrafish homologue (*valentino*) is required for the formation of both r5 and r6 (Moens *et al.*, 1996). Finally, misexpression of *kreisler* in r3 has been shown to ectopically induce or prolong the expression of *FGF-3*, *Krox-20*, *Hoxa3* and *Hoxb3* (Theil *et al.*, manuscript in preparation).

The wildtype expression pattern of *ephrin-B2* is shown in figures III.1 and IV.1. In *kreisler* mutants, the distinctive gap in *ephrin-B2* expression at r5

seen in wildtype animals disappears (fig. IV.1A, E). The high-level r6 domain is shifted forward by one rhombomere so that it is adjacent to r4, while the low-level r3 domain is further downregulated, resembling the expression profile of wildtype r5. These data suggest that, contrary to previous interpretations based on analysis of zebrafish *valentino* (Moens *et al.*, 1996), r6 is still present in *kr* mutant embryos. To investigate this further, the expression of two more molecular markers – *ephrin-B3* and *EphA7* – was examined.

ephrin-B3 expression in the wildtype hindbrain also has a characteristic lack of expression in r5 (fig. IV.1B). This gene is expressed rhombomeres 1-4 and is especially strong in r6, with only dorsally-restricted expression in r7. The pattern in *kreisler* mutants is exactly analogous to that observed for *ephrin-B2:* the r5 domain disappears, bringing forward the r6 domain by one rhombomere so that it abuts r4 (fig. IV.1F). There may be some alteration of the expression level in r3, but if so it is much less pronounced than that seen for *ephrin-B2.*

EphA7 expression is dorsally restricted in the hindbrain and is seen in rhombomeres 1-6, at highest levels in r3 and r5, lower in r2, r4 and r6 and lower still in r1 (fig. IV.1C, D). In the *kreisler* mutant, the r5 expression domain is absent and this marker also shows very clearly that the hindbrain is shortened by approximately one rhombomere's length (fig. IV.1G, H). These results are summarised diagrammatically in fig. IV.2 and indicate that, while r5 is certainly absent in *kr* mutants, r6 is present. The continued expression of *ephrins -B2, -B3* and *EphA7* in r6 of *kr* mutants demonstrates that *kreisler* is not absolutely required for their expression in this rhombomere.

4.2.1 Analysis of *kreisler*$^{3/5}$ embryos

Whilst working in the laboratory of Dr David Wilkinson, Dr Thomas Theil generated a line of transgenic mice (*kreisler*$^{3/5}$) expressing *kreisler* under the control of an r3/5 enhancer from the *ephA4* gene (Theil *et al.*, manuscript in preparation). This results in ectopic *kreisler* expression in r3 and abnormally

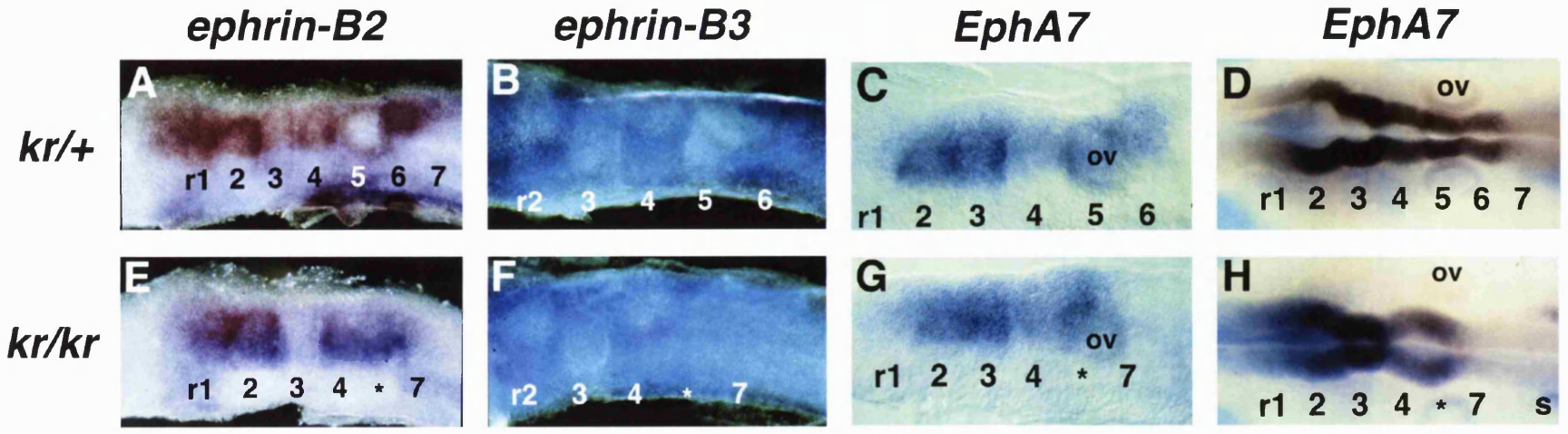

Figure IV.1. *Eph/ephrin* expression in heterozygous and *kreisler* mutant embryos. **A-C** and **E-G** are flatmounts of just the hindbrain region, **D** and **H** are dorsal views of whole-mounts. ov = otic vesicle, s = somite. **A,E.** *ephrin-B2*. In the mutant, the r3 gap becomes considerably more pronounced due to downregulation of *ephrin-B2* while the r5 gap disappears. **B,F.** *ephrin-B3*. The r5 gap disappears in the mutant, bringing forward r6/7. **C,G.** *EphA7*. Expression is highest in r2, r3 and r5 in the wildtype embryo. The r5 domain is lost in the mutant but the r6 domain is retained. The shortening of the hindbrain is clearly seen, the otic vesicle (ov) serving as a useful reference point. **D,H.** Dorsal views of the same embryos seen in C and G respectively.

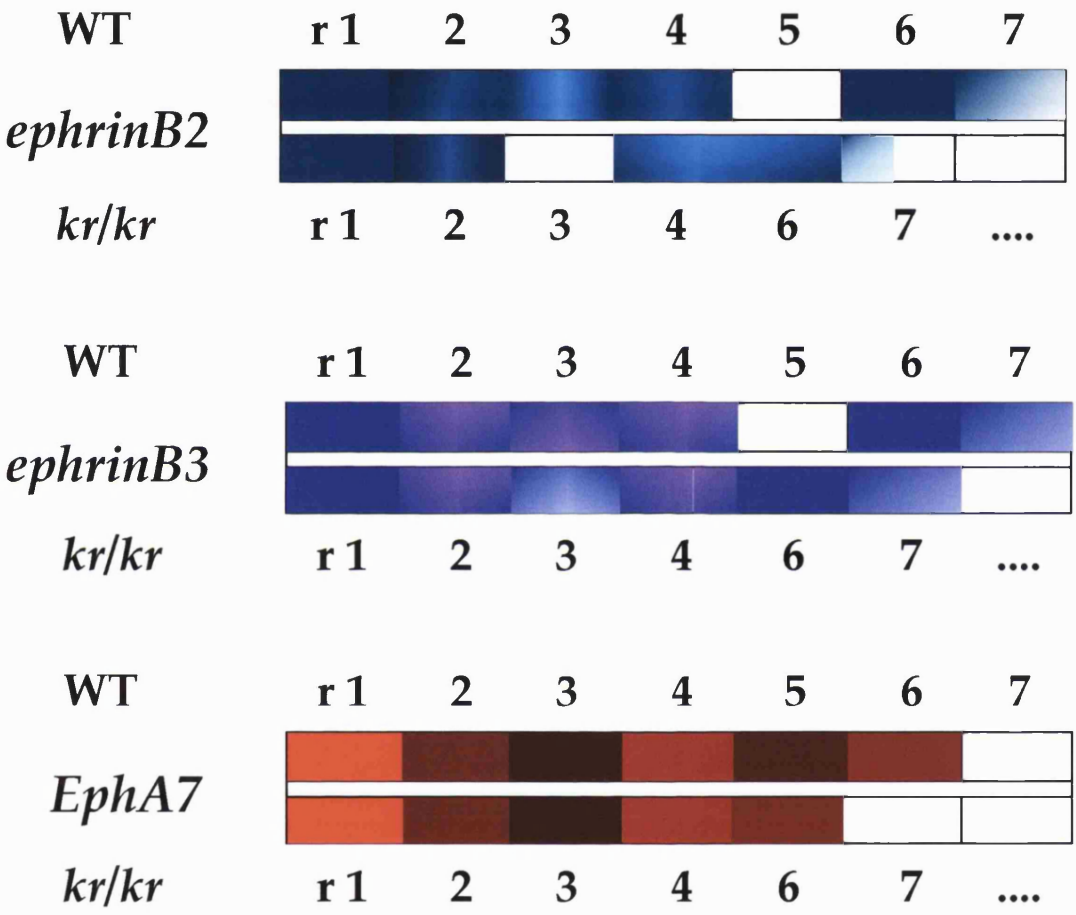

Figure IV.2. Diagrammatic representation of the expression patterns in wildtype and *kreisler* mutant hindbrains of *ephrin-B2*, *ephrin-B3* and *EphA7*.

high and prolonged expression in r5. The ectopic expression of *Fgf-3*, *Hoxa3* and *Hoxb3* and the prolonged expression of *Krox-20* in rhombomere 3 of these animals is suggestive of a partial transformation towards r5 identity. This transgenic line provided an opportunity to investigate the possibility that *kreisler* negatively regulates *ephrin* expression in rhombomere 5. The expression of *ephrin-B2* and *ephrin-B3* was examined in *kreisler*$^{3/5}$ embryos at several stages and a significant difference in r3 expression levels between these and control animals was never observed (not shown). This suggests that *kreisler* is not responsible for the downregulation of *ephrin-B2/-B3*, though a requirement for regionally restricted co-factor(s) cannot be excluded.

I also carried out some further analyses of the *kreisler*$^{3/5}$ mice in order to address an outstanding question regarding the identity of an ectopic motor nucleus which, initial analysis suggested, develops in rhombomere 5. *kreisler*$^{3/5}$ mice were crossed with lines carrying a lacZ reporter gene under the control of *Hox* gene enhancer elements driving expression either in r4 (HL5 Marshall *et al.*, 1992) or in rhombomeres 3 and 5 (ML19 Sham *et al.*, 1993). The line HL5 carries an r4-enhancer from the *Hoxb1* gene (Marshall *et al.*, 1992). Transgene expression is observed in the body of rhombomere 4 and in cells of the facial motor nucleus migrating from r4 into r5 (fig. IV.3 A). In *kreisler*$^{3/5}$ animals, transgene expression in r4 is not affected, but a failure of facial motor neuron migration into r5 is noted (fig. IV.3 B, F). The migrating neurons appear to be unable to cross into r5 territory and instead form a swollen mass at the r4/5 boundary, which protrudes into the ventricle and often fuses across the midline, giving the appearance of an ectopic nucleus. The r4 origin of these neurons was further confirmed by analysis of transgene expression from the ML19 line in *kreisler*$^{3/5}$ mice (fig. IV.3 C–E). The ML19 line carries an enhancer from the *Hoxb2* gene which drives transgene expression in rhombomeres 3 and 5. When combined with the *kreisler*$^{3/5}$ background, this illustrates defects in the development of rhombomeres 3 and 5 and the absence of labelling in the blocked motor neurons at the r4/5 boundary indicates that they are not of r5 origin (fig. IV.3 D, E).

Figure IV.3. Expression of the *Hoxb1-r4* (12.5 dpc; A, B, F–H) and *Hoxb2-r3/r5* (11.5 dpc; C–E) transgenic lines in wildtype (A, C) and *kreisler*$^{3/5}$ (B, D–H) embryos. **A.** Strong expression is observed in r4 and in the facial motor neurons migrating into r5 (black arrow). **B.** Facial motor neuron (black arrow) migration has been arrested at the boundary with r5, piling up into a swollen mass. This is shown at higher magnification in **F.** Parasaggital sections through a similar embryo to that pictured in B and F are shown in **G** and **H.** A section lateral to the blocked facial motor neurons is pictured in G and one through the bulge in H (black arrow). **D** and **E** (at higher magnification) illustrate the sunken appearance of rhombomeres 3 and 5 in the *kreisler*$^{3/5}$ embryo.

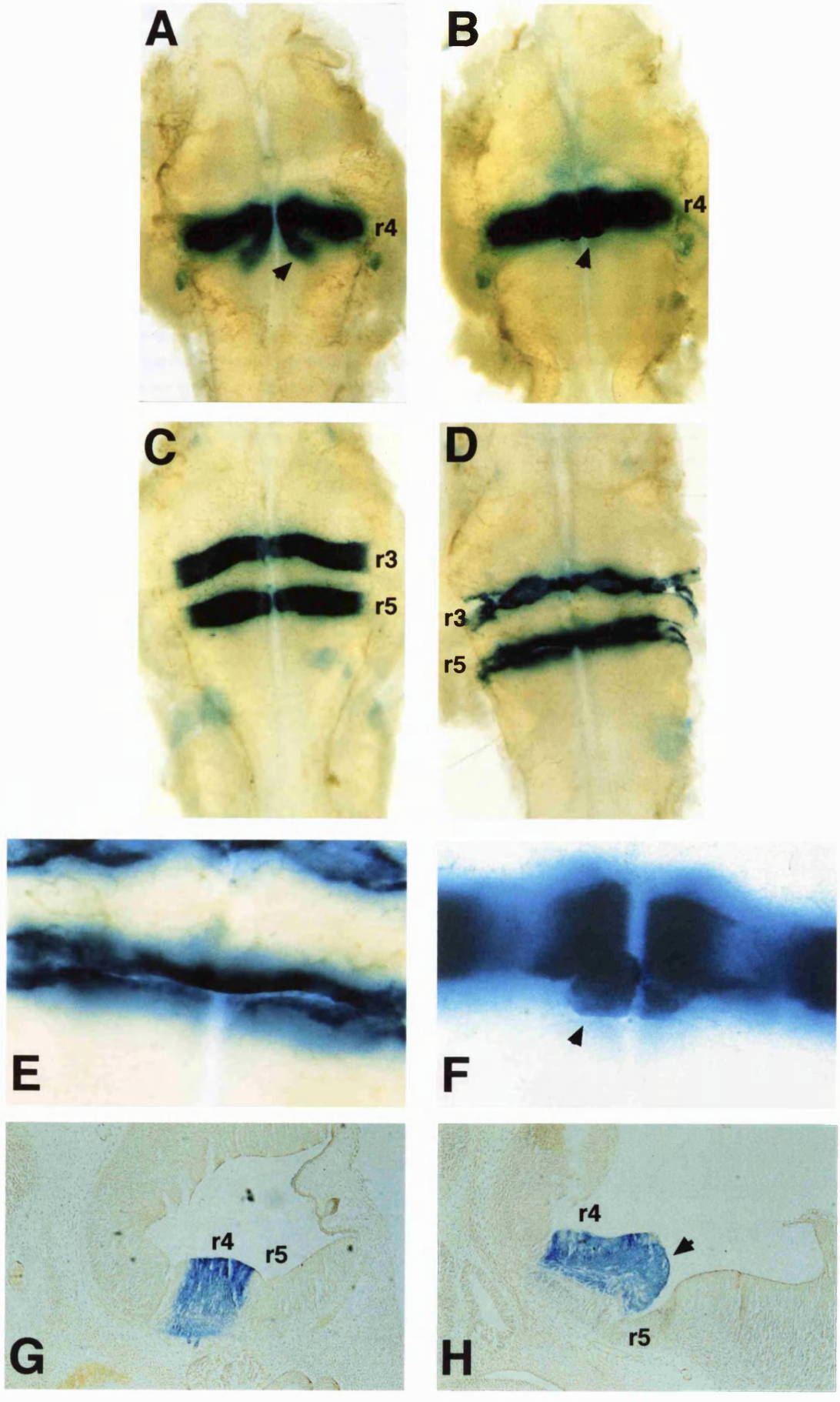
A
r4
B
r4
C
r3
r5
D
r3
r5
E
F
G
r4
r5
H
r4
r5

Altered *Eph/ephrin* expression is considered a possible contributing factor to the altered migration of these neurons. The distribution of EphA4 protein was analysed by immunodetection (using an anti-EphA4 antibody developed by (Irving *et al.*, 1996). The results pictured in fig. IV.4 show a dramatic reduction of EphA4 protein levels in the hindbrain of *kreisler*$^{3/5}$ animals.

4.3 Analysis of *Krox-20* mutant embryos

In *Krox-20* mutant mice, rhombomeres 3 and 5 initially form but are subsequently lost (Schneider-Maunoury *et al.*, 1993; Swiatek and Gridley, 1993). At 9 dpc, r3 has already begun to disappear, but r5 is still present (Schneider-Maunoury *et al.*, 1993), leaving a time-window of approximately one day to examine gene expression in these rhombomeres. *Krox-20* mutant embryos from the line originally generated by Swiatek and Gridley were obtained and analysed by *in situ* hybridisation for *ephrin-B2* expression (fig. IV.5). Comparison of stage-matched control and *Krox-20*$^{-/-}$ embryos at 9 dpc shows alterations to *ephrin-B2* expression in both rhombomeres 3 and 5. The low-level expression domain normally observed for r3 has been replaced by high-level expression indistinguishable from that in r1 and r2. The location of r5 is reliably marked by the presence of the otic vesicle. In *Krox-20*$^{-/-}$ embryos, *ephrin-B2* expression is noted in r5, from which it is normally absent. Although r3 may have been partially lost at this stage, r5 is still present and these results suggest that *Krox-20* negatively regulates *ephrin-B2* expression in rhombomeres 3 and 5.

4.4 Analysis of *Hox* mutant embryos

The group 1 paralogue Hox genes with hindbrain expression domains, *Hoxa1* and *Hoxb1*, play important roles in its development (see section 1.5.1). They are particularly vital in rhombomere 4, which is mis-specified in the *Hoxb1* mutant (Goddard, 1996; Studer *et al.*, 1996), and rhombomere 5, which is absent in the *Hoxa1* mutant (Carpenter *et al.*, 1993; Dollé *et al.*, 1993;

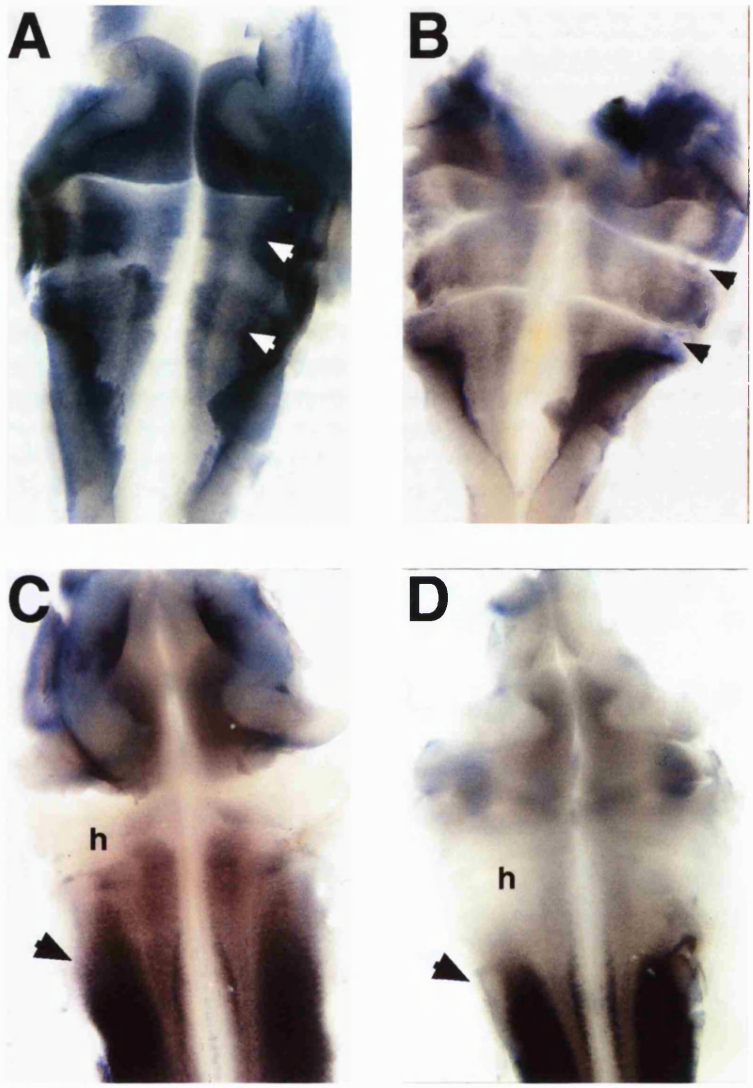

Figure IV.4. Distribution of EphA4 protein, detected by immunolocalisation in wildtype (**A, C**) and *kreisler3/5* (**B, D**) embryos. **A, B.** 11.5 dpc. Bands of expression corresponding to rhombomeres 3 and 5 are observed in the wildtype embryo (white arrows), along with longitudinal columns extending the length of the hindbrain. In the *kreisler3/5* embryo, the r3 and 5 bands are absent (black arrows), although the longitudinal columns are unaffected. **C, D.** At 12.5 dpc., the r3/5 stripes have also been downregulated in the wildtype hindbrain. General EphA4 protein levels in the hindbrain (h) are reduced in the *kreisler3/5* embryo in comparison to wildtype (both relative to somitic expression levels – black arrows).

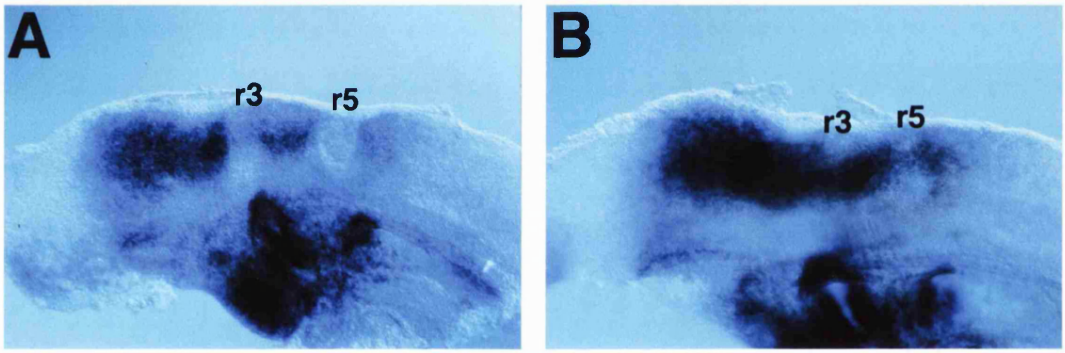

Figure IV.5. Expression of *ephrin-B2* in wildtype (**A**) and *Krox-20* mutant (**B**) embryos at 15–16 somite stage. In the *Krox-20* mutant, *ephrin-B2* expression is upregulated in both rhombomeres 3 and 5.

Mark *et al.*, 1993). r4 is partially deleted in both the *Hoxa1* single mutant (Mark *et al.*, 1993; Studer *et al.*, 1998) and in the *Hoxa1/b1* double mutant (Studer *et al.*, 1998), but is further altered in the double mutant such that it expresses none of the known markers of r4 identity which have been tested. Thus, *Hoxa1* and *Hoxb1* have overlapping roles in the specification of r4.

I analysed *ephrin-B2* expression by *in situ* hybridisation in both *Hoxa1* and *Hoxb1* mutant embryos (fig. IV.6). In the *Hoxa1* mutant embryo, the distinctive r5 domain normally void of *ephrin-B2* is absent – in agreement with earlier findings which demonstrate the deletion of this rhombomere. Expression in the remaining rhombomeres, however, appears unaltered. The low-level expression domain corresponding to r3 is noted, as are high-level domains corresponding to rhombomeres 1, 2, 4 and 6. This finding demonstrates that *Hoxa1* alone is not required for *ephrin-B2* expression in r4 or in more posterior rhombomeres.

In the *Hoxb1* mutant hindbrain, *ephrin-B2* expression appears essentially normal in all respects, displaying its characteristic expression profile in rhombomeres 1–6. This result indicates that, as for *Hoxa1*, *Hoxb1* alone is not absolutely required for *ephrin-B2* expression in rhombomere 4. Unfortunately, owing to the restricted availability of these embryos, I was unable to examine any *Hoxa1/b1* double mutants and so cannot comment on the very real possibility that one compensates for the other in the single mutants.

4.5 Discussion

The investigation of *Eph* and *ephrin* expression patterns in *kreisler* mutant mice has helped resolve two of the outstanding questions regarding that phenotype i.e. are there one or two rhombomeres missing and what is the status of rhombomeric identity posterior to r4? Previous studies looking at molecular markers have concentrated mainly on *Hox* genes (Frohman *et al.*, 1993; Cordes and Barsh, 1994; McKay *et al.*, 1994). The uncertainty associated with the interpretation of these expression patterns in the *kreisler* mutant

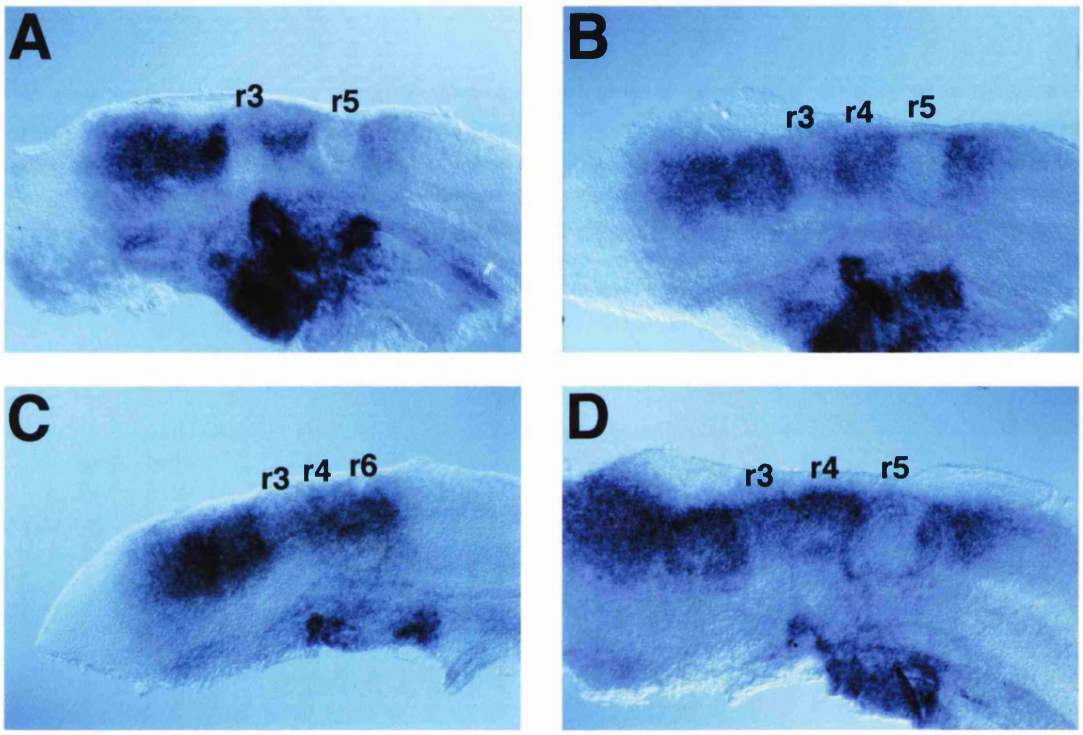

Figure IV.6. Expression of *ephrin-B2* in wildtype (**A**), *Hoxa1* (+/-) *Hoxb1* (+/-) (**B**), *Hoxa1* (-/-) (**C**) and *Hoxa1* (+/-) *Hoxb1* (-/-) (**D**) embryos. Expression levels in the double heterozygote appear indistinguishable from wildtype (although there appears to some extopic expression dorsally in r5). In the *Hoxa1* mutant, expression is comparable to wildtype with the deletion of r5. In the *Hoxa1* (+/-) *Hoxb1* (-/-) embryo, hindbrain expression is essentially the same as wildtype (although the ectopic dorsal r5 expression noted in the double heterzygote appears to be stronger).

hindbrain is due to the fact that the *Hox* gene markers used are expressed to an anterior boundary in the hindbrain but are also expressed in more posterior neural tissue. This can lead to ambiguities in assigning rhombomeric identity (some of the relevant expression patterns are summarised diagrammatically in fig. IV.7). Several possible explanations of the segmentation breakdown in the *kreisler* mutant hindbrain have been tendered: loss of r5 (Cordes and Barsh, 1994), loss of r5 and r6 (McKay *et al.*, 1994; Moens *et al.*, 1996), loss of r5 and homeotic transformation of r6 towards r4 identity (Frohman *et al.*, 1993). The advantages of using *Ephs* and *ephrins* as markers are two-fold. Firstly, the alternating rhombomeric expression of receptors and ligands allows for more definitive identification of rhombomeres and, secondly, they mediate restrictions to cell intermingling, which are altered in *kr* mutants. The loss of r5 is clearly shown by the failure of the r5 *Krox-20* stripe ever to appear (Frohman *et al.*, 1993). The results shown in fig. IV.1 and summarised in fig. IV.3 show quite clearly that, while rhombomere 5 is lost in the *kr* mutant, r6 remains and that the hindbrain is correspondingly shortened by approximately one rhombomere's length. This interpretation is consistent with the expression patterns of the *Hox* genes shown in fig. IV.7 and with the results of transplantation experiments where cells from the neural tube immediately caudal to r4 (here called r* for convenience) in *kreisler* mutants are placed in different wildtype rhombomeres (Manzanares *et al.*, 1999b). The results show that r* cells mix freely into wildtype rhombomeres r2, r4 and r6 and do not mix with r3 or r5. Additionally, the fuzzy boundaries of *Hox* gene expression observed between r4 and r* in *kr* mutants may be explained by the fact that these rhombomeres both express the same complement of *ephrins* and cells would therefore be expected to mix between them. Our interpretation is summarised in fig. IV.8. r* may therefore be said to be r6, though it is not identical to a mature r6 in all respects, as genes known to be downstream of *kreisler*, such as *Fgf-3* (Frohman *et al.*, 1993), are not expressed. This is distinct from the interpretation of the *valentino* mutant phenotype in zebrafish (see section 1.5.3), where it is

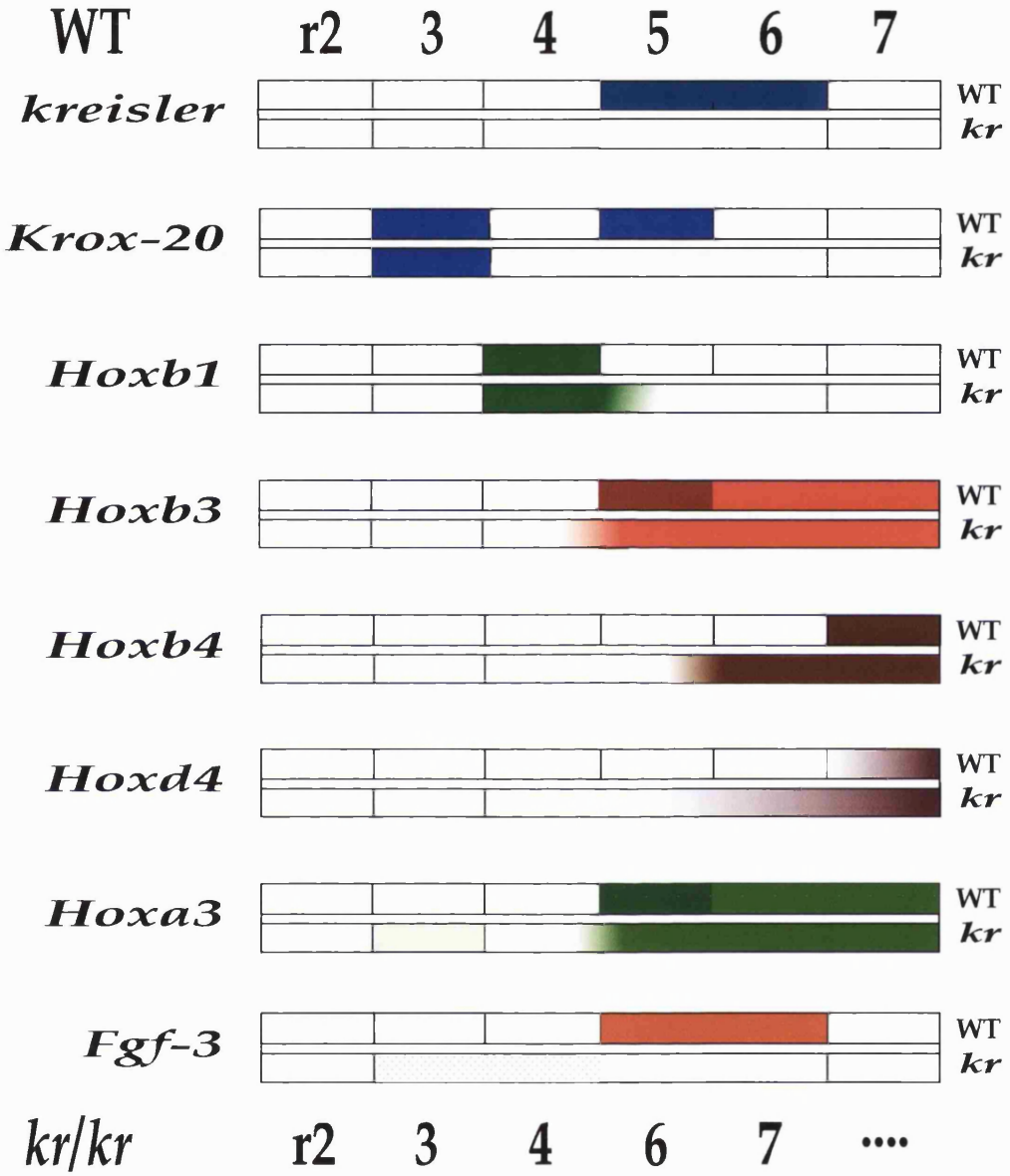

Figure IV.7. Diagrammatic summary of expression in wildtype and *kr* mutant hindbrains of some of the molecular markers previously used in analysing the *kreisler* mutant phenotype. *kreisler* (Cordes and Barsh, 1994); *krox20, hoxb1, hoxb3, hoxb4, Fgf-3* (Frohman *et al.*, 1993); *hoxa3, hoxd4* (McKay *et al.*, 1994). These expression patterns (with the single exception of *Fgf-3*) are all consistent with the presence of r6 in the *kreisler* mutant. Leaching of expression domains between r4 and r6 would be expected based on their similar *Eph/ephrin* expression profiles.

Figure IV.8. Diagrammatic summary of the interpretation of the *kreisler* mutant phenotype based on *Eph/ephrin* expression (*ephrin-B2* expression – data presented here; *EphB2* and *EphA4* expression data from (Becker *et al.*, 1994) and (Irving *et al.*, 1996) respectively). PS = 'protosegment' as proposed by (Moens *et al.*, 1996). Moens *et al.* suggest this is the common precursor of rhombomeres 5 and 6. Their interpretation suggests that, in *valentino* mutants, the protosegment does not undergo further differentiation into mature rhombomeres. Results presented here and in (Manzanares *et al.*, 1999) indicate that r6 is generated while r5 is absent. In the wildtype situation, the expression of *kreisler* and other unknown factors leads to the development of rhombomeres 5 and 6 out of their immature precursor region. In the absence of *kreisler*, r5 development is blocked and only r6 (influenced by unknown factors represented by the question mark) is produced from this region. The *Eph/ephrin* expression profiles provide a mechanistic basis to explain the cell mixing properties of segments from wildtype and *kreisler* mutant hindbrains. Cells from the *kreisler* mutant r6 have a typical *Eph/ephrin* expression profile for an even numbered rhombomere and have been shown to mix freely into wildtype rhombomeres 2 and 6 while being incapable of mixing with r5 cells (Manzanares *et al.*, 1999). If this segment was locked into its prorhombomeric r5/6 state, as suggested for the *valentino* mutant (Moens *et al.*, 1996), cells from it would not be expected to mix into either even or odd numbered rhombomeres.

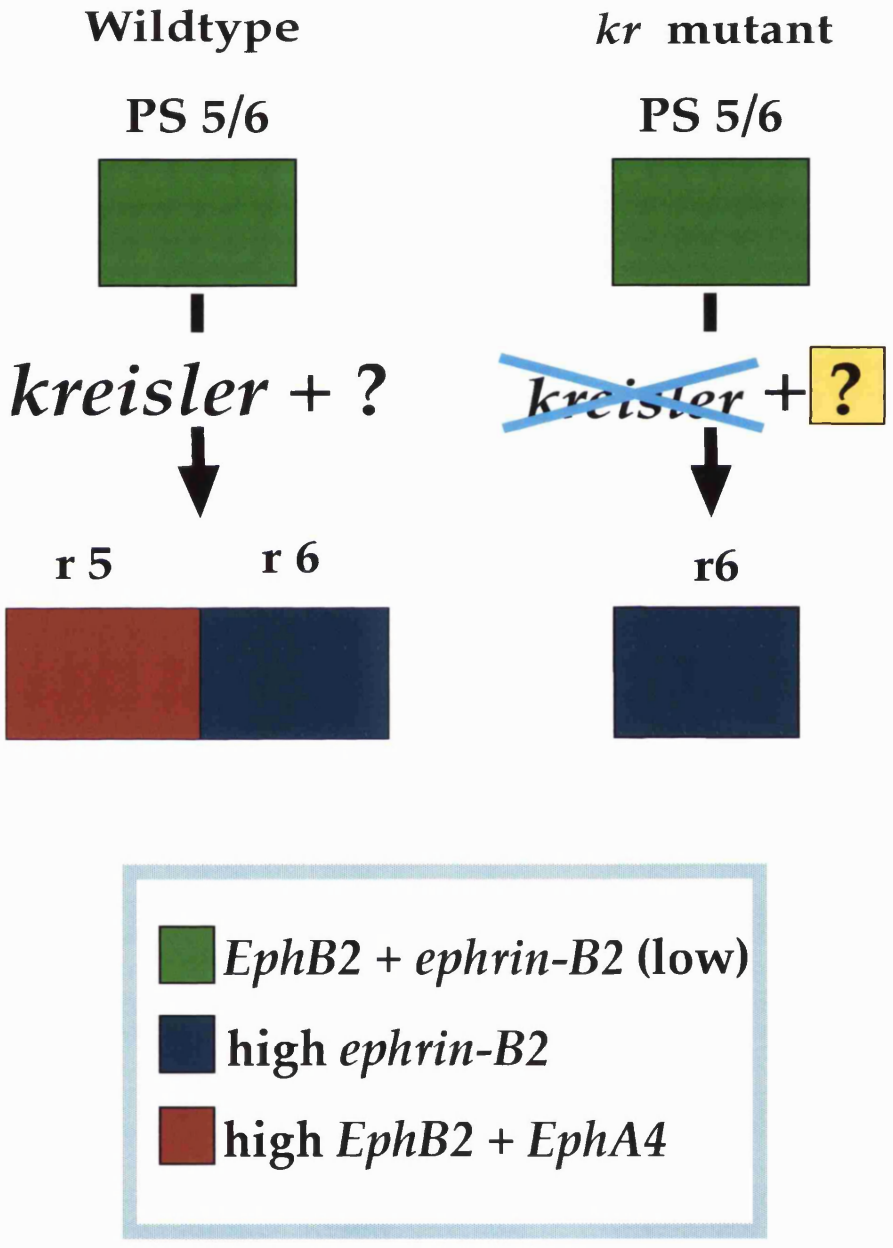
Wildtype
PS 5/6
kreisler + ?
r 5
r 6
kr mutant
PS 5/6
kreisler + ?
r6
EphB2 + ephrin-B2 (low)
high ephrin-B2
high EphB2 + EphA4

suggested that the loss of *val* function results in the failure of the 'r5/6 protosegment' to differentiate into rhombomeres 5 and 6 (Moens *et al.*, 1996). In the *val* mutant, this protosegment persists in a relatively undifferentiated state, developing some characteristics of both r5 and r6, but without fully maturing into either rhombomere. The apparent differences between the results in these two systems may be due to an actual difference between the functions of *kreisler* and *valentino*, which has been introduced through evolutionary time or may result from differences in experimental design.

With regards to the regulation of *ephrins -B2* and *-B3*, the results presented here clearly show that *kreisler* is not required for the upregulation or maintenance of their r6 expression domain as this persists in the *kr* mutant hindbrain. The possibility that *kreisler* represses *ephrin-B2/-B3* expression in rhombomere 5 was addressed by the analysis of *kreisler*$^{3/5}$ mice which ectopically express *kreisler* in r3. Neither *ephrin-B2* nor *ephrin-B3* show abnormally low levels of expression in r3 in these mice, suggesting that (excepting the possible requirement for some regionally-restricted cofactor(s)) *kreisler* does not downregulate these *ephrins* in r5.

The downregulation of *ephrin-B2* expression in rhombomere 3 of *kr* mutants is interesting, if difficult to explain. It suggests a partial transformation of r3 towards r5 identity, agreeing with alterations in r3 noted in other studies. The r3 *Krox-20* expression profile is altered in *kreisler* mutants such that it resembles r5 in terms of its duration (Frohman *et al.*, 1993). Furthermore, weak ectopic r3 domains of *Hoxa3* and *Fgf-3* expression have been detected by *in situ* hybridisation in *kr* mutants (Frohman *et al.*, 1993). This has been confirmed in lacZ transgenic studies with *Hoxa3* r5/6 enhancer elements, where ectopic r3 expression is observed in heterozygous as well as homozygous embryos (Manzanares *et al.*, 1999b). The activation of the *Hoxa3* r5/6 enhancer in r3 of *kr* heterozygotes is particularly intriguing as this rules out the simple possibility of knock-on effects on segment identity resulting from the loss of r5. Together, these results suggest that the loss of *kreisler* in r5 and r6 indirectly results in progressive changes to segmental identity in r3 correlated with the gene dosage.

The additional analyses carried out on *kreisler*$^{3/5}$ mice have addressed the identity of the apparently ectopic motor nucleus evident at the r4/5 boundary of these animals. The labelling of this nucleus in the progeny of crosses between *kreisler*$^{3/5}$ and HL5 mice demonstrates that this results from a block in the migration of cells of the facial motor nucleus from r4 into r5. The exact nature of this block is currently under investigation. One suggestion is that the abnormally prolonged expression of *kreisler* in r5 interferes with its further differentiation. In other words, *kreisler* must be downregulated to allow subsequent changes in gene expression and the cellular environment requisite for the passage of the facial motor neuron cells into rhombomere 5. The altered EphA4 protein levels shown in fig. IV.4 may be a reflection of this but, as with the effects on r3 in the *kr* mutant reported here and elsewhere, this result is difficult to interpret at present. Together, these results hint at an unknown role for *kreisler* in controlling genes involved in longer-range signalling during hindbrain development, which will require further work to elucidate.

The analysis of *Krox-20* mutant embryos has shown that it is required for the repression of *ephrin-B2* expression in at least rhombomere 5 and possibly in r3 also. Precedent exists to support a negative regulatory role for *Krox-20* in this context as it has also been found to be required for the specific downregulation of follistatin in r3 (Seitanidou *et al.*, 1997) (see section 1.5.2). The wildtype expression dynamics of *ephrin-B2* and *Krox-20* are also consistent with a negative regulatory relationship (see fig. IV.9). No indication presently exists as to whether this is a direct or indirect relationship. A negative regulatory role for *Krox-20* on *ephrin-B2* suggests a mechanism for the downregulation of *ephrin-B2* in r3 of *kreisler* mutants through the abnormally prolonged r3 *Krox-20* expression (Frohman *et al.*, 1993) in these animals. This would support a model for the generation of stripes of *ephrin-B2* expression in the hindbrain in which multiple enhancers control the very specific expression levels across the hindbrain. This is then repressed in rhombomeres 3 and 5 through the action of *Krox-20*.

Figure IV.9. A. Diagrammatic summary of the *ephrin-B2* time-course (data presented here) compared with *Krox-20* expression (data from Irving *et al.*, 1996). These expression patterns are consistent with negative regulation of *ephrin-B2* by *Krox-20* in rhombomeres 3 and 5. **B.** Model for the generation of complementary *Eph/ephrin* stripes. *ephrin-B2*, initially expressed throughout the hindbrain is subsequently downregulated by *Krox-20* in rhombomeres 3 and 5. Simultaneously, *EphA4* is upregulated in these rhombomeres, thus ensuring complementary ligand/ receptor expression domains.

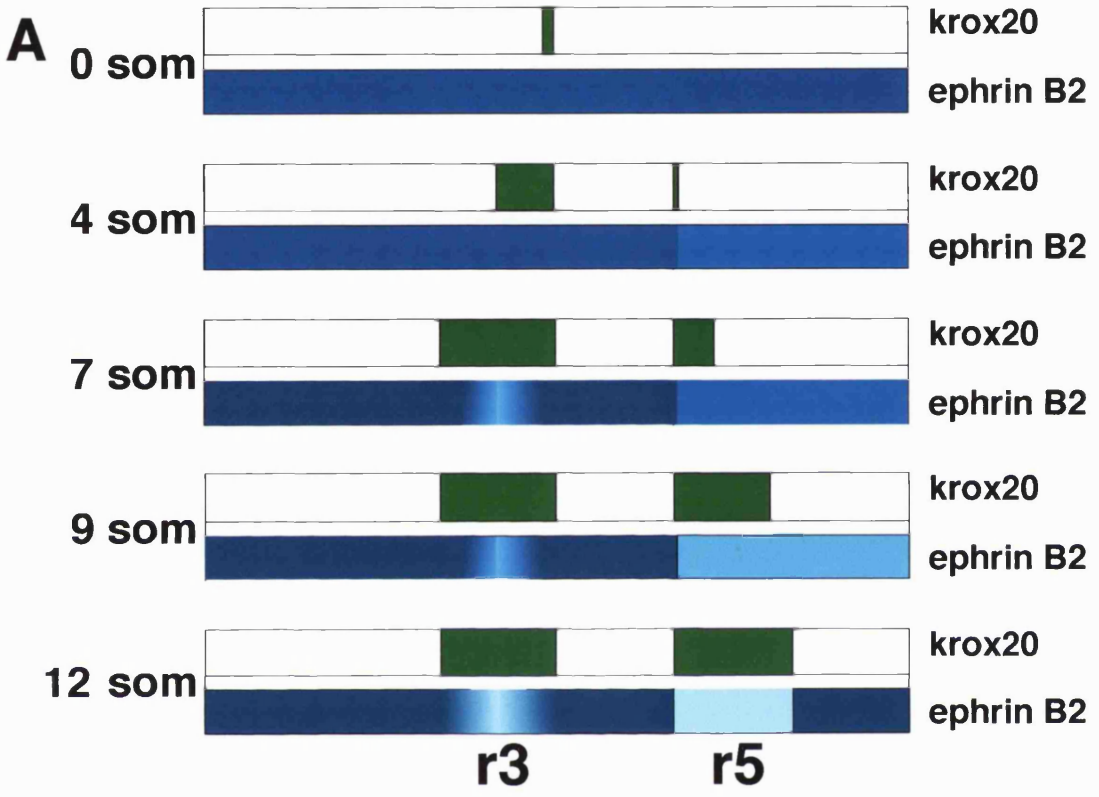
A
0 som
krox20
ephrin B2
4 som
krox20
ephrin B2
7 som
krox20
ephrin B2
9 som
krox20
ephrin B2
12 som
krox20
ephrin B2
r3
r5

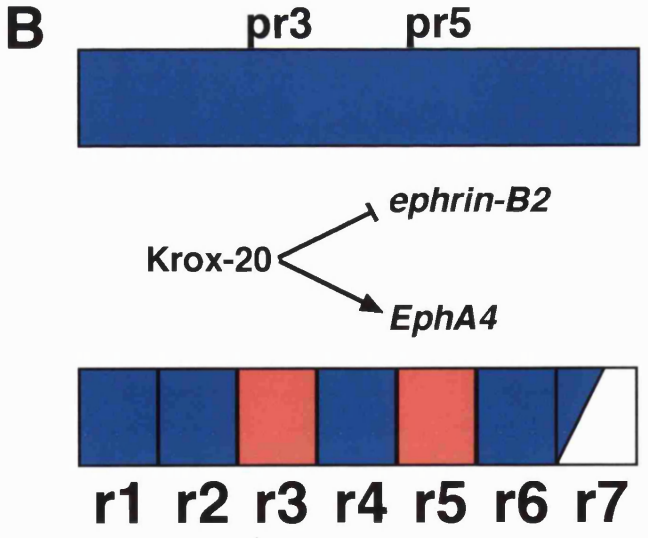
B
pr3
pr5
ephrin-B2
Krox-20
EphA4
r1 r2 r3 r4 r5 r6 r7

Positive regulation of the receptor (as has been established for *EphA4* (Theil *et al.*, 1998) and negative regulation of the ligand (in these rhombomeres, as shown here for *ephrin-B2*) would represent an elegant means of generating complementary receptor-ligand expression domains. Such a speculative model is illustrated in fig. IV.9 B.

It has also been shown here that the single loss of either *Hoxa1* or *Hoxb1* does not affect the upregulation of *ephrin-B2* in rhombomere 4. It would be extremely interesting to know the situation in the double mutant to determine definitively whether these *Hox* genes regulate *ephrin-B2*. None of the known markers of r4 identity which have been looked at are expressed in what remains of rhombomere 4 in the *Hoxa1/b1* double mutant (Studer *et al.*, 1998) (see section 1.5.1).

Chapter 5 – Retinoids in *ephrin* regulation

5.1 Introduction

Retinoids play a central role in hindbrain development (see section 1.3). Severe disruptions in hindbrain patterning are caused by either excess or deficient retinoid signalling (references in section 1.3.3). The nature of the disruptions caused in each case is distinct, but complementary and is manifested as a posteriorisation of rostral rhombomeres or an anteriorisation (or deletion) of caudal rhombomeres respectively. The effects of retinoids on hindbrain patterning are direct, through interactions with key regulatory factors such as *Hoxa1* and *Hoxb1*. Given the known role of retinoids in the regulation of these determinants of segmental identity, it is an attractive possibility that they may also be involved in regulating the *ephrin*s. This would provide a link between A–P identity and cell-intermingling restrictions similar to that of *Krox-20*, which is known to regulate both *Hox* genes and *EphA4* (see section 1.5.2). The hypothesised regulation of *ephrin*s by retinoic acid is supported by the cloning of *ephrin-B1* in a screen for retinoic acid-responsive genes from an embryonal carcinoma cell line (Bouillet *et al.*, 1995). In order to investigate the role of retinoic acid in the regulation of *ephrin-B2*, zebrafish embryos were exposed either to exogenous retinoic acid or to a retinoic acid antagonist (BMS 493) known to block all RAR receptor isotypes (P. Chambon, pers. comm.)

5.2 Analysis of retinoic acid/antagonist-treated embryos

Zebrafish embryos were collected and treated either with all-*trans*-retinoic acid (RA) or BMS 493 (as described in Materials and Methods, sections 2.12.1 and 2.12.2). The effects on hindbrain patterning at the 15 somite stage were examined by *in situ* analysis of *ephrin-B2*, *Krox-20* and *Hoxb1* expression.

The hindbrain phenotype induced by treatment with exogenous retinoic acid has been well documented (see section 1.3.3.1ii). The experiments were repeated here to facilitate comparison with BMS 493-

treated embryos and also because the effects on *ephrin-B2* and *Hoxb1* (in zebrafish) expression had not previously been documented. The effects of retinoic acid treatment on *Krox-20* and *Hoxb1* hindbrain expression are shown in fig. V.1. As has been demonstrated previously (Holder and Hill, 1991; Hill *et al.*, 1995), retinoic acid treatment causes truncations in neural tissues rostral to the hindbrain and also the failure of rhombomeres 1–3 to form morphologically distinct units. Nevertheless, neuronal derivatives of these rhombomeres do form (Holder and Hill, 1991; Hill *et al.*, 1995). As noted in earlier studies (Hill *et al.*, 1995), *Krox-20* expression in the RA-treated hindbrain is always preserved in r5, but is often reduced to two lateral spots in rhombomere 3 (fig. V.1B, C). Zebrafish *Hoxb1*, as in other vertebrate models, is expressed in rhombomere 4 (Prince *et al.*, 1998). Embryos treated with retinoic acid and examined at the 15 somite stage present patchy ectopic *Hoxb1* expression in r3, r2 and often further rostral (fig. V.1E, F). The effects of BMS 493 treatment on *Krox-20* and *Hoxb1* expression are shown in fig. V.2. The most immediately obvious feature of the resulting phenotype is an expansion of rhombomere size along the A–P axis, noted for both markers. Ectopic *Krox-20* expressing cells are often observed in rhombomere 2 and sometimes in r4 and r6 (fig. V.2A–C). Misdirected streams of *Krox-20*-expressing neural crest are also noted. Patchy ectopic *Hoxb1* expression is observed in rhombomeres 5 and 6, while r4 expression (apart from the increase in its total area) is unaffected (fig. V.2F–H).

Zebrafish *ephrin-B2* expression differs somewhat from that seen in the mouse. The wildtype expression pattern at the 15 somite stage is shown in fig. V.3 B. High level expression is observed in r1, with slightly lower-level expression in rhombomeres 4 and 7. There are low level expression domains in r2 and r6 and expression is very low or absent from rhombomeres 3 (low level in posterior r3) and 5. There is strong expression lateral to the neural tube in a population which may be neural crest adjacent to rhombomeres 2–4. The effects of retinoic acid treatment on *ephrin-B2* expression are shown in fig. V.3 A. While the r4, 5 and 6 expression domains appear to be normal, expression equivalent to that seen in r4 extends

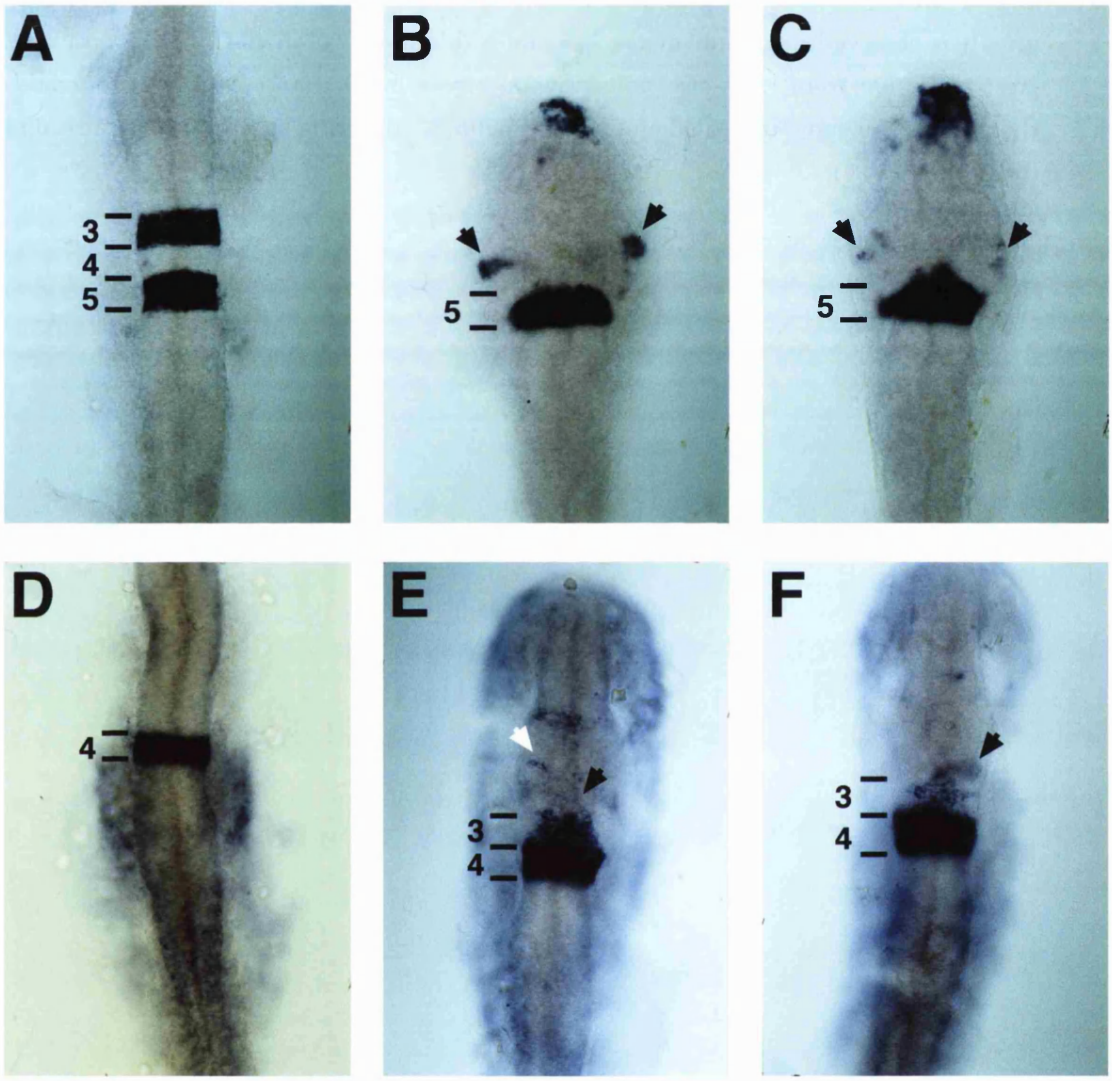

Figure V.1. Expression of *Krox-20* (**A–C**) and *Hoxb1* (**D–F**) in wildtype (**A, D**) and retinoic acid-treated (**B, C, E, F**) embryos at 15 somite stage. r3 *Krox-20* expression is downregulated in treated embryos, often becoming restricted to two lateral spots (black arrows in **B** and **C**). Expression in r5 is not affected, although the shape of the rhombomere is sometimes altered. Severe truncations in anterior neural structures are noted. Ectopic *Hoxb1* expression is observed in rhombomeres rostral to r4 in treated embryos. This is generally patchy and extends into r3, r2 and occasionally further anterior (black and white arrows in **E**). Consolidated patches of expression are sometimes observed in r2 (black arrow in **F**).

Figure V.2. Expression of *Krox-20* (**A–D**) and *Hoxb1* (**E–H**) in wildtype (**D, E**) and embryos treated with BMS 493 from 50% epiboly. Embryos are at the 15 somite stage and all photographs were taken at the same magnification (200X). Large increases in the A–P extent of labelled rhombomeres are observed in treated embryos. Ectopic *Krox-20* expressing cells are often observed in rhombomeres 2, 4 and 6 (black arrows in **A–C**) and aberrant neural crest migration from r5 is also noted (white arrow in **C**). *Hoxb1* expression spreads into rhombomeres 5 and 6 in treated embryos, sometimes appearing as a band of expression in r6 (black arrow in **F**).

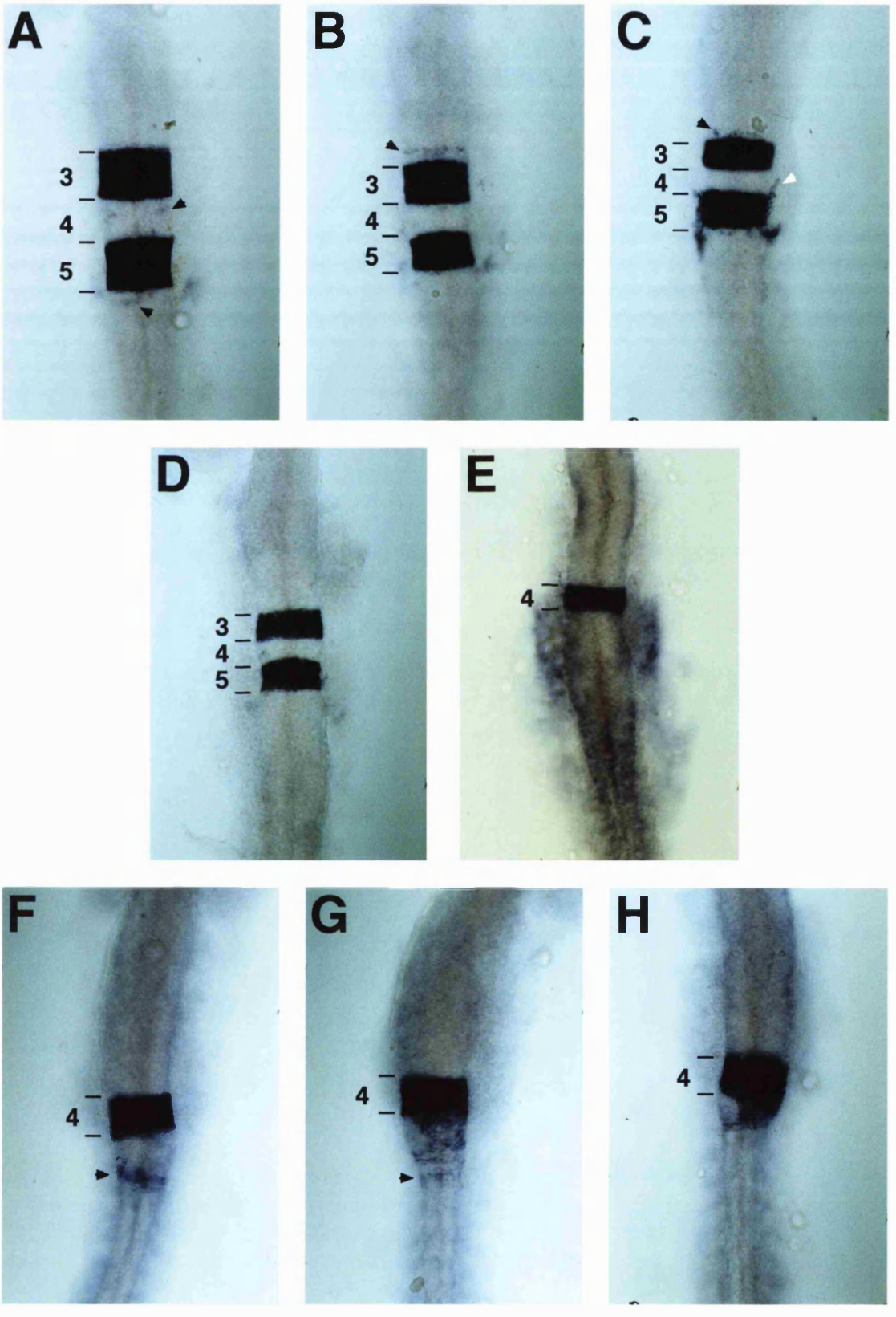
A
3
4
5
B
3
4
5
C
3
4
5
D
3
4
5
E
4
F
4
G
4
H
4

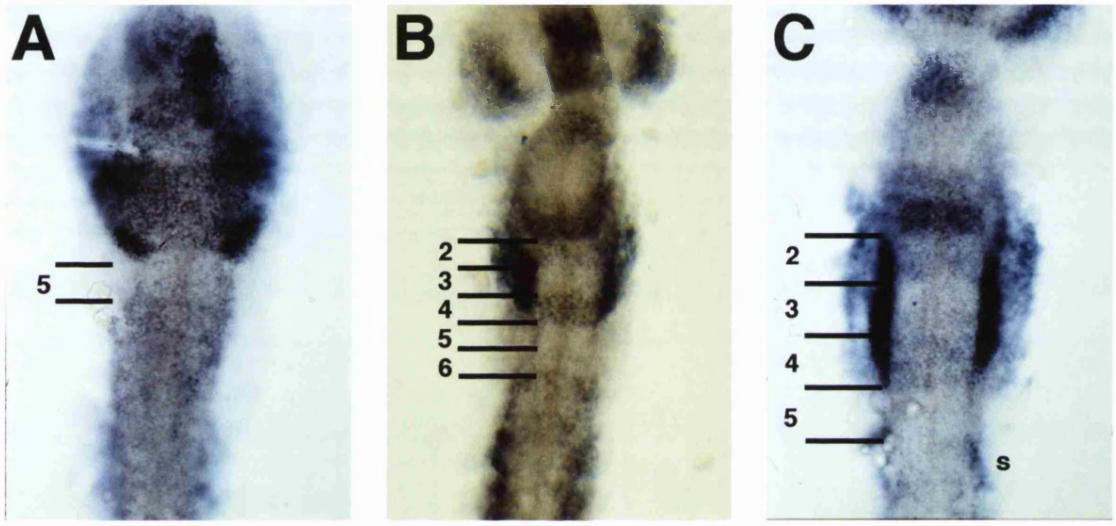

Figure V.3. *ephrin-B2* expression in wildtype (**B**), retinoic acid-treated (**A**) and BMS 493-treated (from 50% epiboly) (**C**) embryos at the 15 somite stage. Wildtype hindbrain expression is observed in at high levels in r1, slightly lower in rhombomeres 4 and 7, lower in r2 and r6, very low in posterior r3 and undetectable in anterior r3 and r5. The strongest region of expression is in the cell population lateral to r2–4. In retinoic acid treated embryos, expression is raised to uniformly high levels rostral to r5. In BMS 493-treated embryos, the expression domains corresponding to r7 and possibly also r6 are absent, with somitic expression (**s**) closely abutting r5. Rhombomeres 2–5 have expanded along the A–P axis as has the population lateral to r2–4. Expression in r4 appears to be downregulated compared to wildtype levels. (See also fig. V.7 for a comparison between the *ephrin-B2* and *Krox-20* expression domains.)

throughout the rostral hindbrain. In animals treated with BMS 493, the same expansion of rhombomeres along the A–P axis is noted for *ephrin-B2* (fig. V.3 C) as for *Krox-20* and *Hoxb1* (fig. V.2). Relative changes in expression levels are also noted, suggestive of alterations in A–P identity. Expression in r4 is reduced relative to that in r1 such that it more closely resembles that seen in r2. The high-level r7 domain is absent and somitic expression is closely juxtaposed to r5 – indicating the deletion of caudal rhombomeres.

In order to address the possibility that retinoid signalling occurring before 50% epiboly was making a significant contribution to hindbrain patterning in embryos treated with BMS 493 at this stage, earlier and more prolonged treatments were also carried out (see Materials and Methods section 2.12.2). The effects on hindbrain patterning of BMS 493 treatment from pre-1000 cell stage until early somite stages are more pronounced than those following treatment from 50% epiboly (figs. V.4–V.6). The increase in rhombomere size along the A–P axis noted after 50% epiboly treatment is also observed following the pre-1000 cell treatment but the caudal hindbrain deletions appear to extend further rostrally. There is a range in severity of the phenotype amongst treated embryos, the most severe end of which is a near-total deletion of r5 and more caudal rhombomeres. This is apparent from examination of the expression patterns of *Krox-20* (fig. V.4) and *ephrin-B2* (fig. V.5). High-level, coherent *Krox-20* expression is always maintained in r3 (fig. V.4 C–F), although the rhombomere is often misshapen, and scattered *Krox-20* expressing cells are often observed in r4. The r2/3 boundary also tends to be fuzzy and poorly defined. Reductions in the extent of the r5 *Krox-20* stripe are noted which, in more severe instances, leave only a scattering of expressing cells (fig. V.4 F). These expression data are complemented by those from the examination of *ephrin-B2* and *Hoxb1* (figs. V.5 and V.6). As is the case with *Krox-20*, the extended period of BMS 493 treatment enhances the resulting phenotype and this ranges in severity within the treated population. The proximity of the r4 expression domain to somitic expression increases until they are directly abutting (fig. V.5 C, D), confirming the deletion of r5 and

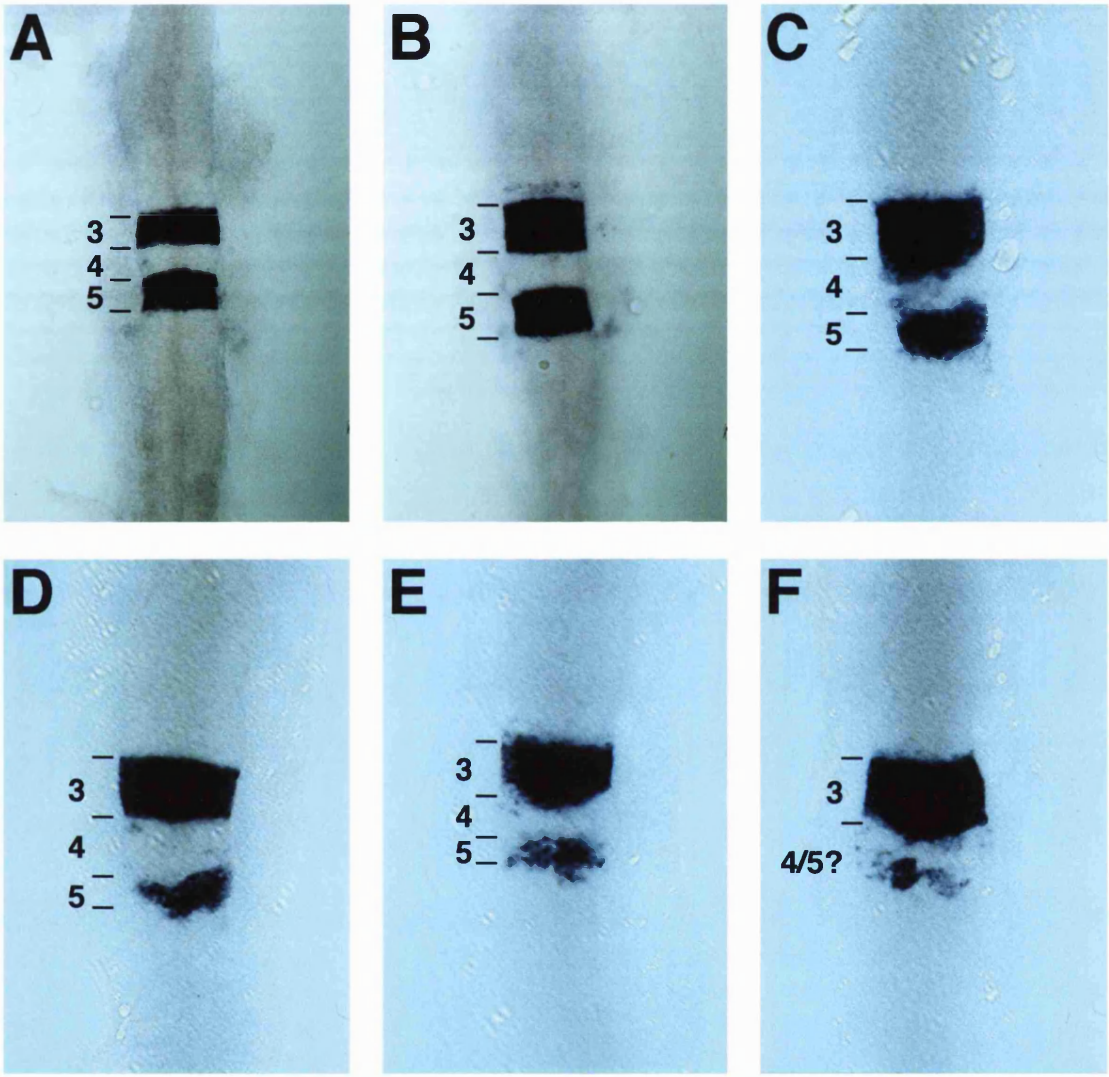

Figure V.4. *Krox-20* expression in wildtype (**A**), BMS 493 – 50% epiboly – treated (**B**) and BMS 493 – pre-1000 cell – treated (**C–F**) embryos (15 somite). The earlier and prolonged exposure to BMS 493 leads to more severe effects over and above those noted in fig. V.2. **C–F** reflect the variability of severity in effects within a treated population. In the most extreme cases, r5 expression is almost completely lost.

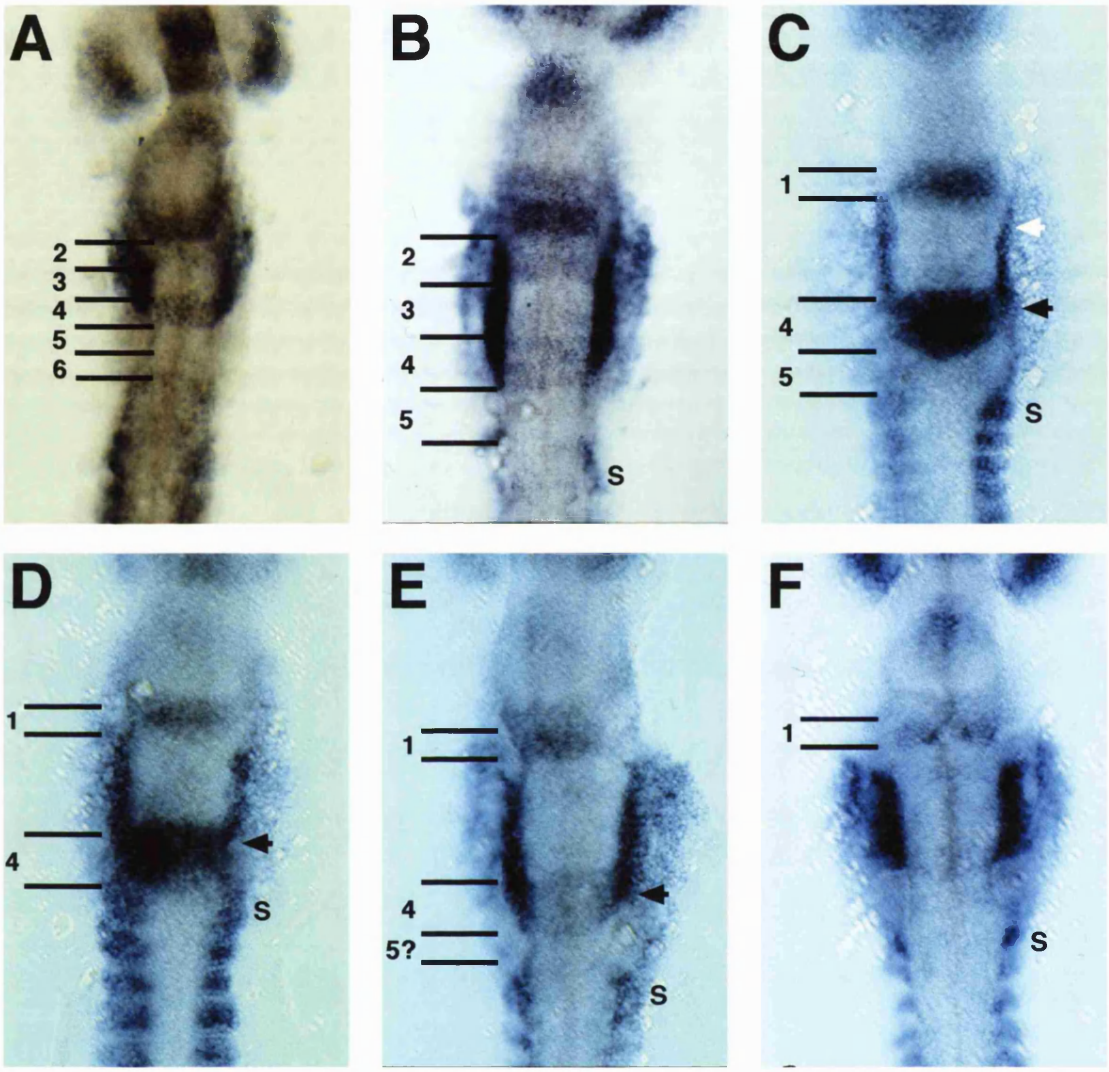

Figure V.5. *ephrin-B2* expression in wildtype (**A**), BMS 493 – 50% epiboly – treated (**B**) and BMS 493 – pre-1000 cell – treated (**C–F**) embryos (15 somite). The more rigorous BMS 493 treatment regime produces correspondingly more severe effects on *ephrin-B2* expression. Variability within the treated population is reflected by the embryos shown in **C–F**. Expression in r2 is downregulated below detectable levels (white arrow in **C**). In less severely affected embryos (**C, D**), r4 expression levels are enhanced above levels observed in both wildtype and 50% epiboly BMS 493-treated embryos. In more extreme cases (**E, F**), all hindbrain expression caudal to r1 is severely downregulated. In many cases, the population lateral to r2–4, which normally extends the full length of these rhombomeres, does not extend to the posterior end of the *ephrin-B2* r4 stripe (black arrow in **C–E**). **s** = somitic expression.

more caudal rhombomeres suggested by the *Krox-20* expression pattern. Further alterations in relative expression levels between the remaining rhombomeres are also noted. Relative to expression in r1 and the lateral staining adjacent to rhombomeres 2–4, r2 expression diminishes to the point where it can no longer be detected (fig. V.5 C, D). Expression levels in r4 (relative to the same standards) are often increased above wildtype levels. In more extreme instances (fig. V.5 E, F), *ephrin-B2* expression is dramatically reduced throughout the hindbrain, to the point where it is almost undetectable above background levels. Even in the most severely affected embryos, the intensity of expression in the lateral population is not affected, although it does not extend along the full length of the r4 stripe in some cases (fig. V.5 C–E). This serves both as an internal control for the *in situ* hybridisation and as a marker for the location of rhombomeres 2–4 as this population is invariably found at the same axial level. The effects on *ephrin-B2* expression in rhombomere 4 are confirmed by analysis of *Hoxb1* expression, which is known to be regulated by retinoids (fig. V.6). In the most severely affected examples, *Hoxb1* r4 expression is reduced to two lateral spots. In contrast to embryos treated at 50% epiboly, the overall length of the hindbrain – from the r1 stripe to the most anterior somitic expression – does appear to be slightly reduced in embryos subjected to the more prolonged treatment (compare figs. V.5 A, B and D).

5.3 Discussion

The widespread involvement of retinoids in hindbrain patterning along with the specific finding that *ephrin-B1* is a retinoid-responsive gene (Bouillet *et al.*, 1995) gave good grounds to suspect a role in *ephrin* regulation. The results of experiments presented here confirm this hypothesis and give added insights into the mechanisms which underlie hindbrain patterning.

In agreement with earlier studies, retinoic acid treatment leads to a partial transformation of rhombomere 2 towards r4 identity. This is supported by the appearance of *Hoxb1* expressing cells in r2 (fig. V.1) and the upregulation of *ephrin-B2* in this rhombomere such that it more closely

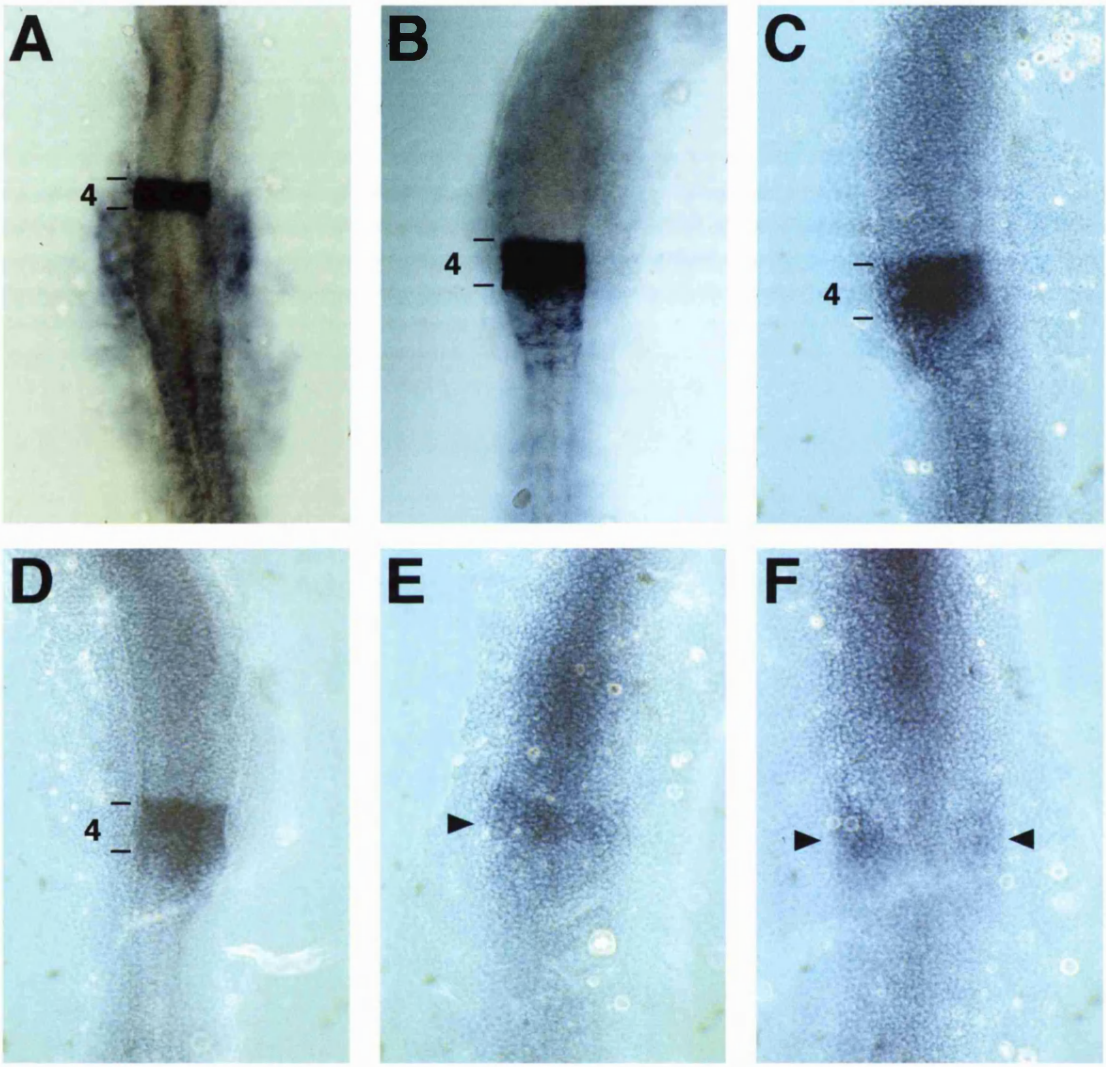

Figure V.6. *Hoxb1* expression in wildtype (**A**), BMS 493 – 50% epiboly – treated (**B**) and BMS 493 – pre-1000 cell – treated (**C–F**) embryos (15 somite). In embryos treated with BMS 493 from pre-1000 cell stages, *Hoxb1* expression levels appear to be reduced compared to wildtype as the *in situ* hybridisations needed to be highly developed in order to detect it. Variation of severity in effects is noted with r4 expression being reduced to weak lateral spots in the most extreme cases (black arrows in **F**).

resembles wildtype r4 levels (fig. V.3). The patchy appearance of *Hoxb1* expression in r2 of RA-treated embryos suggests a more limited r2 to r4 transformation than that reported in the mouse embryo (Marshall *et al.*, 1992). It is possible that this expression may be strengthened at later stages through the establishment of the *Hoxb1* autoregulatory loop (Pöpperl *et al.*, 1995; Studer *et al.*, 1998). Earlier work has revealed differences in the extent of the r2 to r4 transfomation following RA-treatment in mice and zebrafish. Hill and colleagues noted that a hybrid rhombomere was found in the location of r2 which retains some features of r2 and gains some of r4 (Hill *et al.*, 1995). The *Hoxb1* expression observed in r3 following RA-treatment in this study has also been noted in previously published work (Morriss-Kay *et al.*, 1991; Wood *et al.*, 1994). In the mouse, this has been found to be subsequently downregulated, leaving expression in r2 and r4 (Wood *et al.*, 1994; Marshall *et al.*, 1992). It seems probable that this will also be the case in zebrafish. The reduction of r3 *Krox-20* expression to two lateral spots (fig. V.1) agrees with the results of earlier studies (Hill *et al.*, 1995) and, along with the appearance of *Hoxb1* expression in r3, suggests a partial transformation of this rhombomere towards r4 identity at the stage examined (Morriss-Kay *et al.*, 1991; Wood *et al.*, 1994). It is interesting to note the absolute correlation between *Krox-20* expression and *ephrin-B2* repression which persists in retinoic acid-treated embryos (fig. V.7). The downregulation of *Krox-20* expression in r3 coincides with the upregulation of *ephrin-B2*, adding further support to the conjecture that *Krox-20* negatively regulates *ephrin-B2* (see section 4.5).

As discussed in section 1.3.3.2, numerous approaches have been used in different experimental systems to interfere with retinoid signalling and determine the effects on hindbrain development. The most complete absence of retinoid signalling is seen in the retinoid-deficient quail embryos produced by Maden and colleagues (Maden *et al.*, 1996; Gale *et al.*, 1999). This may perhaps be regarded as the achievable endpoint of retinoid signalling reduction and the phenotype – expansion of r1–3 and loss of rhombomeres

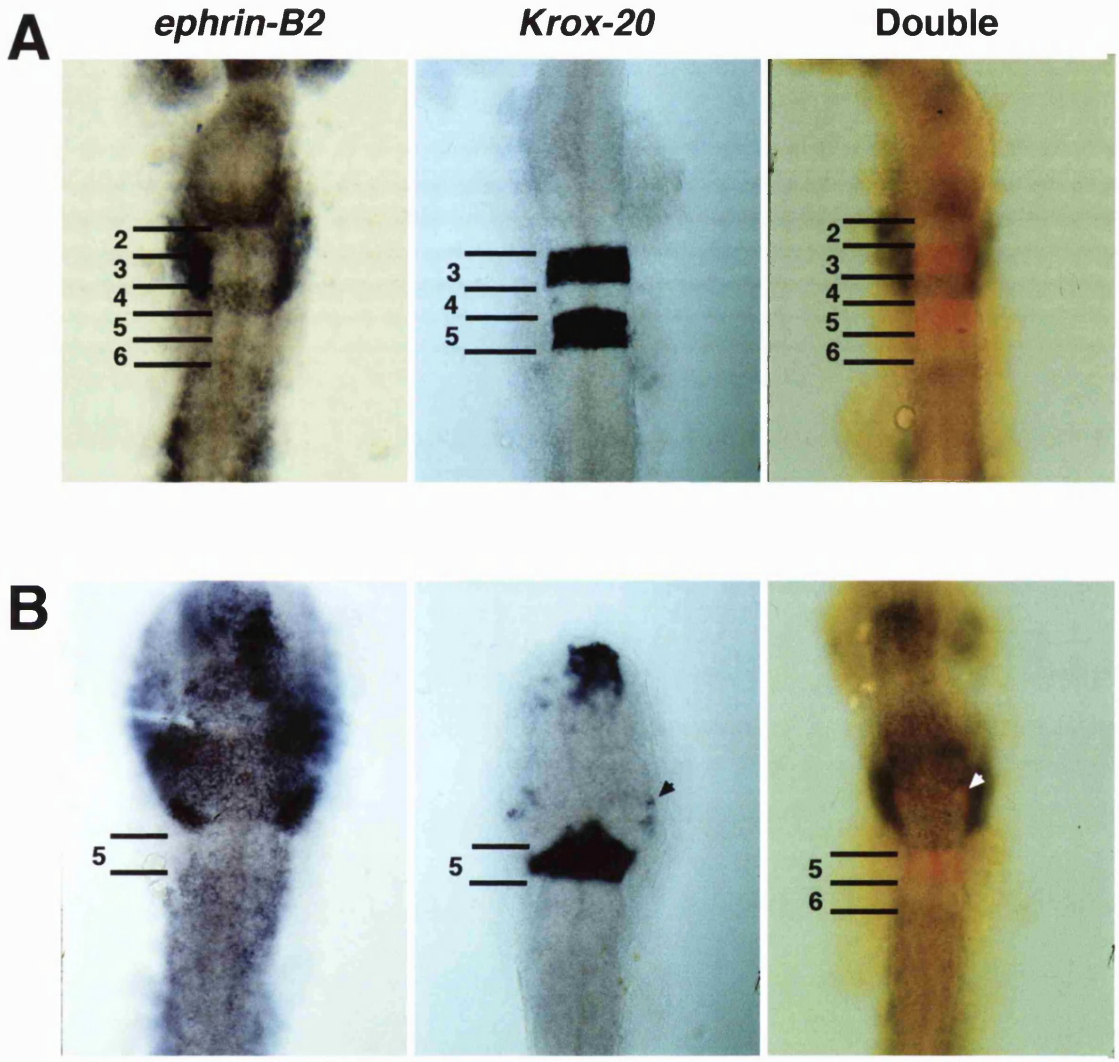

Figure V.7. Comparison of *ephrin-B2* and *Krox-20* expression in wildtype (**A**) and retinoic acid-treated (**B**) embryos. Domains of high level *ephrin-B2* expression and *Krox-20* expression are mutually exclusive as observed in the respective single and double *in situ* hybridisations. In the doubles, *Krox-20* expression is stained in red and *ephrin-B2* in brown.

4–7 – as the most extreme possible. Other methods – such as the overexpression of retinoic acid metabolising enzymes or dominant negative retinoic acid receptors in *Xenopus* embryos (Hollemann *et al.*, 1998; Kolm *et al.*, 1997; van der Wees *et al.*, 1998), or the targeted disruption of retinoic acid synthesising enzymes or receptors in mice (Niederreither *et al.*, 1999; Lohnes *et al.*, 1994; Dupé *et al.*, 1999) – more or less closely approach this endpoint, depending on their efficacy in reducing overall retinoid signalling. This gradation of phenotype is also observed between the two BMS 493 treatment regimes employed in this study. There are several advantages in using a chemical retinoid antagonist on zebrafish embryo for retinoid-blocking experiments. Firstly, there is the ease of accessibility and application of the agent inherent to the zebrafish system. The second advantage is in overcoming the uncertain perdurance of injected RNA. The third advantage relates to BMS 493 specifically, as it is reported to block all RAR isotypes (P. Chambon, pers. comm.), thus circumventing the difficulties surrounding redundancy and compensation between individual receptors encountered when injecting a dominant-negative version of any given member.

50% epiboly was initally selected as the point for beginning BMS 493 treatment as this had previously been determined as the optimal time point for retinoic acid treatment in inducing the hindbrain phenotype (Holder and Hill, 1991). Embryos have entered gastrulation at this stage, reaching the point of maximum hindbrain-sensitivity to retinoids in other vertebrate species (Durston *et al.*, 1989; Morriss-Kay *et al.*, 1991). Zebrafish embryos treated with BMS 493 from 50% epiboly present with deletions of caudal rhombomeres, alterations in the size of the remaining rhombomeres and differences in relative expression levels along the A–P axis of at least one *ephrin*. The deletion of caudal rhombomeres is indicated by analysis of the *ephrin-B2* and *Krox-20* expression patterns (figs. V.2 and V.3). The absence of the normal r7 expression domain and the close juxtaposition of r5 *Krox-20* expression with somitic *ephrin-B2* expression suggests the deletion of r7 at least. The fate of r6 is more difficult to determine, as *ephrin-B2* is normally expressed at low levels in r6 (fig. V.3 B). *ephrin-B2* expression in r4 of treated embryos appears to be reduced compared with wildtype levels and

expression in surrounding tissues (fig. V.3 C). Its close resemblance to r2 expression levels may indicate a partial anteriorisation of this rhombomere towards r2 identity.

The appearance of ectopic *Krox-20* expressing cells in rhombomeres adjacent to r3 and r5 and misdirections of neural crest migration (fig. V.2) are reminiscent of effects seen following injection of dominant negative RARβ in *Xenopus* embryos (van der Wees *et al.*, 1998). This type of defect is also observed following disruptions of Eph/ephrin signalling (Xu *et al.*, 1995; Smith *et al.*, 1997), a correlation suggestive of a link between retinoid signalling and Eph/ephrin regulation. The altered rhombomeric expression levels of *ephrin-B2* described above may contribute to a partial breakdown in the restriction of cell intermingling between rhombomeres.

Hoxb1 expression expands from r4 into more posterior rhombomeres, occasionally appearing as a discrete band in what remains of r6 (fig. V.2). This too is suggestive of anterior transformations within the caudal rhombomeres, although the continued strong r4 expression of *Hoxb1* indicates that this aspect of its identity is maintained despite the reduced levels of *ephrin-B2* expression noted above. These results suggest that rhombomeres may often be of mixed identity following this treatment. The enlargement of the remaining rhombomeres to fill the normal area occupied by the hindbrain is also interesting. This accords with the finding in other studies (Maden *et al.*, 1996; Gale *et al.*, 1999; Niederreither *et al.*, 2000; Kolm *et al.*, 1997) but see (van der Wees *et al.*, 1998) that the specification of generic hindbrain fate and its extent in the neural tube are set by mechanisms independent from those involved in hindbrain segmentation.

The persistence of r5 *Krox-20* expression in embryos treated with BMS 493 at 50% epiboly suggested that a significant level of retinoid signalling was still occurring. In both the retinoid-deficient quail embryo (Maden *et al.*, 1996) and the *Raldh2* mutant mouse (Niederreither *et al.*, 2000), rhombomere 5 is absent and in the quail system r4 is also missing. I therefore altered the treatment regime in an attempt to reduce this residual signalling level by exposing the embryos to BMS 493 from the pre-1000 cell stage onwards. This prolonged treatment did enhance the hindbrain phenotype (figs. V.4 and

V.5). Within treated populations and between treatment regimes there was a gradation in the severity of the phenotype apporoaching the endpoint set by the retinoid-deficient quail or the *Raldh2* mutant mouse. r5 *Krox-20* expression was severely reduced and nearly eliminated in some cases (fig. V.4), indicating the loss of r5 fate. This is supported by the analysis of *ephrin-B2* expression which, in less severely affected examples, shows close juxtaposition of rhombomere 4 and somite expression (fig. V.5). Further differences in rhombomeric expression levels of *ephrin-B2* over and above those seen following 50% epiboly treatment suggest an important role for retinoids in the regulation of this gene. In less severely affected embryos, expression is not detected in r2 while it actually appears to be enhanced above wildtype levels in r4 (fig. V.5 C, D). In more severely affected embryos, *ephrin-B2* expression is almost completely elimintated from the hindbrain (fig. V.5 E, F), indicating that retinoid signalling is essential for *ephrin-B2* expression. Even in the most extreme instances (fig. V.5 F), expression is maintained in r1 (although at a reduced level) and r1 also appears to be refractive to the size increase noted in other rhombomeres. This points to a dependence on other signalling pathways (most likely isthmic in origin) for r1 development (Wassef and Joyner, 1997; Wingate and Hatten, 1999; Irving and Mason, 2000). Intriguingly, *ephrin-B2* expression in the midbrain itself is altered as two domains are absent following pre-1000 cell treatment (fig. V.5 E, F).

The high-level *ephrin-B2* expression domain adjacent to rhombomeres 2, 3 and 4 may represent a neural crest cell population. This is consistently labelled to a high degree, regardless of treatment applied, and is always found laterally to the same rhombomeres. As mentioned above, this serves as a useful internal control and axial marker. It also demonstrates that *ephrin-B2* is regulated by separate mechanisms in the hindbrain and neural crest (assuming this population is in fact crest), a feature also noted for some *Hox* genes, e.g. (Saldivar *et al.*, 1996; Mallo and Brändlin, 1997; Trainor and Krumlauf, 2000).

Figure V.8. Summary of the effects of BMS 493-treatment on hindbrain patterning. The diagrammatic representations on the left include the *ephrin-B2* expression pattern, *ephrin-B2* expression is shown in the middle and *Krox-20* on the righthand side. **A.** Wildtype. **B.** 50% epiboly BMS 493 treatment. **C, D.** Pre-1000 cell stage BMS 493 treatment.

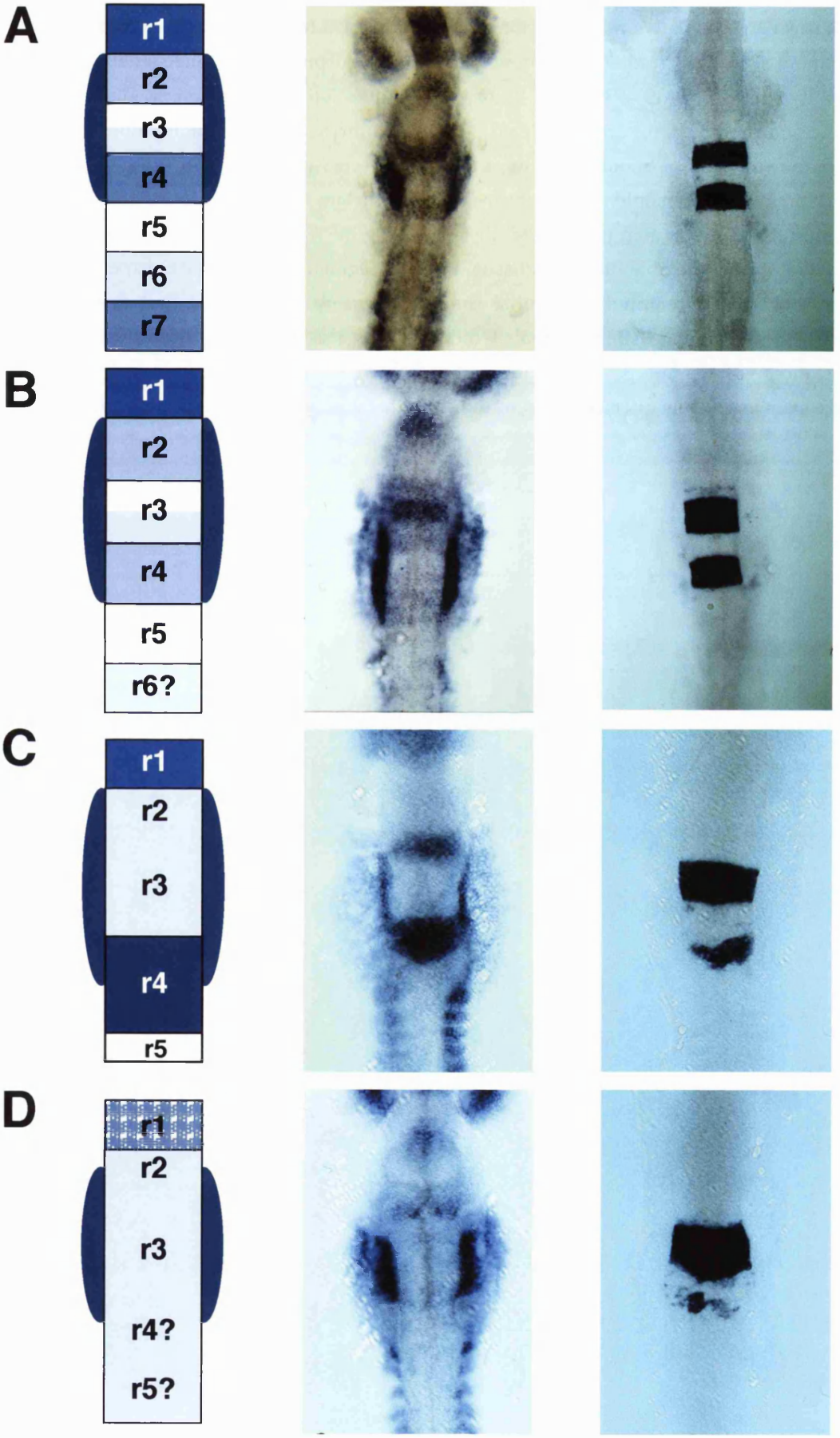
A
r1
r2
r3
r4
r5
r6
r7
B
r1
r2
r3
r4
r5
r6?
C
r1
r2
r3
r4
r5
D
r1
r2
r3
r4?
r5?

Figure V.9. Speculative model for the effects of BMS 493 treatment on hindbrain patterning. The retinoid signalling gradient is represented in blue and putative isthmic signals in orange in **A.** wildtype and **B.** BMS 493-treated embryos. The question of rhombomeric identity is left aside here and rhombomeres are considered purely in numerical order from anterior to posterior. The effect of blocking retinoid signalling may be to decrease the angle of the gradient across the hindbrain. The threshold levels which somehow dictate the extent of individual rhombomeres would then be separated by a greater distance along the A–P axis, extending rhombomere length to take up the available hindbrain tissue. Links to segment identity must also exist as the higher threshold levels required for caudal rhombomeres are not reached and these domains are consequently absent. Isthmic signals would perhaps also be expected to diffuse over a greated distance, with the interposition of fewer rhombomere boundaries. The maintenance of normal r1 size even in severely affected embryos indicates that it is set by independent mechanisms.

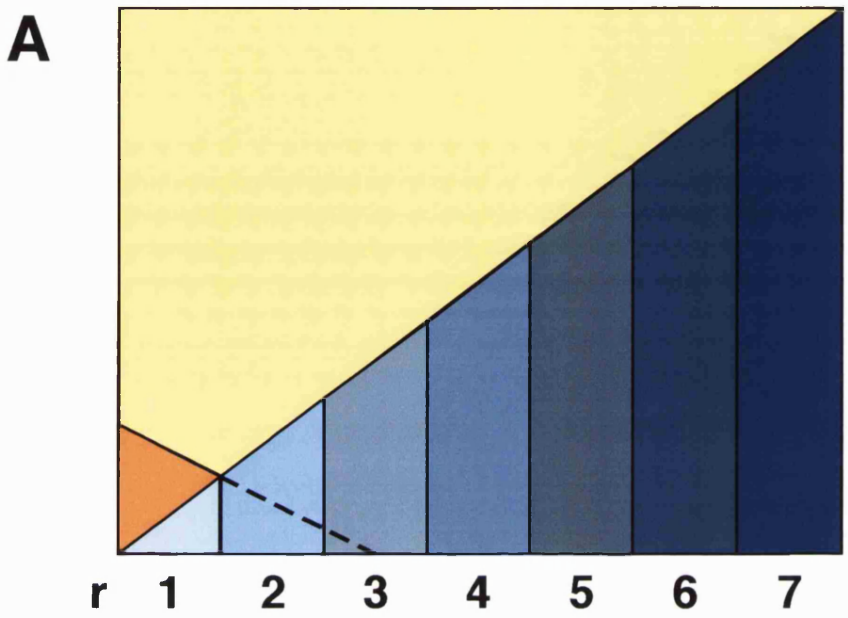
A
r 1 2 3 4 5 6 7

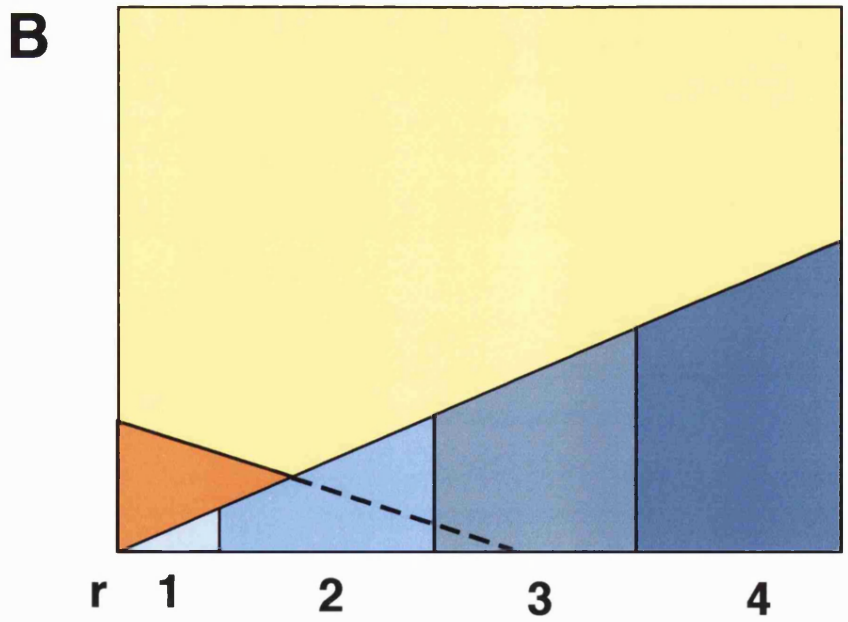
B
r 1 2 3 4

The effects of BMS 493 treatment on hindbrain patterning are summarised diagrammatically in fig. V.8 and a model is presented in fig. V.9 to account for the increase in rhombomere length on the basis of retinoid signalling levels.

Chapter 6 – Summary and future perspectives

6.1 The search for *ephrin-B2* regulatory elements

The work comprising this section of the project, while demanding the greatest amount of time and efffort, is essentially preliminary in nature. The key elements required to carry the work forward are now in place. A large amount of genomic DNA including and surrounding the *ephrin-B2* locus has been isolated in two PAC clones – 383-I11 and 548-N22 (section 3.3.2.1). The reason for selecting this approach was to maximise the probability of the isolated genomic fragments containing the relevant *ephrin-B2* regulatory elements, as these can be located tens of kilobases distant from the coding region. A strategy has been devised for the introduction of a *lacZ* reporter gene near the *ephrin-B2* start codon by the ET-cloning method of homologous recombination in bacteria and the plasmid constructs required to execute this method have been generated (sections 3.3.2 and 3.3.2.2). The efficacy of this approach has been proved in principle by the successful introduction of tetracycline resistance into both PAC clones (section 3.3.2.3). Technical difficulties have been encountered with the final step in this procedure – the introduction of the *lacZ* reporter in place of tetracycline resistance – but it should be possible to overcome these, beginning with the steps outlined in section 3.4. Following the successful completion of this step, the next will be the generation of transgenic mice by pronuclear injection with the modified PAC constructs and their analysis for *lacZ* expression. The production of transgenic animals with such large DNA fragments is reportedly no greater a technical challenge than standard procedures (M. Martinez pers. comm.). The continuation of this work should represent a fruitful line of future enquiry.

The time-course analysis of wildtype *ephrin-B2* expression (section 3.2) has revealed that its pattern and dynamics are more complex than suggested by previously published results (Bergemann *et al.*, 1995). Its dynamic spatiotemporal expression is reminiscent of that noted for *EphA4* (Irving *et al.*, 1996) and the *Hox* genes (e.g. Gould *et al.*, 1998), suggesting that it may be

regulated by similar mechanisms, with discrete early, late and segment-specific enhancer elements.

6.2 The analysis of candidate upstream genes

The other approach to identifying factors involved in *ephrin* regulation was the analysis of embryos mutant for genes whose known functions indicate a potential role. *Krox-20, kreisler, Hoxa1* and *Hoxb1* were all examined in this way. From these analyses, it has been determined that *kreisler* is not required for *ephrin-B2* expression in r6 (section 4.5) and that neither *Hoxa1* or *Hoxb1* are individually essential for expression in r4 or more caudal rhombomeres. The possibility remains that, in the absence of one of these *Hox* paralogues, the other functionally compensates for it. In order to test this, it is essential to examine the *Hoxa1/b1* double-mutant. I have been unable to do so, owing to the restricted availability of embryos from these lines, but double-mutant embryos should be ultimately obtainable.

Krox-20 has been shown to have a role in repressing *ephrin-B2* expression in rhombomeres 3 and 5 as novel high-level expression domains are observed in both rhombomeres prior to their disappearance in the *Krox-20* mutant (section 4.3 figs. IV.5 and IV.9). Several other pieces of evidence discussed below add support to this conjecture, but none give any indication as to the direct/indirect nature of this relationship. The definitive proof required can only come from the analysis of *ephrin-B2* regulatory elements. The link between *Krox-20* and *ephrin-B2* is an important one as it brings together the regulation of *ephrins*, *Eph* receptors (Theil *et al.*, 1998) and *Hox* genes (Sham *et al.*, 1993; Nonchev *et al.*, 1996) – co-ordinating the restriction of cell mixing across rhombomere boundaries with the determination of A–P identity in a single step.

In addition to eliminating it as a potential regulator of the *Eph/ephrins* examined in r6, the results from analysis of *kreisler* mutant embryos were also valuable in resolving outstanding questions regarding the *kr* phenotype (section 4.5 and Manzanares *et al.*, 1999b). The *Eph/ephrin* expression patterns examined in *kreisler* mutants demonstrate the continued presence of

rhombomere 6 (fig. IV.3). This indicates that *kreisler* is not absolutely required for the development of r6 as has been suggested in the mouse (McKay *et al.*, 1994) and as may be the case in the zebrafish embryo (Moens *et al.*, 1996). It would be of considerable interest to examine *Eph/ephrin* expression patterns in the *valentino* mutant. The finding that *ephrin-B2* expression is downregulated in r3 of *kr* mutants ties in with other previously reported changes in its molecular identity. Ectopic expression of *Hoxa3, Fgf-3* and abnormally prolonged *Krox-20* expression in r3 have all been observed in *kr* mutants (Frohman *et al.*, 1993; Manzanares *et al.*, 1999b). The finding reported here that *Krox-20* is required for repression of *ephrin-B2* in rhombomeres 3 and 5 provides a possible explanation for the sub-normal expression level in *kr* mutant r3.

The possibility of a role for *kreisler* in the repression of *ephrin* expression in r5 was investigated by analysis of embryos from the *kreisler*$^{3/5}$ line created by Thomas Theil. In this line, *kreisler* is misexpressed in rhombomere 3 under the control of the *EphA4* promoter (Theil *et al.*, manuscript in preparation). The finding that neither *ephrin-B2* or *ephrin-B3* are downregulated in r3 of these animals argues against negative regulation of these genes by *kreisler* in r5, although the requirement for a regionally-restricted cofactor cannot be excluded. The analysis of *kreisler*$^{3/5}$ embryos was extended to address the outstanding issue of an ectopic motor nucleus which intial findings suggested develops in r5. By crosses with *Hox* enhancer-driven *lacZ* transgenic lines and analysis of the resulting embryos (described in section 4.2.1), this nucleus was determined to be comprised of facial motor neurons arrested in their migration from r4 into r5. The exact nature of this block is currently under investigation in a collaborative effort with Linda Ariza-McNaughton in the laboratory of Robb Krumlauf.

6.3 Retinoids in *ephrin* regulation

The major role of retinoids in hindbrain patterning and the specific cloning of *ephrin-B1* as a retinoic acid-responsive gene (Bouillet *et al.*, 1995) made this an obvious candidate regulator of the *ephrins*. Results presented here from the

analysis of *ephrin-B2* expression following treatment with all-*trans*-retinoic acid and the retinoid antagonist, BMS 493, demonstrate a role in regulating *ephrin-B2*. The well-documented transformation of r2 towards r4 identity in retinoic acid-treated embryos has here been shown to include an upregulation of *ephrin-B2* (section 5.2). This may either be a direct effect, or indirect through other genes such as *Hoxa1/b1*. Again, this question could be partially resolved by the examination of *ephrin-B2* expression in a *Hoxa1/b1* double mutant to determine whether its regulation is independent of these genes in r4. Coincident with the downregulation of *Krox-20* in r3 of retinoic acid-treated embryos is the upregulation of *ephrin-B2* in this rhombomere (fig. V.6). This supports the role, noted above, of *Krox-20* in downregulating *ephrin-B2* expression in rhombomeres 3 and 5.

The near total elimination of *ephrin-B2* expression in the hindbrain of BMS 493-treated embryos demonstrates conclusively that retinoids are absolutely required for this expression. Again, as with the *Krox-20* result, whether this effect is direct or indirect can only finally be determined by transgenic analysis of the *ephrin-B2* promoter region. In any case, these results provide important clues about what to look for when carrying out this analysis.

The BMS 493 work has also produced some more general clues about hindbrain development. The progressive deletion of caudal rhombomeres and the respecification of hindbrain tissue by expansion of the remaining rhombomeres to take their place reveal the separability of mechanisms which specify hindbrain fate (fig. V.8) from those involved in patterning it. Again the central role of retinoids in hindbrain patterning is highlighted, while the specification of hindbrain fate is likely to be dependent on earlier signals from the mesoderm directing the regionalisation of the neural tube. The findings presented here could be extended by the examination of more molecular markers, such as *valentino*, *Fgf-3*, *Hoxa2* and *Hoxa3/b3*. Given a less restricted supply of BMS 493, it would also be of interest to test the effects of increasing antagonist concentration.

A general point that emerges from the studies undertaken here and by many others is the complexity which underlies the concept of rhombomere

identity. Many manipulations affecting hindbrain patterning – whether mutation of regulatory genes or their misexpression, by direct methods or indirectly through treatement with agents such as retinoic acid or BMS 493 – alter some aspects of rhombomeric identity, while leaving others unchanged. To what extent does a rhombomere have to be altered before it should be considered to have changed its identity to that of another rhombomere? To phrase the question differently, what is a suitable definition for rhombomere identity at this level? The obvious functional definition would relate to the structures which are ultimately derived from a given rhombomere. There is some doubt regarding the adequacy of this simple definition owing to the transient nature of rhombomeric organisation and intertwining of the fates of their derivatives. Subtle and temporary alterations in early molecular identity are often compensated for and masked at later stages in this robust developmental system. It may be that the concept of rhombomere identity at these stages is too broad to be rigorously defined. That is not to deny the usefulness of the concept as it does undoubtedly aid in grasping the complexity of hindbrain patterning. It was stated in the introduction that the study of hindbrain development is useful as an accessible microcosm of CNS development. It seems likely that the principles grasped through the study of the hindbrain will apply within the wider system. Perhaps the most striking feature is its robustness, achieved through overlap and compensatory mechanisms, which must be essential in the generation of so much complexity.

Appendix 1 – *ephrin-B2* cDNA sequence

(Bennett, B. D. *et al.*, 1995)

```
        10        20        30        40        50        60        70        80        90       100
CCCACGCGTCCGCGCGCGCTGAGGGACGCGCAGGGTGAGCGCACCTGGCCTCGGCGACCGCGGGAGCGGCGCGGCGTGTCCGCCCCGGAGGATTGGGGGT
GGGTGCGCAGGCGCGCGCGACTCCCTGCGCGTCCCACTCGCGTGGACCGGAGCCGCTGGCGCCCTCGCCGCGCCGCACAGGCGGGGCCTCCTAACCCCCA

                                                    >NcoI
                                                      |
       >EagI                                          >MscI
         |                                            ||
       110       120       130       140       150       160   ||  170       180       190       200
CGCTGCCCGCGGCCGGTCCCAACGCGTCCCGGAGTGCGCAGAACTGGGAGCGGCTTGGGCATGGCCATGGCCCCGGTCCAGGAGGGACTCTGTGTGGAAGT
GCGACGGGCGCCGGCCAGGGTTGCGCAGGGCCTCACGCGTCTTGACCCTCGCCGAACCCGTACCGGTACCGGGCCAGGTCCTCCCTGAGACACACCTTCA

                                        >ClaI                   >EcoRI
                                          |                       |
       210       220       230       240       250       260       270   |   280       290       300
ACTGTTGGGGACTTTTGATGGTTTTGTGCAGAACTGCGATCTCCAGATCGATAGTTTTAGAGCCTATCTACTGGAATTCCTCGAACTCCAAATTTCTACC
TGACAACCCCTGAAAACTACCAAAACACGTCTTGACGCTAGAGGTCTAGCTATCAAAATCTCGGATAGATGACCTTAAGGAGCTTGAGGTTTAAAGATGG

      >StuI                                                                 >MscI
        |                                                                     |
       310       320       330       340       350       360       370       380|      390       400
CGGACAAGGCCTGGTACTATACCCACAGATAGGAGACAAATTGGATATTATTTGCCCCAAAGTGGACTCTAAAACTGTTGGCCAGTATGAATATTATAAA
GCCTGTTCCGGACCATGATATGGGTGTCTATCCTCTGTTTAACCTATAATAAACGGGGTTTCACCTGAGATTTTGACAACCGGTCATACTTATAATATTT

       410       420       430       440       450       460       470       480       490       500
GTTTATATGGTTGATAAAGACCAAGCAGACAGATGCACAATTAAGAAGGAGAATACCCCGCTGCTCAACTGTGCCAGACCAGACCAAGATGTGAAATTCA
CAAATATACCAACTATTTCTGGTTCGTCTGTCTACGTGTTAATTCTTCCTCTTATGGGGCGACGAGTTGACACGGTCTGGTCTGGTTCTACACTTTAAGT
```

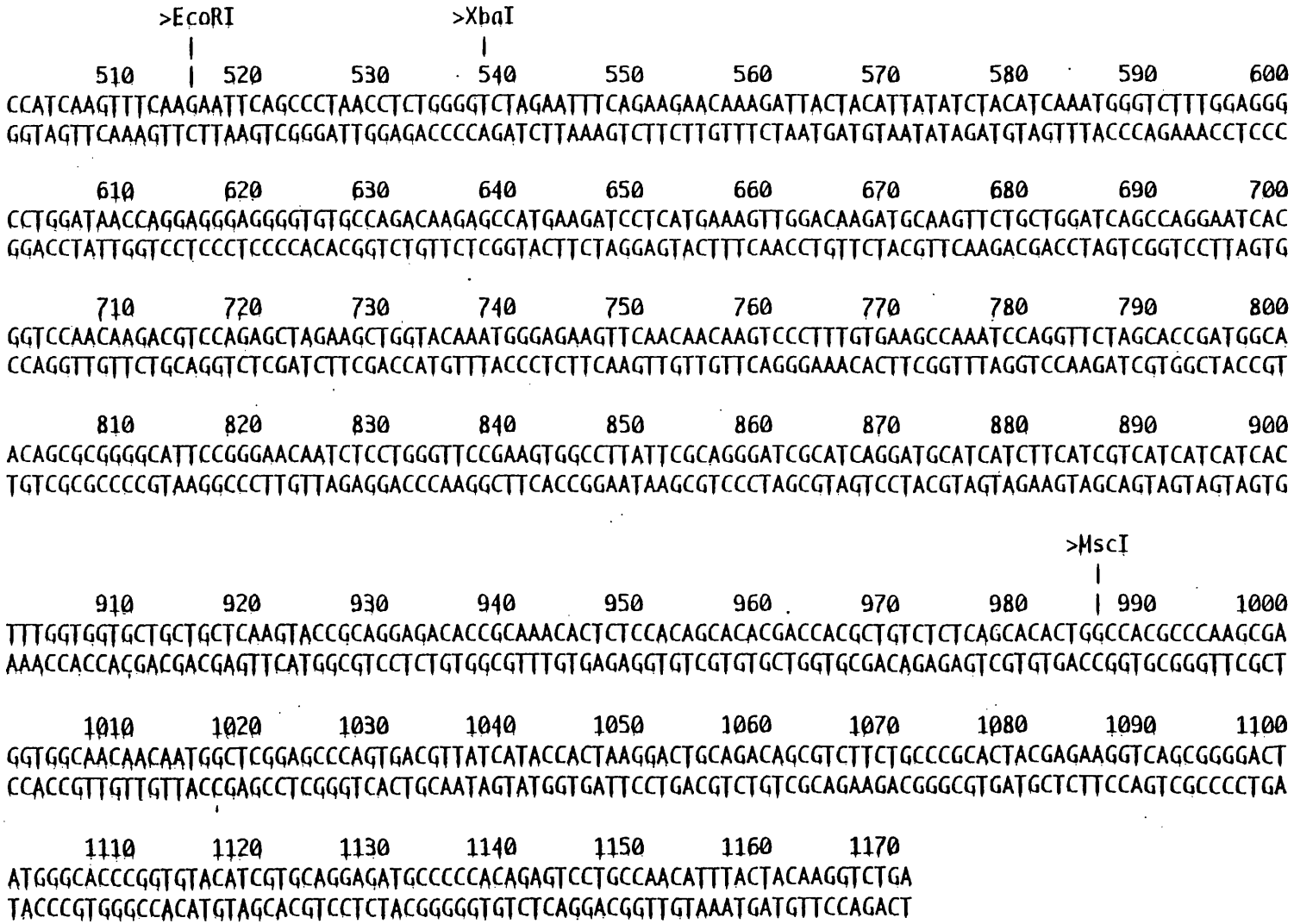
>EcoRI
>XbaI
510 520 530 540 550 560 570 580 590 600
CCATCAAGTTTCAAGAATTCAGCCCTAACCTCTGGGGTCTAGAATTTCAGAAGAACAAAGATTACTACATTATATCTACATCAAATGGGTCTTTGGAGGG
GGTAGTTCAAAGTTCTTAAGTCGGGATTGGAGACCCCAGATCTTAAAGTCTTCTTGTTTCTAATGATGTAATATAGATGTAGTTTACCCAGAAACCTCCC
610 620 630 640 650 660 670 680 690 700
CCTGGATAACCAGGAGGGAGGGGTGTGCCAGACAAGAGCCATGAAGATCCTCATGAAAGTTGGACAAGATGCAAGTTCTGCTGGATCAGCCAGGAATCAC
GGACCTATTGGTCCTCCCTCCCCACACGGTCTGTTCTCGGTACTTCTAGGAGTACTTTCAACCTGTTCTACGTTCAAGACGACCTAGTCGGTCCTTAGTG
710 720 730 740 750 760 770 780 790 800
GGTCCAACAAGACGTCCAGAGCTAGAAGCTGGTACAAATGGGAGAAGTTCAACAACAAGTCCCTTTGTGAAGCCAAATCCAGGTTCTAGCACCGATGGCA
CCAGGTTGTTCTGCAGGTCTCGATCTTCGACCATGTTTACCCTCTTCAAGTTGTTGTTCAGGGAAACACTTCGGTTTAGGTCCAAGATCGTGGCTACCGT
810 820 830 840 850 860 870 880 890 900
ACAGCGCGGGGCATTCCGGGAACAATCTCCTGGGTTCCGAAGTGGCCTTATTCGCAGGGATCGCATCAGGATGCATCATCTTCATCGTCATCATCATCAC
TGTCGCGCCCCGTAAGGCCCTTGTTAGAGGACCCAAGGCTTCACCGGAATAAGCGTCCCTAGCGTAGTCCTACGTAGTAGAAGTAGCAGTAGTAGTAGTG
>MscI
910 920 930 940 950 960 970 980 990 1000
TTTGGTGGTGCTGCTGCTCAAGTACCGCAGGAGACACCGCAAACACTCTCCACAGCACACGACCACGCTGTCTCTCAGCACACTGGCCACGCCCAAGCGA
AAACCACCACGACGACGAGTTCATGGCGTCCTCTGTGGCGTTTGTGAGAGGTGTCGTGTGCTGGTGCGACAGAGAGTCGTGTGACCGGTGCGGGTTCGCT
1010 1020 1030 1040 1050 1060 1070 1080 1090 1100
GGTGGCAACAACAATGGCTCGGAGCCCAGTGACGTTATCATACCACTAAGGACTGCAGACAGCGTCTTCTGCCCGCACTACGAGAAGGTCAGCGGGGACT
CCACCGTTGTTGTTACCGAGCCTCGGGTCACTGCAATAGTATGGTGATTCCTGACGTCTGTCGCAGAAGACGGGCGTGATGCTCTTCCAGTCGCCCCTGA
1110 1120 1130 1140 1150 1160 1170
ATGGGCACCCGGTGTACATCGTGCAGGAGATGCCCCCACAGAGTCCTGCCAACATTTACTACAAGGTCTGA
TACCCGTGGGCCACATGTAGCACGTCCTCTACGGGGGTGTCTCAGGACGGTTGTAAATGATGTTCCAGACT

Appendix 2

The Yang method for targeted modification of bacterial artificial chromosomes (BACs) (Yang *et al.*, 1997)

I. Construction of the recA(+) and temperature sensitive shuttle vector

1) Clone two small genomic fragments (>500 bp each) into the building vector (pBV1)

2) Transfer the recombination cassette into the Ts-RecA(+) shuttle vector (pSV1.RecA)

II. Transformation of the shuttle vector into the *E. coli* host strain of BACs and selection for co-integrates

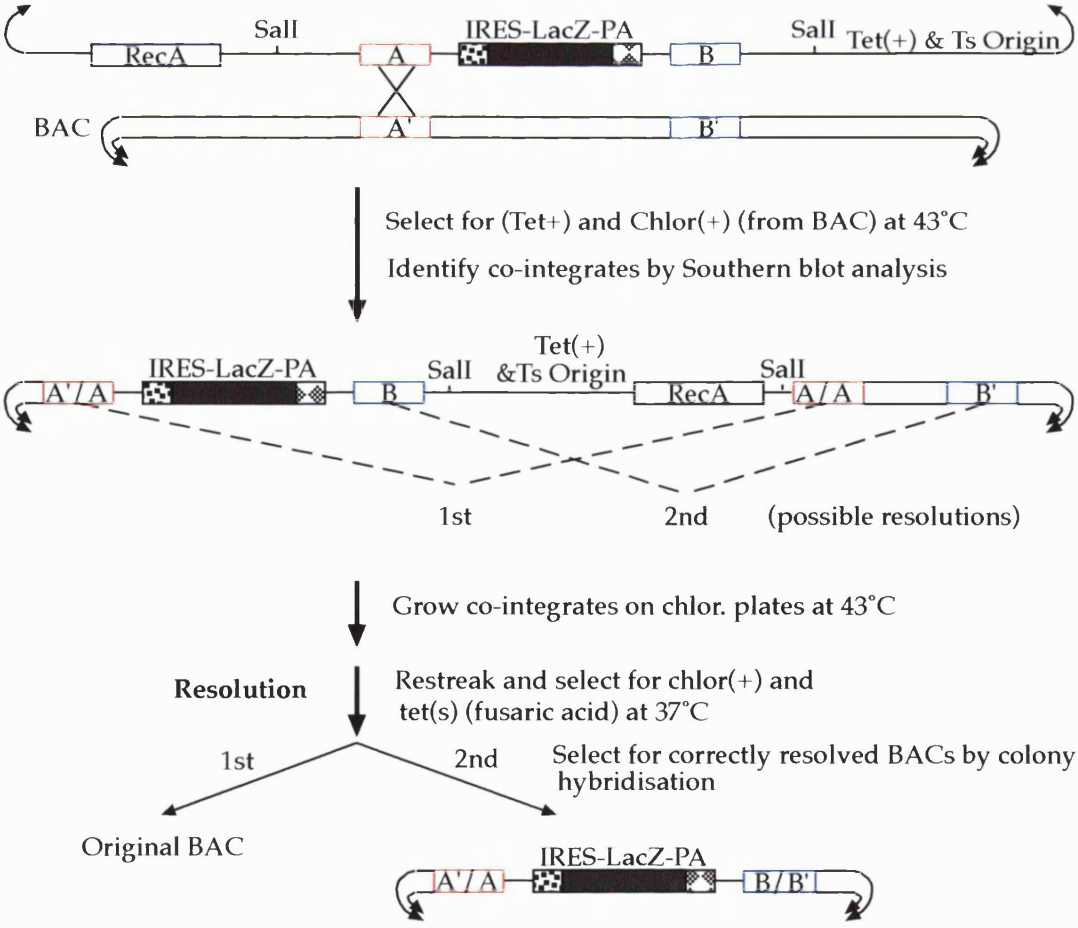

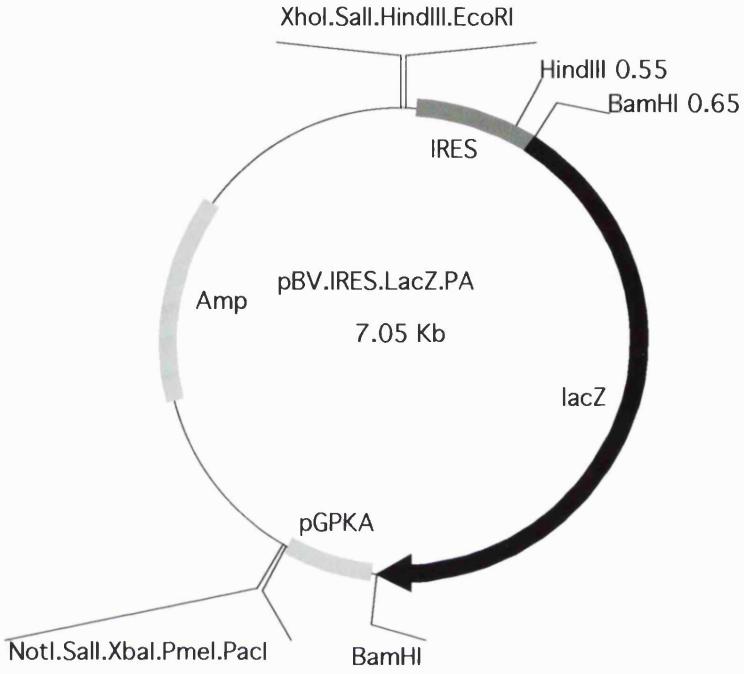
XhoI.SalI.HindIII.EcoRI
HindIII 0.55
BamHI 0.65
IRES
pBV.IRES.LacZ.PA
7.05 Kb
Amp
lacZ
pGPKA
NotI.SalI.XbaI.PmeI.PacI
BamHI

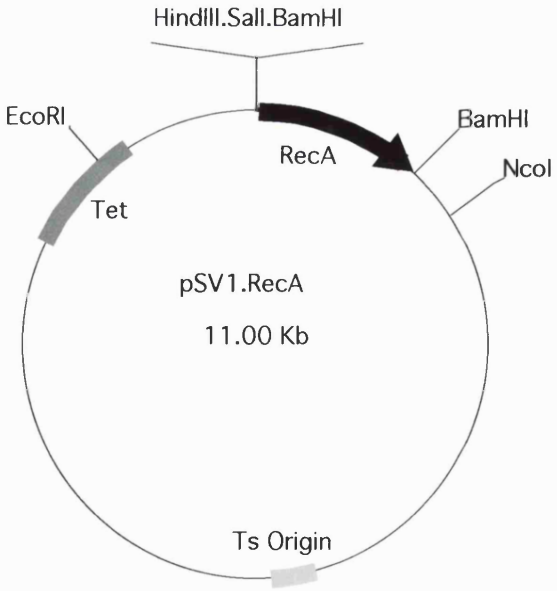
HindIII.SalI.BamHI
EcoRI
BamHI
RecA
NcoI
Tet
pSV1.RecA
11.00 Kb
Ts Origin

Appendix 3 – Vector maps

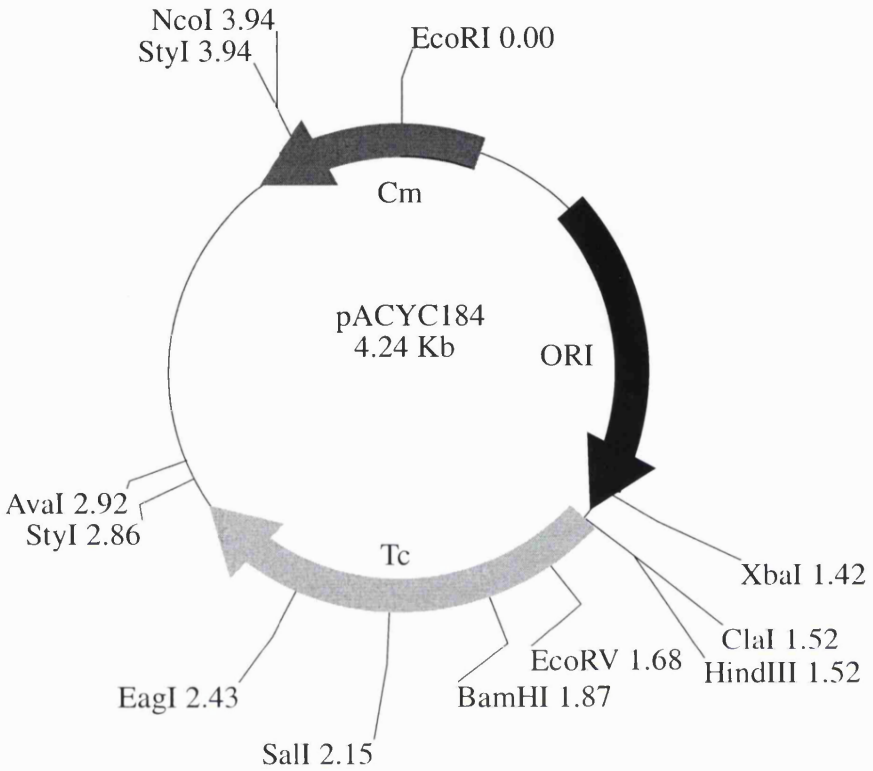

(New England Biolabs)

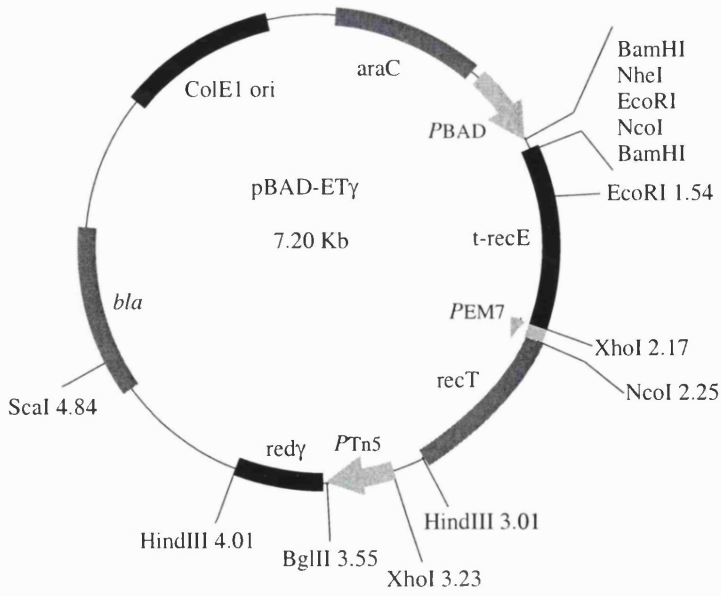

(Zhang *et al.*, 1998)

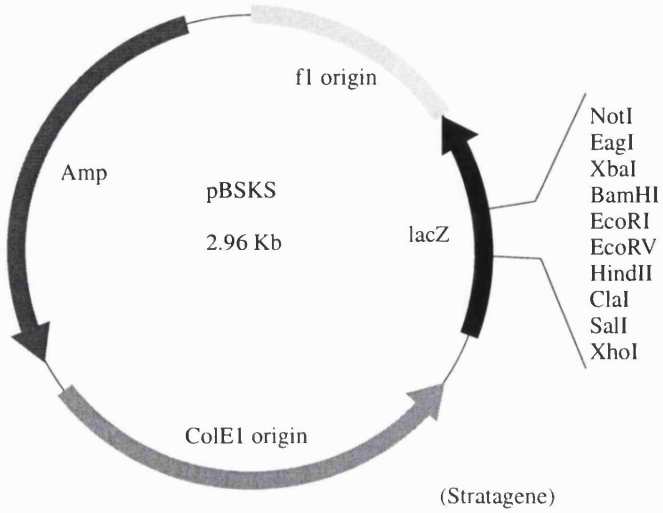

(Stratagene)

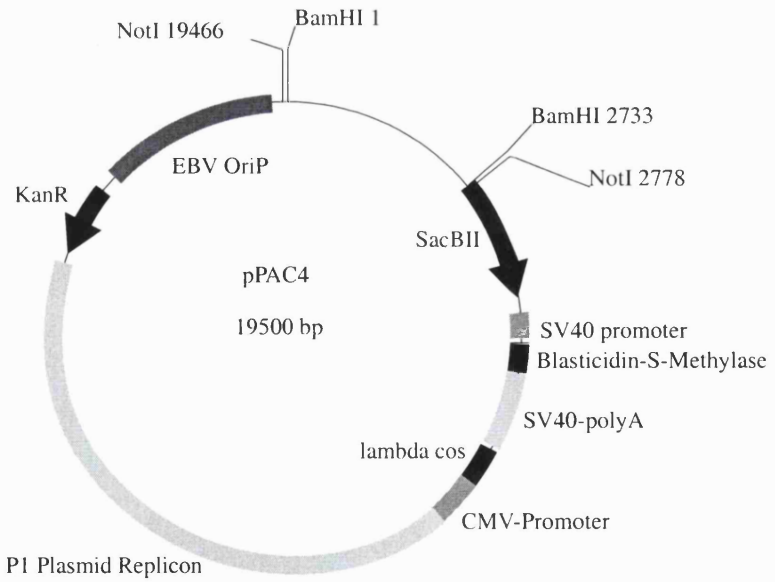

(Osoegawa and de Jong, http://www.chori.org/bacpac/)

Appendix 4 – PCR primers and programmes

Primer pair: 008/009

PCR program: 1 cycle x 5 min. 95°C; 20 cycles x 1 min. 95°C, 1 min. 64°C, 2 min. 72°C; 1 cycle x 1 min. 95°C, 2 min. 64°C, 10 min. 72°C

Primer pair: LZR/B2P

PCR program: 1 cycle x 3 min. 94°C; 30 cycles x 20 sec. 94°C, 1 min. 59.6°C, 2 min. 72°C; 1 cycle x 3 min. 72°C

Primer pair: TetF/B2P

PCR program: as for LZR/B2P but with an annealing temperature of 63.0°C

Primer sequence:

008 – 5′-GGCTGAGGGACGCGCAGG

009 – 5′-GGACGCGTTGGGACCGGC

LZR – 5′-GTGCTGCAAGGCGATTAAGTTG

B2P – 5′-CGGAGTGCGCAGAACTGGGAG

TetF – CAGGAGTCGCATAAGGGAGAGCG

References

Alexandre, D., J. D. W. Clarke, E. Oxtoby, Y. Yan, T. Jowett and N. Holder (1996). Ectopic expression of *Hoxa1* in the zebrafish alters the fate of the mandibular arch neural crest and phenocopies a retinoic acid-induced phenotype. *Development* **122**: 735–746.

Ang, H. L. and G. Duester (1997). Initiation of retinoid signaling in primitive streak mouse embryos: spatiotemporal expression patterns of receptors and metabolic enzymes for ligand synthesis. *Developmental Dynamics* **208**: 536–543.

Ang, S., R. A. Conlon, O. Jin and J. Rossant (1994). Positive and negative signals from mesoderm regulate the expression of mouse *Otx2* in ectoderm explants. *Development* **120**: 2979–2989.

Barrow, J. R. and M. R. Capecchi (1996). Targeted disruption of the *Hoxb-2* locus in mice interferes with expression of *Hoxb-1* and *Hoxb-4*. *Development* **122**: 3817–3828.

Barrow, J. R., H. S. Stadler and M. R. Capecchi (2000). Roles of *Hoxa1* and *Hoxa2* in patterning the early hindbrain of the mouse. *Development* **127**: 933–944.

Becker, N., T. Seitanidou, P. Murphy, M.-G. Mattei, P. Topilko, M. A. Nieto, D. G. Wilkinson, P. Charnay and P. Gilardi-Hebenstreit (1994). Several receptor tyrosine kinase genes of the *Eph* family are segmentally expressed in the developing hindbrain. *Mechanisms of Development* **47**: 3–17.

Beddington, R. S. P. (1994). Induction of a second neural axis by the mouse node. *Development* **120**: 613–620.

Beddington, R. S. P. and E. J. Robertson (1998). Anterior patterning in mouse. *Trends in Genetics* **14**(7): 277–284.

Bell, E., R. J. T. Wingate and A. Lumsden (1999). Homeotic transformation of rhombomere identity after localized *Hoxb1* misexpression. *Science* **284**: 2168–2171.

Bennett, B.D., F. C. Zeigler, Q. Gu, B. Fendly, A.D. Goddard, N. Gillett, and W. Matthews (1995). Molecular cloning of a ligand for the EPH-related receptor protein-tyrosine kinase Htk. *Proceedings of the National Academy of Sciences of the USA* **92**: 1866–1870

Bergemann, A. D., H.-J. Cheng, R. Brambilla, R. Klein and J. G. Flanagan (1995). ELF-2, a new member of the Eph ligand family, is segmentally expressed in the region of the hindbrain and newly formed somites. *Molecular and Cellular Biology* **15**: 4921–4929.

Berggren, K., P. McCaffery, U. Dräger and C. J. Forehand (1999). Differential distribution of retinoic acid synthesis in the chicken embryo as determined by immunolocalization of the retinoic acid synthetic enzyme, RALDH-2. *Developmental Biology* **210**: 288–304.

Birgbauer, E. and S. E. Fraser (1994). Violation of cell lineage restriction compartments in the chick hindbrain. *Development* **120**: 1347–1356.

Blumberg, B., J. J. Bolado, T. A. Moreno, C. Kintner, R. M. Evans and N. Papalopulu (1997). An essential role for retinoid signaling in anteroposterior neural patterning. *Development* **124**: 373–379.

Bockman, D. E. and M. L. Kirby (1984). Dependence of thymus development on derivatives of the neural crest. *Science* **223**: 498–500.

Bouillet, P., M. Oulad-Abdelghani, S. Vicaire, J.-M. Garnier, B. Schuhbaur, P. Dollé and P. Chambon (1995). Efficient Cloning of cDNAs of Retinoic Acid-Responsive Genes in P19 Embryonal Carcinoma Cells and Characterisation of a Novel Mouse Gene, Stra1 (Mouse LERK-2/Eplg2). *Developmental Biology* **170**: 420–433.

Bruckner, K., E. B. Pasquale and R. Klein (1997). Tyrosine phosphorylation of transmembrane ligands for Eph receptors. *Science* **275**: 1640–1643.

Carpenter, E. M., J. M. Goddard, O. Chisaka, N. R. Manley and M. R. Capecchi (1993). Loss of *Hoxa-1 (Hox-1.6)* expression results in the reorganisation of the murine hindbrain. *Development* **118**: 1063–1075.

Chambon, P. (1996). A decade of molecular biology of retinoic acid receptors. *FASEB Journal* **10**: 940–954.

Chavrier, P., M. Zerial, P. Lemaire, J. Almendral, R. Bravo and P. Charnay (1988). A gene encoding a protein with zinc fingers is activated during G_0/G_1 transition in cultured cells. *The EMBO Journal* **7**: 29–35.

Chen, J. (1998). An enhancer element in the *EphA2* (*Eck*) gene sufficient for rhombomere-specific expression is activated by HOXA1 and HOXB1 homeobox proteins. *The Journal of Biological Chemistry* **273**(38): 24670–24675.

Chen, Y., L. Huang and M. Solursh (1993). A concentration gradient of retinoids in the early *Xenopus laevis* embryo. *Developmental Biology* **161**: 70–76.

Clarke, J. D. and A. Lumsden (1989). Segmental repetition of neuronal phenotype sets in the chick embryo hindbrain. *Development* **118**: 151–162.

Conlon, R. A. and J. Rossant (1992). Exogenous retinoic acid rapidly induces anterior expression of murine *Hox-2* genes in vivo. *Development* **116**: 357–368.

Cordes, S. P. and G. S. Barsh (1994). The mouse segmentation gene *kr* encodes a novel basic domain-leucine zipper transcription factor. *Cell* **79**: 1025–1034.

Couly, G. F., P. M. Coltey and N. Le Douarin (1993). The triple origin of skull in higher vertebrates: a study in quail-chick chimaeras. *Development* **117**: 409–429.

Davenne, M., M. K. Maconochie, R. Neun, A. Pattyn, P. Chambon, R. Krumlauf and F. Rijli (1999). *Hoxa2* and *Hoxb2* control dorsoventral patterns of neuronal development in the rostral hindbrain. *Neuron* **22**: 677–691.

Davis, S., N. W. Gale, T. H. Aldrich, P. C. Maisonpierre, V. Lhotak, T. Pawson, M. Goldfarb and G. D. Yancopoulos (1994). Ligands for EPH-related receptors that require membrane attachment or clustering for activity. *Science* **266**: 816–819.

Deol, M. S. (1964). The abnormalities of the inner ear in *Kreisler* mice. *Journal of Embryology and Experimental Morphology* **12**(475–490).

Dollé, P., T. Lufkin, R. Krumlauf, M. Mark, D. Duboule and P. Chambon (1993). Local alterations of *Krox-20* and *Hox* gene expression in the hindbrain suggest lack of rhombomeres 4 and 5 in homozygote null *Hoxa-1 (Hox-1.6)* mutant embryos. *Proceedings of the National Academy of Sciences of the USA* **90**: 7666–7670.

Duboule, D. and P. Dollé (1989). The structural and functional organisation of the murine *HOX* gene family resembles that of *Drosophila* homeotic genes. *EMBO Journal* **8**: 1497–1505.

Dupé, V., M. Davenne, J. Brocard, P. Dollé, M. Mark, A. Dierich, P. Chambon and F. Rijli (1997). *In vivo* functional analysis of the *Hoxa1* 3' retinoid response element (3' RARE). *Development* **124**: 399–410.

Dupé, V., N. B. Ghyselinck, O. Wendling, P. Chambon and M. Mark (1999). Key roles of retinoic acid receptors alpha and beta in patterning of the caudal hindbrain, pharyngeal arches and otocyst in the mouse. *Development* **126**: 5051–5059.

Durston, A. J., J. P. M. Timmermans, W. J. Hage, H. F. J. Hendriks, N. J. de Vries, M. Heideveld and P. D. Nieuwkoop (1989). Retinoic acid causes an anteroposterior transformation in the developing central nervous system. *Nature* **340**: 140–144.

Flenniken, A. M., N. W. Gale, G. D. Yancopoulos and D. G. Wilkinson (1996). Distinct and overlapping expression of ligands for Eph-related receptor tyrosine kinases during mouse embryogenesis. *Developmental Biology* **179**: 382–401.

Foley, A. C., K. G. Storey and C. D. Stern (1997). The prechordal region lacks neural inducing ability, but can confer anterior character to more posterior neuroepithelium. *Development* **124**: 2983–2996.

Fraser, S., R. Keynes and A. Lumsden (1990). Segmentation in the chick embryo hindbrain is defined by cell lineage restrictions. *Nature* **344**: 431–435.

Frisén, J., J. Holmberg and M. Barbacid (1999). Ephrins and their Eph receptors: multitalented directors of embryonic development. *The EMBO Journal* **18**(19): 5159–5165.

Frohman, M. A., G. R. Martin, S. P. Cordes, L. P. Halamek and G. S. Barsh (1993). Altered rhombomere-specific gene expression and hyoid bone differentiation in the mouse segmentation mutant, *kreisler* (*kr*). *Development* **117**: 925–936.

Fujii, H., T. Sato, S. Kaneko, O. Gotoh, Y. Fujii-Kuriyama, K. Osawa, S. Kato and H. Hamada (1997). Metabolic inactivation of retinoic acid by a novel P450 differentially expressed in developing mouse embryos. *The EMBO Journal* **16**(14): 4163–4173.

Gale, E., M. Zile and M. Maden (1999). Hindbrain respecification in the retinoid-deficient quail. *Mechanisms of Development* **89**: 43–54.

Gale, N. W., S. J. Holland, D. M. Valenzuela, A. Flenniken, L. Pan, T. E. Ryan, M. Henkemeyer, K. Strebhardt, H. Hirai, D. G. Wilkinson, T. Pawson, S. Davis and G. D. Yancopoulos (1996). Eph receptors and ligands comprise two major specificity subclasses and are reciprocally compartmentalised during embryogenesis. *Neuron* **17**: 9–19.

Garcia-Bellido, A., G. Morata and P. Ripoll (1973). Developmental compartmentalisation of the wing disc of Drosophila. *Nature New Biology* **245**: 251–253.

Gavalas, A., M. Davenne, A. Lumsden, P. Chambon and F. M. Rijli (1997). Role of *Hoxa-2* in axon pathfinding and rostral hindbrain patterning. *Development* **124**: 3693–3702.

Goddard, J. M. (1996). Mice with targeted disruption of *Hoxb-1* fail to form the motor nucleus of the facial nerve. *Development* **122**: 3217–3228.

Godsave, S. F., C. H. Koster, A. Getahun, M. Hooiveld, J. Van der Wees and J. Hendriks (1998). Graded retinoid responses in the developing hindbrain. *Developmental Dynamics* **213**: 39–49.

Gould, A., N. Itasaki and R. Krumlauf (1998). Initiation of rhombomeric *Hoxb4* expression requires induction by somites and a retinoid pathway. *Neuron* **21**: 39–51.

Gould, A., A. Morrison, G. Sproat, R. A. H. White and R. Krumlauf (1997). Positive cross-regulation and enhancer sharing: two mechanisms for specifying overlapping *Hox* expression patterns. *Genes & Development* **11**: 900–913.

Graham, A. and A. Lumsden (1996). Interactions between rhombomeres modulate *Krox-20* and *follistatin* expression in the chick embryo hindbrain. *Development* **122**: 473–480.

Graham, A., N. Papalopulu and R. Krumlauf (1991). The murine and Drosophila homeobox clusters have common features of organisation and expression. *Cell* **57**: 367–378.

Grapin-Botton, A., M. Bonnin, L. Ariza McNaughton, R. Krumlauf and N. M. Le Douarin (1995). Plasticity of transposed rhombomeres: Hox gene induction is correlated with phenotypic modifications. *Development* **121**: 2707–2721.

Grapin-Botton, A., M. Bonnin and N. M. Le Douarin (1997). Hox gene induction in the neural tube depends on three parameters: competence, signal supply and paralogue group. *Development* **124**: 849–859.

Grapin-Botton, A., M.-A. Bonnin, M. Sieweke and N. M. Le Douarin (1998). Defined concentrations of a posteriorizing signal are critical for *MafB/kreisler* segmental expression in the hindbrain. *Development* **125**: 1173–1181.

Grapin-Botton, A., F. Cambronero, H. L. Weiner, M. Bonnin, L. Puelles and N. M. Le Douarin (1999). Patterning signals acting in the spinal cord override the organizing activity of the isthmus. *Mechanisms of Development* **84**: 41–53.

Guthrie, S. (1991). Patterns of cell division and interkinetic nuclear migration in the chick embryo hindbrain. *Journal of Neurobiology* **22**(7): 742–754.

Guthrie, S. and A. Lumsden (1991). Formation and regeneration of rhombomere boundaries in the developing chick hindbrain. *Development* **112**: 221–229.

Guthrie, S., I. Muchamore, A. Kuroiwa, H. Marshall, R. Krumlauf and A. Lumsden (1992). Neuroectodermal autonomy of *Hox-2.9* expression revealed by rhombomere transplants. *Nature* **356**: 157–159.

Guthrie, S., V. Prince and A. Lumsden (1993). Selective dispersal of avian rhombomere cells in orthotopic and heterotopic grafts. *Development* **118**: 527–538.

Hamburger, V. and H. Hamilton (1951). A series of normal stages in the development of the chick embryo. *Journal of Morphology* **88**: 49–92.

Hanahan, D. (1983). Studies on transformation of *Escherichia coli* with plasmids. *Journal of Molecular Biology* **166**: 557–580.

Helmbacher, F., C. Pujades, C. Desmarquet, M. Frain, F. Rijli, P. Chambon and P. Charnay (1998). *Hoxa1* and *Krox-20* synergize to control the development of rhombomere 3. *Development* **125**: 4739–4748.

Henkemeyer, M., D. Orioli, J. T. Henderson, T. M. Saxton, J. Roder, T. Pawson and R. Klein (1996). Nuk controls pathfinding of commissural axons in the mammalian central nervous system. *Cell* **86**: 35–46.

Hertwig, P. (1942). Sechs neue Mutationen bei der Hausmaus in ihrer Bedeutung für allgemeine Vererbungsfragen. *Zutaten Lehre* **26**: 1–21.

Hertwig, P. (1944). Die Genese der Hirn- und Gehörorganmissbildungen bei röntgenmutierten Kreislermäusen. *Zutaten KonstLehre* **28**: 327–354.

Heyman, I., A. Faissner and A. Lumsden (1995). Cell and matrix specialisations of rhombomere boundaries. *Developmental Dynamics* **204**: 301–315.

Heyman, I., A. Kent and A. Lumsden (1993). Cellular morphology and extracellular space at rhombomere boundaries in the chick embryo hindbrain. *Developmental Dynamics* **198**: 241–253.

Hill, J., J. D. W. Clarke, N. Vargesson, T. Jowett and N. Holder (1995). Exogenous retinoic acid causes specific alterations in the development of the midbrain and hindbrain of the zebrafish embryo including positional respecification of the Mauthner neuron. *Mechanisms of Development* **50**: 3–16.

Himanen, J.-P., M. Henkemeyer and D. B. Nikolov (1998). Crystal structure of the ligand-binding domain of the receptor tyrosine kinase EphB2. *Nature* **396**: 486–491.

Hogan, B. L. M., C. Thaller and G. Eichele (1992). Evidence that Hensen's node is a site of retinoic acid synthesis. *Nature* **359**: 237–241.

Holder, N. and J. Hill (1991). Retinoic acid modifies development of the midbrain-hindbrain border and affects cranial ganglion formation in zebrafish embryos. *Development* **113**: 1159–1170.

Holland, S. J., N. W. Gale, G. Mbamalu, G. D. Yancopolous, M. Henkemeyer and T. Pawson (1996). Bidirectional signalling through the Eph-family receptor Nuk and its transmembrane ligands. *Nature* **383**(722–725).

Hollemann, T., Y. Chen, H. Grunz and T. Pieler (1998). Regionalised metabolic activity establishes boundaries of retinoic acid signalling. *The EMBO Journal* **17**(24): 7361–7372.

Hunt, P., M. Guilisano, M. Cook, M. Sham, A. Faiella, D. G. Wilkinson, E. Boncinelli and R. Krumlauf (1991). A distinct Hox code for the branchial region of the vertebrate head. *Nature* **353**: 861–864.

Irving, C. and I. Mason (2000). Signalling by FGF8 from the isthmus patterns anterior hindbrain and establishes the anterior limit of Hox gene expression. *Development* **127**: 177–186.

Irving, C., M. A. Nieto, R. DasGupta, P. Charnay and D. G. Wilkinson (1996). Progressive spatial restriction of Sek-1 and Krox-20 gene expression during hindbrain segmentation. *Developmental Biology* **173**: 26–38.

Itasaki, N., J. Sharpe, A. Morrison and R. Krumlauf (1996). Reprogramming *Hox* expression in the vertebrate hindbrain: Influence of paraxial mesoderm and rhombomere transposition. *Neuron* **16**: 487–500.

Kalter, H. and J. Warkany (1959). Experimental production of congenital malformations in mammals by metabolic procedure. *Physiological Review* **39**: 69–115.

Kimmel, C. B., W. W. Ballard, S. R. Kimmel, B. Ullmann and T. F. Schilling (1995). Stages of embryonic development of the zebrafish. *Developmental Dynamics* **203**: 253–310.

Kolm, P. J., V. Apekin and H. Sive (1997). *Xenopus* hindbrain patterning requires retinoid signaling. *Developmental Biology* **192**: 1–16.

Kolm, P. J. and H. L. Sive (1997). Retinoids and posterior neural induction: a re-evaluation of Nieuwkoop's two-step hypothesis. *Cold Spring Harbor Symposia on Quantitative Biology* **LXII**: 511–521.

Könteges, G. and A. Lumsden (1996). Rhombencephalic neural crest segmentation is perserved throughout craniofacial ontogeny. *Development* **122**: 3229–3242.

Krumlauf, R. (1993). *Hox* genes and pattern formation in the branchial region of the vertebrate head. *Trends in Genetics* **9**: 106–112.

Krumlauf, R. (1994). *Hox* genes in vertebrate development. *Cell* **78**: 191–201.

Kuratani, S. C. and G. Eichele (1993). Rhombomere transplantation repatterns the segmental organisation of cranial nerves and reveals cell-autonomous expression of a homeodomain protein. *Development* **117**: 105–117.

Labrador, J. P., R. Brambilla and R. Klein (1997). The N-terminal globular domain of Eph-receptors is sufficient for ligand binding and receptor signalling. *EMBO Journal* **16**: 3889–3897.

Lackmann, M., R. J. Mann, L. Kravets, F. M. Smith, T. A. Bucci, K. F. Maxwell, G. J. Howlett, J. E. Olsson, T. V. Bos, D. P. Cerretti and A. W. Boyd (1997). Ligand for EPH-related kinase (LERK) 7 is the preferred high affinity ligand for the HEK receptor. *Journal of Biological Chemistry* **272**: 16521–16530.

Langston, A. W. and L. J. Gudas (1992). Identification of a retinoic acid response enhancer 3' of the murine homeobox gene Hox-1.6. *Mechanisms of Development* **38**: 217–228.

Langston, A. W., J. R. Thompson and L. J. Gudas (1997). Retinoic acid-responsive enhancers located 3' of the Hox A and Hox B homeobox gene clusters. *The Journal of Biological Chemistry* **272**(4): 2167–2175.

Lawrence, P. A. and G. Struhl (1996). Morphogens, Compartments, and Pattern: Lessons from Drosophila? *Cell* **85**: 951–961.

Le Lievre, C. S. and N. M. Le Douarin (1975). Mesenchymal derivatives of the neural crest: analysis of chimaeric quail and chick embryos. *Journal of Embrology and Experimental Morphology* **34**: 125–154.

Lewis, E. (1978). A gene complex controlling segmentation in *Drosophila*. *Nature* **276**(565–570).

Lohnes, D., M. Mark, C. Mendelsohn, P. Dollé, A. Dierich, P. Gorry, A. Gansmuller and P. Chambon (1994). Function of the retinoic acid receptors (RARs) during development. (I) Craniofacial and skeletal abnormalities in RAR double mutants. *Development* **120**: 2723–2748.

Lumsden, A. (1990). The cellular basis of segmentation in the developing hindbrain. *Trends in Neurosciences* **13** (8): 329–335.

Lumsden, A. and R. Keynes (1989). Segmental patterns of neuronal development of the chick hindbrain. *Nature* **337**: 424–428.

Machonochie, M. K., S. Nonchev, M. Studer, S.-K. Chan, H. Pöpperl, M.-H. Sham, R. Mann and R. Krumlauf (1997). Cross-regulation in the mouse *HoxB* complex: the expression of *Hoxb2* in rhombomere 4 is regulated by *Hoxb1*. *Genes & Development* **11**: 1885–1896.

Maden, M., E. Gale, I. Kostetskii and M. Zile (1996). Vitamin A-deficient quail embryos have half a hindbrain and other neural defects. *Current Biology* **6**(4): 417–426.

Maden, M., E. Sonneveld, P. T. van der Saag and E. Gale (1998). The distribution of endogenous retinoic acid in the chick embryo: implications for developmental mechanisms. *Development* **125**: 4133–4144.

Mallo, M. and I. Brändlin (1997). Segmental identity can change independently in the hindbrain and rhombencephalic neural crest. *Developmental Dynamics* **210**: 146–156.

Maloy, S. R. and W. D. Nunn (1981). Selection for loss of tetracycline resistance by *Escherichia coli*. *Journal of Bacteriology* **145** (2): 1110–1112.

Manzanares, M., S. Cordes, L. Ariza-McNaughton, V. Sadl, K. Maruthainar, G. Barsh and R. Krumlauf (1999a). Conserved and distinct roles of *kreisler* in regulation of the paralogous *Hoxa3* and *hoxb3* genes. *Development* **126**: 759–769.

Manzanares, M., S. Cordes, C.-T. Kwan, M. H. Sham, G. S. Barsh and R. Krumlauf (1997). Segmental regulation of *Hoxb-3* by *kreisler*. *Nature* **387**: 191–195.

Manzanares, M., P. A. Trainor, S. Nonchev, L. Ariza-McNaughton, J. Brodie, A. Gould, H. Marshall, A. Morrison, C. Kwan, M. Sham, D. G. Wilkinson and R. Krumlauf (1999b). The role of *kreisler* in segmentation during hindbrain development. *Developmental Biology* **211**: 220–237.

Marín, F. and P. Charnay (2000). Positional regulation of *Krox-20* and *mafB/kr* in the developing hindbrain: Potentialities of prospective rhombomeres. *Developmental Biology* **218**: 220–234.

Mark, M., T. Lufkin, J.-L. Vonesch, E. Ruberte, J.-C. Olivo, P. Dolle, P. Gorry, A. Lumsden and P. Chambon (1993). Two rhombomeres are altered in *Hoxa-1* mutant mice. *Development* **119**: 319–338.

Marshall, H., S. Nonchev, M.-H. Sham, I. Muchamore, A. Lumsden and R. Krumlauf (1992). Retinoic acid alters the hindbrain Hox code and induces the transformation of rhombomeres 2/3 into a rhombomere 4/5 identity. *Nature* **360**: 737–741.

Marshall, H., M. Studer, H. Poepperl, S. Aparicio, A. Kuroiwa, S. Brenner and R. Krumlauf (1994). A conserved retinoic acid response element required for early expression of the homeobox gene *Hoxb-1*. *Nature* **370**: 567–571.

Matsuo, I., S. Kuratani, C. Kimura, N. Takeda and S. Aizawa (1995). Mouse *Otx2* functions in the formation and patterning of rostral head. *Genes & Development* **9**: 2646–2658.

McGinnis, W. and R. Krumlauf (1992). Homeobox genes and axial patterning. *Cell* **68**: 283–302.

McKay, I. J., J. Lewis and A. Lumsden (1997). Organisation and development of facial motor neurons in the *kreisler* mutant mouse. *European Journal of Neuroscience* **9**: 1499–1506.

McKay, I. J., I. Muchamore, R. Krumlauf, M. Maden, A. Lumsden and J. Lewis (1994). The *kreisler* mouse: a hindbrain segmentation mutant that lacks two rhombomeres. *Development* **120**: 2199–2211.

McMahon, A. P., A. L. Joyner, A. Bradley and J. A. McMahon (1992). The midbrain-hindbrain phenotype of *Wnt1*$^{-}$/*Wnt1*$^{-}$ mice results from stepwise deletion of *engrailed*-expressing cells by 9.5 days postcoitum. *Cell* **69**: 581–595.

Mechta-Grigoriou, F., S. Garel and P. Charnay (2000). Nab proteins mediate a negative feedback loop controlling Krox-20 activity in the developing hindbrain. *Development* **127**: 119–128.

Mellitzer, G., Q. Xu and D. G. Wilkinson (1999). Eph receptors and ephrins restrict cell intermingling and communication. *Nature* **400**: 77–81.

Millet, S., K. Campbell, D. J. Epstein, K. Losos, E. Harris and A. L. Joyner (1999). A role for *Gbx2* in repression of *Otx2* and positioning the mid/hindbrain organizer. *Nature* **401**: 161–164.

Moens, C. B., S. P. Cordes, M. W. Giorgianni and G. S. Barsh (1998). Equivalence in the genetic control of hindbrain segmentation in fish and mouse. *Development* **125**: 381–391.

Moens, C. B., Y.-L. Yan, B. Appel, A. G. Force and C. B. Kimmel (1996). *valentino:* a zebrafish gene required for normal hindbrain segmentation. *Development* **122**: 3981–3990.

Morriss-Kay, G. M., P. Murphy, R. E. Hill and D. R. Davidson (1991). Effects of retinoic acid excess on expression of *Hox2.9* and *Krox-20* and on morphological segmentation in the hindbrain of mouse embryos. *The EMBO Journal* **10**: 2985–2995.

Morriss-Kay, G. M. and Sokolova (1996). Embryonic development and pattern formation. *FASEB Journal* **10**: 961–968.

Muhr, J., E. Graziano, S. Wilson, T. M. Jessell and T. Edlund (1999). Convergent inductive signals specify midbrain, hindbrain, and spinal cord identity in gastrula stage chick embryos. *Neuron* **23**: 689–702.

Muyrers, J. P. P., Y. Zhang, G. Testa and A. F. Stewart (1999). Rapid modification of bacterial artificial chromosomes by ET-recombination. *Nucleic Acids Research* **27**(6): 1555–1557.

Newman, S. A. (1993). Is Segmentation Generic? *BioEssays* **15**(4): 277–283.

Niederreither, K., P. McCaffery, U. C. Dräger, P. Chambon and P. Dollé (1997). Restricted expression and retinoic acid-induced downregulation of the retinaldehyde dehydrogenase type 2 (RALDH-2) gene during mouse development. *Mechanisms of Development* **62**: 67–78.

Niederreither, K., V. Subbarayan, P. Dollé and P. Chambon (1999). Embryonic retinioc acid synthesis is essential for early mouse post-implantation development. *Nature Genetics* **21**: 444–448.

Niederreither, K., J. Vermot, B. Schuhbaur, P. Chambon and P. Dollé (2000). Retinoic acid synthesis and hindbrain patterning in the mouse embryo. *Development* **127**: 75–85.

Niehrs, C. (1999). Head in the WNT – the molecular nature of Spemann's head organiser. *Trends in Genetics* **15**(8): 314–319.

Nieto, M. A., P. Gilardi-Hebenstreit, P. Charnay and D. G. Wilkinson (1992). A receptor protein tyrosine kinase implicated in the segmental patterning of the hindbrain and mesoderm. *Development* **116**: 1137–1150.

Nieuwkoop, P. D., E. C. Boterenbrood, A. Kremer, E. F. S. N. Bloesma, E. L. M. J. Hoessels, G. Meyer and F. J. Verheyen (1952). Activation and organization of the central nervous system in amphibians. *Journal of Experimental Zoology* **120**: 1–108.

Noden, D. M. (1983). The role of the neural crest in patterning of avian cranial skeletal, connective, and muscle tissues. *Developmental Biology* **96**: 144–165.

Nonchev, S., C. Vesque, M. Machonochie, T. Seitanidou, L. Ariza-McNaughton, M. Frain, H. Marshall, M. H. Sham, R. Krumlauf and P. Charnay (1996). Segmental expression of *Hoxa-2* in the hindbrain is directly regulated by *Krox-20*. *Development* **122**: 534–554.

Papalopulu, N., J. Clarke, L. Bradley, D. Wilkinson, R. Krumlauf and N. Holder (1991). Retinoic acid causes abnormal development and segmental patterning of the anterior hindbrain in *Xenopus laevis*. *Development* **113**: 1145–1158.

Pasquale, E. B. (1991). Identification of chicken embryo kinase 5, a developmentally regulated receptor-type kinase of the Eph family. *Cell Regulation* **2**: 523–534

Pata, I., M. Studer, J. H. van Dooninck, J. Briscoe, S. Kuuse, J. D. Engel, F. Grosveld and A. Karis (1999). The transcription factor GATA3 is a downstream effector of *Hoxb1* specification in rhombomere 4. *Development* **126**: 5523–5531.

Pera, E. M. and K. Kessel (1997). Patterning of the chick forebrain anlage by the prechordal plate. *Development* **124**: 4153–4162.

Pöpperl, H., M. Bienz, M. Studer, S. K. Chan, S. Aparicio, S. Brenner, R. S. Mann and R. Krumlauf (1995). Segmental expression of Hoxb-1 is controlled by a highly conserved autoregulatory loop dependent upon exd/pbx. *Cell* **81**: 1031–1042.

Pöpperl, H. and M. S. Featherstone (1993). Identification of a retinoic acid response element upstream of the murine Hox-4.2 gene. *Molecular and Cellular Biology* **13**: 257–265.

Prince, V. and A. Lumsden (1994). *Hoxa-2* expression in normal and transposed rhombomeres: independent regulation in the neural tube and neural crest. *Development* **120**: 911–923.

Prince, V. E., C. B. Moens, C. B. Kimmel and R. K. Ho (1998). Zebrafish *hox* genes: expression in the hindbrain region of wild-type and mutants of the segmentation gene, *valentino*. *Development* **125**: 393–406.

Rhinn, M., A. Dierich, W. Shawlot, R. R. Behringer, M. Le Meur and S. Ang (1998). Sequential roles for *Otx2* in visceral endoderm and neurectoderm for forebrain and midbrain induction and specification. *Development* **125**: 845–856.

Rijli, F. M., M. Mark, S. Lakkaraju, A. Dietrich, P. Dolle and P. Chambon (1993). A homeotic transformation is generated in the rostral branchial region of the head by disruption of *Hoxa-2* which acts as a selector gene. *Cell* **5**: 1333–1349.

Rossant, J., R. Zirngibl, D. Cado, M. Shago and G. V. (1991). Expression of a retinoic acid response element-*hsplacZ* transgene defines specific domains of transcriptional activity during mouse embryogenesis. *Genes & Development* **5**: 1333–1344.

Rossel, M. and M. R. Capecchi (1999). Mice mutant for both *Hoxa1* and *Hoxb1* show extensive remodeling of the hindbrain and defects in craniofacial development. *Development* **126**: 5027–5040.

Saldivar, J. R., C. E. Krull, R. Krumlauf, L. Ariza-McNaughton and M. Bronner-Fraser (1996). Rhombomere of origin determines autonomous versus environmentally regulated expression of *Hoxa3* in the avian embryo. *Development* **122**: 895–904.

Sambrook, J., E. F. Fritsch and T. Maniatis (1989). *Molecular cloning: a laboratory manual*. Cold Spring Harbour, Cold Spring Harbour Press.

Sasai, Y. and E. De Robertis (1997). Ectodermal patterning in vertebrate embryos. *Developmental Biology* **182**: 5–20.

Schneider-Maunoury, S., T. Seitanidou, P. Charnay and A. Lumsden (1997). Segmental and neuronal architecture of the hindbrain of *Krox-20* mouse mutants. *Development* **124**: 1215–1226.

Schneider-Maunoury, S., P. Topilko, T. Seitanidou, G. Levi, M. Cohen-Tannoudji, S. Pournin, C. Babinet and P. Charnay (1993). Disruption of Krox-20 results in alteration of rhombomeres 3 and 5 in the developing hindbrain. *Cell* **75**: 1199–1214.

Seitanidou, T., S. Schneider-Maunoury, C. Desmarquet, D. G. Wilkinson and P. Charnay (1997). Krox-20 is a key regulator of

rhombomere-specific gene expression in the developing hindbrain. *Mechanisms of Development* **65**: 31–42.

Sham, M. H., C. Vesque, S. Nonchev, H. Marshall, M. Frain, R. D. Gupta, J. Whiting, D. Wilkinson, P. Charnay and R. Krumlauf (1993). The zinc finger gene *Krox-20* regulates *HoxB2* (*Hox2.8*) during hindbrain segmentation. *Cell* **72**: 183–196.

Shawlot, W. and R. R. Behringer (1995). Requirement for *Lim1* in head-organizer function. *Nature* **374**: 425–430.

Shih, J. and S. E. Fraser (1996). Characterizing the zebrafish organiser: microsurgical analysis at the early-shield stage. *Development* **112**: 1313–1322.

Simeone, A., D. Acampora, V. Nigro, A. Faiella, M. D'Eposito, A. Stornaiuolo, F. Mavilio and E. Boncinelli (1991). Differential regulation by retinoic acid of the homeobox genes of the four HOX loci in human embryonal carcinoma cells. *Mechanisms of Development* **33**: 215–228.

Sive, H. L., B. W. Draper, R. M. Harland and H. Weintraub (1990). Identification of a retinoic acid-sensitive period during primary axis formation in *Xenopus laevis*. *Genes & Development* **4:** 932–942.

Slack, J. M. W. and D. Tannahill (1992). Mechanism of anteroposterior axis specification in vertebrates. Lessons from the amphibians. *Development* **114**: 285–302.

Smith, A., V. Robinson, K. Patel and D. G. Wilkinson (1997). The EphA4 and EphB1 receptor tyrosine kinases and ephrin-B2 ligand regulate targeted migration of branchial neural crest cells. *Current Biology* **7**: 561–570.

Spemann, H. and H. Mangold (1924). Über Induktion von Embryonalanlagen durch Implantation artfremder Organisatoren. *Arch. Mikrosk. Anat. Entwicklungsmechan.* **100**: 599–638.

Stevens, C. F. (1998). Neuronal diversity: too many cell types for comfort? *Current Biology* **8**: R708–R710.

Storey, K. G., J. M. Crossley, E. M. De Robertis, W. E. Norris and C. D. Stern (1992). Neural induction and regionalisation in the chick embryo. *Development* **122**: 729–741.

Studer, M., A. Gavalas, H. Marshall, L. Ariza-McNaughton, F. Rijli, P. Chambon and R. Krumlauf (1998). Genetic interactions between *Hoxa1* and *Hoxb1* reveal new roles in regulation of early hindbrain patterning. *Development* **125**: 1025–1036.

Studer, M., A. Lumsden, L. Ariza-McNaughton, A. Bradley and R. Krumlauf (1996). Altered segmental identity and abnormal migration of motor neurons in mice lacking *Hoxb-1*. *Nature* **384**: 630–634.

Studer, M., H. Pöpperl, H. Marshall, A. Kuroiwa and R. Krumlauf (1994). Role of a conserved retinoic acid response element in rhombomere restriction of *Hoxb-1*. *Science* **265**: 1728–1732.

Swiatek, P. J. and T. Gridley (1993). Perinatal lethality and defects in hindbrain development in mice homozygous for a targeted mutation of the zinc finger gene *Krox20*. *Genes & Development* **7**(2071–2084).

Swindell, E. C., C. Thaller, S. Sockanathan, M. Petkovich, T. M. Jessel and G. Eichele (1999). Complementary domains of retinoic acid

production and degradation in the early chick embryo. *Developmental Biology* **216**: 282–296.

Taneja, R., B. Thisse, F. M. Rijli, C. Thisse, P. Bouillet, P. Dollé and P. Chambon (1996). The expression pattern of the mouse receptor tyrosine kinase gene *MDK1* is conserved through evolution and requires *Hoxa-2* for rhombomere-specific expression in mouse embryos. *Developmental Biology* **177**: 397–412.

Theil, T., M. Frain, P. Gilardi-Hebenstreit, A. Flenniken, P. Charnay and D. G. Wilkinson (1998). Segmental expression of the *EphA4* (*Sek-1*) receptor tyrosine kinase in the hindbrain is under direct transcriptional control of Krox-20. *Development* **125**: 443–452.

Trainor, P. and R. Krumlauf (2000). Plasticity in mouse neural crest cells reveals a new patterning role for cranial mesoderm. *Nature Cell Biology* **2**: 96–102.

van der Wees, J., J. G. Schilthuis, C. H. Koster, H. Diesveld-Schipper, G. E. Folkers, P. T. van der Saag, M. I. Dawson, K. Shudo, B. van der Burg and A. J. Durston (1998). Inhibition of retinoic acid receptor-mediated signalling alters positional identity in the developing hindbrain. *Development* **125**: 545–556.

Vesque, C., M. Maconochie, S. Nonchev, L. Ariza-McNaughton, A. Kuroiwa, P. Charnay and R. Krumlauf (1996). *Hoxb-2* transcriptional activation in rhombomeres 3 and 5 requires an evolutionarily conserved *cis*-acting element in addition to the Krox-20 binding site. *The EMBO Journal* **15** (19): 5383–5396.

Wassarman, K. M., M. Lewandoski, K. Campbell, A. L. Joyner, J. L. R. Rubenstein, S. Martinez and G. R. Martin (1997). Specification of the

anterior hindbrain and establishment of a normal mid/hindbrain organizer is dependent on *Gbx2* gene function. *Development* **124**: 2923–2934.

Wassef, M. and A. L. Joyner (1997). Early mesencephalon/ metencephalon patterning and the development of the cerebellum. *Perspectives in Developmental Neurobiology* **5**: 3–16.

White, J. C., V. N. Shankar, M. Highland, M. L. Epstein, H. F. DeLuca and M. Clagett-Dame (1998). Defects in embryonic hindbrain development and fetal resorption resulting from vitamin A deficiency in the rat are prevented by feeding pharmacological levels of all-*trans*-retinoic acid. *Proceedings of the National Academy of Sciences of the USA* **95**: 13459–13464.

Wilkinson, D. G. (2000). Eph receptors and ephrins: regulators of guidance and assembly. *International Review of Cytology* **196**: 177–244.

Wilkinson, D. G., S. Bhatt, P. Chavrier, R. Bravo and P. Charnay (1989b). Segment-specific expression of a zinc-finger gene in the developing nervous system of the mouse. *Nature* **337**: 461–464.

Wilkinson, D. G., S. Bhatt, M. Cook and E. Boncinelli (1989a). Segmental expression of Hox-2 homeobox-containing genes in the developing mouse hindbrain. *Nature* **341**: 405–409.

Wilson, P. A. and A. Hemmati-Brivanlou (1997). Vertebrate neural induction: inducers, inhibitors, and a new synthesis. *Neuron* **18**: 699–710.

Wingate, R. J. T. and M. E. Hatten (1999). The role of the rhombic lip in avian cerebellum development. *Development* **126**: 4395–4404.

Wizenmann, A. and A. Lumsden (1997). Segregation of rhombomeres by differential chemoaffinity. *Mollecular and Cellular Neuroscience* **9**: 448–459.

Wolpert, L. (1969). Positional information and the spatial pattern of cellular differentiation. *Journal of Theoretical Biology* **25**: 1–47.

Woo, K. and S. E. Fraser (1997). Specification of the zebrafish nervous system by nonaxial signals. *Science* **277**: 254–257.

Woo, K. and S. E. Fraser (1998). Specification of the hindbrain fate in the zebrafish. *Developmental Biology* **197**: 283–296.

Wood, H., G. Pall and G. Morriss-Kay (1994). Exposure to retinoic acid before or after the onset of somitogenesis reveals separate effects on rhombomeric segmentation and 3' HoxB gene expression domains. *Development* **120**: 2279–2285.

Xu, Q., G. Alldus, N. Holder and D. G. Wilkinson (1995). Expression of truncated Sek-1 receptor tyrosine kinase disrupts the segmental restriction of gene expression in the Xenopus and zebrafish hindbrain. *Development* **121**: 4005–4016.

Xu, Q., G. Mellitzer, V. Robinson and D. G. Wilkinson (1999). *In vivo* cell sorting in complementary segmental domains mediated by Eph receptors and ephrins. *Nature* **399**: 267–271.

Yan, Y., T. Jowett and J. H. Postlethwait (1998). Ectopic expression of *hoxb2* after retinoic acid treatment or mRNA injection: disruption of

hindbrain and craniofacial morphogenesis in zebrafish embryos. *Developmental Dynamics* **213**: 370–385.

Yang, X. W., P. Model and N. Heintz (1997). Homologous recombination based modification in *Escherichia coli* and germline transmission in transgenic mice of a bacterial artificial chromosome. *Nature Biotechnology* **15**(9): 859–865.

Zhang, M., H.-J. Kim, H. Marshall, M. Gendron-Maguire, D. Lucas, A. Baron, L. Gudas, T. Gridley, R. Krumlauf and J. Grippo (1994). Ectopic *Hoxa-1* induces rhombomere transformation in the mouse hindbrain. *Development* **120**: 2431–2442.

Zhang, Y., F. Buchholz, J. P. P. Muyrers and A. F. Stewart (1998). A new logic for DNA engineering using recombination in *Escherichia coli*. *Nature Genetics* **20**: 123–128.

Developmental Biology 211, 220–237 (1999)
Article ID dbio.1999.9318, available online at http://www.idealibrary.com on IDEAL®

The Role of *kreisler* in Segmentation during Hindbrain Development

Miguel Manzanares,* Paul A. Trainor,* Stefan Nonchev,*,[1] Linda Ariza-McNaughton,* Jim Brodie,* Alex Gould,*,[2] Heather Marshall,* Alastair Morrison,*,[3] Chung-Tin Kwan,† Mai-Har Sham,† David G. Wilkinson,* and Robb Krumlauf*,[4]

**Division of Developmental Neurobiology, MRC National Institute for Medical Research, The Ridgeway, Mill Hill, London NW7 1AA, United Kingdom; and †Department of Biochemistry, University of Hong Kong, 5 Sassoon Road, Hong Kong*

The mouse *kreisler* gene is expressed in rhombomeres (r) 5 and 6 during neural development and *kreisler* mutants have patterning defects in the hindbrain that are not fully understood. Here we analyzed this phenotype with a combination of genetic, molecular, and cellular marking techniques. Using *Hox/lacZ* transgenic mice as reporter lines and by analyzing *Eph/ephrin* expression, we have found that while r5 fails to form in these mice, r6 is present. This shows that *kreisler* has an early role in the formation of r5. We also observed patterning defects in r3 and r4 that are outside the normal domain of *kreisler* expression. In both heterozygous and homozygous *kreisler* embryos some r5 markers are induced in r3, suggesting that there is a partial change in r3 identity that is not dependent upon the loss of r5. To investigate the cellular character of r6 in *kreisler* embryos we performed heterotopic grafting experiments in the mouse hindbrain to monitor its mixing properties. Control experiments revealed that cells from even- or odd-numbered segments only mixed freely with themselves, but not with cells of opposite character. Transposition of cells from the r6 territory of *kreisler* mutants reveals that they adopt mature r6 characteristics, as they freely mix only with cells from even-numbered rhombomeres. Analysis of *Phox2b* expression shows that some aspects of later neurogenesis in r6 are altered, which may be associated with the additional roles of *kreisler* in regulating segmental identity. Together these results suggest that the formation of r6 has not been affected in *kreisler* mutants. This analysis has revealed phenotypic and mechanistic differences between *kreisler* and its zebrafish equivalent *valentino*. While *valentino* is believed to subdivide preexisting segmental units, in the mouse *kreisler* specifies a particular segment. The formation of r6 independent of r5 argues against a role of kreisler in prorhombomeric segmentation of the mouse hindbrain. We conclude that the mouse *kreisler* gene regulates multiple steps in segmental patterning involving both the formation of segments and their A-P identity.

***Key Words:* *kreisler*; segmentation; hindbrain; transgenic mice; and *Hox* genes.**

INTRODUCTION

The vertebrate hindbrain is organized and patterned as a segmented structure during early neural development. Its metameric units, the rhombomeres (r), are lineage-restricted cellular compartments that provide the basic ground plan by which segmental patterns of gene expression, neural crest migration, and neuronal differentiation occur in the hindbrain (Lumsden and Krumlauf, 1996). A number of the components which function in diverse aspects of segmental patterning have been identified based on expression patterns, as well as mutational and transgenic analysis. In this way it has been shown that the transcription factors *Krox20* and *kreisler* directly regulate segmental expression of multiple *Hox* genes (Manzanares *et al.*, 1997, 1999; Nonchev *et al.*, 1996; Sham *et al.*, 1993) and that *Hox* genes themselves have a role in conferring and

[1] Present address: Université Joseph Fourrier, Institut Albert Bonniot, Domaine de la Merci, 38706 La Tronche, Cedex France.
[2] Present address: Division of Mammalian Development, MRC National Institute for Medical Research, The Ridgeway, Mill Hill, London NW7 1AA, UK.
[3] Present address: Imperial Cancer Research Fund, 44 Lincoln's Inn Fields, London WC2A 3PX, UK.
[4] To whom correspondence should be addressed. Fax: 0181-913-8658. E-mail: r-krumlauf@nimr.mrc.ac.uk.

0012-1606/99

maintaining segmental identity (Gavalas *et al.*, 1997, 1998; Goddard *et al.*, 1996; Studer *et al.*, 1996, 1998; Zhang *et al.*, 1994). This has helped to unravel part of the network controlling the individual anteroposterior (A-P) identity of specific rhombomeres.

In contrast to segmental identity, very little is known about the mechanisms and genes governing segmentation itself. One gene involved in segmental processes is *Krox20*, which displays conserved early expression domains in r3 and r5 (Nieto *et al.*, 1991; Wilkinson *et al.*, 1989). In *Krox20* mutants territories for presumptive r3 and r5 arise, but they fail to develop properly and are eventually lost (Schneider-Maunoury *et al.*, 1993, 1997; Swiatek and Gridley, 1993). Recently it has been shown that *Krox20* directly regulates not only *Hox* genes, but also an *Eph* tyrosine kinase receptor involved in restricting cell migration between rhombomeres (Theil *et al.*, 1998; Xu *et al.*, 1995). Together with the mutant phenotype, this suggests that *Krox20* is involved initially in the maintenance of segments and later in steps that regulate the A-P identity and lineage restrictions of rhombomeres. There is also some evidence that *Hoxa1* may have a role in aspects of segmentation, as there is a partial reduction (Dollé *et al.*, 1993; Mark *et al.*, 1993) or a loss of r5 (Carpenter *et al.*, 1993) in targeted mutations of this gene. Therefore, *Hox* genes are involved in multiple steps of segmental patterning ranging from segmentation to segmental identity.

A candidate for regulating earlier steps in vertebrate hindbrain segmentation is *kreisler* (*kr*). Mice mutant for this gene, induced by X-ray mutagenesis, were first identified by Hertwig due to their circling behavior and deafness, which are phenotypes associated with vestibular-accoustic defects (Hertwig, 1944). Deol studied these mutants in early embryogenesis and found defects in the hindbrain, where there was an apparent loss of overt segments posterior to r4 (Deol, 1964). This led him to conclude that the adult phenotype was secondary to the early neural tube defects. The *kreisler* gene has been isolated by positional cloning and shown to encode a transcription factor of the b-zip Maf family (Kml1) expressed in r5 and r6 (Cordes and Barsh, 1994). Two independent studies have been performed, using molecular markers, to monitor changes in the *kreisler* hindbrain. One concluded that r5 and r6 are missing through a combination of changes in A-P identity and fate, followed by subsequent cell death (McKay *et al.*, 1994). The other study interpreted the data as the loss of overt segmentation of the hindbrain posterior to r4 leading to abnormal expression of markers in the region (Frohman *et al.*, 1993). While these reports clearly demonstrate that the posterior hindbrain in *kreisler* mutants has an abnormal organization, they do not address which processes (formation, maintenance, or the identity of segments) are affected.

A further complication in understanding the role of *kreisler* in segmentation comes from analysis of its zebrafish homologue, *valentino* (*val*). The *val* gene was first identified in a genetic screen as a mutation that affected the expression of *Krox20* in the hindbrain (Moens *et al.*, 1996) and later it was shown to be caused by mutations in a fish homologue of the mouse *kreisler* gene (Moens *et al.*, 1998). The general *val* phenotype resembles in some aspects that of *kreisler*. The interpretation of the *val* phenotype, based on marker gene expression and cell grafting experiments, is that *val* is involved in the subdivision of a prorhombomere into r5 and r6 and that in the *val* mutant the prospective r5–r6 territory is frozen at an early stage. This leads to an immature rhombomere (rX) lacking any specific segmental identity in place of r5 and r6 (Moens *et al.*, 1996, 1998). Based on this model, it was concluded that mouse *kreisler* has a similar function to *valentino* and that the different interpretations of the mouse phenotype (Frohman *et al.*, 1993; McKay *et al.*, 1994) could be reconciled by this mechanism (Moens *et al.*, 1998; Prince *et al.*, 1998). Hence, this model argues that *kreisler* functions in the maturation and identity of a definitive pair of segments and that the developments of r5 and r6 are tightly coupled because they arise from a common prorhombomeric territory.

To investigate the nature of the segmental defects in *kreisler* mutants and their relationship to the fish *valentino* phenotype, we have examined *kreisler* mutants with a combination of genetic, molecular, and cellular marking techniques. Using transgenic analysis we have previously identified a number of *cis*-regulatory components that direct rhombomere-restricted expression of *Hox* genes (reviewed in Maconochie *et al.*, 1996). Here we have taken advantage of 10 different transgenic lines carrying a *lacZ* reporter gene under the control of these segmental enhancers and systematically bred them into the *kreisler* mutant background. We have also analyzed the expression of additional marker genes and carried out cell grafting experiments in order to analyze the character of the territory affected in the *kreisler* mutant. Our results show that r5 is missing and that r6 is actually present in the *kreisler* hindbrain. Hence, with respect to r5, *kreisler* is essential for the formation of this segment. Segmentation and boundary formation in the rest of the hindbrain are primarily normal and there is no evidence for an immature or early common precursor of r5 and r6 that fails to subdivide. Furthermore, there are effects in r3 and r4 outside of the normal domain of *kreisler* expression. This shows that *kreisler* has a role in the early formation of a single segment, in addition to its later roles in regulating segmental identity.

MATERIALS AND METHODS

Mouse Breeding

kreisler mice were bred, maintained, and genotyped as described (Frohman *et al.*, 1993). Colonies of *kr;lacZ* transgenic mice were obtained by crossing *kr/kr* males to homozygote or heterozygote females for the transgenes. The F1 progeny was genotyped for both the *kr* allele (where necessary) and the transgene and embryos of the desired stage and genotype were obtained by intercrossing of the F1 or by backcrossing to *kr/kr* males or *kr/+* females. Some of these colonies were further expanded and maintained. Among these was the *kr;b1-r4* colony, from where *kr/kr* transgenic males

Copyright © 1999 by Academic Press. All rights of reproduction in any form reserved.

were used to generate double transgenic embryos. The genotype of the embryos was determined visually between 9.0 and 10.5 days postcoitum (dpc) and by PCR for other stages. Expression patterns of the transgenes or *in situs* were indistinguishable between +/+ and *kr*/+ embryos, so both are referred to as wt (wild type) throughout the text. The only exception is the *a3-r5/r6* line (see Results). *LacZ* reporter expression was detected as described (Whiting *et al.*, 1991) and reporter transgenic lines used in this study are listed with a brief description in Table 1.

Cell Grafting and Tracing

Embryos of the desired genotype were obtained as described above or from CBA × C57/BL6 crosses for wild-type embryos. Host embryos (8.5 dpc) were dissected from the uterus with an intact visceral yolk sac, amnion, and ectoplacental cone (Trainor and Tam, 1995; Trainor *et al.*, 1994). Isochronic donor *kr/kr* embryos and donor wild-type embryos were initially bisected along the midline and neuromeric junctions were used as landmarks for isolating specific rhombomeres (Trainor and Tam, 1995). In *kreisler* mutants the position of presumptive r6 was defined as the territory immediately posterior to the otic sulcus, in agreement with our marker analysis. This corresponds to r5 in wild-type embryos. Finely polished alloy and glass needles were used to separate the neuroectoderm from adjacent tissues. Rhombomeric fragments that could not be cleanly separated from adjacent tissues were then incubated in a solution of 0.5% trypsin, 0.25% pancreatin, 0.2% glucose, and 0.1% polyvinylpyrolidone in PBS for 20 min at 37°C to ensure a pure rhombomeric donor population. Individual rhombomeres were then labeled by soaking in a 1:1 mix of DiI (1,1-dioctadecyl-3,3,3′,3′-tetra-methylindocarbocyanine perchlorate): DR50 (DiI:50% Dulbecco's modified Eagle's medium, 50% rat serum) for 1 min, washed in DR50, dissected into fragments containing approximately 10–15 cells, and grafted into the dorsal neuroectoderm of 8.5-day (5-somite-stage) host CBA × C57/BL6 embryos. Previous work has established that the first neural crest cells to migrate leave the dorsal caudal midbrain/rostral hindbrain neuroepithelium at the 5- to 6-somite stage (Chan and Tam, 1988; Jacobson and Tam, 1982; Nichols, 1981). Therefore, in order to catch the earliest waves of migrating neural crest cells in both cell grafting and neural crest cell labeling experiments, only donor and host embryos having five or less pairs of somites were used. After cell grafting or neural crest cell labeling by DiI injection, embryos were cultured *in vitro* for 24 h in DR50 in a 5% CO_2, 5% O_2, 90% N_2 atmosphere (Sturm and Tam, 1993). The genotype of the donor embryos was determined by PCR as described above. Solutions (0.05%, w/v) of DiI were made from 0.5% stock ethanolic solutions diluted 1:10 in 0.3 M sucrose.

We labeled the facial (VII) motor neurons by retrograde tracing using DiI (Molecular Probes) at a concentration of 1 mg/ml in dimethyl formamide. Embryos were dissected from the uterus in PBS and the cranial roots were injected using a pressure injector (Picospritzer). Following injection, embryos were fixed in 4% paraformaldehyde and stored at room temperature for up to a week. The labeled hindbrains were dissected of any surrounding tissue and flat mounted in glycerol/PBS. The labeled neurons were viewed using a Leica TCS NT confocal microscope, with an argon/krypton laser (excitation 567 nm) and a 10×/0.3 NA Leica lens.

In Situ Hybridization and Immunochemistry

Immunostaining using a monoclonal antibody specific for mouse HOXB4 was as described (Gould *et al.*, 1997). Whole-mount *in situ* hybridization with digoxigenin-labeled RNA probes was performed as described (Xu and Wilkinson, 1998). The *ephrin-B2* and *ephrin-B3* probes correspond to the full coding region of cDNA clones (Gale *et al.*, 1996), the *EphA7* probe to a fragment of the extracellular domain of the protein (nucleotide residues 636–1211), and the *Phox2b* probe as previously described (Pattyn *et al.*, 1997).

RESULTS

To analyze the nature of the segmental defects in *kreisler* mice, we have intercrossed them with 10 different transgenic *Hox/lacZ* reporter lines containing rhombomere-specific regulatory elements from the *Hoxb1* to *Hoxb4* and *Hoxa3* genes. These control elements are well characterized and have important roles in segmental regulation of their respective *Hox* genes. The benefit of these genetic markers is that they allow us to monitor specific subsets of the normal expression pattern of the respective endogenous genes and permit a clear-cut identification of specific hindbrain territories. In this way we have been able to study the loss or change in identity of individual rhombomeres and rhombomeric boundaries, due to the mutation of the *kreisler* gene. Table 1 provides a list of the lines used, relevant control regions, and a brief description of their expression patterns. In this analysis we will refer to transgene expression in the +/+ or *kr*/+ backgrounds as the wild-type or normal pattern and in the *kr/kr* background as the mutant pattern (except for the *a3-r5/r6* line; see below).

Analysis of Defects in r4

To mark r4 and its derivatives we have used two transgenic lines where reporter expression is directed by an r4-specific enhancer from *Hoxb1* [*b1-r4* line (Marshall *et al.*, 1992)] or *Hoxb2* [*b2-r4* line (Maconochie *et al.*, 1997)]. Figure 1 shows a comparison of normal and mutant staining patterns from 8.5 to 12.5 dpc for the *b1-r4* line. Between 8.5 and 9.0 dpc the r4 stripe of reporter expression in the mutant background appears relatively normal, except that its overall size is slightly larger and the posterior border appears more diffuse (Figs. 1A, 1B, 1H, and 1I). This is in agreement with previous analysis of *Hoxb1* expression by *in situ* hybridization (Frohman *et al.*, 1993; McKay *et al.*, 1994). However, temporal analysis shows that this is not a stable property of the r4 territory in the mutants. From 9.5 to 12.5 dpc there is a gradual reduction in the size of r4 expression as well as a clear disorganization of the posterior boundary (Figs. 1C–1F and 1J–1M). Using whole-mount *in situ* hybridization and antibody staining we have found that a similar size reduction in r4 occurs in the endogenous *Hoxb1* expression domain (data not shown).

This transgene is also expressed in facial branchiomotor (fbm) neurons which undergo a characteristic series of movements, whereby they normally migrate from r4 into r5 along the ventral midline at 11.5 dpc [Fig. 1E (Studer *et al.*, 1996)]. By 12.5 dpc they have migrated posteriorly and then laterally into r6 forming the nucleus of the facial (VII) nerve (Fig. 1F). In the mutant background fbm neurons expressing

Copyright © 1999 by Academic Press. All rights of reproduction in any form reserved.

TABLE 1

Gene	Line	Lab name	Wt pattern	*kr/kr* pattern	Main reference
Hoxb1	*b1-r4*	HL5	r4 facial neurons	Fuzzy posterior boundary, defective migration	Marshall *et al.* (1992)
Hoxb2	*b2-r4*	ML22	r4 ba2 crest	Fuzzy posterior boundary, defective migration	Maconochie *et al.* (1997)
	b2-r3/r5	ML19	r3 + r5	Missing r5 stripe	Sham *et al.* (1993)
	b2-r3/r4/r5	ML24	r3 + r5 r4 (late)	Missing r5 stripe, fuzzy posterior boundary	Sham *et al.* (1993)
Hoxb3	*b3-r5*	EL-IV	r5	Missing r5 stripe	Kwan *et al.* (unpublished) Manzanares *et al.* (1997)
	b3-r5/6	EL-IIIA	r5–r6 boundary	Anterior 1/2 rhombomere shift	Kwan *et al.* (unpublished)
Hoxa3	*a3-r5/r6*	A3-K146	r5 + r6	Missing r5 + r6 domain, ectopic activation in r3	Manzanares *et al.* (1999)
Hoxb4	*b4-r6/7*	JL64	r6–r7 boundary	Anterior 1 rhombomere shift	Whiting *et al.* (1991)
	b4-r6/7 early	AG17	r6–r7 boundary	Anterior 1 rhombomere shift	Gould *et al.* (1998)
	b4-r6/7 late	AG8	r6–r7 boundary	Anterior 1 rhombomere shift	Gould *et al.* (1997)

the transgene migrate along the midline into the segment posterior to r4 but they form a highly disorganized nucleus that immediately begins to migrate laterally (Figs. 1L and 1M). To test if the pattern with the *lacZ*-positive cells faithfully represents the behavior of the major components of the facial motor nerve we performed DiI retrograde labeling in normal and mutant embryos [see Studer *et al.* (1996) for a brief description of the organization of the facial nerve]. These results show that in mutant embryos axonal projections and cell bodies of the facial motor nerve are abnormally located immediately posterior to r4 and do not display the one rhombomere gap seen in normal embryos (Figs. 1G and 1N). In agreement with analysis by McKay *et al.*, the population of visceromotor neurons (vm) which arises in r5 and exits through r4 is absent (McKay *et al.*, 1997). In contrast, the contralateral vestibuloaccoustic neurons (cva) that cross the midline specifically at the level of r4 appear normal. This population does not extend more posteriorly in the mutant (Figs. 1G and 1N), suggesting that the r4 territory has not expanded in a posterior direction.

Similar analysis using the *b2-r4* line confirmed that initial transgene expression in r4 appears normal, but between 9.5 and 11.5 dpc there is a marked reduction in the size of the r4 domain and abnormal migration of the fbm neurons (Figs. 2A, 2B, 2F, and 2G and data not shown). This *b2-r4* line also expresses the reporter at high levels in the cranial neural crest derived from r4, which normally migrates rostral to the otic vesicle and into the second branchial arch (Fig. 2C). In mutant embryos we noted an accumulation of *lacZ*-expressing cells between the hindbrain and the laterally displaced otic vesicle (Fig. 2H). This is interesting because it has been reported that there are defects in the hyoid bone of *kreisler* mutants that could be interpreted as a partial transformation of third arch structures into a second arch identity (Frohman *et al.*, 1993). This phenotype could arise because the accumulating r4 crest might be able to migrate rostrally and caudally around the laterally positioned otic vesicle and contribute to both the second and third branchial arches. To assess whether there are changes in the patterns of neural crest migration in *kr* mutants, we performed lineage analysis by direct focal injection of DiI at 8.5 dpc into the dorsal hindbrain of normal and mutant embryos followed by 24 h in culture. The results showed that in both cases when presumptive r4 was labeled, cells only contributed to the second branchial arch (Figs. 2D and 2I). In contrast, when the presumptive segment immediately posterior to r4 was labeled, cells are able to contribute to both the second and third branchial arches in normal and mutant embryos (Figs. 2E and 2J). More posterior injections in the mutant only label neural crest cells migrating into the third arch (Fig. 2K). This argues that the hyoid defects do not arise by abnormal migration of r4-derived cells into the third arch and that the lateral displacement of the otic vesicle does not prevent crest arising posterior to r4 from migrating into the second arch. Therefore, the hyoid defects could arise because *kreisler* or its targets (*Hoxb3* and *Hoxa3*) have an important role in patterning third arch crest, which is in line with the loss of hyoid structures observed in *Hoxa3* mouse mutants (Chisaka and Capecchi, 1991). It is also possible that these are secondary patterning defects due to the unusual contribution of r6-derived crest cells to both the second and third arches.

Together, these results show that in *kreisler* mutants there is a progressive failure to maintain a normal-sized r4 territory. The anterior boundary with r3 is distinct and normal in appearance; however, the posterior border is always more diffuse. Furthermore, the spatial pattern of facial motor neuron migration is severely affected once they leave r4. This is in contrast to the changes in r4 patterning observed in early *kreisler* mutants and the fish *valentino* mutants on the basis of *Hoxb1* expression, which reported a posterior expansion of the r4 territory (Frohman *et al.*, 1993; McKay *et al.*, 1994; Prince *et al.*, 1998).

Copyright © 1999 by Academic Press. All rights of reproduction in any form reserved.

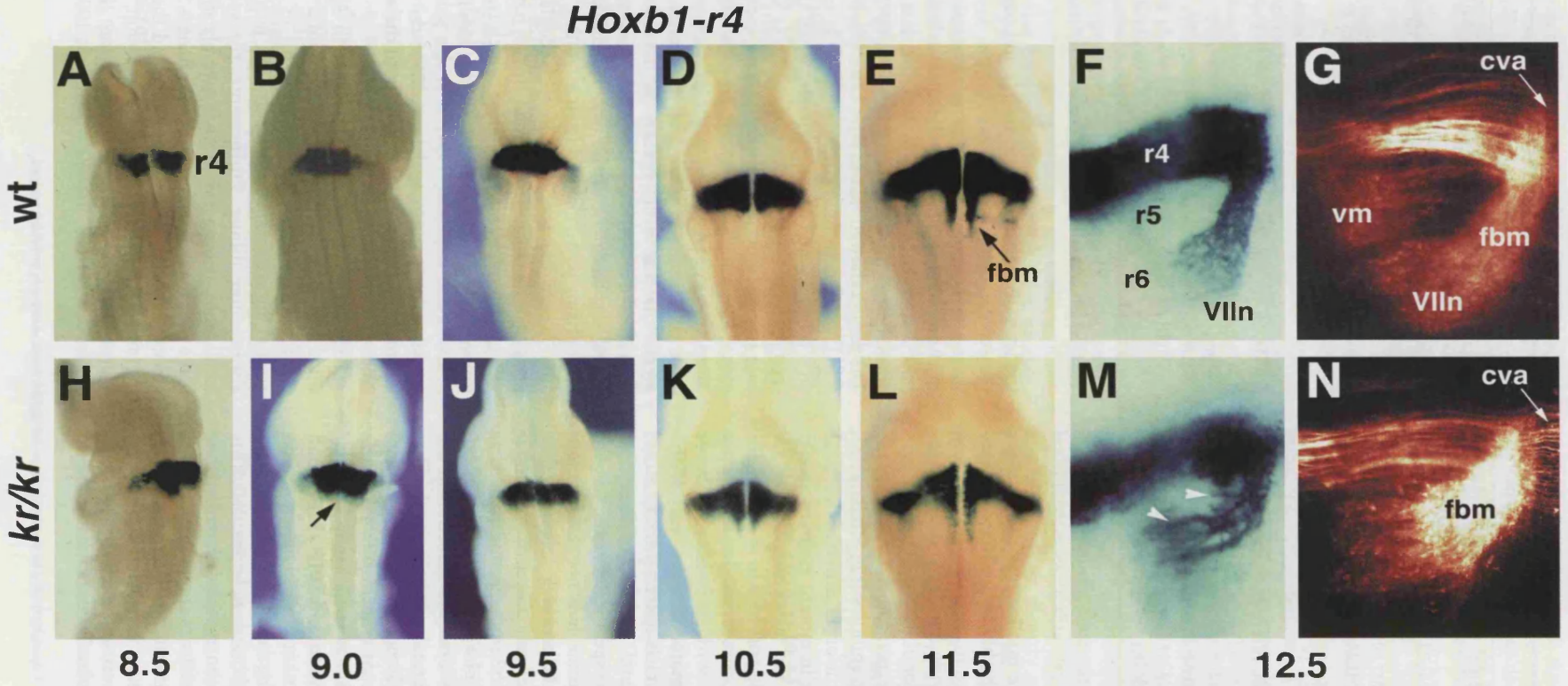

FIG. 1. Expression of the *Hoxb1-r4* transgenic line in wt (A–F) and *kr/kr* (H–M) embryos. Up to 9.5 dpc the stripe corresponding to r4 is broader in *kr/kr* (H, I) than in wt (A, B), but from that moment on it is reduced (J–L) compared to wt (C–E). The projections of the facial branchiomotor (fbm; arrow in E) neurons migrate posterior to r4 normally in the mutant (K) but are misrouted once they turn into the nuclei of the facial ganglion (VIIn; F, M). White arrowheads in M point to branching of the fbm projections shortly after leaving the r4 territory. DiI retrograde tracing of the facial nerve (G, N) shows the same misrouting of the fbm neurons, normal behavior of the cva (contralateral vestibuloaccoustic) neurons, and the absence of the visceromotor neurons (vm) in the mutant (N), compared to normal embryos (G). Embryonic stage in dpc is shown below the panels.

Copyright © 1999 by Academic Press. All rights of reproduction in any form reserved.

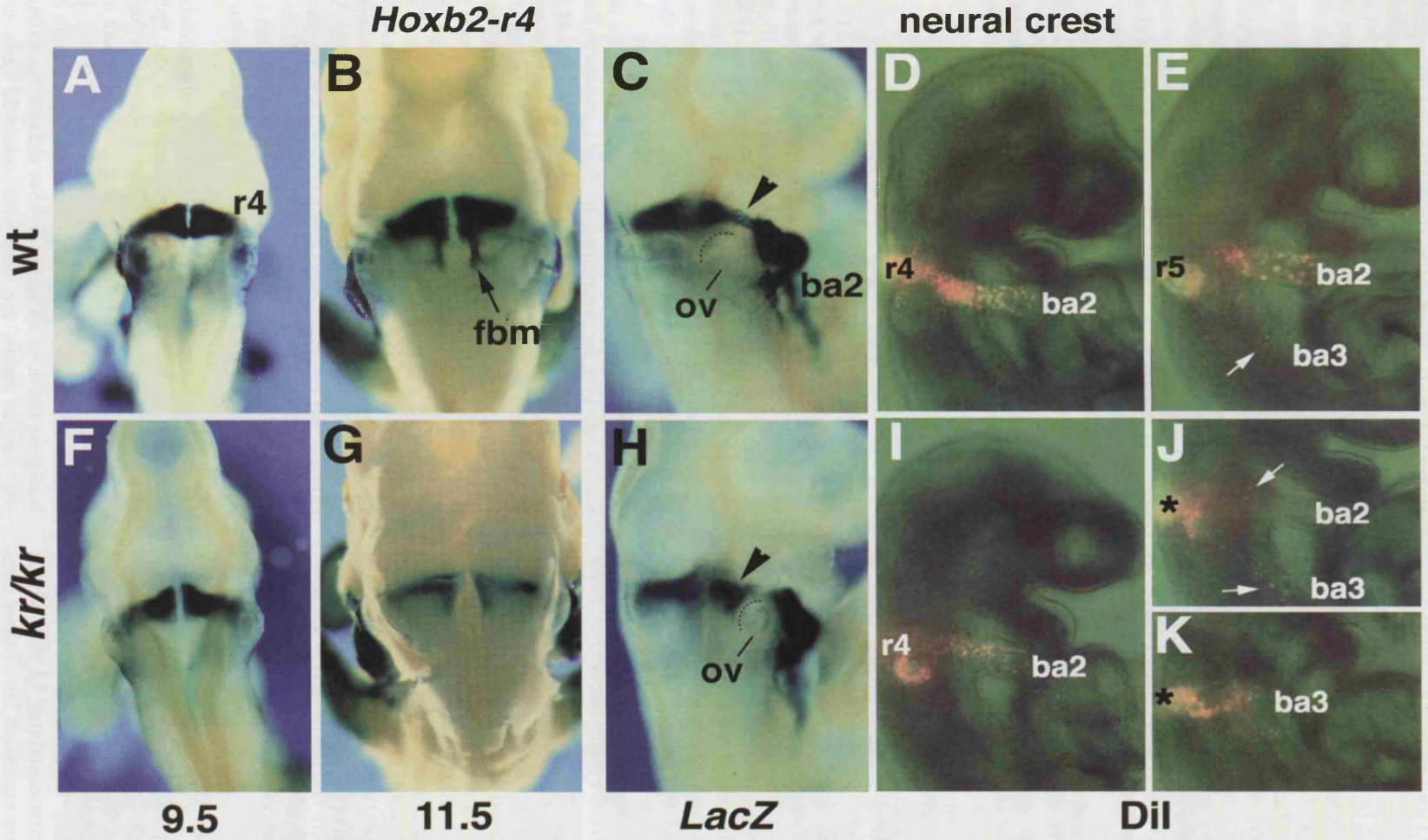

FIG. 2. Expression of the *Hoxb2-r4* transgenic line in wt (A–C) and *kr/kr* (D–F) embryos. The r4 stripe is of similar width at 9.5 dpc in the mutant (F) and wt (A), but clearly thinner at 11.5 dpc in mutant embryos (B, G). The migratory patterns of neural crest cells were analyzed in wt (C–E) and *kreisler* (H–K) embryos by both *LacZ* staining of the *Hoxb2-r4* transgenic reporter (C, H) and DiI focal injections to label migrating cells leaving the hindbrain (D, E, I–K). In wt embryos, there is a thin and contiguous stream of *LacZ*-positive cells leaving r4 (arrowhead in C) and migrating into the second branchial arch (ba2). In contrast, *LacZ* staining is observed in a population of cells located between the otic vesicle (outlined) and the neural tube in *kreisler* embryos (arrowhead in H). The fate of cells leaving the neural tube was followed by DiI tracing, in order to see if this ectopically located population of neural crest cells in kr embryos could contribute to the third arch (ba3). When the focal injection of DiI was performed on presumptive r4, labeled cells were only observed in ba2 in both wt (D) and mutant (I). When the rhombomere immediately posterior to r4 was labeled, cells were found in ba2 and ba3 in both mutant and wt (arrows in E and J). Labeling cells two rhombomeres posterior to r4 in the mutants showed that DiI-labeled cells were only present in ba3 (K). Embryos shown in C–E and H–K are 9.5 dpc.

Analysis of Defects in r3 and r5

All studies to date on *kreisler* phenotypes have identified r5 as a major functional domain of the gene, exemplified by the absence of an r5 stripe of *Krox20* expression. However, the stage of segmentation at which these defects arise, e.g., formation or maintenance, has not been determined. To examine if there is a transient appearance of r5 at very early stages we have used two transgenic lines containing a *Krox20*-dependent enhancer from the *Hoxb2* gene that direct reporter expression specifically to r3 and r5 [*b2-r3/r5* and *b2-r3-r5* (Sham *et al.*, 1993)]. Over a detailed early time course, the temporal dynamics and parameters of transgene expression in r3 are identical in normal and mutant embryos (Fig. 3). In wild-type embryos the onset of expression in r5 occurs later than in r3 (Figs. 3A–3C); however, throughout this time course we never detect a second stripe or even a few lacZ-expressing cells in *kreisler* mutant embryos (Figs. 3F–3J). This suggests that r5 never forms, unlike *Krox20* mutants in which r5 is lost at later stages (Schneider-Maunoury *et al.*, 1993, 1997).

We have previously identified an r5-specific enhancer from the *Hoxb3* gene that is a transcriptional target of *kreisler* (Manzanares *et al.*, 1997). To determine if reporter expression in r5 is strictly dependent upon *kreisler* we mated a line with this enhancer (*b3-r5*) into the mutant background. Reporter staining in r5 of mutant embryos is never observed in any of the stages examined from 7.5 to 10.5 dpc (Figs. 4A–4F and data not shown). This shows that *kreisler* is required to establish and maintain segmental expression mediated by this enhancer. Recently we have also isolated an enhancer from the paralogous *Hoxa3* gene that directs expression in r5 and r6 (Figs. 4G and 4J) and is a transcriptional target of *kreisler* (Manzanares *et al.*, 1999). Here we used a reporter line with this enhancer (*a3-r5/r6*) and crossed it into the *kreisler* mutant background. In homozygous mutant embryos, expression in r5 and r6 is completely absent (Figs. 4I and 4L), showing that in these domains the *Hoxa3* enhancer activity is dependent upon *kreisler*. Surprisingly, analysis in both *kr*/+ and *kr/kr* embryos revealed an ectopic induction of the *Hoxa3* reporter in r3 (Figs. 4H, 4I, 4K, and 4L). This is consistent with a previous report on the appearance of some *Hoxa3*-positive cells in the r3 territory of homozygous *kreisler* mutants, as detected by radioactive *in situ* analysis (McKay *et al.*, 1994). This suggests that there may also be progressive changes in the identity of r3 dependent on the dosage of *kreisler*.

Analysis of Defects in the Posterior Hindbrain

To study the posterior defects in the hindbrain of *kreisler* embryos, we intercrossed the mutants with three different lines which contain combinations of neural enhancers from *Hoxb4* that direct lacZ reporter expression up to an anterior limit at the r6–r7 boundary (Gould *et al.*, 1997, 1998; Whiting *et al.*, 1991). Immunostaining of endogenous HOXB4 protein and reporter expression for all three lines shows that in mutant embryos the rostral limit of expression at 9.5 dpc is shifted anteriorly closer to the otic vesicle (Figs. 5A–5F and data not shown). In all cases, the anterior boundary in the mutants is as sharp as in normal embryos. This anterior shift is maintained through later stages, as evidenced by a clear reduction in the distance between the pontine flexure (pf) and the anterior limit of transgene expression at 11.5 dpc (Figs. 5G and 5H).

To more precisely map the position of this anterior shift in *Hoxb4* expression, we generated double transgenic embryos with the *b4-r6/7* line and the *b1-r4* reporter line in normal and mutant backgrounds (Fig. 6). By marking r4 and r6/7 in this manner, in the normal embryos there is a clear two-rhombomere gap between the domains of *lacZ* expression (Figs. 6A, 6C, and 6E). In contrast, in *kr mutants* this is reduced to a one-segment gap (Figs. 6B, 6D, and 6F). Our detailed time course of these lines indicates that this spatial relationship is maintained at later stages and these domains do not overlap. Therefore, in *kreisler* mutants *Hoxb4* expression has shifted anteriorly by a single rhombomere and a sharp anterior boundary is maintained.

The Presence of an r6-like Territory

Previous studies in mouse and zebrafish have argued that in *kreisler/valentino* mutants r5 and r6 are lost, adopt new mixed identities, or become locked in a prerhombomeric state and fail to express markers for either segment (Frohman *et al.*, 1993; McKay *et al.*, 1994; Moens *et al.*, 1996, 1998). From our analysis above, the presence of a single segment between the r4 and r6/r7 marker domains raises a question concerning its identity. Since we have found that r5-specific markers are missing, we also tested for the presence of r6 markers. While there are currently no r6-specific markers, for this purpose we used a transgenic line carrying a neural regulatory element from *Hoxb3* that is expressed up to an anterior limit at the r5/r6 boundary and also ventrally in r5 (*b3-r5/6* line; Kwan *et al.*, unpublished). Generating double transgenic embryos for this reporter and the *b1-r4* line shows that in normal embryos there is a lateral gap in *lacZ* expression, corresponding to r5 (Figs. 7A, 7C, and 7E). The staining along the ventral midline in r5 is due to both the posterior migration of the fbm neurons labeled with the *b1-r4* reporter and the anterior expression of the *b3-r5/6* line into ventral r5 (Figs. 7C and 7E). In contrast, the two domains of reporter expression are completely fused in *kreisler* mutant embryos (Figs. 7B, 7D, and 7F). This shows that the segment located between the r4 and r7 in the *kreisler* embryos expresses a marker indicative of an r6-like or more caudal identity.

To extend this analysis we have also examined segmental expression of several receptors and ligands of the *Eph/ephrin* families. *Ephrin-B2* is normally expressed at high levels in r1, r2, r4, and r6, with lower levels in r3 and no expression in r5 [Fig. 8A (Bergemann *et al.*, 1995)]. In *kreisler* embryos the gap of expression corresponding to r5 is missing and there is a fusion of the r4 and r6 domains (Fig. 8B). Similar results are seen with *ephrin-B3* (data not shown). The *EphA7* receptor is normally expressed at high

Copyright © 1999 by Academic Press. All rights of reproduction in any form reserved.

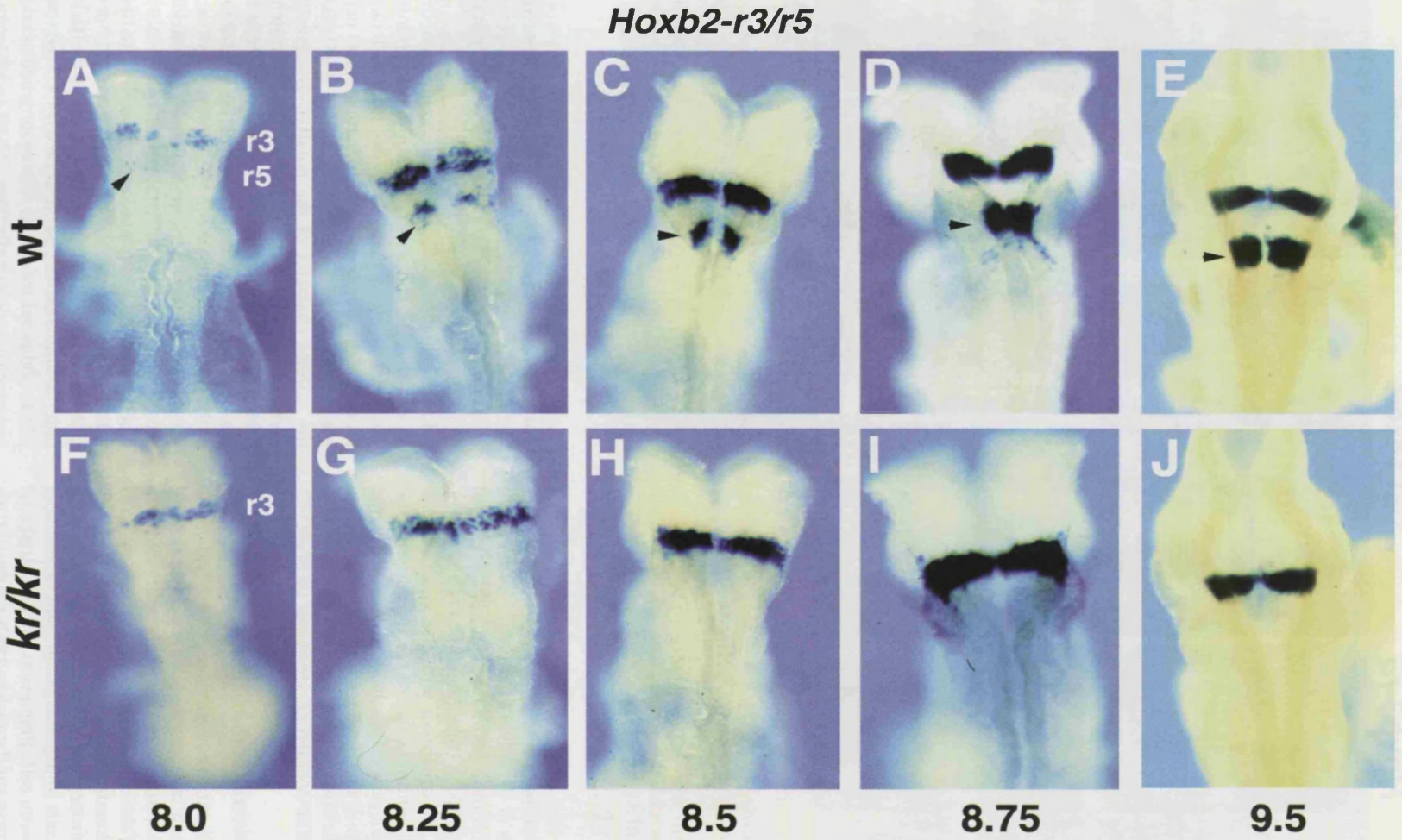

FIG. 3. Expression of the *Hoxb2-r3/r5* transgenic line in wt (A–E) and *kr/kr* (F–J) embryos. In wt embryos the stripe corresponding to r3 appears first and only later does the stripe for r5 begin expressing the transgene (A). Gradually the r5 stripe becomes broader (B–D) and by stage 9.5 both stripes are of comparable intensity. In *kr/kr* embryos, not a single cell in the prospective r5 territory turns on the transgene from the earliest stages examined. Arrowheads in A to E point to the r5 stripe of *lacZ* expression. Embryonic stage in dpc is shown below the panels.

Copyright © 1999 by Academic Press. All rights of reproduction in any form reserved.

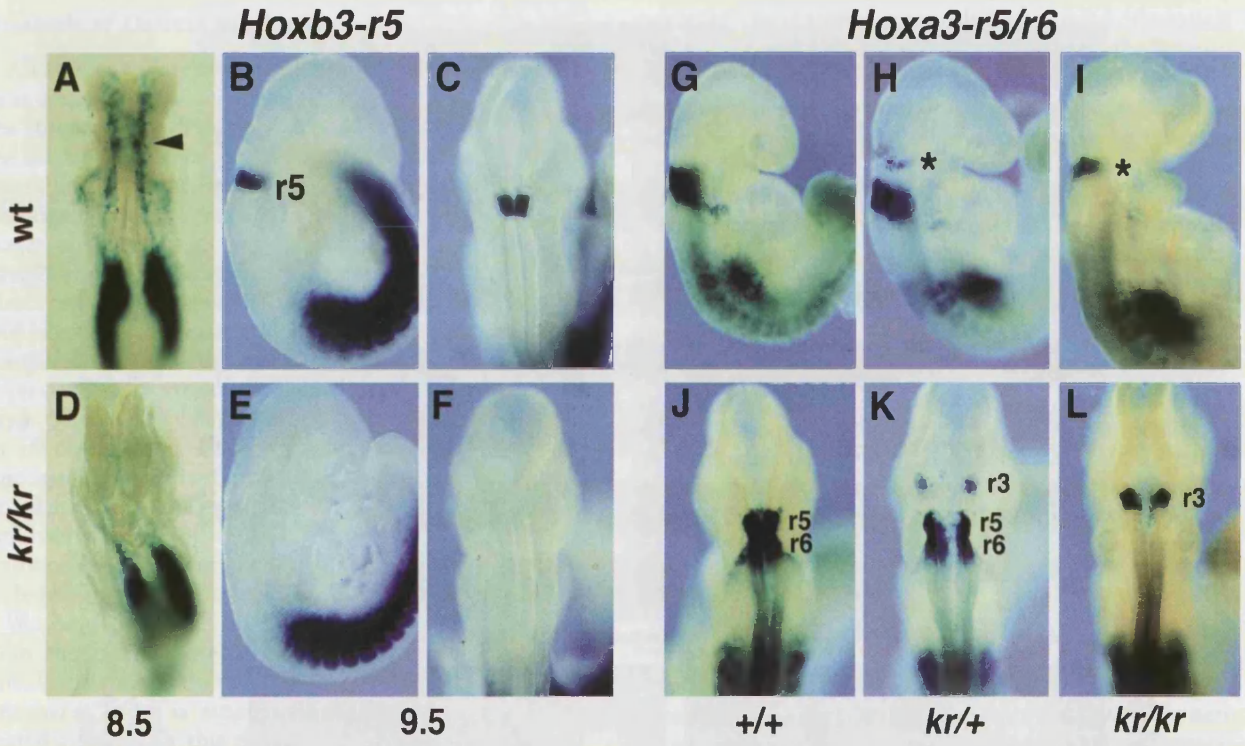

FIG. 4. Expression of the *Hoxb3-r5* (A–F) and *Hoxa3-r5/r6* (G–L) transgenic lines. The reporter for the *b3-r5* line is never turned on in the prospective r5 territory of the mutant from the earliest stages examined (A–C, normal embryos; D–F, mutants). The *a3-r5/r6* line exhibits a peculiar behavior in that it shows differences between wild-type (+/+; G, J), heterozygote (*kr*/+; H, K), and homozygote (*kr/kr*; I, L) embryos for the *kreisler* mutation. This transgene is normally expressed in r5 and r6 (J), but in *kr*/+ embryos a weak extra domain of expression (asterisk in H and I) is observed in r3 (K). In *kr/kr* embryos, the r5/r6 domain is lost but the ectopic r3 domain is stronger than in *kr*/+ embryos (L). All embryos are 9.5 dpc except for A and D that are 8.5 dpc.

levels in r3 and r5, at lower levels in r2, r4, and r6, but not in r7 [Fig. 8C (Ellis *et al.*, 1995)]. In *kreisler* mutants the high-level expression in r5 is missing and there is a fused domain of lower expression corresponding to r4 and r6 (Fig. 8D). These results are consistent with the idea that r5 is deleted and that r6 continues to express its characteristic pattern of *Eph/ephrin* genes. Together with the data on the *b3-r5/6* reporter line, our findings suggest that in the *kreisler* mutant r5 is missing but that r6 is actually formed and initially adopts an appropriate segmental identity.

Cell-Mixing Properties in the kreisler Hindbrain

Rhombomeres act as cell compartments, with little or no cell mixing between adjacent segments (Birgbauer and Fraser, 1994; Fraser *et al.*, 1990). This has been attributed to differences in both the cell adhesive and repulsive properties of alternating rhombomeres. It has been shown in chick embryos that cells from even-numbered rhombomeres will freely mix, as will cells from odd segments, but intermixing does not occur between cells from even- and odd-numbered rhombomeres (Guthrie and Lumsden, 1991; Guthrie *et al.*, 1993; Wizenmann and Lumsden, 1997). The *Eph* receptors and *ephrins* have been implicated in these restrictions of cell intermingling (Xu *et al.*, 1995, 1999). Therefore differences in mixing properties reflect the odd or even character of a segment along the A-P axis.

In the zebrafish model for *valentino* function, the inability of *val*$^{-}$ cells and wild-type r5 or r6 cells to intermingle was used to argue that the rX territory is locked in an immature prorhombomeric state that possesses neither odd nor even character (Moens *et al.*, 1996, 1998). To address the cellular character of the putative r6 segment in the *kreisler* embryos, we carried out grafting experiments in the mouse by transposing small populations of cells from the otic region of *kreisler* or wt embryos. As mixing properties of rhombomeric cells have not been previously examined in the mouse, we first performed a series of control experiments. Donor cells from wild-type 8.5 dpc embryos were labeled with DiI and grafted orthotopically and heterotopically into wild-type hindbrains. After 24 h of embryo culture we visualized the distribution of the DiI label in order to follow the fate of the grafted cells. Even to even and odd to odd grafts mix freely, but even to odd or odd to even transpositions do not mix (Figs. 9D–9F and data not shown). This further supports the idea that a restriction to mixing

Copyright © 1999 by Academic Press. All rights of reproduction in any form reserved.

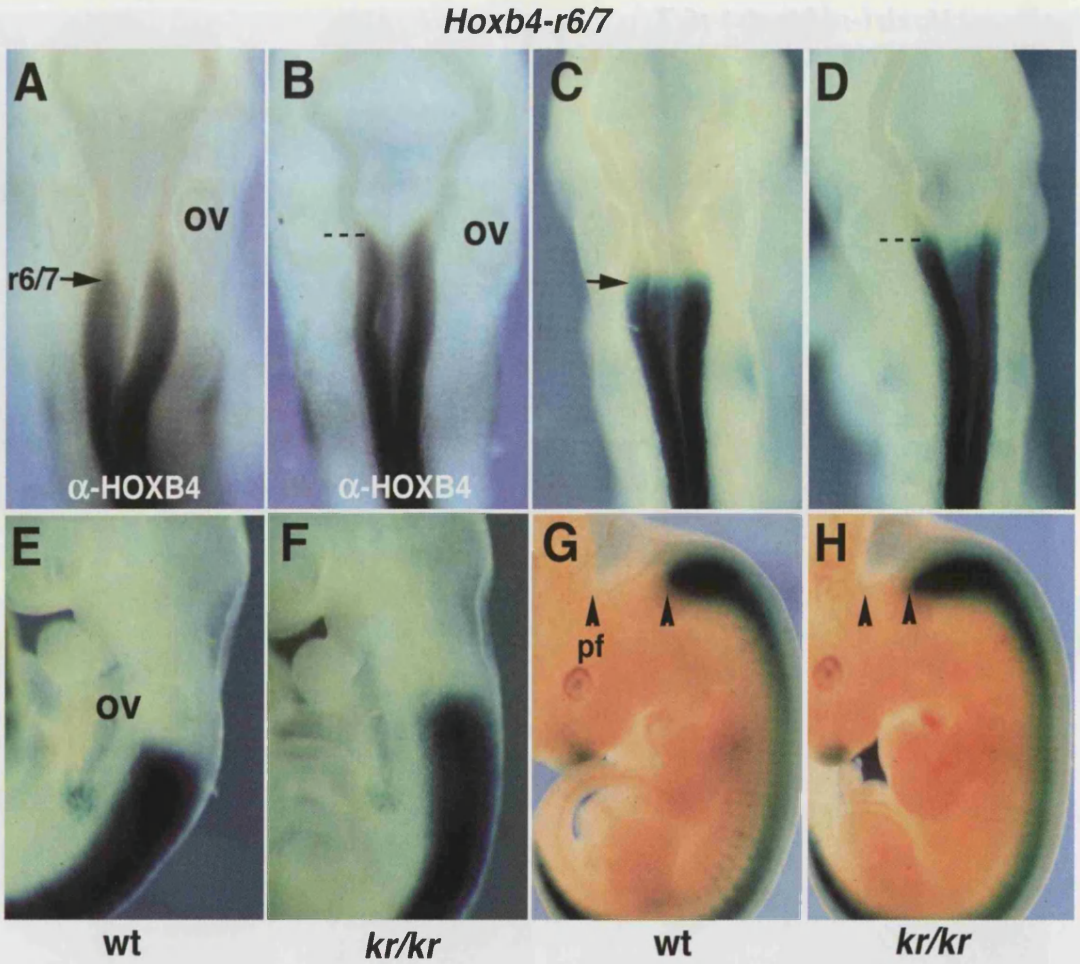

FIG. 5. Expression of HOXB4 protein (A, B) and the *Hoxb4-r6/7* transgenic line (C–H) in wt (A, C, E, G) and *kr/kr* (B, D, F, H) embryos. The expression of the endogenous protein is faithfully mimicked by the transgene at 9.5 dpc (A–F). An anterior shift of one rhombomere length is observed in the mutant embryos with both the α-HOXB4 antibody (A, B) and the reporter line (C–F). A sharp anterior limit of expression is observed at the r6/r7 boundary for wt (arrows in A and C) and adjacent to the otic vesicle (ov) in *kr/kr* embryos (dashed lines in B and D). This anterior shift in expression is still maintained at a later stage (11.5 dpc) as is evident in the smaller distance between the anterior limit of the expression of the transgene and the pontine flexure (pf; arrowheads in G and H) in *kr/kr* (H) compared to wt (G).

between odd and even segments is a general property of the vertebrate hindbrain.

In an analogous manner, grafts of rhombomeric tissue from *kreisler* donor embryos, corresponding to presumptive r6, were transplanted to r2, r5, or r6 in wild-type hosts (Figs. 9A–9C). The *kreisler*-derived cells mix freely with even-numbered rhombomeres and also contribute to neural crest derived from them that migrates into the branchial arches (Figs. 9A and 9C). However, when grafted into odd-numbered rhombomeres, such as r5, they remain as a tight clump of labeled cells with no mixing (Figs. 9A and 9B). Therefore, presumptive r6 from *kreisler* mutant embryos displays cell-mixing properties in the hindbrain characteristic of a mature even-numbered rhombomere. This is in clear contrast to the results in zebrafish, arguing that in the mouse, even in the absence of r5, r6 forms and it is not locked in an immature prorhombomeric state.

Late Characteristics of r6 in kreisler Mutants

The fact that r6 is formed and initially adopts an appropriate identity in *kreisler* mutants does not exclude the possibility that there could be later defects in this rhombomere. For example, the lack of *Hoxa3* upregulation in r6 that occurs because it is a direct transcriptional target of *kreisler* [Figs. 4G–4L and Manzanares *et al.* (1999)] could result in later or subtle changes in its identity. Therefore, we used *Phox2b* as a marker to monitor rhombomeric patterns of neurogenesis. In wild-type embryos at 10.0 dpc, *Phox2b* is expressed in two longitudinal columns, one

Copyright © 1999 by Academic Press. All rights of reproduction in any form reserved.

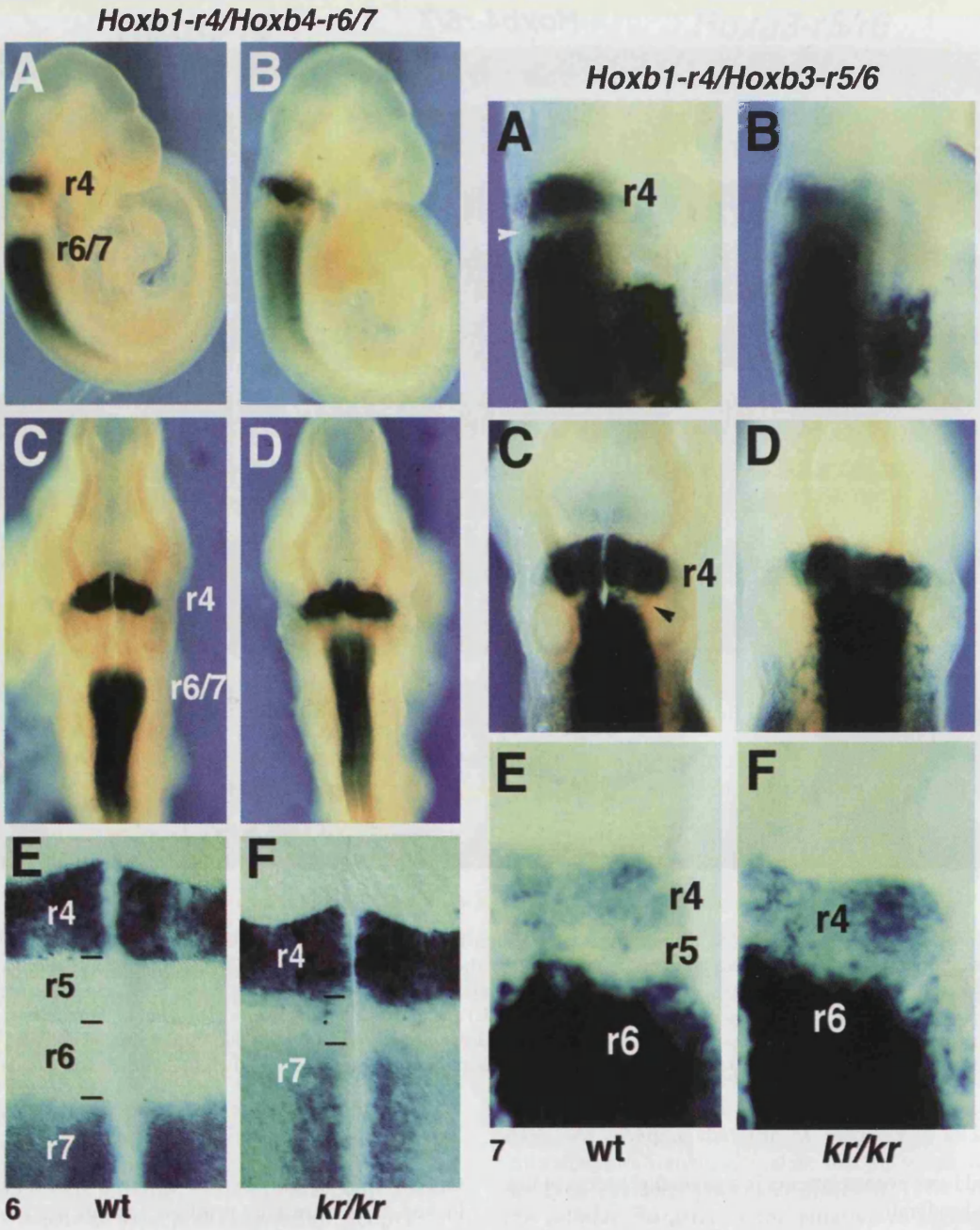

FIG. 6. Expression of the *Hoxb1-r4; Hoxb4-r6/e late* double transgene in wt (A, C, E) and *kr/kr* (B, D, E) embryos. The two-rhombomere gap between r4 and the r6/r7 boundary of the normal embryo is reduced to one or less in the mutant. In the flat mount of the wt (E) a sharp posterior boundary for the r4 stripe is observed, as well as the morphological r5/r6 boundary and the anterior limit of the *b4-r6/e late* line. In the mutant (F), the r4 stripe is less well defined at the posterior boundary, no visible boundary exists in between, and the anterior limit of the *b4-r6/e late* line is as clear as in the wt. No mixing of cells expressing *lacZ* from the *b1-r4* and the *b4-r6/e late* lines is observed. All embryos shown are 9.5 dpc.

FIG. 7. Expression of the *Hoxb1-r4; Hoxb3-r5/6* double transgene in wt (A, C, E) and *kr/kr* (B, D, E) embryos. A gap between the two domains of transgene expression in r4 and r6 is clearly seen in wt embryos and corresponds to r5 (arrowheads in A and C). The r5 domain of unstained cells is absent in the mutants (B, D). In the flat mounts (E, F) the level of expression is lower for the *b1-r4* line than for the *b3-r5/6* line, so that the difference between the r4 and r6 domains is evident. In wt embryos, there is staining in the most ventral portion of r5 (C, E) which corresponds to fbm neurons migrating posterior from r4. All embryos shown are 9.5 dpc.

Copyright © 1999 by Academic Press. All rights of reproduction in any form reserved.

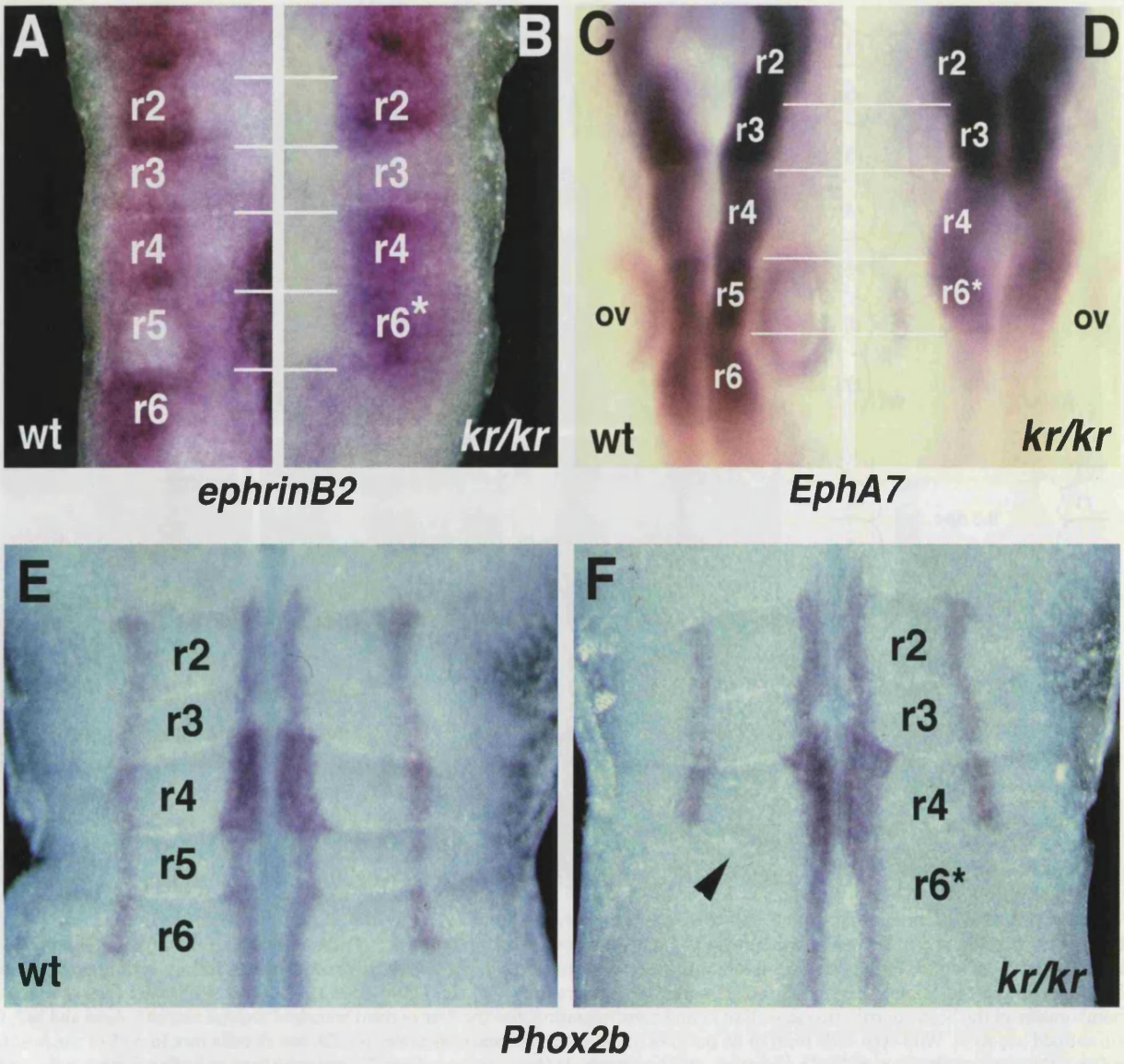

FIG. 8. Expression of *Eph* receptors, *ephrin* ligands, and *Phox2b* in the *kreisler* hindbrain. (A, B) *ephrin-B2* is normally expressed at a high level in r1, r2, r4, and r6 and at lower levels in r3 and is absent in r5 (A). In *kr/kr* embryos expression in r4 is contiguous with the more caudal domain corresponding to r6 (B). (C, D) *EphA7* expression normally occurs in r2–r6, with higher levels of expression in r3 and r5 (C). In *kr/kr* embryos high levels of expression occur only in r3 and the domain of expression posterior to r4 is reduced by one rhombomere in length (D). These data (A–D) indicate that in *kreisler* mutants the territory immediately caudal to r4 expresses molecular markers normally present in r6. (E, F) At 10.0 dpc *Phox2b* is normally expressed in two longitudinal columns in the hindbrain positioned ventrally and laterally (E). The ventral column is expanded in r4 and the lateral column extends from r2 to r6. In *kr/kr* embryos expression in the ventral column is largely unchanged, except for the altered shape of the r4 domain (F). However, the lateral column runs only from r2 to r4. The arrowhead in F indicates the presence of a morphologically distinct boundary between r4 and r6. ov, otic vesicle; r6* refers to the anteriorly shifted r6 due to the deletion of r5. All embryos shown are 9.5 dpc except E and F which are 10.0 dpc. A and B and E and F represent flat-mounted hindbrains, while C and D are dorsal views.

ventral and one lateral [Fig. 8E and Pattyn *et al.* (1997)]. The ventral column extends from the r1/r2 boundary more posteriorly into the spinal cord and the domain in r4 corresponding to the developing facial motor neurons is markedly thickened. The lateral column spans r2 through r6. In *kreisler* mutant embryos at this stage, the ventral column appears generally unaffected except for the shape of the r4 domain (Fig. 8F). This change in r4 correlates with the defects we previously noted using the *b1-r4* and *b2-r4* transgenic lines (Figs. 1 and 2). Expression of *Phox2b* in the

Copyright © 1999 by Academic Press. All rights of reproduction in any form reserved.

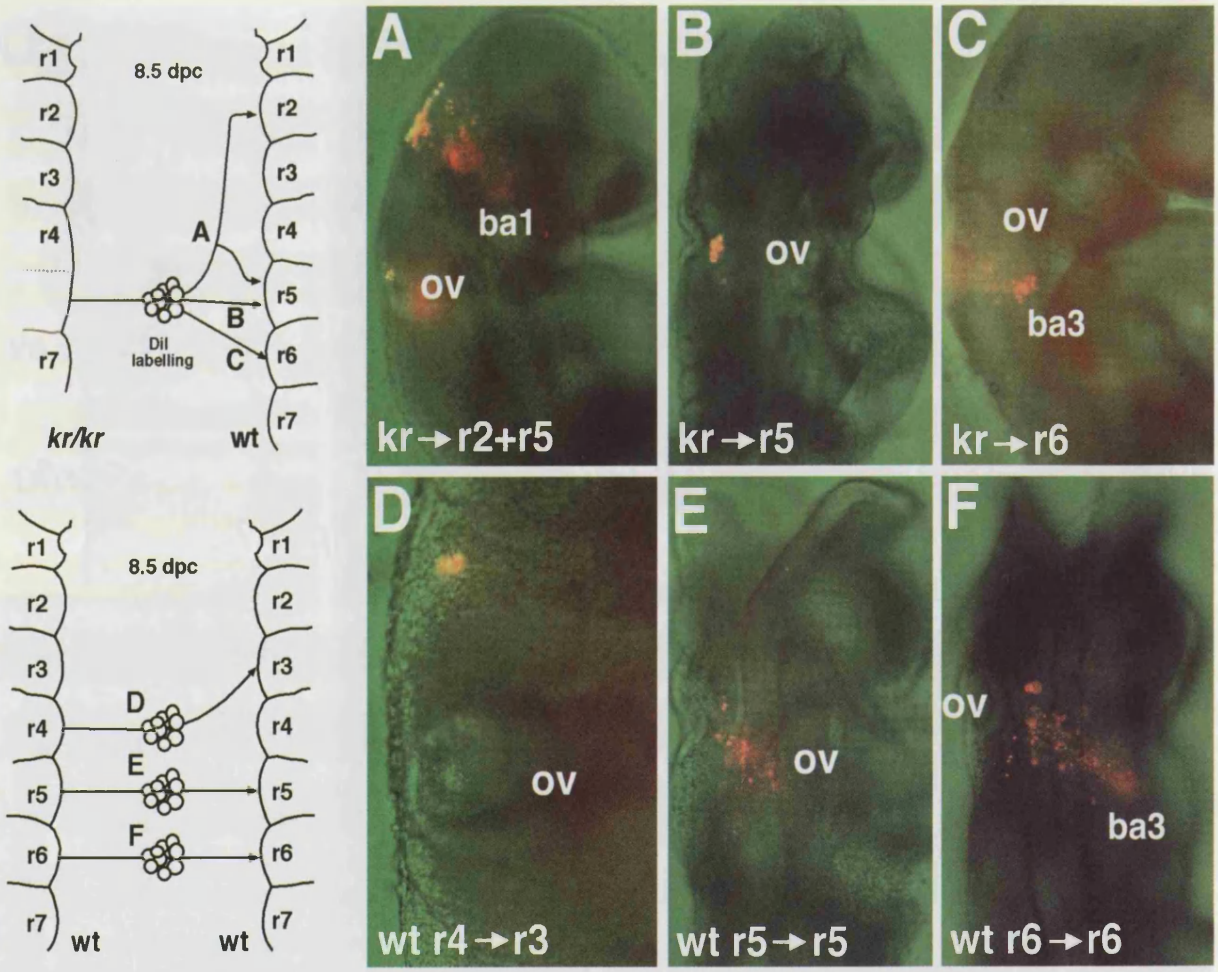

FIG. 9. Grafting of cells from *kr/kr* (A–C) and wt (D, E) donor embryos into isochronic wt hosts. On the left-hand side, diagrams depict the grafting experiments shown. A small group of cells from 8.5 dpc *kreisler* (A–C) or wt (D–F) donors were labeled with DiI and grafted to the indicated rhombomere level of wt CBA isochronic hosts. Embryos were grown in culture for a further 24 h. *kreisler* mutant cells from the otic region of the donor were grafted into r2 and r5 of the same host (A) or into r5 (B) or r6 (C). These cells mix freely with even rhombomeres of the host, contributing as well to neural crest migrating into the first or third branchial arch (r2 and ba1, A; r6 and ba3, C), but not odd (r5; A, B). Wild-type cells from r4 do not mix in an odd rhombomere territory (r3, D), but r5 cells mix into r5 of the host (E), and r6 cells mix into the host r6 (F). The position of the otic vesicle (ov) is indicated in all panels. All embryos shown are 9.5 dpc.

lateral column does not extend posterior to r4, indicating that both the r5 and r6 domains are missing (Fig. 8F). The loss of expression in r5 was expected since this segment does not form in *kreisler* embryos. However, the loss of the subrhombomeric r6 domain shows that not all aspects of r6 patterning are normal. This indicates that *kreisler* does have a later role in conferring specific aspects of r6 identity that could be mediated through its effect on *Hox* genes or other targets.

DISCUSSION

In this study we have examined the hindbrain phenotype in the mouse *kreisler* mutant using *Hox/lacZ* transgenic marker lines, lineage analysis, cell grafting and mixing assays, and *Eph/ephrin* and *Phox2b* gene expression. This analysis reveals that r5 is missing and fails to form. There are also alterations to r3 and r4, which are outside the normal domains of *kreisler* expression, suggesting that it has indirect influences to patterning in other hindbrain segments. The combination of markers characteristic of r6 and grafting experiments examining cellular mixing properties show that r6 is present, initially adopts an appropriate identity, and generates neural crest cells. This indicates that *kreisler* has an early role in segmentation in addition later roles in regulating segmental identity through the *Hox* genes. This also provides an interesting contrast to the role of its zebrafish homolog, *valentino*, in hindbrain patterning.

Copyright © 1999 by Academic Press. All rights of reproduction in any form reserved.

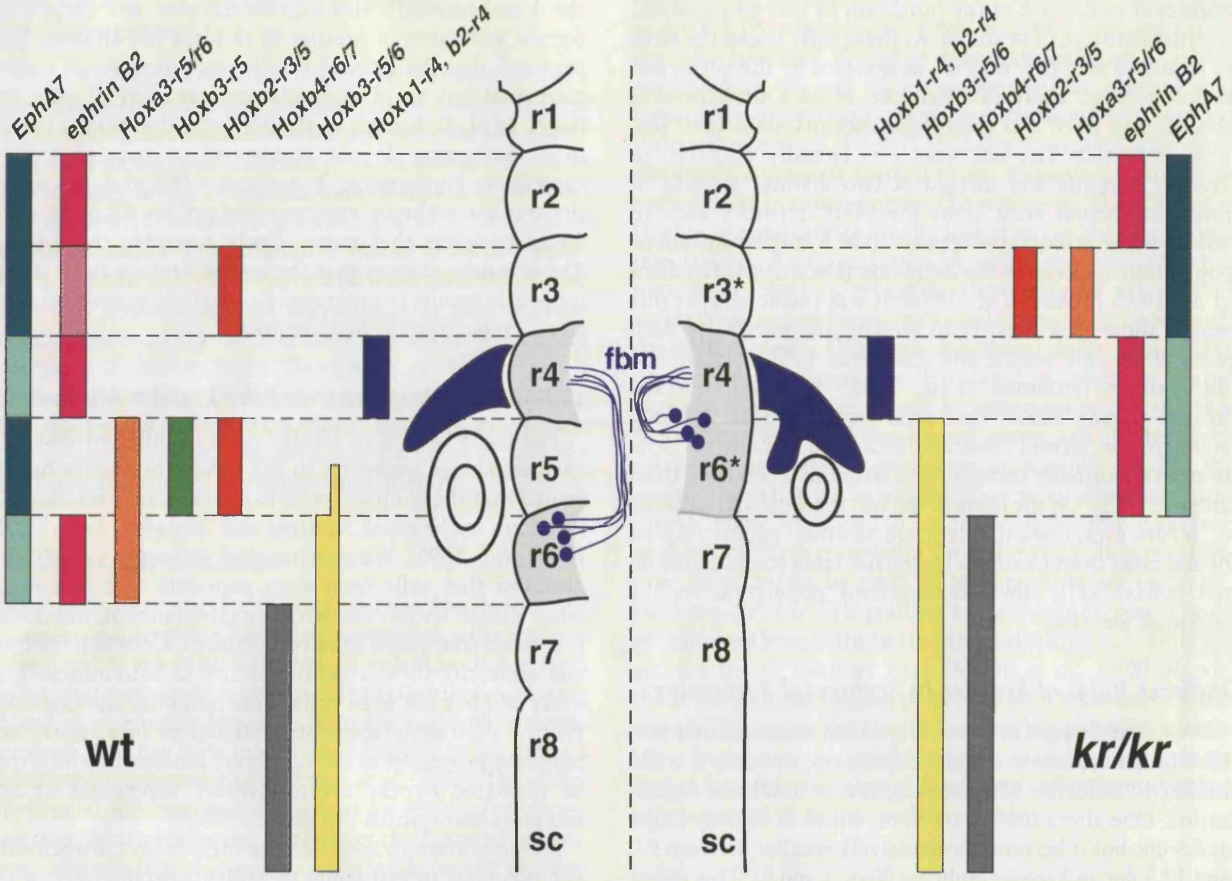

FIG. 10. Diagram depicting the phenotypic effects of the *kreisler* mutation on the mouse hindbrain with the markers used in this study. Migrating neural crest from r4 and the fbm population were detected with the *Hoxb1* and *Hoxb2* r4 lines; therefore, they are represented in the same color. Different levels of *EphA7* and *ephrin B2* are indicated by shades of coloring. The density of stippling over the rhombomeres indicates their even or odd mixing properties. In *kr/kr*, an asterisk indicates the partial transformation of r3 toward an r5 identity and the changes in *Phox2b* expression in r6. All of the markers shown are depicted at 9.5 dpc, except for the migration of the fbm that represent the situation at 12.5 dpc. sc, spinal cord.

kreisler and Its Roles in Segmentation

The summary diagram in Fig. 10 compares the patterns of segmental expression in wild-type and *kreisler* mutant embryos with respect to markers used in this study. In agreement with previous analyses there is an absence of any marker specific to or characteristic of r5. Furthermore, the temporal analysis with different reporter lines extended this to show that expression of the r5 markers is never initiated, arguing that r5 is not simply lost at later stages due to a failure in its maintenance (Figs. 3 and 4). Hence, we believe *kreisler* is required for the initial specification of the r5 territory.

One of the major reasons for embarking upon this study was to resolve the confusion over whether r6 was present, deleted, transformed to r4, or locked in an altered or immature prerhombomeric state in the mouse mutants. Analysis with two r4 reporter lines shows that r4 has not expanded posteriorly, arguing against an r6 to r4 transformation (Figs. 1 and 2). Double transgenic embryos carrying the *Hoxb1-r4* and the *Hoxb4-r6/7* reporters clearly indicate that between the r4 and r7 territories there is a group of unstained cells, approximately one segment wide (Fig. 6). We have found that this putative segment has molecular and cellular characteristics of r6. The expression profile of the *Eph/ephrin* genes and the *Hoxb3-r5/6* reporter line in this territory, immediately posterior to r4, resemble wild-type r6 (Figs. 7 and 8). Heterotopic grafts reveal that these cells also have mixing properties identical to that of r6 and mature even-numbered rhombomeres (Fig. 9). Furthermore, the r4-derived fbm neurons, which migrate ventrally in r5 and then turn laterally in r6 of wild-type embryos, undergo a lateral migration immediately after emerging from r4 in *kreisler* embryos (Fig. 1). Together these results support the idea that this segment displays an r6 identity or character.

Our analysis suggests that in the absence of *kreisler* there is a block in the formation of r5 that leads to an overall

Copyright © 1999 by Academic Press. All rights of reproduction in any form reserved.

reduction in the size of the hindbrain by one segment and the juxtaposition of r4 and r6. At these early stages the sizes of r4 and r6 are fairly normal, as assessed by the single and double reporter analyses. Therefore, r4 does not expand at the expense of r6 and these segments maintain their distinct identities. The otic vesicle is laterally displaced in *kreisler* mutants and instead of two distinct streams of migrating neural crest from the r4–r6 territory seen in wild-type embryos, there appears to be a single continuous population adjacent to the hindbrain (Deol, 1964; Frohman *et al.*, 1993; McKay *et al.*, 1994). It was predicted that this would allow crest from r4 to migrate abnormally on both sides of the otic vesicle and contribute to the second and third arches (Frohman *et al.*, 1993). However, our DiI lineage tracing shows that cells emerging from r4 only populate the second branchial arch, and in contrast cells from r6 abnormally contribute to both the second and third arches (Fig. 2). On the basis of the cell marking and patterns of reporter expression, there are distinct populations of neural crest from r4 and r6 in *kreisler* embryos and they do not behave as a single homogenous population with a common identity.

Indirect Roles of kreisler in Segmental Patterning

We noted changes in patterning and in markers outside of the normal domain of *kreisler* expression, showing it could indirectly influence additional aspects of hindbrain organization. One alteration occurs in r4, which is slightly larger at 8.5 dpc but it becomes progressively smaller between 9.0 and 12.5 dpc in *kreisler* embryos (Figs. 1 and 2). This defect could be a consequence of inappropriate interrhombomeric signaling due to the absence of r5 and the juxtaposition of r4 and r6. Signaling processes between odd- and even-numbered rhombomeres have been shown to be important in chick grafting experiments for the proper maintenance of some aspects of segmental gene expression (Graham and Lumsden, 1996). It is interesting that it has previously been observed, on the basis of acridine orange staining, that there is increased apoptosis over r4 in *kreisler* mutants (McKay *et al.*, 1994). Hence, the reduction of r4 could be mediated by ectopic activation of the cell death program in this territory due to improper signaling.

The induction of the *Hoxa3 r5/r6* reporter indicates that r3 is also affected in the *kreisler* mutants. The activation of the r5/r6 reporter in r3 also occurs in *kr*/+ heterozygous embryos, where hindbrain segmentation was believed to be completely normal. Therefore, since r5 is present in these embryos, this induction cannot simply be explained by changes in signaling arising from its absence. Other than in r5 and r6 *kreisler* is not normally expressed in the hindbrain, except for a dorsal population of cells in the roof plate (Cordes and Barsh, 1994; Eichmann *et al.*, 1997). Hence, it is possible that these dorsal cells normally prevent the induction of the respective r5 markers in r3 or that *kreisler* itself is ectopically activated in r3 in the mutants. However, we analyzed the expression of *kreisler* in *kr/kr* embryos and found that while the domain in r5 and r6 is completely lost, the dorsal roof cells still express the gene and there is no ectopic induction of *kreisler* in r3 (data not shown). This confirms that the original *kreisler* mutation is not a complete null but an r5/r6 regulatory mutation (Cordes and Barsh, 1994; Eichmann *et al.*, 1997) and that these changes in r3 patterning do not correspond to sites of *kreisler* expression. Furthermore, in support of this idea, in some of the mutant embryos expression of *ephrin-B2* in r3 is reduced to levels that more closely resemble those in r5. These results suggest that the loss of *kreisler* in r5 and r6 indirectly results in progressive changes to segmental identity correlated with the gene dosage.

Cell-Mixing Properties and the kreisler Mutants

The transposition of labeled cells to different odd- and even-numbered segments in the mouse hindbrain has revealed that the ability of cells to intermix follows a similar paradigm to the chick (Guthrie and Lumsden, 1991; Guthrie *et al.*, 1993; Wizenmann and Lumsden, 1997). We observed that cells from even segments will mix freely when placed within another even environment, but do not mix when transposed to an odd segment. Cells derived from odd segments show a similar ability to intermingle with other odd but not even cells. This reiterates the conservation of alternating segmental differences in adhesive and repulsive properties in the vertebrate hindbrain, which may be mediated by the complementary expression of Eph receptors and ephrins (Xu *et al.*, 1995).

It is important to note that the miscibility between even and odd cells in cell grafts or explants occurs only in the absence of a boundary between these populations, but if a boundary is present they tend not to mix and remain as discrete coherent groups (Guthrie *et al.*, 1993). Analysis in the chick has previously shown that in at least 25% of the cases, new morphologically detectable boundaries were formed when even segments were placed adjacent to each other (Guthrie and Lumsden, 1991). Furthermore, in *Krox20* mutants when r5 is lost and r4 and r6 are brought together, a boundary is maintained (Schneider-Maunoury *et al.*, 1997). This is relevant to the *kreisler* mutants, as the absence of r5 brings r4 and r6 in to direct opposition, which could potentially lead to considerable intermixing between the segments. However, we noted that at the r4/r6 interface the expression boundaries of the *lacZ* reporters are only slightly more diffuse compared with wild-type embryos (Figs. 1, 2, and 5–7). This could arise due to reprogramming of the patterns of expression following extensive intermingling, but we also observed in the neural crest marking experiments that DiI placed into r4 or r6 of *kreisler* embryos remained confined primarily to a single segment (Fig. 2 and data not shown). Furthermore, in some of the flat-mounted hindbrain preparations of mutant embryos a morphological boundary between r4 and r6 is detected (arrowhead in Fig. 8F). This supports the idea that there is relatively little intermixing between these segments and a boundary has formed or been maintained between r4 and r6 in the *kreisler* mutants.

Copyright © 1999 by Academic Press. All rights of reproduction in any form reserved.

Roles for kreisler in Late r6 Patterning and Neurogenesis

While we have shown that r6 forms and initially adopts a correct segmental identity, the analysis of *Phox2b* expression in neurogenesis demonstrates that there are some later changes in its regional character (Figs. 8E and 8F). The loss of expression in the r6-specific subpopulation of neurons from the lateral column might arise due to the absence of *kreisler*-dependent upregulation of *Hoxa3* in r6. In support of this, a recent study has shown that the *Hoxa2* and *Hoxb2* genes play a role in differentially regulating rhombomere-specific subsets of *Phox2b* and other neurogenic markers in patterning of the hindbrain (Davenne *et al.*, 1999). Even if these alterations are mediated through other *kreisler* targets, the results demonstrate that in addition to its early roles in segmentation, *kreisler* has some direct or indirect input into the control of rhombomere identity.

kreisler versus valentino

Our analysis of alterations in the mouse *kreisler* mutant provides an interesting basis for comparison with those of *valentino*, its zebrafish homolog. In *valentino* it has been shown that mutant cells are not able to contribute to future r5 and r6 territories but do mix freely with other rhombomeres. This has been interpreted as failure in acquiring a definitive rhombomeric fate (Moens *et al.*, 1996). Therefore, the general mechanism put forward for *kreisler/valentino* function, derived from this analysis of the zebrafish phenotype, suggests that this gene is responsible for the maturation and subdivision of a prorhombomeric territory into definitive r5 and r6 (Moens *et al.*, 1996, 1998). The loss of *valentino* locks this territory into its immature prorhombomeric state, and the cells display no mature characteristics of r5 or r6.

However, our analysis of the *kreisler* phenotype does not easily fit such a model. r5 is absent but r6 is present and acquires the correct identity. Therefore, the mouse *kreisler* gene is involved in the formation of r5, but the generation of a definitive r6 territory is independent of both *kreisler* and r5. There are other differences in the phenotypes between these species. For example, in *valentino* mutants r4 dramatically expands in a posterior direction (Prince *et al.*, 1998), while in *kreisler* r4 is actually reduced in size. Hence, while many of the same segments are affected in the mouse and fish mutants, the nature of these changes is distinctly different.

There are several reasons that could account for the *kr/val* differences between the species. First, in fish *val* is expressed throughout r5 and r6 at all stages (Moens *et al.*, 1998). In mouse, high levels of *kreisler* are initially observed in r5 and rostral r6 and expression in the entire r6 territory only appears at later stages (Cordes and Barsh, 1994; Manzanares *et al.*, 1999). Hence, the lack of an early role for *kreisler* in mouse r6 is consistent with the fact that it is not present in this segment until later stages. Another possibility arises from ploidy differences between the species and the potential for additional *valentino/kreisler*-related genes in the fish (Wittbrodt *et al.*, 1998). Recently a second Kr/val homolog has been cloned in zebrafish, although it is not expressed in r5 and r6, it is detected in somites and transiently in reticulospinal and occulomotor neurons (Schvarzstein *et al.*, 1999). This helps to explain why these neurons are properly formed in *val* mutants despite other early defects in neurogenesis. The new gene, *Zkrml2*, might be able to compensate for the loss of *val* in these neuronal populations. As three copies of single mammalian genes have been found in zebrafish, there may be yet another *val/kr* homolog and new roles could have evolved for such duplicated genes. Common functional roles could have been divided between the duplicated members or shared between them. Hence, it will be important to determine if there are other *valentino*-related genes and if they have roles in segmentation analogous to *kreisler*. Finally, the assumption that rX in val mutants is an immature prorhombomeric territory and not r6-like is due to the absence of those markers tested and its cell-mixing defects. However, there might be early r6 markers that are on in rX. Furthermore, the fish grafting experiments to test mixing potential utilized early gastrulating cells from *val*$^-$ embryos and not the rX territory itself (Moens *et al.*, 1998). Hence, the actual cellular mixing properties of rX were not directly tested. This raises the possibility that the r5 and r6 phenotypes in *val* mutants might be more analogous to those we find in *kreisler*, such that r5 is missing and r6 forms but has only a partial r6 or incomplete identity.

CONCLUSION

This study illustrates that *kreisler* has roles in regulating multiple steps of hindbrain patterning. The complete absence of r5 in *kreisler* mutants shows that it has an early role in the specification of this segment. The formation of r6 independent of r5 argues against a strict prorhombomeric model for segmentation of this region of the hindbrain in mouse. In addition, through the direct regulation of *Hox* genes, *kreisler* participates in the control of segmental identity. Ectopic expression of *kreisler* in r3 leads to its transformation toward an r5 identity (Theil *et al.*, 1999). The correct dosage of *kreisler* also appears to be critical for indirectly maintaining the proper identity of r3. Therefore, rather than being restricted to a single aspect of patterning, it appears to be an emerging theme that genes involved in controlling segmental processes in the hindbrain can act at several different levels.

ACKNOWLEDGMENTS

We thank Amanda Hewett, Peter Mealyer, and Rosemary Murphy for help in animal husbandry; Christiana Ruhrberg for help with *in situs*; Christo Goridis and Jean-François Brunet for the gift of the *Phox2b* probe; and Drs. Greg Barsh, Thomas Theil, Sabine Cordes, and Patrick Tam and members of the Krumlauf lab for valuable discussions. M.M. was supported by HFSP and EEC Marie

Copyright © 1999 by Academic Press. All rights of reproduction in any form reserved.

Curie postdoctoral fellowships, P.T. by EMBO and HFSP postdoctoral fellowships, S.N. by an EEC Biotechnology Network grant (BIO4 CT-960378), A.G. by a Bait Memorial Fellowship, A.M. by an MRC Training Fellowship, and J.B. by an MRC studentship. This work was funded by Core MRC Programme support and EEC Biotechnology Network grants to R.K. (BIO4 CT-960378) and D.W. (BIO4 CT-960659) and by grants from the Hong Kong RGC to C-T.K. and M.S.

REFERENCES

Bergemann, A. D., Cheng, H.-J., Brambilla, R., Klein, R., and Flanagan, J. G. (1995). *ELF-2,* a new member of the *Eph* ligand family, is segmentally expressed in mouse embryos in the region of the hindbrain and newly forming somites. *Mol. Cell. Biol.* **15,** 4921–4929.

Birgbauer, E., and Fraser, S. E. (1994). Violation of cell lineage restriction compartments in the chick hindbrain. *Development* **120,** 1347–1356.

Carpenter, E. M., Goddard, J. M., Chisaka, O., Manley, N. R., and Capecchi, M. R. (1993). Loss of *Hoxa-1 (Hox-1.6)* function results in the reorganization of the murine hindbrain. *Development* **118,** 1063–1075.

Chan, W. Y., and Tam, P. P. L. (1988). A morphological and experimental study of the mesencephalic neural crest cells in the mouse embryo using wheat-germ agglutinin gold conjugate as the cell marker. *Development* **102,** 427–442.

Chisaka, O., and Capecchi, M. (1991). Regionally restricted developmental defects resulting from targeted disruption of the mouse homeobox gene *hox1.5. Nature* **350,** 473–479.

Cordes, S. P., and Barsh, G. S. (1994). The mouse segmentation gene *kr* encodes a novel basic domain–leucine zipper transcription factor. *Cell* **79,** 1025–1034.

Davenne, M., Maconochie, M., Neun, R., Brunet, J.-F., Chambon, P., Krumlauf, R., and Rijli, F. (1999). *Hoxa2* and *Hoxb2* control dorsoventral patterns of neuronal development in the rostral hindbrain. *Neuron* **22,** 677–691.

Deol, M. S. (1964). The abnormalities of the inner ear in *kreisler* mice. *J. Embryol. Exp. Morphol.* **12,** 475–490.

Dollé, P., Lufkin, T., Krumlauf, R., Mark, M., Duboule, D., and Chambon, P. (1993). Local alterations of *Krox-20* and *Hox* gene expression in the hindbrain suggest lack of rhombomeres 4 and 5 in homozygote null *Hoxa-1 (Hox-1.6)* mutant embryos. *Proc. Natl. Acad. Sci. USA* **90,** 7666–7670.

Eichmann, A., Grapin-Botton, A., Kelly, L., Graf, T., Le Douarin, N. M., and Sieweke, M. (1997). The expression pattern of the *mafB/kr* gene in birds and mice reveals that the *kreisler* phenotype does not represent a null mutant. *Mech. Dev.* **65,** 111–122.

Ellis, J., Liu, Q., Breitman, M., Jenkins, N., Gilbert, G., Copeland, N., Tempest, H., Warren, S., Muir, E., Schilling, H., Fletcher, F., Ziegler, S., and Rogers, J. (1995). Embryo brain kinase: A novel gene of the Eph/Elk receptor tyrosine kinase family. *Mech. Dev.* **52,** 319–349.

Fraser, S., Keynes, R., and Lumsden, A. (1990). Segmentation in the chick embryo hindbrain is defined by cell lineage restrictions. *Nature* **344,** 431–435.

Frohman, M. A., Martin, G. R., Cordes, S., Halamek, L. P., and Barsh, G. S. (1993). Altered rhombomere-specific gene expression and hyoid bone differentiation in the mouse segmentation mutant *kreisler (kr). Development* **117,** 925–936.

Gale, N., Flenniken, A., Compton, D., Jenkins, N., Copeland, N., Gilbert, D., Davis, S., Wilkinson, D., and Yancopoulos, G. (1996). Elk-L3, a novel transmembrane ligand for the Eph family of receptor tyrosine kinases, expressed in embryonic floor plate, roof plate and hindbrain segments. *Oncogene* **13,** 1343–1352.

Gavalas, A., Davenne, M., Lumsden, A., Chambon, P., and Rijli, F. (1997). Role of *Hoxa-2* in axon pathfinding and rostral hindbrain patterning. *Development* **124,** 3693–3702.

Gavalas, A., Studer, M., Lumsden, A., Rijli, F., Krumlauf, R., and Chambon, P. (1998). *Hoxa1* and *Hoxb1* synergize in patterning the hindbrain, cranial nerves and second pharyngeal arch. *Development* **125,** 1123–1136.

Goddard, J., Rossel, M., Manley, N., and Capecchi, M. (1996). Mice with targeted disruption of *Hoxb1* fail to form the motor nucleus of the VIIth nerve. *Development* **122,** 3217–3228.

Gould, A., Itasaki, N., and Krumlauf, R. (1998). Initiation of rhombomeric *Hoxb4* expression requires induction by somites and a retinoid pathway. *Neuron* **21,** 39–51.

Gould, A., Morrison, A., Sproat, G., White, R., and Krumlauf, R. (1997). Positive cross-regulation and enhancer sharing: Two mechanisms for specifying overlapping *Hox* expression patterns. *Genes Dev.* **11,** 900–913.

Graham, A., and Lumsden, A. (1996). Interactions between rhombomeres modulate *Krox-20* and follistatin expression in the chick embryo hindbrain. *Development* **122,** 473–480.

Guthrie, S., and Lumsden, A. (1991). Formation and regeneration of rhombomere boundaries in the developing chick hindbrain. *Development* **112,** 221–229.

Guthrie, S., Prince, V., and Lumsden, A. (1993). Selective dispersal of avian rhombomere cells in orthotopic and heterotopic grafts. *Development* **118,** 527–538.

Hertwig, P. (1944). Die Genese der Hirn- und GehörorganmiBbildungen bei röntgenmutierten Kreisler-mäusen. *Z. KonstLehnre* **28,** 327–354.

Jacobson, A. G., and Tam, P. P. L. (1982). Cephalic neurulation in the mouse embryo analyzed by sem and morphometry. *Anat. Rec.* **203,** 375–396.

Lumsden, A., and Krumlauf, R. (1996). Patterning the vertebrate neuraxis. *Science* **274,** 1109–1115.

Maconochie, M., Nonchev, S., Studer, M., Chan, S.-K., Pöpperl, H., Sham, M.-H., Mann, R., and Krumlauf, R. (1997). Cross-regulation in the mouse *HoxB* complex: The expression of *Hoxb2* in rhombomere 4 is regulated by *Hoxb1. Genes Dev.* **11,** 1885–1896.

Maconochie, M. K., Nonchev, S., Morrison, A., and Krumlauf, R. (1996). Paralogous *Hox* genes: Function and regulation. *Annu. Rev. Genet.* **30,** 529–556.

Manzanares, M., Cordes, S., Ariza-McNaughton, L., Sadl, V., Maruthainar, K., Barsh, G., and Krumlauf, R. (1999). Conserved and distinct roles of *kreisler* in regulation of the paralogous *Hoxa3* and *Hoxb3* genes. *Development* **126,** 759–769.

Manzanares, M., Cordes, S., Kwan, C.-T., Sham, M.-H., Barsh, G., and Krumlauf, R. (1997). Segmental regulation of *Hoxb3* by *kreisler. Nature* **387,** 191–195.

Mark, M., Lufkin, T., Vonesch, J.-L., Ruberte, E., Olivo, J.-C., Dollé, P., Gorry, P., Lumsden, A., and Chambon, P. (1993). Two rhombomeres are altered in *Hoxa-1* mutant mice. *Development* **119,** 319–338.

Marshall, H., Nonchev, S., Sham, M. H., Muchamore, I., Lumsden, A., and Krumlauf, R. (1992). Retinoic acid alters hindbrain Hox code and induces transformation of rhombomeres 2/3 into a 4/5 identity. *Nature* **360,** 737–741.

McKay, I., Lewis, J., and Lumsden, A. (1997). Organization and development of facial motor neurons in the *kreisler* mutant mouse. *Eur. J. Neurosci.* **9,** 1499–1506.

Copyright © 1999 by Academic Press. All rights of reproduction in any form reserved.

McKay, I. J., Muchamore, I., Krumlauf, R., Maden, M., Lumsden, A., and Lewis, J. (1994). The *kreisler* mouse: A hindbrain segmentation mutant that lacks two rhombomeres. *Development* **120,** 2199–2211.

Moens, C. B., Cordes, S. P., Giorgianni, M. W., Barsh, G. S., and Kimmel, C. B. (1998). Equivalence in the genetic control of hindbrain segmentation in fish and mouse. *Development* **125,** 381–391.

Moens, C. B., Yan, Y.-L., Appel, B., Force, A. G., and Kimmel, C. B. (1996). *valentino:* A zebrafish gene required for normal hindbrain segmentation. *Development* **122,** 3981–3990.

Nichols, D. (1981). Neural crest formation in the head of the mouse embryo as observed using a new histological technique. *JEEM* **64,** 105–120.

Nieto, M. A., Bradley, L. C., and Wilkinson, D. G. (1991). Conserved segmental expression of *Krox-20* in the vertebrate hindbrain and its relationship to lineage restriction. *Development Suppl.* **2,** 59–62.

Nonchev, S., Vesque, C., Maconochie, M., Seitanidou, T., Ariza-McNaughton, L., Frain, M., Marshall, H., Sham, M. H., Krumlauf, R., and Charnay, P. (1996). Segmental expression of Hoxa-2 in the hindbrain is directly regulated by Krox-20. *Development* **122,** 543–554.

Pattyn, A., Morin, X., Cremer, H., Goridis, C., and Brunet, J.-F. (1997). Expression and interactions of the two closely related homeobox genes *Phox2a* and *Phox2b* during neurogenesis. *Development* **124,** 4065–4075.

Prince, V. E., Moens, C. B., Kimmel, C. B., and Ho, R. K. (1998). Zebrafish *hox* genes: Expression in the hindbrain region of wild-type and mutants of the segmentation gene, *valentino*. *Development* **125,** 393–406.

Schneider-Maunoury, S., Seitanidou, T., Charnay, P., and Lumsden, A. (1997). Segmental and neuronal architecture of the hindbrain of *Krox-20* mouse mutants. *Development* **124,** 1215–1226.

Schneider-Maunoury, S., Topilko, P., Seitanidou, T., Levi, G., Cohen-Tannoudji, M., Pournin, S., Babinet, C., and Charnay, P. (1993). Disruption of *Krox-20* results in alteration of rhombomeres 3 and 5 in the developing hindbrain. *Cell* **75,** 1199–1214.

Schvarzstein, M., Kirn, A., Haffter, P., and Cordes, S. (1999). Expression of *Zkrml2*, a homologue of the *Krml1/val* segmentation gene, during embryonic patterning of the zebrafish (*Danio rerio*). *Mech. Dev.* **80,** 223–226.

Sham, M. H., Vesque, C., Nonchev, S., Marshall, H., Frain, M., Das Gupta, R., Whiting, J., Wilkinson, D., Charnay, P., and Krumlauf, R. (1993). The zinc finger gene *Krox-20* regulates *Hoxb-2* (*Hox2.8*) during hindbrain segmentation. *Cell* **72,** 183–196.

Studer, M., Gavalas, A., Marshall, H., Ariza-McNaughton, L., Rijli, F., Chambon, P., and Krumlauf, R. (1998). Genetic interactions between *Hoxa1* and *Hoxb1* reveal new roles in regulation of early hindbrain patterning. *Development* **125,** 1025–1036.

Studer, M., Lumsden, A., Ariza-McNaughton, L., Bradley, A., and Krumlauf, R. (1996). Altered segmental identity and abnormal migration of motor neurons in mice lacking *Hoxb-1*. *Nature* **384,** 630–635.

Sturm, K., and Tam, P. P. L. (1993). Isolation and culture of whole postimplantation embryos and germ layer derivatives. *Methods Enzymol.* **225,** 164–190.

Swiatek, P. J., and Gridley, T. (1993). Perinatal lethality and defects in hindbrain development in mice homozygous for a targeted mutation of the zinc finger gene *Krox-20*. *Genes Dev.* **7,** 2071–2084.

Theil, T., Ariza-McNaughton, L., Manzanares, M., Krumlauf, R., and Wilkinson, D. (1999). *kreisler* regulates rostrocaudal identity in the hindbrain. *Development,* in press.

Theil, T., Frain, M., Gilardi-Hebenstreit, P., Flenniken, A., Charnay, P., and Wilkinson, D. (1998). Segmental expression of the *EphA4* (*Sek-1*) receptor tyrosine kinase in the hindbrain is under the direct transcriptional control of Krox20. *Development* **125,** 443–452.

Trainor, P. A., and Tam, P. P. L. (1995). Cranial paraxial mesoderm and neural crest of the mouse embryo-codistribution in the craniofacial mesenchyme but distinct segregation in the branchial arches. *Development* **121,** 2569–2582.

Trainor, P. A., Tan, S. S., and Tam, P. P. L. (1994). Cranial paraxial mesoderm-regionalization of cell fate and impact on craniofacial development in mouse embryos. *Development* **120,** 2925–2932.

Whiting, J., Marshall, H., Cook, M., Krumlauf, R., Rigby, P. W. J., Stott, D., and Allemann, R. K. (1991). Multiple spatially specific enhancers are required to reconstruct the pattern of *Hox-2.6* gene expression. *Genes Dev.* **5,** 2048–2059.

Wilkinson, D. G., Bhatt, S., Chavrier, P., Bravo, R., and Charnay, P. (1989). Segment-specific expression of a zinc finger gene in the developing nervous system of the mouse. *Nature* **337,** 461–464.

Wittbrodt, J., Meyer, A., and Schartl, M. (1998). More genes in fish? *Bioessays* **20,** 511–515.

Wizenmann, A., and Lumsden, A. (1997). Segregation of rhombomeres by differential chemoaffinity. *Mol. Cell. Neurosci.* **9,** 448–459.

Xu, Q., Alldus, G., Holder, N., and Wilkinson, D. G. (1995). Expression of truncated *Sek-1* receptor tyrosine kinase disrupts the segmental restriction of gene expression in the *Xenopus* and zebrafish hindbrain. *Development* **121,** 4005–4016.

Xu, Q., Mellitzer, G., Robinson, V., and Wilkinson, D. (1999). *In vivo* cell sorting in complementary segmental domains mediated by *Eph* receptors and *ephrins*. *Nature* **399,** 267–271.

Xu, Q., and Wilkinson, D. (1998). "*In Situ* Hybridisation of mRNA with Hapten Labelled Probes." IRL Press, Oxford.

Zhang, M., Kim, H.-J., Marshall, H., Gendron-Maguire, M., Lucas, A. D., Baron, A., Gudas, L. J., Gridley, T., Krumlauf, R., and Grippo, J. F. (1994). Ectopic *Hoxa-1* induces rhombomere transformation in mouse hindbrain. *Development* **120,** 2431–2442.

Received for publication March 15, 1999
Revised April 26, 1999
Accepted April 26, 1999

Copyright © 1999 by Academic Press. All rights of reproduction in any form reserved.